

Radiation-Induced, Solid-State Polymerization of Derivatives of Methacrylic Acid. I. Postirradiation Polymerization of Zinc Methacrylate

J. H. O'DONNELL and R. D. SOTHMAN, *Chemistry Department, University of Queensland, Brisbane, Australia*

Synopsis

The postirradiation polymerization of the crystalline, anhydrous, monohydrate, and dihydrate forms of zinc methacrylate was studied. The anhydrous salt polymerized readily in the temperature range 50–150°C., the monohydrate did not polymerize at all, and the dihydrate polymerized at about 100°C. Aging of the anhydrous salt greatly affected the rate of polymerization; this was shown to be due mainly to the formation of peroxides by reaction with air. Polymerization could be initiated thermally, without irradiation, in monomer which had been aged in contact with air, apparently by decomposition of the peroxides. The rate of the postirradiation polymerization was increased when air was present during irradiation and decreased when air was present during polymerization. The rate of polymerization increased with temperature, corresponding to an apparent activation energy of 10 kcal./mole. The dihydrate lost one molecule of water rapidly under vacuum at 20°C. and slowly on heating at 50°C. in a sealed vessel, forming a crystalline monohydrate. Slow thermal polymerization and rapid postirradiation polymerization occurred at 100°C. without the formation of any monohydrate, indicating that the polymerization was concurrent with the phase change.

INTRODUCTION

Polymerization in the solid state is now recognized to be possible for a wide variety of monomers,¹ but there is little fundamental understanding of the process or even of the relative importance of chemical and physical parameters.²

Many techniques used in the liquid state, including the use of chemical initiators, have limited applicability, and the most satisfactory method of obtaining a reasonably uniform distribution of initiating centers in a solid monomer is to use high-energy radiation, such as gamma rays.

If polymerization is carried out by warming after irradiation at a low temperature, at which polymer formation is negligible, i.e. by postirradiation polymerization, then initiation is distinct from propagation; moreover, termination by small radicals, particularly hydrogen atoms, will be reduced and the complexity of the reaction reduced to a minimum.³

Progress in understanding solid-state polymerization depends on a detailed study of suitable systems, which should include study of their

crystal structures, but only a few monomers, such as trioxane⁴ and vinyl stearate,⁵ have been studied in this way.

The postirradiation polymerization of a series of metal salts of acrylic and methacrylic acids has been investigated by Morawetz and his co-workers.⁶⁻⁹ They showed that polymerization can occur in crystalline solids at least 100°C. below the melting (or decomposition) point. Local melting and vapor-phase transport, alternatives to true solid-state polymerization, are unlikely to be important in such semi-ionic crystals at these temperatures. Furthermore, polymerization was shown to occur over a temperature range and not associated with any known solid-state phase transitions. The rate of polymerization (even the possibility of polymerization) varied between different metal salts and different hydrates of the same salt, but there was no correlation with the nature of the metal ion or the degree of hydration. The conclusion drawn from these results was that the parameters of the crystalline lattice determined the rate of polymerization. The crystal structures of the compounds are not known, except for calcium acrylate and in part barium methacrylate, but it is apparently the separation and spatial arrangement of double bonds which determines the polymerizability. Such topochemical control is well known in inorganic solids,¹⁰ and there are also many examples of reactions in organic solids.^{11,12} In all the acrylate and methacrylate salts studied the polymers produced were completely amorphous; this has also been the case in other free-radical polymerizations in the solid state.^{5,13,14}

The present investigation of the solid-state polymerization of zinc methacrylate was undertaken to determine whether a crystalline polymer was formed in this case, since new peaks had been observed in the x-ray diffraction pattern of the irradiated monomer.

EXPERIMENTAL

Zinc methacrylate was prepared by neutralization of methacrylic acid (Rohm and Haas, distilled under 100 mm. Hg of oxygen-free nitrogen at 60°C.) with Analar-grade zinc oxide (B.D.H.). The reaction was carried out at room temperature with vigorous stirring, with either water or methanol as solvent. A slight excess of methacrylic acid was added, and then the zinc methacrylate was allowed to crystallize on standing. The dihydrate crystallized from aqueous solution and was stored over saturated calcium chloride, to prevent dehydration.

The anhydrous salt crystallized from methanol solution, but care had to be taken to avoid contamination with dihydrate, which sometimes also crystallized. It was found necessary to make the anhydrous zinc methacrylate free from peroxides, and for this purpose the procedure described above was carried out in a dry box flushed with oxygen-free nitrogen. Anhydrous zinc methacrylate was also prepared by reaction of zinc metal with methacrylic acid in methanol, but since both water and oxygen were found necessary for the reaction to proceed, this method could not be used for preparing peroxide-free monomer.

The monohydrate was prepared by evacuation of the dihydrate at 10^{-3} mm. Hg for 8 hr. at 25°C . There was rapid and complete loss of one molecule of water of hydration, and crystalline monohydrate was produced. Further dehydration could not be induced by continued evacuation.

The three crystalline forms of zinc methacrylate were characterized by their x-ray diffraction patterns; these are shown in Figure 1. They were used to ensure the purity of each preparation, since contamination by the other forms can readily occur. The water contents were determined by

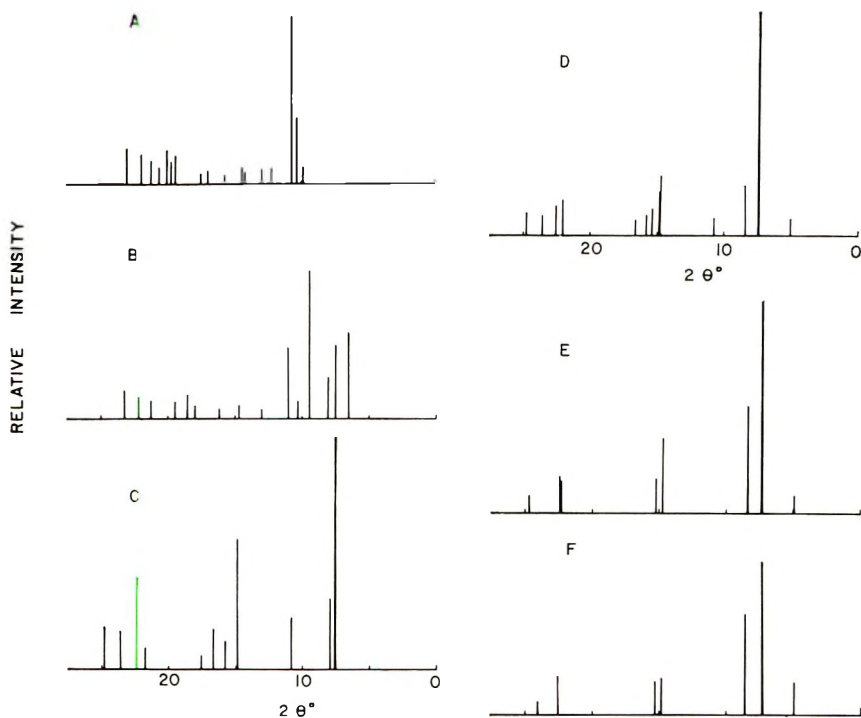


Fig. 1. X-ray diffraction patterns of zinc methacrylate salts: (A) anhydrous; (B) monohydrate; (C) dihydrate; (D-F) dihydrate after 1 Mrad of gamma irradiation at -196°C . followed by heating at 100°C .; (D) 1 day, 17% polymer; (E) 2 days, 23% polymer; (F) 4 days, 35% polymer.

Karl Fischer titrations,¹⁵ and the zinc was analyzed by EDTA titration.¹⁶ Peroxide was measured colorimetrically with ferrous thiocyanate.¹⁷

Approximately 2-g. samples were sealed under vacuum (10^{-3} mm. Hg), air, or nitrogen. The dihydrate could not be sealed under vacuum, since it was converted to the monohydrate. The samples were then irradiated at -196 or -78°C . in the radiation pond facility at the Australian Atomic Energy Commission Research Establishment with ^{60}Co gamma rays at a dose rate of 500,000 rad/hr., measured by ferrous sulfate dosimetry, and corrected for absorption by the liquid nitrogen and for the different electron density of the monomer.

The irradiated samples were stored at -196°C . until the postirradiation polymerization runs were carried out in an oil bath in the temperature range 50 – 150°C . Samples were removed from the bath after various times, and the polymer was separated gravimetrically. The anhydrous zinc methacrylate was dissolved in methanol, the mixture centrifuged, and the monomer solution decanted from the insoluble polymer. No suitable differential solvent was found for the dihydrate, so the complete sample was dissolved in 1% w/v hydrochloric acid in methanol and the polymer precipitated as poly(methacrylic acid) by the addition of concentrated HCl. The polymer yields were measured after drying in a vacuum oven at 50°C . for 12 hr.

The gravimetric determination of polymer yield is valid only if negligible polymerization occurs during the dissolution process. In the present work the monomer dissolved rapidly, provided it was vigorously stirred, and no polymer was detected at zero time. Therefore, it is considered that the polymer yields obtained were reasonably accurate. However, it was found most important to crush large crystals to a fine powder, or inflated yields resulted from the increased time required for dissolution.

RESULTS

Anhydrous Zinc Methacrylate

Aging of Monomer

The rate of postirradiation polymerization of polycrystalline, anhydrous zinc methacrylate was found to vary widely with the history of the sample. This is shown in Figure 2, where the polymer yield after 24 hr. at 100°C . after 1 Mrad of gamma irradiation varies from 10 to 90%. There is a correlation between the polymer yield and the age of the sample. The wide scatter in the points was found to reflect different methods of storage;

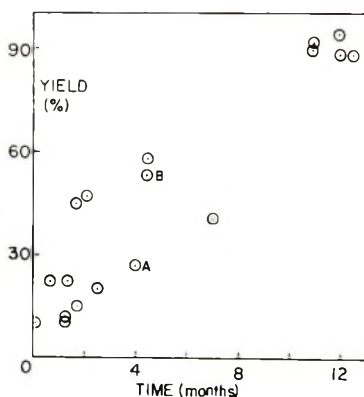


Fig. 2. Yield of polymer from anhydrous zinc methacrylate after 24 hr. at 100°C . following 1 Mrad of gamma irradiation, plotted against period of storage of monomer in air.

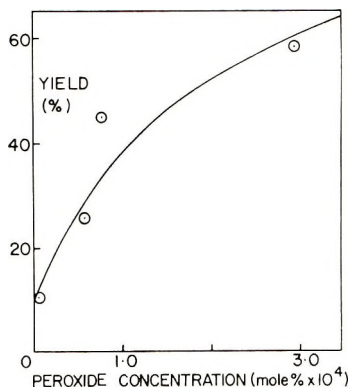


Fig. 3. Polymer yield from anhydrous zinc methacrylate after 24 hr. at 100°C. following 1 Mrad of gamma irradiation, plotted against peroxide content of monomer.

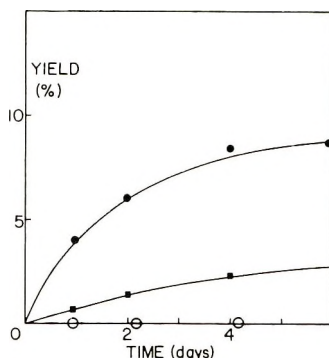


Fig. 4. Rate of thermal polymerization of anhydrous zinc methacrylate at 100°C.: (○) peroxide-free monomer; (■) monomer prepared and stored in air, age 3 days; (●) monomer prepared and stored in air, age 2 months.

higher yields resulted from storage in containers (*a*) with a large air space and (*b*) made of clear glass. The effect of air was especially marked if the samples were crushed; for example, a particular sample of crystals gave a yield of 27% after 16 weeks of storage (A in Fig. 2), but after being crushed to a fine powder and exposed to the air for a further 7 days it gave a yield of 50% (B in Fig. 2).

Peroxide formation was suspect as the cause of the enhanced rate of polymerization, and its presence was confirmed by colorimetric analysis with ferrous thiocyanate. A direct relationship between peroxide content of the monomer and postirradiation polymerization rate was observed and is illustrated in Figure 3. The measured peroxide content did not increase linearly with age, apparently because of thermal (and photolytic) decomposition, which produced some thermal polymerization, and up to 15% polymer was found in the samples stored for 1 year at room temperature (20°C.). The samples become yellow with age; this effect appeared to depend on the presence of air and was accelerated by light. The nature of

this change is unknown. Polymerization occurred in anhydrous zinc methacrylate after storage in air at 20°C. on heating to 100°C., as shown in Figure 4, and the rate of polymerization was related to the length of the storage period. This thermal polymerization apparently resulted from decomposition of the peroxides. The postirradiation polymerization measurements were made with samples of anhydrous zinc methacrylate prepared and stored in an atmosphere of oxygen-free nitrogen. These samples contained no peroxides and showed no thermal polymerization. However, a slight increase in polymerization rate with age was observed.

Polymerization Rate

Effect of Oxygen. The rates of polymerization of powdered samples in air and vacuum at 100°C. are given in Figure 5 and show very marked but

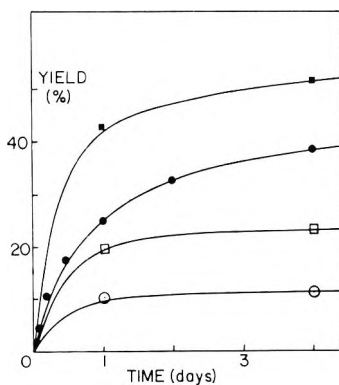


Fig. 5. Effect of oxygen on rate of polymerization of anhydrous zinc methacrylate at 100°C. after 1 Mrad of gamma irradiation. Oxygen during irradiation and during postirradiation heating, respectively: (■) present, absent; (●) absent, absent; (□) present, present; (○) absent, present.

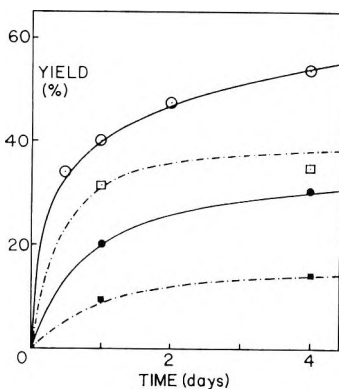


Fig. 6. Effect of crystal size on polymerization of anhydrous zinc methacrylate at 100°C. after 1 Mrad of gamma irradiation in vacuum: (○) large crystals heated in vacuum; (□) large crystals heated in air; (●) polycrystalline sample heated in vacuum; (■), polycrystalline sample heated in air.

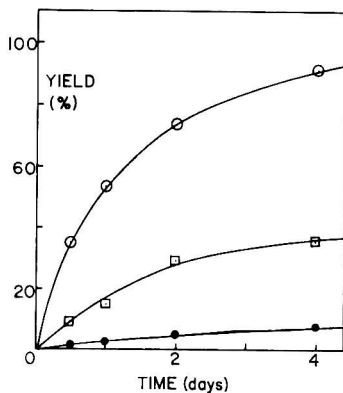


Fig. 7. Effect of temperature on polymerization of peroxide-free anhydrous zinc methacrylate after 1 Mrad of gamma irradiation at -196°C .: (○) 141°C .; (□) 100°C .; (●) 60°C .

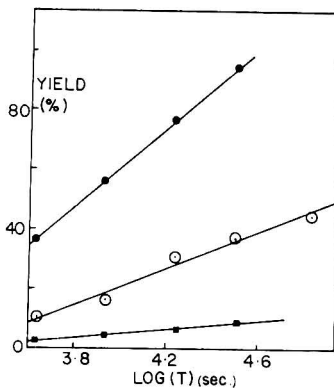


Fig. 8. Relationship between polymer yield and log time for polymerization of peroxide-free anhydrous zinc methacrylate after 1 Mrad of gamma irradiation at -196°C .: (●) 141°C .; (○) 100°C .; (■) 60°C .

separate effects of oxygen during (a) irradiation and (b) polymerization. The maximum rate was found in samples irradiated in air and polymerized in vacuum; the minimum rate, in samples irradiated in vacuum and polymerized in air. It is evident that oxygen increased the initiation rate but decreased the propagation rate.

Effect of Crystal Size. Powdered samples showed much lower rates of polymerization than large crystals, as shown in Figure 6. This effect was observed in samples (a) irradiated and heated under vacuum and (b) irradiated under vacuum and heated in air. The presence of air during polymerization decreased the rate for both large crystals and powdered samples.

Effect of Temperature. The rate of polymerization increased with temperature from 60 to 140°C ., as shown in Figure 7. A plot of log initial rate versus reciprocal temperature was linear, giving an apparent activation energy of 10 kcal./mole.

Linear relationships were obtained between yield and log time, as shown in Figure 8.

Zinc Methacrylate Monohydrate

No polymer was obtained from zinc methacrylate monohydrate after heating for 7 days at 50, 100, or 150°C. subsequent to 1 Mrad of gamma irradiation at -78 or -196°C .

Zinc Methacrylate Dihydrate

Effect of Air. Zinc methacrylate dihydrate could not be evacuated, owing to rapid dehydration to monohydrate. The net effect of air was observed by irradiating at -78°C . and heating at 100°C . samples which had been sealed under (a) nitrogen, (b) air, and (c) oxygen. Figure 9 shows that lower yields were obtained with increasing oxygen content.

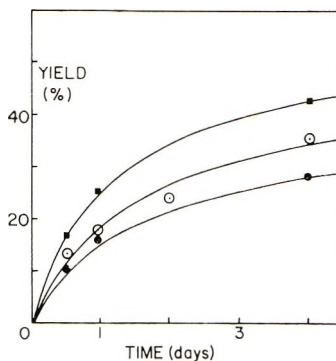


Fig. 9. Effect of oxygen on polymerization of zinc methacrylate dihydrate at 100°C . after 1 Mrad of gamma irradiation. Irradiated and polymerized in an atmosphere of: (■) nitrogen; (○) air; (●) oxygen.

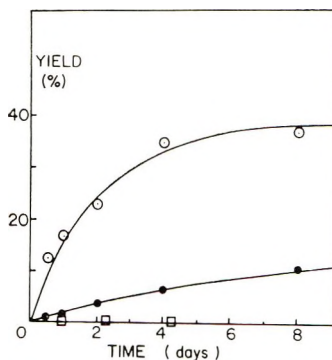


Fig. 10. Effect of temperature on polymerization of zinc methacrylate dihydrate: (○) 100°C ., postirradiation polymerization; (●) 100°C ., thermal polymerization; (◻) 50°C ., postirradiation polymerization. Irradiation: 1 Mrad of gamma irradiation at -78°C . in air.

Effect of Temperature. The yield of polymer from postirradiation polymerization was negligible at 50°C. and reached 40% in 4 days at 100°C. Thermal polymerization was negligible at 50°C. but gave 8% polymer in 4 days at 100°C. These results are shown in Figure 10. There was slow dehydration to the monohydrate at 50°C., and this would be expected to increase at 100°C. No monohydrate was produced at 100°C., although the rates of thermal and postirradiation polymerization were quite high. This suggests that at 100°C. polymerization occurs in association with the solid-state phase change, producing polymer instead of monohydrate.

Effect of Crystal Size. The yields of polymer from powdered zinc methacrylate dihydrate and from large crystals after postirradiation polymerization at 100°C. under a nitrogen atmosphere were the same.

DISCUSSION

Anhydrous Zinc Methacrylate

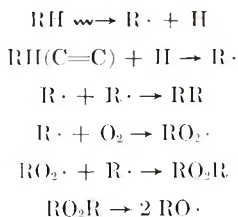
Aging

An outstanding feature of anhydrous zinc methacrylate is its sensitivity to oxygen before, during, and after irradiation. Such a remarkable increase in monomer reactivity due to the presence of air during storage has not been previously reported. Fadner and Morawetz¹⁸ noticed that the yield of polymer from the postirradiation polymerization of acrylamide did depend on the time and nature of storage, but they attributed this to annealing of defects. The formation of peroxide has been shown to be mainly responsible for this effect. The rate of peroxide formation was greatly enhanced by crushing of the crystals, suggesting that the reaction took place readily at the surface. Reduction in the particle size would also enhance the extent of diffusion of oxygen into the lattice, which must be the limiting factor in large crystals. Both the rate of diffusion of oxygen into the crystal and the rate of reaction at the surface must vary from one monomer to another; for example, Adler¹⁹ found that the electron spin resonance spectrum of acrylamide was unaffected by exposure to air at room temperature. We have not noticed any significant effect of storage in air on the rate of polymerization of barium methacrylate in the form of large crystals or of powder.

A likely explanation of the difference in behavior of the zinc and barium salts is the relative permeability of the lattice to oxygen, since a difference in reactivity of the double bond would not be expected. However, the effect would be expected to occur generally, the magnitude depending on the characteristics of the particular monomer. Caution should therefore be exercised in comparing rates of solid-state polymerization measured with samples of different ages or in accepting rates of any samples which have been stored in air.

Acceleration by Air

The marked increase in the rate of postirradiation polymerization of anhydrous zinc methacrylate when the monomer was irradiated in air suggests that oxygen reacts to increase the total radical concentration. Many of the initial radicals will be formed in localized areas or spurs during gamma radiolysis, and a high proportion of them would normally recombine immediately or subsequently on heating. However, when oxygen is present it may react with the initial radicals to form peroxy radicals. When recombination of radicals involving a peroxy radical does occur, the resultant peroxide will decompose thermally, giving two oxy radicals. Thus, the total number of radicals available for starting chains and, hence, the rate of initiation are increased. The reactions involved in initiation would be



This effect depends on the availability of oxygen in the lattice, which must be related to the permeability of the lattice and will obviously vary among monomers.

Inhibition by Air

Inhibition or retardation of free-radical polymerization by oxygen is well known in liquid-phase reactions. It is due to the addition of oxygen to radicals with a monomer end ($\text{R}\cdot$), forming peroxy radicals ($\text{RO}_2\cdot$), which have a lower reactivity with monomer and which disappear, causing the formation of nonradical products. The magnitude of the effect would be expected to vary with the nature of the monomer, the structure of the lattice, and the temperature. The present work has shown that oxygen decreases the rate of polymerization of anhydrous ZnMA. This suggests that propagation occurs by a free-radical mechanism. There is a reduction in the number of propagating radicals, i.e. inhibition, rather than in the radical reactivity, i.e. retardation, since ESR spectra showed that the total radical concentration of a sample irradiated in vacuum at -196°C . was decreased by about 30% on warming to 50°C . in vacuum but then disappeared within 10 min. when air was admitted.

Net Effect of Air

Obviously, the effect of oxygen on radiation-induced solid-state polymerization must be divided into the effects which occur (a) during irradiation and (b) during polymerization. These two effects would normally

oppose each other, and the net effect would depend on the permeability of the lattice to oxygen, the temperatures of irradiation and polymerization (affecting the rate of oxygen diffusion and reaction), and the crystal size of the monomer (determining the importance of initiation and retardation at the surface). Various effects of air on postirradiation polymerization rates have been reported; for example, Morawetz and his co-workers observed a slight decrease in acrylamide,¹⁸ no effect in barium methacrylate dihydrate,⁹ and an increase in butadiene-1-carboxylic acid.²⁰ Amagi and Chapiro²¹ found a decrease in a methyl methacrylate-paraffin oil mixture, but Chen and Grabar²² found an increase in tributylvinyl phosphonium bromide at 0°C. and a decrease at 30°C. A probable explanation of much of this variation is the failure of the investigators to separate the effects of oxygen during irradiation and during polymerization. Hayashi et al.²³ examined the separate effects in trioxane, but concluded that there was no difference between (a) irradiation and postpolymerization both carried out in air, (b) irradiation in vacuum and postpolymerization in air, and (c) irradiation in air and postpolymerization in vacuum, although the yield was markedly reduced if both irradiation and postpolymerization were carried out in vacuum. However, the mechanism in trioxane is uncertain, and there are possibly several competing processes.

Crystal Size

The rate of polymerization is markedly greater in large crystals than in polycrystalline samples after irradiation in vacuum, whether polymerization is carried out in vacuum or in air. Similar increased rates in large crystals have been observed for acetaldehyde²⁴ and trioxane,²⁵ but Fadner and Morawetz¹⁵ observed no effect from crushing acrylamide, although shock-frozen samples gave lower yields, probably because of a more imperfect crystalline structure. Charlesby² predicted that larger crystals should have a higher rate when the polymerization occurs preferentially in certain crystallographic directions.

Temperature

The observed increase in postirradiation polymerization rate with temperature is to be expected with free-radical polymerizations in the solid state. The apparent activation energy gives an indication of the temperature dependence of the rate but it has limited quantitative applications because it is not derived from rate constants. The kinetics of solid-state polymerization are not understood, and the reason for the linear plots of yield versus log time is unknown. However, the apparent activation energy of 10 kcal./mole is less than the values obtained from some other systems. Morawetz and his co-workers reported 17 kcal./mole for potassium acrylate⁸ and 25 kcal./mole for acrylamide.¹⁸

Zinc Methacrylate Monohydrate

Since both the anhydrous and dihydrate crystalline forms polymerized, the failure of the monohydrate to polymerize apparently is not due to the water of hydration. The metal ion and the organic molecule are the same in all cases, which suggests that the physical properties of the crystalline lattice must be responsible. Probably the spatial separation and orientation of the double bonds are the key factors, but the mobility of the molecules may also be important.

Zinc Methacrylate Dihydrate

The thermal and postirradiation polymerization of zinc methacrylate dihydrate is complicated by the dehydration reaction to the monohydrate. The reaction occurs rapidly under vacuum at ambient and higher temperatures and also takes place slowly in air. It is a transformation between two crystalline structures with the evolution of water, well below the melting point of the solid (the melting point of zinc methacrylate monohydrate, with decomposition, is about 220°C.) and can occur without the formation of polymer. At 100°C. irradiated samples polymerized without any formation of monohydrate, which strongly suggests that polymerization occurred concurrently with the phase change.

This is in agreement with the idea that the increased mobility of molecules during the disorder of phase transitions, including solid-solid transitions, is highly effective in promoting chemical reactions,^{11,26} including polymerization. It may well be that zinc methacrylate dihydrate is intrinsically nonpolymerizable, as is the monohydrate, and that polymerization can only take place at the phase change. This may apply to the reported polymerization of other monomer hydrates in the solid state. It has been postulated that the controlling factors for true crystalline chemical reaction are the separations of the atoms between which new bonds must be formed, for which a maximum of 4 Å. has been suggested,¹² and the spatial arrangement of the reactive sites. Further evidence is required in the methacrylate from detailed crystal structures.

The x-ray diffraction peaks of the irradiated dihydrate decreased during heating at 100°C., corresponding to the loss of monomer structure accompanying polymerization; this is shown in Figure 1. A shift in position, corresponding to a decrease in cell dimensions, of some of the dihydrate peaks also occurred, suggesting that polymerization was taking place within the monomer crystallites. New, large, broad peaks also appeared, which could not be attributed to the monohydrate or anhydrous salts. They may be due to an ordered structure in the polymer or to a new, unknown monomer form but it was not possible to distinguish between these alternatives.

CONCLUSIONS

The presence of air (*a*) before, (*b*) during, and (*c*) after irradiation affects the postirradiation polymerization of zinc methacrylate in the solid

state. Peroxide formation results in thermal polymerization and enhanced radiation-induced polymerization.

The crystal structure of the monomer is of critical importance; the polymerizability cannot be correlated with the nature of the metal ion or the degree of hydration and probably depends on the separation and orientation of double bonds.

The rate of polymerization is increased by air present during irradiation, apparently owing to a greater rate of initiation, resulting from enhanced trapping of radicals by reaction with oxygen. During polymerization air retards the propagation, as would be expected in free-radical propagation. Therefore, the overall effect of air obviously has little meaning, being the net result of two opposing effects, and a negligible effect of air on a solid-state polymerization obviously cannot be taken as evidence against a free-radical mechanism. The effect of air is further complicated by the importance of the permeability of the monomer to oxygen.

Dehydration of hydrated monomers may provide the molecular disorder and consequent mobility necessary for solid-state polymerization, even if the two crystalline forms do not have the requisite disposition of double bonds for crystalline polymerization.

We are pleased to acknowledge support for this work from the Australian Institute of Nuclear Science and Engineering. We should like to thank the Australian Atomic Energy Commission for carrying out the irradiations and the Geology Department of the University of Queensland for use of their x-ray diffraction facilities.

References

1. A. Chapiro, in *Macromolecular Chemistry, Paris, 1963* (*J. Polymer Sci. C*, **4**), M. Magat, Ed., Interscience, New York, 1964, p. 1551.
2. A. Charlesby, *Rept. Progr. Phys.*, **28**, 463 (1965).
3. H. Morawetz, *J. Polymer Sci. C*, **1**, 65 (1963).
4. S. Okamura, K. Hayashi, and Y. Kitanishi, *J. Polymer Sci.*, **58**, 925 (1962).
5. N. Morosoff, H. Morawetz, and B. Post, *J. Am. Chem. Soc.*, **87**, 3035 (1965).
6. A. Restaino, R. B. Mesrobian, H. Morawetz, D. S. Ballantine, C. J. Dienes, and D. J. Metz, *J. Am. Chem. Soc.*, **78**, 2939 (1956).
7. T. A. Fadner, I. D. Rubin, and H. Morawetz, *J. Polymer Sci.*, **37**, 549 (1959).
8. H. Morawetz and I. D. Rubin, *J. Polymer Sci.*, **57**, 669 (1962).
9. J. B. Lando and H. Morawetz, in *Macromolecular Chemistry, Paris, 1963* (*J. Polymer Sci. C*, **4**), M. Magat, Ed., Interscience, New York, 1964, p. 789.
10. L. S. Dent, F. P. Glasser, and H. F. W. Taylor, *Quart. Rev. (London)*, **16**, 343 (1962).
11. H. Morawetz, in *Physics and Chemistry of the Organic Solid State*, D. Fox, M. M. Labes, and A. Weissberger, Eds., Interscience, New York: Vol. 1, p. 287, 1963; Vol. 2, p. 853, 1965.
12. F. L. Hirshfeld and G. M. J. Schmidt, *J. Polymer Sci. A*, **2**, 2181 (1964).
13. A. Chapiro and M. Pertessis, *J. Chem. Phys.*, **61**, 991 (1964).
14. G. Adler and W. Reams, *J. Chem. Phys.*, **32**, 1698 (1960).
15. J. Mitchell and D. M. Smith, *Aquametry*, Interscience, New York, 1948, p. 19.
16. A. I. Vogel, *Quantitative Inorganic Analysis*, 3rd Ed., Longmans, London, 1961, p. 433.
17. F. Feigl, *Spot Tests in Organic Analysis*, Academic Press, New York, 1943, p. 534.
18. T. A. Fadner and H. Morawetz, *J. Polymer Sci.*, **45**, 475 (1960).

19. G. Adler, *U.S. At. Energy Comm., TID 7643*, 127 (1962).
20. H. Morawetz and I. D. Rubin, *J. Polymer Sci.*, **57**, 687 (1962).
21. Y. Amagi and A. Chapiro, *J. Chem. Phys.*, **59**, 537 (1962).
22. C. S. Chen and D. G. Grabar, in *Macromolecular Chemistry, Paris, 1963* (*J. Polymer Sci. C*, **4**), M. Magat, Ed., Interscience, New York, 1964, p. 849.
23. K. Hayashi, H. Ochi, and S. Okamura, *J. Polymer Sci. A*, **2**, 2929 (1964).
24. C. Chachaty, reported in M. Magat, *Polymer*, **3**, 449 (1962).
25. S. Okamura and K. Hayashi, *J. Chem. Phys.*, **59**, 429 (1962).
26. R. Bensasson, M. Durup, A. Dworkin, M. Magat, R. Marx, and H. Szwarc, *Discussions Faraday Soc.*, **36**, 177 (1963).

Received May 10, 1967

Revised September 7, 1967

Polymerization of Isocyanates. III. Chemical Behavior and Structure of Polyisocyanates

YOSHIO IWAKURA, KEIKICHI UNO, and NORIO KOBAYASHI,
*The Department of Synthetic Chemistry, Faculty of Engineering,
University of Tokyo, Bunkyo-ku, Tokyo, Japan*

Synopsis

The chemical behavior of polyisocyanates was investigated. Dissociation of the polymer to the monomer was observed directly by infrared spectra. Aminolysis of the polymer gave cyclic trimer and asymmetric urea as reaction products, and the formation of the latter was ascribed to the reaction of amine with the monomer dissociated from the polymer. It was concluded that polyisocyanates are composed of disubstituted amide structure only.

INTRODUCTION

Isocyanates were found by Shashoua and his co-workers¹ to undergo homopolymerization to high molecular weight polymers. Since then a number of studies on isocyanate polymerization have been reported, but there are few works on the chemical behavior of polyisocyanates. Shashoua found that the polymer was unstable and degraded when a solution of polymer in *N,N*-dimethylformamide (DMF) was allowed to stand overnight at room temperature in the presence of sodium cyanide.

In the present paper, the chemical behavior of polyisocyanates, especially toward amines, will be described. From the results and the infrared (IR) data it was concluded that the polymers have only a structure formed by opening of the carbon-nitrogen double bond, namely a disubstituted amide structure.

RESULTS AND DISCUSSION

Chemical Behavior of the Polymers

The reactions of aliphatic polyisocyanates with di-*n*-butylamine were examined in various conditions; the results are summarized in Table I. All the polymers recovered from the reaction mixture gave IR spectra identical with those of the original polymers. The inherent viscosity of the polymer recovered was not decreased even after 90% of the reaction, as shown in Figure 1. From these facts it would be reasonable to consider that the reaction of the polymer took place at the end of the polymer chain, and

TABLE I
 Reactions of Aliphatic Polyisocyanates with Di-*n*-butylamine

R	Polym., g.	Amine/polym., mole	Medium	Temp., °C.	Time, hr.	Polymer recovd., %	Prod., g.	Urea yield to tot. prod., %
<i>n</i> -C ₄ H ₉ -	1.2	2.9	DMF	30	70	100		
<i>n</i> -C ₄ H ₉ -	1.4	2.9	DMF ^b	30	26	0	Trimer ^c 1.1	
<i>n</i> -C ₄ H ₉ -	0.9	3.5	Acetone	reflux	55	78	Trimer, trace	
<i>n</i> -C ₄ H ₉ -	1.5	2.0	DMF	45	2 ^d	9 ^e	Trimer + urea ^f 1.4	9
<i>n</i> -C ₃ H ₇ -	1.3	3.1	DMF	30	75	100		
<i>n</i> -C ₃ H ₇ -	2.2	2.5	DMF ^b	30	65	0	Trimer ^g 2.1	
<i>n</i> -C ₃ H ₇ -	1.0	2.0	Benzene	reflux	8	97	Trimer, trace	
<i>n</i> -C ₃ H ₇ -	1.0	2.0	DMF	80-85	8	93	Trimer + urea ^h trace	8
<i>n</i> -C ₃ H ₇ -	1.0	2.0	Toluene	reflux	9	31	Trimer, 0.6	
<i>n</i> -C ₃ H ₇ -	1.0	2.0	DMF	reflux	3	0	Trimer + urea, 1.1	40

^a Calculated from relative intensity of carbonyl bands of trimers (near 1690 cm.⁻¹) and ureas (near 1630 cm.⁻¹).

^b A catalytic amount of sodium cyanide was present.

^c 1,3,5-Tri-*n*-butyl isocyanurate.

^d With continuous stirring.

^e Inherent viscosity of recovered polymer was 0.80; that of parent polymer, 0.82 (at a concentration of 0.5 g. per 100 ml. of benzene and at 30°C.).

^f *N,N',N''*-Tri-*n*-Butylurea.

^g 1,3,5-Tri-*n*-pentyl isocyanurate.

^h *N,N*-Di-*n*-butyl-*N',N'*-*n*-pentylurea.

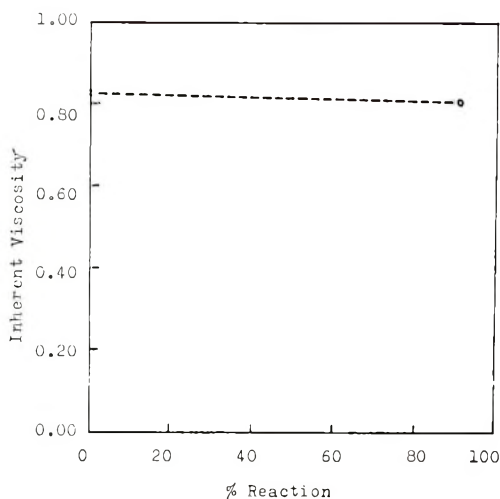


Fig. 1. Effect of reaction percentage on inherent viscosity of poly(*n*-butyl isocyanate) recovered.

it proceeded very fast along the polymer back bone. Reaction products were cyclic trimers (isocyanurates) and a small amount of asymmetric ureas (*N*-alkyl-*N'*,*N'*-di-*n*-butylureas). The ratio of the products was different according to the experimental conditions, and the yield of asymmetric ureas increased with temperature.

Aromatic polyisocyanates reacted more readily with di-*n*-butylamine. The reactions of poly(phenyl isocyanate) with the amine are listed in Table II. This polymer, which is insoluble in organic solvents, reacted completely at 100°C. in DMF within 5 hr. The amount of the amine consumed here was larger, if compared with the case of aliphatic polymers. Reaction products were also only a cyclic trimer and an asymmetric urea.

When a solution of some soluble aromatic polymer stood at room temperature, the appearance of isocyanate was observed by IR spectra; the

TABLE II
Reactions of Poly(phenyl Isocyanate) with Di-*n*-butylamine

Polym., g.	Amine/ polym.,		Temp., °C.	Time, hr.	Polym. re- covd., %	Prod., g.		Urea yield to tot. prod., %
	mole	Medium				Trim. ^a	Urea ^b	
1.61	3.2	DMF	30	53	0	0.62	1.00	44
2.32	5.7	DMF	30	28	0	1.00	1.40	43
2.00	2.0	Acetone	reflux	49	6.0	0.76	1.49	49
1.00	18.5	—	30	168	0	0.34	0.90	56
2.30	1.5	DMF	100	5	0	0.63	2.45	65

^a 1,3,5-Triphenyl isocyanurate.

^b *N,N*-Di-*n*-butyl-*N'*-phenylurea.

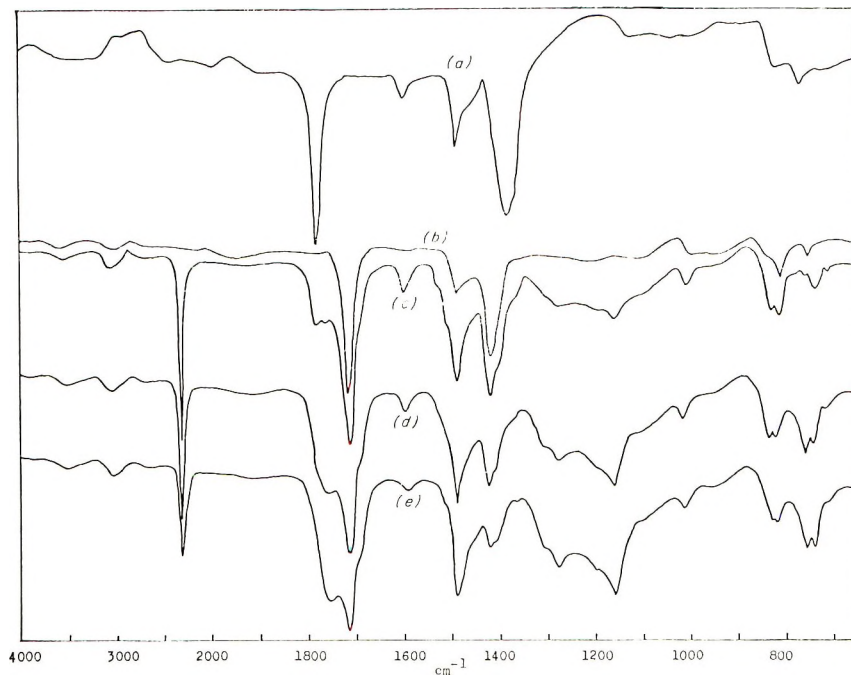
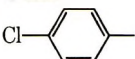
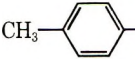
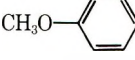


Fig. 2. IR spectra of poly(*p*-chlorophenyl isocyanate) in THF: (e) 10 min. after dissolving polymer; (d) 30 min. after dissolving polymer; (c) 80 min. after dissolving polymer; (b) trimer of *p*-chlorophenyl isocyanate; (a) dimer of *p*-chlorophenyl isocyanate.

qualitative results are shown in Table III. Polymers with an electron-donating group at the *p* position gave the characteristic absorptions of isocyanate only in DMF, the most basic solvent used. On the other hand, poly(*p*-chlorophenyl isocyanate) have the bands of isocyanate even in tetrahydrofuran (THF). The depolymerization of poly(*p*-chlorophenyl

TABLE III
Dissociation of Aromatic Polyisocyanates in Solution

R	Solvent ^a			
	Chloroform	THF	DMSO	DMF
	-	+		
	-	-	-	+
	-		-	+

^a Signs: +, appearance of $\nu_{\text{N}=\text{C}=\text{O}}$ observed; -, appearance of $\nu_{\text{N}=\text{C}=\text{O}}$ not observed.

isocyanate) was followed by IR spectra, as shown in Figure 2. As the absorptions of the polymer decreased, those of the monomer and the cyclic trimer increased. After 80 min. almost all of the polymer disappeared and the monomer, trimer, and a small amount of dimer remained. In the presence of an amine such a depolymerization reaction was accelerated. When triethylamine was added to a solution of poly(*p*-tolyl isocyanate) in dimethylsulfoxide (DMSO) in air, the viscosity of the solution decreased, and finally a cyclic trimer and a symmetric urea (*N,N'*-di-*p*-tolylurea), which would be formed by the reaction of the isocyanate with

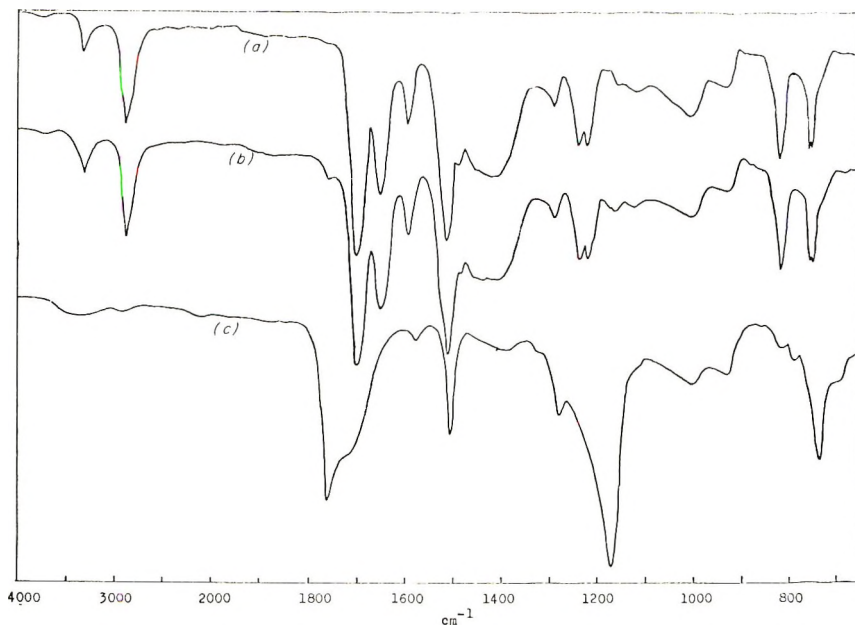
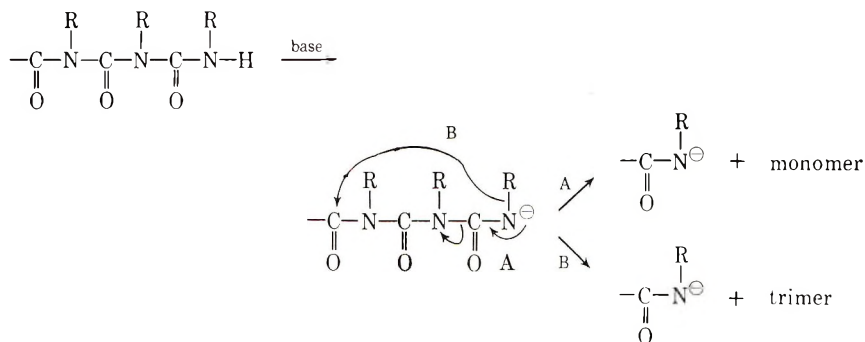


Fig. 3. IR spectra of poly(*p*-tolyl isocyanate) in DMSO: (c) before addition of di-*n*-butylamine; (b) 2 min. after addition of equimolar amount of di-*n*-butylamine; (a) 100 min. after addition of equimolar amount of di-*n*-butylamine.

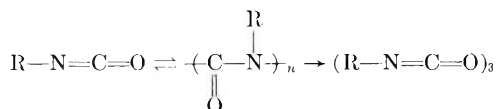
moisture, were obtained. A much faster reaction was observed between the polymer and an equimolar amount of di-*n*-butylamine. As shown in Figure 3, most of the bands characteristic of the polymer disappeared even 2 min. after the addition of the amine, and absorptions of cyclic trimer and asymmetric urea appeared.

From the results, the following may be considered. The depolymerization of polyisocyanates would be initiated by the abstraction of a proton at the end of the polymer chain, since basic substance, such as amines or DMF, accelerated the depolymerization, and the reaction rate of aliphatic polymers was smaller than that of aromatic polymers, according to the following scheme:



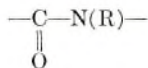
If a nitrogen anion is produced by the abstraction of the proton at the chain end, succeeding depolymerization will occur in two ways. The one is dissociation to isocyanate; this reaction is favored by the electron-withdrawing character of R. The other is degradative trimerization by an intramolecular attack of a nitrogen anion at the carbonyl carbon in the sixth position; this reaction is irreversible and seems to be favored by the electron-donating property of R.

Since isocyanate polymerizes at a low temperature with an anionic initiator and the polymer depolymerizes at room temperature to give monomer and cyclic trimer if a polymer anion is produced, there seems to be a ceiling temperature in the polymerization of isocyanate as in the anionic polymerization of α -methylstyrene.² However, in the case of the polyisocyanate there is an irreversible depolymerization to trimer in addition to a reversible one to monomer:



Chemical Structure of Polyisocyanates

The homopolymer of monoisocyanates depolymerized as described above. Consequently, the depolymerization products would reflect the structure of the polymer. They were symmetric trimers and monomers, and there were no asymmetric trimers and symmetric trimers with iminoacetal structure. Thus it could be concluded that the polymer is composed exclusively of a uniform repeating unit,



The IR spectra of the polymers and the trimers support such a configuration.

Aliphatic polymers gave a single carbonyl band at about 1700 cm^{-1} , as shown in Figure 4. On the other hand, aromatic polymers in Nujol mull afford some carbonyl bands, and these bands become single-peak in solution

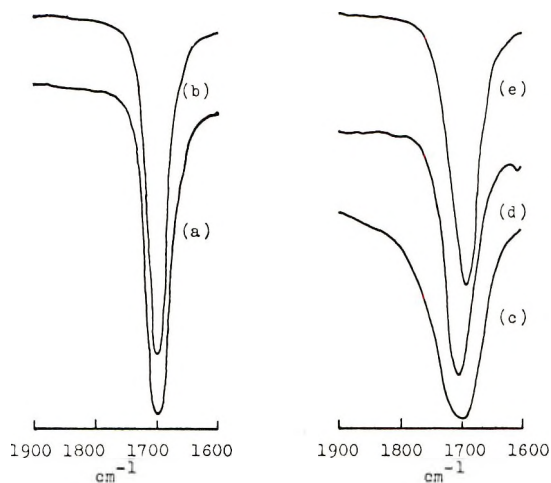


Fig. 4. IR spectra of aliphatic polyisocyanates: (a) *n*-butyl (film); (b) *n*-pentyl (film); (c) ethyl (in Nujol mull); (d) benzyl (in Nujol mull); (e) cyclohexyl (in Nujol mull).

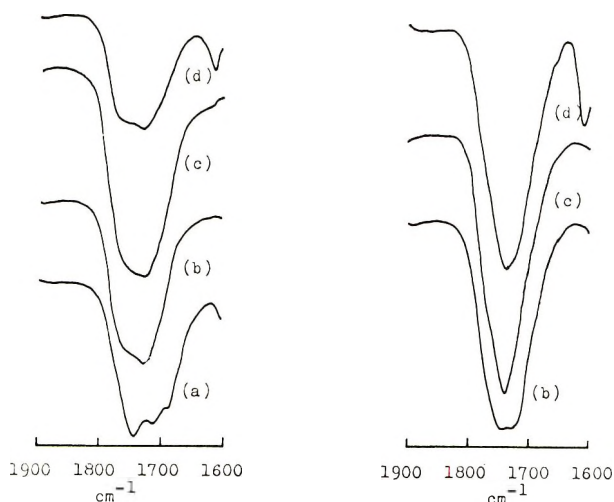
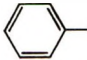
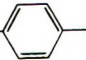
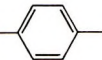
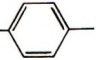


Fig. 5. IR spectra of aromatic polyisocyanates in (left) Nujol mull, (right) chloroform solution: (a) phenyl; (b) *p*-chlorophenyl; (c) *p*-tolyl; (d) *p*-methoxyphenyl.

(Figure 5). Aryl isocyanurates that are *p*-substituted gave three distinct absorptions around 1700 cm^{-1} in Nujol mull but only one band when in chloroform (Table IV). These findings would support that the polyisocyanates contain only one kind of repeating unit.

In the polymerization of isocyanates additions through either a carbon-nitrogen double bond or a carbon-oxygen double bond are possible, and both additions were expected by some workers.^{4,5} In an earlier paper⁶

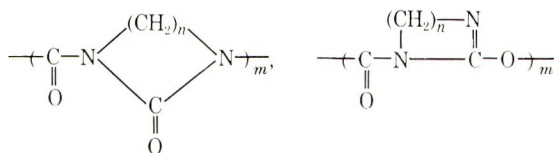
TABLE IV
 Carbonyl Bands of Triaryl Isoocyanurates

R	In Nujol mull, cm. ⁻¹	In KBr pellets, ^a μ	In chloro- form, ^b cm. ⁻¹
	1710	5.85	1705
CH ₃ - 	1765, 1715, 1690	5.63, 5.84, 6.17	1708
CH ₃ O- 	1765, 1715, 1690		1707
Cl- 	1770, 1715, 1690		1715

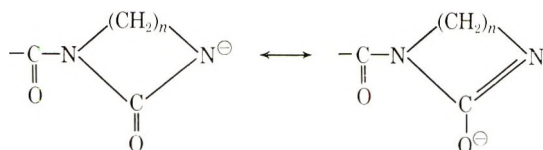
^a Data of Taub and McGinn.³

^b In 0.6% solution.

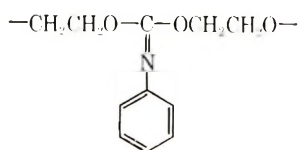
we proposed two kinds of repeating unit in the polymer of α,ω -polymethylene diisocyanates:



The formation of both units has been interpreted by the delocalization of a charge in the intermediate anion, and their ratio is affected by the ring size.



Recently Furukawa and his co-workers⁷ showed that the copolymer of phenyl isocyanate with ethylene oxide has an iminoacetal unit in the polymer chain. In this case the polymerization proceeded through coordinating anionic polymerization.



Although in the polymerization of isocyanates with the NaCN-DMF system units enchaind through carbon-oxygen bonds have been expected to some extent, it is suggested, from the structure of the polymers, that polymerization took place only through carbon-nitrogen double bonds.

EXPERIMENTAL

Materials

Isocyanates were synthesized from the corresponding carboxylic hydrazides and nitrous acid through the Curtius rearrangement. All the monomers were freshly distilled just before the polymerization reaction. Solvents and amines were purified by the usual methods. Sodium cyanide was obtained commercially.

Preparation of Polymers

The polymerization of monoisocyanates was carried out in DMF by using sodium cyanide as catalyst. The procedure was virtually the same as that given by Shashoua et al.¹ Since their polymerization procedure was inapplicable to *p*-chlorophenyl isocyanate because of its poor solubility in DMF at low temperature, the following modification was adopted.

Polymerization of *p*-Chlorophenyl Isocyanate. Into a cooled solution containing 50 ml. of DMF and 1 ml. of initiator solution a solution of 10 g. of monomer in 10 ml. of THF was added with vigorous stirring. The mixture became highly viscous immediately. After 10 min., methanol was added to quench the reaction. The precipitated polymer was filtered, washed with methanol, and dried under vacuum. The yield was 95%. The polymer was soluble in DMF, DMSO, THF, chloroform, and acetone, and was purified by reprecipitation from chloroform solution into methanol; m.p., 177–178°C. (decompd.). The inherent viscosity was 0.14 in chloroform at concentration 0.5 g. per 100 ml. and at 30°C.

ANAL. Calcd. for $(C_7H_4NOCl)_n$: C, 54.74%; H, 2.63%; N, 9.12%; Cl, 23.09%. Found: C, 54.71%; H, 3.09%; N, 9.27%; Cl, 22.63%.

Characterization of the Polymers

Inherent viscosity was measured at 30°C. in an Ostwald viscometer. The IR spectra were obtained by a double-beam Hitachi EPI-S2 IR spectrophotometer.

Reactions of Polyisocyanates with Di-*n*-butylamine

The reactions were carried out in various conditions; the results are summarized in Tables I and II. The following are typical reaction procedures.

Reaction of Poly(*n*-pentyl Isocyanate) with Di-*n*-butylamine. In a 100-ml. round-bottomed flask were placed 1.00 g. (0.00885 mole of *n*-pentyl isocyanate unit) poly(*n*-pentyl isocyanate), 2.38 g. (0.0177 mole) of di-*n*-butylamine, and 50 ml. of DMF. The mixture was kept at 80–85°C. for 8 hr., cooled, and then poured into 300 ml. of methanol. The precipitate was filtered, washed with methanol, and dried and gave 0.93 g. (93%) of the polymer. The filtrate was distilled under reduced pressures so as to remove the methanol, DMF, and di-*n*-butylamine. The residual pale-yellow viscous liquid was a mixture of 1,3,5-tri-*n*-pentyl isocyanurate and

N,N-di-*n*-butyl-*N'*-*n*-pentylurea. The ratio of the asymmetric urea to the total products was estimated at 8% from IR spectra of the residue.

Reaction of Poly(phenyl Isocyanate) with Di-*n*-butylamine. A mixture of 1.61 g. (0.0136 mole of phenyl isocyanate unit) of poly(phenyl isocyanate), 5.81 g. (0.0435 mole) of di-*n*-butylamine, and 50 ml. of DMF was kept at 30°C. for 53 hr. and then poured into 300 ml. of methanol. No precipitation was observed. After removal of methanol, DMF, and di-*n*-butylamine by distillation under reduced pressure pale-yellow crystals were obtained. They were treated with 50 ml. of ether and gave 0.75 g. of a 1:1 complex of 1,3,5-triphenyl isocyanurate with DMF.⁸ It was recrystallized from methanol to 1,3,5-triphenyl isocyanurate; m.p., 280°C. The ethereal filtrate was distilled for removal of ether and then treated with 50 ml. of water so that 1.00 g. of cottonlike needles of *N,N*-di-*n*-butyl-*N'*-phenylurea precipitated; m.p., 83°C. (from methanol-water).

References

1. V. E. Shashoua, W. Sweeny, and R. F. Tietz, *J. Am. Chem. Soc.*, **82**, 866 (1960).
2. V. Vrancken, J. Smid, and M. Szwarc, *J. Am. Chem. Soc.*, **83**, 2772 (1961).
3. B. Taub and C. E. McGinn, *Dyestuffs*, **42**, 266 (1958).
4. G. Natta, J. Di Pietro, and M. Cambini, *Makromol. Chem.*, **56**, 200 (1962).
5. N. S. Schneider, S. Furusaki, and R. W. Lenz, *J. Polymer Sci. A*, **3**, 933 (1965).
6. Y. Iwakura, K. Uno, and K. Ichikawa, *J. Polymer Sci. A*, **2**, 3387 (1964).
7. J. Furukawa, S. Yamashita, M. Maruhashi, and K. Harada, *Makromol. Chem.*, **85**, 80 (1965).
8. Y. Iwakura, K. Uno, and N. Kobayashi, *Bull. Chem. Soc. Japan*, **39**, 2551 (1966).

Received April 25, 1967

Revised July 12, 1967

Aromatic Polydiketopiperazines

YOSHIO IWAKURA, SHIN-ICHI IZAWA, and FUSAKAZU HAYANO,
*Department of Synthetic Chemistry, Faculty of Engineering,
 University of Tokyo, Tokyo, Japan*

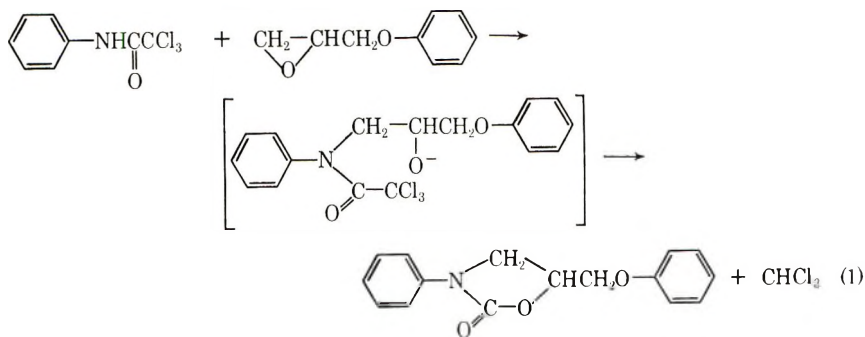
Synopsis

Aromatic polydiketopiperazines have been prepared from bis-2-chloroacetamides of aromatic diamines in the presence of an epoxide as HCl acceptor and a quaternary ammonium halide catalyst. The structures of the polymers were characterized by infrared and NMR spectra. These polymers were soluble in organic acids such as formic acid, dichloroacetic acid, and trifluoroacetic acid but insoluble in common organic solvents such as dimethylformamide, dimethylacetamide, and dimethyl sulfoxide. Thermogravimetric analysis indicated that these polymers decomposed at 300–340°C.

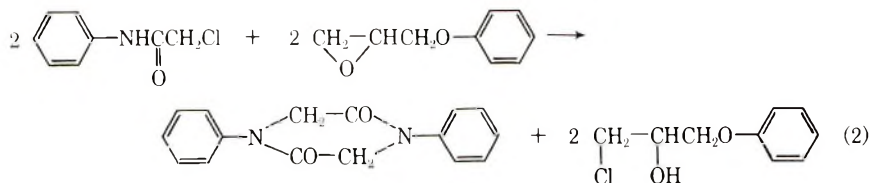
INTRODUCTION

Aliphatic polydiketopiperazines were prepared from hexamethylenebis(iminoacetic acid) by Allen and Drewitt.¹ However, there has been no study reported to date on aromatic polydiketopiperazines.

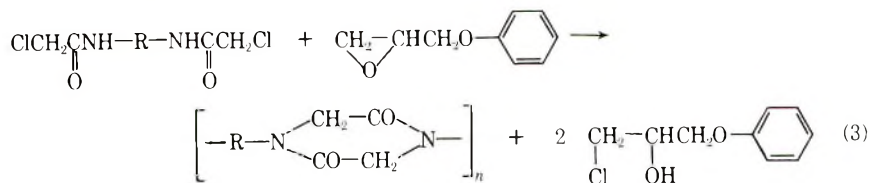
In our previous paper on the reaction of aromatic urethans and ureas with phenyl glycidyl ether, formation of the 2-oxazolidone ring was reported.² 2,2,2-Trichloroacetanilide was also found to form 2-oxazolidone through C—C bond cleavage in the trichloroacetyl group, as a result of the strong electron-withdrawing property of CCl₃.³



On the contrary, 2-chloroacetanilide was found to give *N,N'*-diphenyldiketopiperazine as a major product in the presence of phenyl glycidyl ether and quaternary ammonium halide [eq. (2)]. Phenyl glycidyl ether acted as an HCl acceptor in this reaction.



The present study describes the formation of polydiketopiperazines from bis(2-chloroacetamides) of aromatic diamines as an extension of reaction (2).



EXPERIMENTAL

Monomers

Monomers were prepared from various aromatic diamines and 2-chloroacetyl chloride by the method reported by Phillips and Wnuek.⁴ Yields, melting points, and analytical data are listed in Table I.

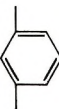
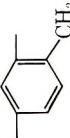


Commercially available phenyl glycidyl ether was used after purification by distillation.

Polycondensation

Polycondensation in Dimethylacetamide. In an ampule were put 0.783 g. (0.003 mole) of *N,N'*-*m*-phenylenebis(2-chloroacetamide), 0.990 g. (0.0066 mole) of phenyl glycidyl ether, 0.07 g. (0.0003 mole) of triethylbenzylammonium chloride, 0.224 g. of lithium chloride, and 5 ml. of dimethylacetamide. The ampule was flushed with nitrogen and sealed. After heating of the mixture at 100°C. for 50 hr. it was poured into 200 ml. of acetone. The precipitated polymer was collected by filtration and washed with 50 ml. of methanol to remove catalyst. The isolated polymer was washed with acetone in a Soxhlet extractor for 6 hr. and dried at 100°C. in vacuum for 6 hr. to give 0.317 g. (56%) of polydiketopiperazine. The inherent viscosity was 0.12 (0.5 g./100 ml. in dichloroacetic acid at 30°C.).

Polycondensation in Phenyl Glycidyl Ether. An ampule was charged with 0.738 g. (0.0028 mole) of *N,N'*-*m*-phenylenebis(2-chloroacetamide), 0.137 g. (0.0006 mole) of triethylbenzylammonium chloride, and 10 ml. of phenyl glycidyl ether. The ampule was sealed and heated at 150°C. After heating for 1 hr. the reaction mixture was poured into 200 ml. of acetone. The precipitated polymer was isolated in the same way as described above. It weighed 0.421 g. (79%). The inherent viscosity was 0.21 (0.5 g./100 ml. in dichloroacetic acid at 30°C.).

TABLE I
 Bis(2-chloroacetamides) $\text{ClCH}_2\text{CNH}-\text{R}-\text{NHCCl}_2$

R	Yield, %	Melting point, °C.	C, %		H, %		N, %	
			Calcd.	Found	Calcd.	Found	Calcd.	Found
	85	217-218	45.00	45.99	3.86	3.87	10.73	10.50
	56	218-219	48.02	47.81	4.40	4.31	10.18	9.81
	68	234-235 (dec.)	58.13	58.20	4.59	4.74	7.98	8.10
	81	187-189	47.89	45.45	3.52	3.95	6.98	6.63

^a Very hygroscopic.

Polycondensation in Phenyl Glycidyl Ether with Stirring. In a 50-ml. three-necked flask equipped with a mechanical stirrer and reflux condenser 1.053 g. (0.003 mole) of 4,4'-bis(2-chloroacetamido)diphenylmethane was dissolved in 10 ml. of phenyl glycidyl ether at 180°C. To the solution was added 0.227 g. (0.001 mole) of triethylbenzylammonium chloride. The mixture was heated for 1 hr. and poured into 200 ml. of acetone. The precipitated polymer was isolated as above and found to weigh 0.591 g. (71%). The inherent viscosity was 0.33 (0.5 g./100 ml. in dichloroacetic acid at 30°C.).

Model Compounds

***N,N'*-Diphenyldiketopiperazine.** A mixture of 3.392 g. (0.02 mole) of 2-chloroacetanilide, 6.000 g. (0.04 mole) of phenyl glycidyl ether, and 0.454 g. (0.002 mole) of triethylbenzylammonium chloride was heated at 180°C. for 1 hr. A crystalline product was filtered and washed with 5 ml. of methanol to give 1.866 g. (70%) of *N,N'*-diphenyldiketopiperazine. It was recrystallized from acetone; m.p. 263–264°C. (lit. m.p.: 265–267°C.⁵ 273–275°C.⁶).

ANAL. Calcd. for C₁₆H₁₄O₂N₂: C, 72.16%; H, 5.30%; N, 10.52%. Found: C, 72.14%; H, 5.29%; N, 10.40%.

The filtrate was evaporated under reduced pressure of 2 mm. Hg to remove excess phenyl glycidyl ether and a part of the 1-chloro-2-hydroxy-3-phenoxypropane. To the residual mixture were added 5 ml. of acetic anhydride and 4 ml. of pyridine, and this was allowed to stand overnight at room temperature. Pyridine and acetic anhydride were removed under reduced pressure, and the residue was distilled in vacuum to give 1.36 g. of 1-chloro-2-acetoxy-3-phenoxypropane, b.p. 106–110°C./0.25 mm. Hg, and a viscous oil, b.p. 190°C./0.25 mm. Hg. The viscous oil gave crystals from isopropyl ether, 0.244 g. (4.3%) of 3-oxo-4-phenyl-6-phenoxyethylmorpholine; m.p. 99–100°C.

ANAL. Calcd. for C₁₇H₁₇O₃N: C, 72.06%; H, 6.05%; N, 4.94%. Found: C, 71.87%; H, 6.26%; N, 4.83%.

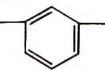
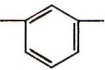
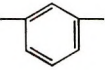
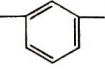
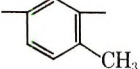
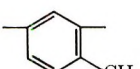
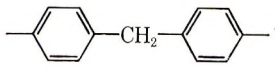
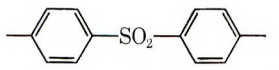
RESULTS AND DISCUSSION

Polycondensation

The results of the polycondensation reactions are summarized in Table II. The polycondensation reaction of these monomers in dimethylacetamide in the presence of a catalytic amount of triethylbenzylammonium chloride and equimolar amount of phenyl glycidyl ether did not give high molecular weight polymer even if the reaction was carried out at high temperature for a long period. On the contrary, the reaction in excess phenyl glycidyl ether without solvent gave relatively high molecular weight polymers in a short period. The polymers obtained were yellowish-brown

TABLE II

Polydiketopiperazines $\left[-R-N \begin{array}{l} \diagup \text{CH}_2-\text{CO} \\ \diagdown \text{CO}-\text{CH}_2 \end{array} N- \right]_n$

R	Solvent	Reaction temp., °C.	Time, hr.	Yield, %	η_{inh}^a
	DMAc ^b	100	50	56	0.12
	"	160	50	60	0.14
	PGE ^c	140	1	75	0.21
	"	180	1	71	0.21
	DMAc ^b	160	50	37	0.13
	PGE ^c	180	2	68	0.18
	"	180	1	71	0.33
	"	180	1	63	0.18

^a Measured at a concentration of 0.5 g./100 ml. in dichloroacetic acid at 30°C.

^b Dimethylacetamide containing 5 wt.-% lithium chloride.

^c Phenyl glycidyl ether.

powders, soluble in organic acids such as formic acid, dichloroacetic acid, and trifluoroacetic acid but insoluble in common organic solvents such as dimethylformamide, dimethylacetamide, and dimethyl sulfoxide.

The infrared spectra of the model compound (*N,N'*-diphenyldiketopiperazine), the monomer [*N,N'*-*m*-phenylenebis(2-chloroacetamide)], and the polymer prepared from it are shown in Figure 1. Absorption bands at 3350 cm^{-1} (NH stretching) and 1550 cm^{-1} (NH deformation) of the monomer disappeared in the polymer. The broad absorption in the spectrum of the polymer around 3300 cm^{-1} was attributed to water which adsorbed in the polymer.

The NMR spectra of the polydiketopiperazine prepared from *N,N'*-*m*-phenylenebis(2-chloroacetamide) and the model compound, *N,N'*-diphenyldiketopiperazine, have singlet signals at τ values of 5.14 and 5.20, respec-

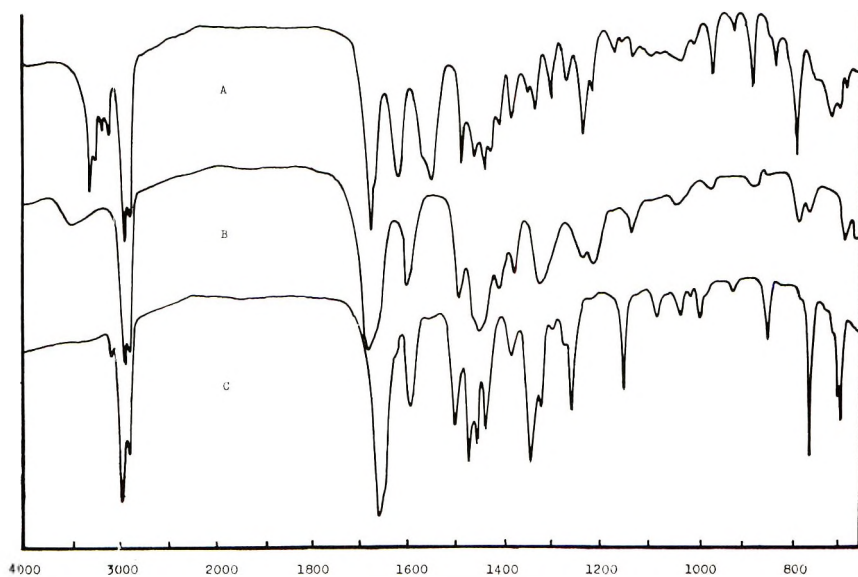
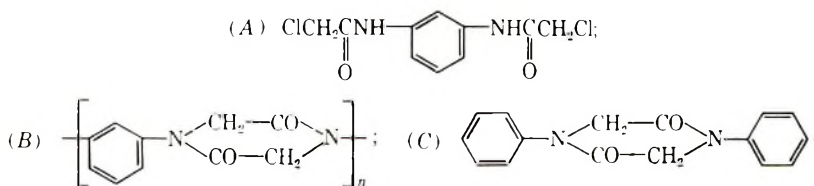


Fig. 1. Infrared spectra of the monomer, polymer, and model compound:



tively, which were assigned to methylene proton in diketopiperazine rings (Fig. 2). Weak absorptions at 5.3–6.0 τ in the polymer were attributed to the polymer endgroups as discussed below.

Although the polycondensation reaction was accelerated in excess phenyl glycidyl ether, high molecular weight polymer was not obtained, presumably because of some side reaction of the 2-chloroacetamide group with phenyl glycidyl ether and/or the poor solubility of polymers in phenyl glycidyl ether. Figure 3 shows that yield and inherent viscosity of polydiketopiperazine derived from *N,N'*-*m*-phenylenebis(2-chloroacetamide) were not improved in reactions at 150 and 180°C. in spite of prolonged reaction time. At these temperatures, polymer began to precipitate within a few minutes. Consequently, the low molecular weight of the polymer obtained here might be a result of its insolubility. On the other hand, the polymer derived from *N,N'*-2,4-tolylenebis(2-chloroacetamide) did not precipitate during the polymerization, but the inherent viscosity of the polymer was not very high. These results seem to indicate the presence of some side reactions which prevent chain growth. In a previous paper,³ the reaction of 2,2,2-trichloroacetanilide with phenyl glycidyl ether was described [eq. (1)]. This reaction suggests the occurrence of a similar reaction between

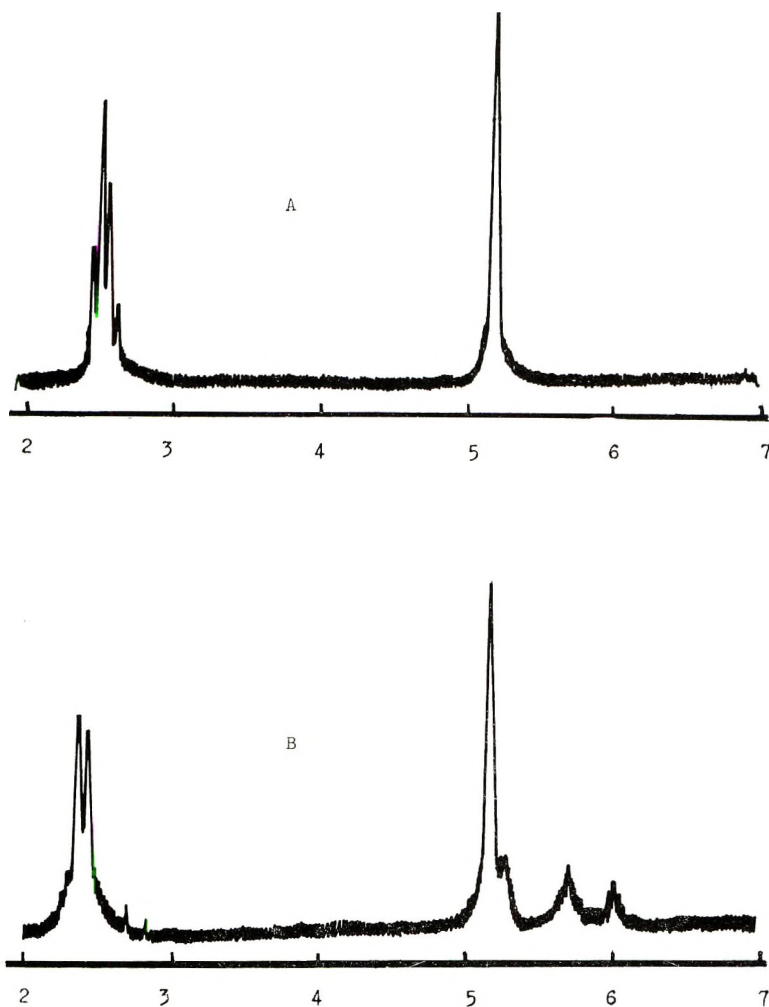
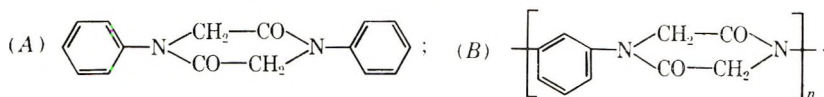


Fig. 2. NMR spectra in trifluoroacetic acid at 70°C. (60 Mc.):



2-chloroacetamide group and phenyl glycidyl ether. Such a reaction would destroy the functional group for chain growth and would result in a low molecular weight of the polymer.

As mentioned above, there is the possibility of an addition reaction of 2-chloroacetanilide with phenyl glycidyl ether, so the reaction of 2-chloroacetanilide with phenyl glycidyl ether was reinvestigated. The reaction was carried out with excess phenyl glycidyl ether and catalytic amount of triethylbenzylammonium chloride at 180°C. for 1 hr. *N,N'*-Diphenyldiketopiperazine was obtained as crystals (70%). After separating the

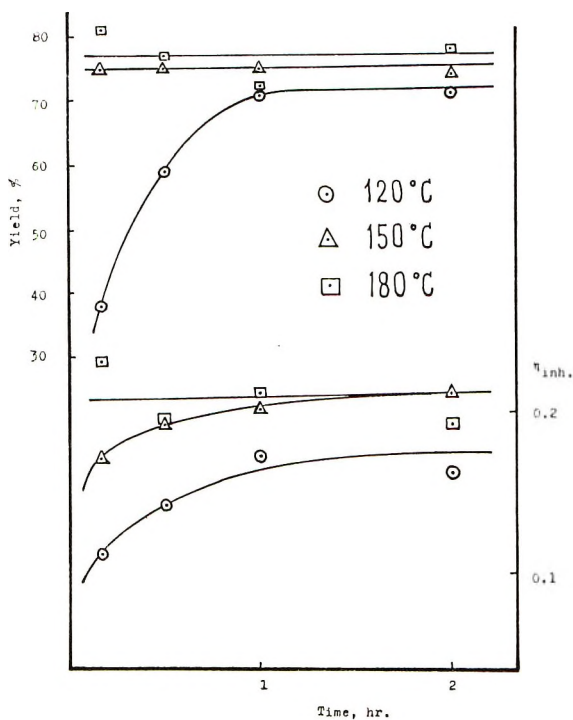


Fig. 3. Effect of reaction time and temperature.

crystals, excess phenyl glycidyl ether was removed under reduced pressure, and the residual liquid was acetylated with acetic anhydride and pyridine. The distillation of the reaction product under reduced pressure gave compound II which was derived from 2-chloroacetanilide and phenyl glycidyl ether in 4% yield, in addition to 2-acetoxy-1-chloro-3-phenoxypropane (IV)

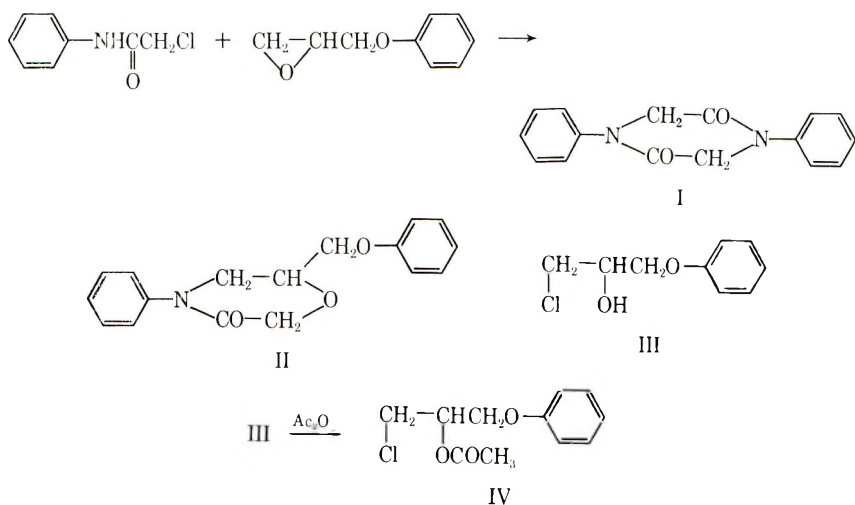
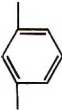
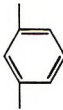
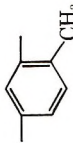




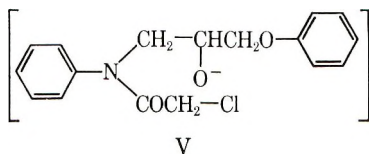
TABLE III
Elemental Analyses of Polymers^a

R	Reaction temp., °C.	Time, hr.	η_{inh}	C, %	H, %	N, %	C/N
	120	1/6	0.11	59.27	4.88	13.22	4.48
	150	2	0.21	63.02	5.08	12.31	5.12
	180	1	0.16	64.88	5.90	10.31	6.28
	180	1	0.33	72.01	5.74	8.74	8.24
	180	1	0.18	60.50	4.77	6.50	9.30

^a Calculated for polydiketopiperazine, $\left[-R-N \begin{array}{c} \text{CH}_2-CO \\ \diagup \quad \diagdown \\ N- \\ \diagdown \quad \diagup \\ CO-CH_2 \end{array} \right]_n$; *m*-Phenylene(C₁₀H₈O₂N₂): C, 63.82%; H, 4.29%; N, 14.89%; C/N, 4.29.

2,4-Tolylene(C₁₁H₁₀O₂N₂): C, 65.33%; H, 4.98%; N, 13.86%; C/N, 4.71. Diphenylmethane(C₁₇H₁₄O₂N₂): C, 73.36%; H, 5.07%; N, 10.07%; C/N, 7.28. Diphenylsulfone(C₁₆H₁₂O₄N₂S): C, 58.53%; H, 3.68%; N, 8.53%; C/N, 6.87.

The addition product (II), 3-oxo-4-phenyl-6-phenoxyethylmorpholine, was considered to be formed through an intermediate (V) similar to that through which 2-oxazolidone was formed from 2,2,2-trichloroacetanilide and phenyl glycidyl ether [eq. (1)]:



The NMR spectrum of the addition product (II) has the signals at 5.29, 5.73, and 5.9–6.2 τ . These signals correspond to the signals at 5.28, 5.67, and 6.0 τ of the polymer.

Moreover, elemental analysis of the polymer indicates the occurrence of an addition reaction of the polymer end with phenyl glycidyl ether. If the polymers were formed merely by repeated condensation of the 2-chloroacetamide group, the ratio of carbon content to nitrogen content (C/N) would be constant. However, if addition of the polymer end to phenyl glycidyl ether occurred, this ratio would increase. The analytical data for some polymers (Table III) show values of C/N larger than the calculated value; this coincides with the results of NMR, and confirms the consideration of the side reaction described above as a cause of termination of polycondensation.

Thermal Stability

The thermal stability of the polydiketopiperazines in nitrogen atmosphere and in air was determined by the thermogravimetric analysis; the

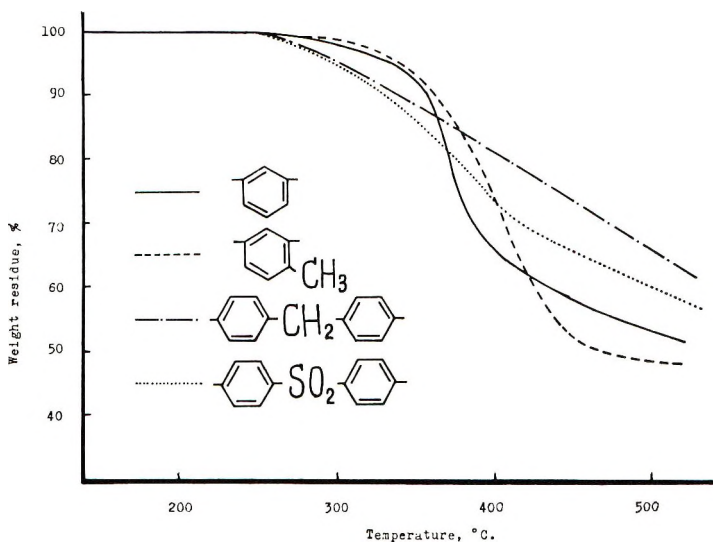


Fig. 4. Thermogravimetric analysis curves for polydiketopiperazines in N_2 atmosphere.

curves are shown in Figures 4 and 5. In nitrogen, *m*-phenylene and tolylene derivatives showed different curves from diphenylmethane and diphenylsulfone derivatives; the former showed minor weight loss below

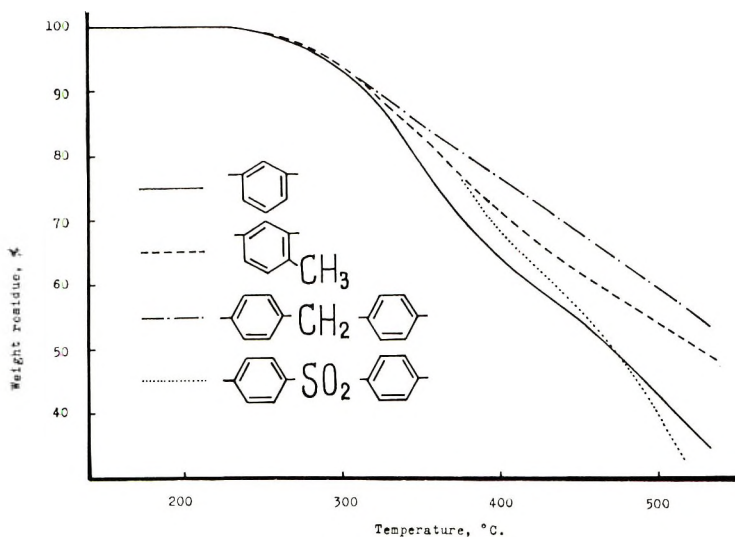


Fig. 5. Thermogravimetric analysis curves for polydiketopiperazines in air.

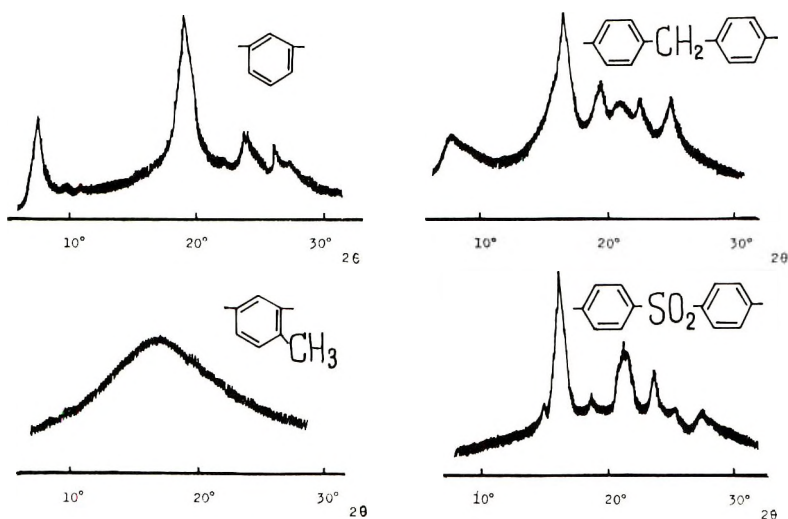


Fig. 6. X-ray diffraction pattern of polydiketopiperazines with Ni-filtered $\text{CuK}\alpha$ radiation.

340°C. and abrupt weight loss above 340°C., the latter began to show weight loss below 300°C., but the decomposition proceeded slowly. In air this difference was not observed, and the polymers decomposed below 300°C. exothermally.

Crystallinity

The x-ray diffraction diagrams of polydiketopiperazine shown in Figure 6 were obtained by the powder method with the use of nickel-filtered $\text{CuK}\alpha$ radiation. The diagrams indicate that the polydiketopiperazines are crystalline except for the tolylene derivative, which did not precipitate in polymerization.

References

1. S. T. Allen and J. G. Drewitt, Brit. Pat., 610,304 (Oct. 14, 1948).
2. Y. Iwakura and S. Izawa, *J. Org. Chem.*, **29**, 379 (1964).
3. Y. Iwakura and S. Izawa, *Bull. Chem. Soc. Japan*, **39**, 2490 (1966).
4. A. P. Phillips and A. L. Wnuck, U.S. Pat. 2,759,941 (Aug. 21, 1956).
5. F. Wessely, H. Pawloy, and W. Rizzi, *Monatsh.*, **86**, 75 (1955).
6. C. E. Cosgrove and R. A. La Forge, *J. Org. Chem.*, **21**, 197 (1956).

Received July 18, 1967

Revised August 25, 1967

Radiation-Induced Polymerization of Isoprene in Aqueous Solution of Silver Nitrate

SYUJI FUJIOKA, TADAO ICHIMURA, and
YASUO SHINOHARA, *Central Research Laboratories,
Toyo Rayon Co., Ltd., Sonoyama Otsu-shi, Japan,* and
KOICHIRO HAYASHI, *Faculty of Engineering, Kyoto University,
Yoshida, Sakyo-ku, Kyoto, Japan*

Synopsis

The rate of radiation-induced polymerization of isoprene in aqueous solution of silver nitrate is 20-50 times as fast as the rate of radiation-induced polymerization of pure isoprene. The formation of a 1:2 complex of isoprene and silver nitrate was confirmed spectrometrically, and this complex seems to polymerize by attack of an active species. The equilibrium constant K_f and the extinction coefficient E of the complex were estimated to be 0.18 and 1.4, respectively. The polymerization mechanism was concluded to be a radical one, based on the effects of inhibitors. The polyisoprene obtained had a crosslinked structure, was insoluble, and did not give a distinct melting point. The 1,2 structure was the predominant polyisoprene configuration. This was interpreted on the basis of the frontier electron density of isoprene.

INTRODUCTION

It has previously been reported that polymerization of ethylene occurred in aqueous solutions of silver nitrate by both catalytic¹ and radiation-induced² reactions. The polymerization rates reported in these literature reports are very fast; in the radiation polymerization the G value (absolute number of ethylene molecules polymerized per 100 e.V.) is 1,000,000.

It is assumed that ethylene and silver cation form a 1:1 complex in the aqueous solution and that this complex takes part in the polymerization. It is well known that ethylene forms complexes³ with various metal ions. Ohdan et al.⁴ reported that the polymerization of acrylonitrile is accelerated by the presence of silver nitrate. Sumitomo et al.⁵ obtained a complex of zinc chloride and acrylonitrile and attempted radiation polymerization of this complex. Yamashita et al.⁶ reported the polymerization of butadiene in the presence of various metal salts and inorganic complexes, and investigated the microstructure of the polymer obtained. It is interesting that Kraus and Stern⁷ reported that butadiene and silver cation form an intermolecular crosslinking type complex.

It is very interesting that the monomer-metal ion complexes are reported to form before polymerization and take part in the polymerization reaction at quite a high rate.

The objects of this paper are to clarify the quantitative relationships between the complex and the polymerization rate, and between the complex and the microstructure of polymer obtained in the system isoprene-silver nitrate.

EXPERIMENTAL

Polymerization Procedure

Silver nitrate (reagent grade) was obtained commercially. Isoprene was distilled by use of a Widmer distiller column. A typical experiment was carried out as follows. Given amounts of aqueous silver nitrate solution and isoprene were added to an L-type ampule. Water was then added to the monomer mixture to a total volume of 15 ml. The L-type ampule was used in this experiment in order to prevent the ampule from rupture by solidification of water during the degassing procedure. The L-type ampule was connected to the vacuum line and was cooled with liquid nitrogen. Degassing was repeated twice by a solidifying-melting method, and then the ampule was sealed under vacuum (10^{-3} mm. Hg). All irradiations were performed with a 800 c. ^{60}Co source. The reaction temperature was automatically maintained constant within $\pm 1^\circ\text{C}$. during the reaction. Immediately after the polymerization reaction, the ampule was opened. The polymer obtained was washed with water and dried to a constant weight in vacuum at room temperature. Dosimetry was performed by the ferrous-ferric dosimeter method.

Polymer Analysis

Since the polymer obtained includes silver nitrate, the latter was determined quantitatively; the polymerization yield was then calculated for pure polyisoprene. The analytical method of for silver nitrate was as follows. Washed and dried polymer was first burned completely in a platinum crucible. The residue was dissolved in 10 ml. of 5*N* nitric acid, diluted with water, and silver chloride precipitated by adding a slight excess of aqueous saturated NaCl solution. The silver content thus calculated is on the basis of the amount of silver chloride precipitated.

Optical Measurement

The ultraviolet and visible light absorption spectra of an isoprene-silver nitrate aqueous solution were obtained with the Hitachi ultraviolet spectrophotometer. The infrared absorption spectrum of a polymer was obtained by the KBr disk method.

RESULTS

Influence of Isoprene and Silver Nitrate Mole Ratios

The polymer yield as a function of the irradiation time at a silver nitrate concentration of 5.32 mole/l. and isoprene concentrations of 1.33, 0.67,

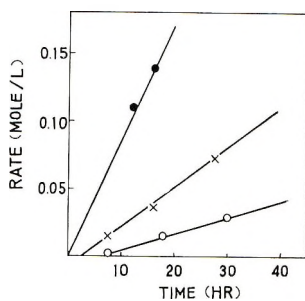


Fig. 1. Effect of mole ratio of silver nitrate and isoprene on polymerization rate at various isoprene concentrations: (●) 1.33 mole/l. (×) 0.67 mole/l.; (○) 0.33 mole/l.; $[\text{Ag}^+]$, 5.32 mole/l.; temperature, 30°C.; dose rate, 0.78×10^4 r/hr.

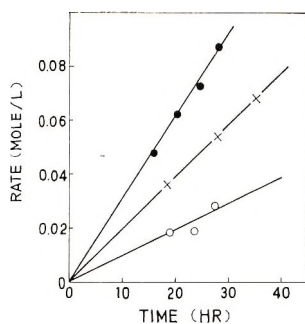


Fig. 2. Effect of mole ratio of silver nitrate and isoprene on polymerization rate at various $[\text{Ag}^+]$: (●) 4.00 mole/l.; (×) 2.67 mole/l.; (○) 1.33 mole/l.; [isoprene], 0.67 mole/l.; temperature, 30°C.; dose rate, 0.78×10^4 r/hr.

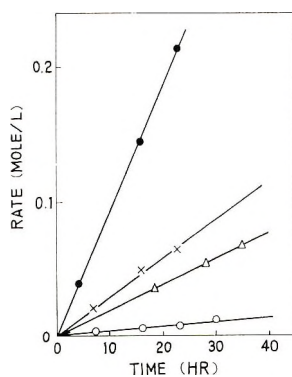


Fig. 3. Effect of concentration of silver nitrate and isoprene on polymerization rate: (●) [isoprene], 1.33 mole/l., $[\text{Ag}^+]$, 5.42 mole/l.; (×) [isoprene], 1.00 mole/l., $[\text{Ag}^+]$, 4.00 mole/l.; (Δ) [isoprene], 0.67 mole/l., $[\text{Ag}^+]$, 2.67 mole/l.; (○) [isoprene], 0.33 mole/l., $[\text{Ag}^+]$, 1.33 mole/l. $\text{Ag}^+/\text{isoprene} = 4$; temperature, 30°C.; dose rate, 0.78×10^4 r/hr.

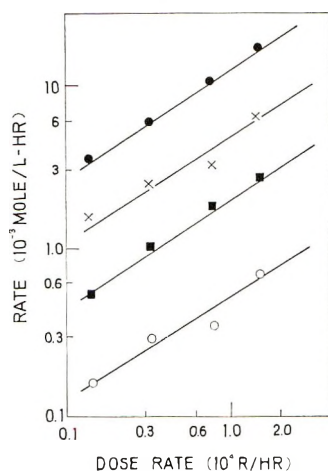


Fig. 4. Effect of dose rate on polymerization rate: (●) [isoprene], 1.33 mole/l., $[Ag^+]$ 5.42 mole/l.; (×) [isoprene], 1.00 mole/l., $[Ag^+]$, 4.00 mole/l.; (■) [isoprene], 0.67 mole/l., $[Ag^+]$, 2.67 mole/l.; (○) [isoprene], 0.33 mole/l., $[Ag^+]$, 1.33 mole/l. Temperature, 30°C.

and 0.33 mole/l. is shown in Figure 1. Figure 2 indicates the polymer yield as a function of irradiation time of a fixed isoprene concentration of 0.67 mole/l. and the concentrations of silver nitrate of 4.00, 2.67, or 1.33 mole/l.

These figures show the existence of the induction period for the lower concentration of isoprene. It is worth noticing that the rate of polymerization in this experiment is 20–50 times as much as that in radiation-induced polymerization of pure isoprene.⁸

In subsequent runs, the experiments were performed under a fixed mole ratio of silver nitrate: isoprene of 4:1, since under this condition the monomer solution is homogeneous and there is no induction period (Figs. 3 and 4).

Temperature Dependence

The polymerization was performed at 2 and 15°C., and the conversion is plotted versus the irradiation time in Figures 5 and 6, respectively. The polymerization temperature was restricted to the range between the melting point and the boiling point of the monomer solution.

In Figure 7, Arrhenius plots obtained from the results of Figures 3, 5, and 6 are shown. In view of Figure 7, it is obvious that a linear relationship is obtained with respect to solutions having equal complex concentrations. We obtained an apparent activation energy of 8 kcal./mole.

Influence of Inhibitors

In order to determine the polymerization mechanism of this system, polymerizations were carried out in the presence of various radical inhibitors.

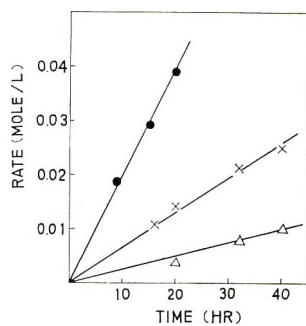


Fig. 5. Effect of temperature on polymerization rate at 2°C.: (●) [isoprene], 1.33 mole/l., $[Ag^+]$, 5.42 mole/l.; (×) [isoprene], 1.00 mole/l., $[Ag^+]$, 4.00 mole/l.; (Δ) [isoprene], 0.67 mole/l., $[Ag^+]$, 2.67 mole/l. Dose rate, 0.78×10^4 r/hr.

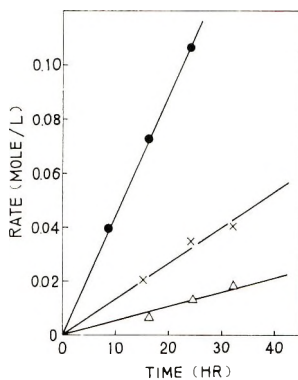


Fig. 6. Effect of temperature on polymerization rate at 15°C. Dose rate 0.78×10^4 r/hr.; symbols as in Fig. 5.

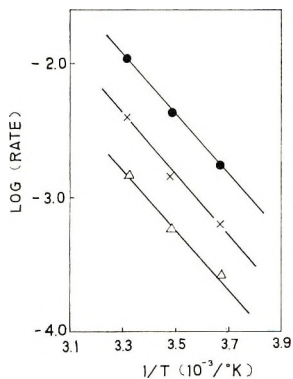


Fig. 7. Effect of temperature on polymerization rate at various concentrations of complex: (●) 1.2 mole/l.; (×) 0.6 mole/l.; (Δ) 0.3 mole/l. Dose rate, 0.78×10^4 r/hr.; $[Ag^+]/[isoprene] = 4$.

It is obvious from Table I that a small amount of polymer was produced in spite of the coexistence of radical inhibitors. The polymers obtained are assumed to be of low molecular weight, in view of the high solubility in acetone. As the polymerization is almost inhibited by radical inhibitors, it may be possible to conclude that the polymerization proceeds through a radical mechanism.

TABLE I
Influence of Inhibitor^a

Inhibitor	Yield, moles
None	0.213
<i>p</i> -Benzoquinone	0.0037
DPPH	0.0025

^a Reaction conditions: isoprene, 2×10^{-2} mole/15 ml.; silver nitrate, 8×10^{-2} mole/l.; inhibitor, 1 mole-% (based on isoprene); dose rate, 0.78×10^4 r/hr.; temperature, 30°C.; time, 23 hr.

Detection of Complex

To determine the reaction mechanism, a spectrophotometric study of the complex was carried out. In Figure 8 the transmittance of the following solutions in visible region are shown; 8 mole/l. aqueous silver nitrate solution with reference to pure water, 8 mole/l. aqueous silver nitrate solution (10 ml.) + 0.25×10^{-2} mole isoprene solution, and 8 mole/l. aqueous silver nitrate solution (10 ml.) + 0.50×10^{-2} mole isoprene solution with reference to 8 mole/l. aqueous silver nitrate solution, and 50 vol.-% isoprene in solution methanol with reference to methanol. It is obvious from Figure 8 that the spectra of silver nitrate-isoprene solutions show an absorption peak at 375 $m\mu$, which the spectrum isoprene does not show. This fact indicates that a complex between silver nitrate and isoprene is formed in aqueous solution.

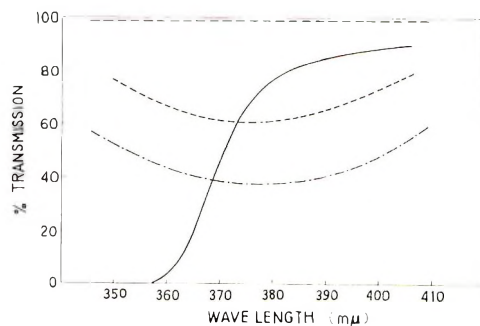


Fig. 8. Absorption spectra of polymerization solution in visible region: (---) 50% isoprene in methanol; (—) 8 mole/l. silver nitrate aqueous solution; (---) 0.244 mole/l. isoprene + 8 mole/l. silver nitrate, aqueous solution; (-·-) 0.500 mole/l. isoprene + 8 mole/l. silver nitrate, aqueous solution.

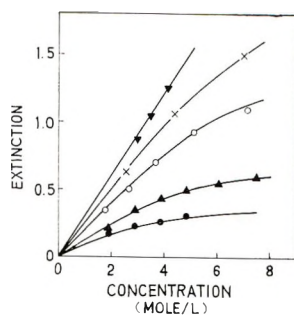


Fig. 9. Extinction of silver nitrate and isoprene aqueous solution at $380\text{ m}\mu$ at various isoprene concentrations: (▼) 1.5 mole/l.; (×) 1.3 mole/l.; (○) 0.91 mole/l.; (▲) 0.48 mole/l.; (●) 0.24 mole/l.; silver nitrate, transverse.

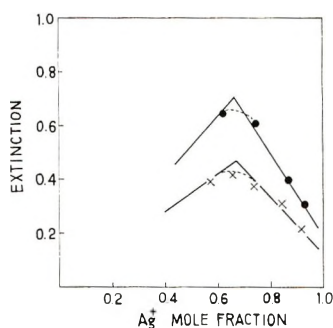


Fig. 10. Determination of complex composition by continuous variation method at $380\text{ m}\mu$: (●) [isoprene] + $[\text{Ag}^+] = 4.0$ mole/l.; (×) [isoprene] + $[\text{Ag}^+] = 3.0$ mole/l.

In order to determine the composition and the concentration of complex, the following experiments were undertaken. The extinctions (optical density) of isoprene-aqueous silver nitrate solution with reference to the aqueous solution of equal concentration of silver nitrate were determined at 30°C . since the extinction coefficient of silver nitrate in the region of wavelengths more than $380\text{ m}\mu$ was very small, while that of the complex was fairly large.

The extinctions of the aqueous solution of complex in the case of constant isoprene concentration are shown in Figure 9. The determination of the complex composition was made by using the continuous variation method^{9,10} on the basis of Figure 9. Figure 10 shows the relationship between mole fraction of silver nitrate and the extinction as a function of mole ratio of isoprene and silver nitrate at fixed total concentrations. The mole fraction of silver nitrate at the maximum extinction is 0.67 (i.e., $2/3$). The complex accordingly, consists of two silver ions and one isoprene molecule.

From the above results, the extinction coefficient and the equilibrium constant of complex were determined as follows. The equilibrium constant K_f is given by eq. (1)

$$K_f = [\text{Ag}_2^+\text{B}]/[\text{Ag}^+]^2[\text{B}] \quad (1)$$

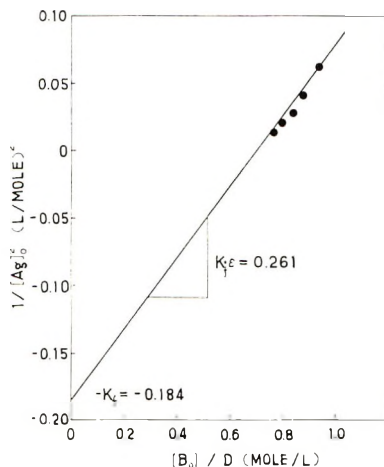


Fig. 11. Determination of equilibrium constant K_f and extinction coefficient E of complex.

where $[Ag^+]$, $[B]$, and $[Ag_2+B]$ are the concentrations of silver ion isoprene, and complex, respectively.

In the case of $[Ag^+] \gg [B]$, eq. (2) can be written:

$$1/[Ag^+]_0^2 = K_f \cdot E \cdot \frac{[B]_0}{D} - K_f \quad (2)$$

where $[Ag^+]_0$ and $[B]_0$ are the initial concentrations, $[Ag^+]$, $[B]$, and $[Ag_2+B]$ are the concentrations at equilibrium, and D and E are the extinction coefficients of aqueous silver nitrate-isoprene solutions, and the complex, respectively.

$[Ag^+]_0$ and $[B]_0$ are known values, and D can be determined spectroscopically. Thus, the linear relationship should be given by plotting $1/[Ag^+]_0^2$ against $[B]_0/D$, so that K_f and E can be determined graphically. By plotting the determined values at $[B]_0 = 0.244$ mole/l. in Figure 8

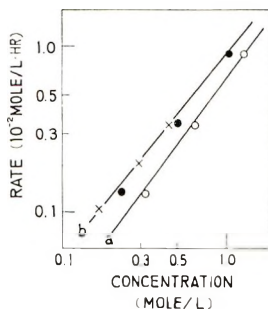


Fig. 12. Effect of (a) isoprene and (b) complex concentration on polymerization rate: (O) polymerization rate from isoprene concentration according to Fig. 1, (●) rate from complex concentration according to Fig. 1, (X) rate from complex concentration according to Fig. 2.

according to eq. (2), Figure 11 was obtained, and therefore, K_f and E are given as 0.18 and 1.4, respectively.

Relationship between Concentration of Complex and Polymerization Rate

Figure 12, which was obtained from Figures 1 and 2, shows the dependence of the polymerization rate on the concentrations of isoprene and complex. A similar dependence is shown in Figure 13, where the mole ratio of silver nitrate and isoprene is 4:1.

As shown in Figures 12 and 13, the same linear relationships are obtained under the conditions of these experiments, and the exponent found is 1.3.

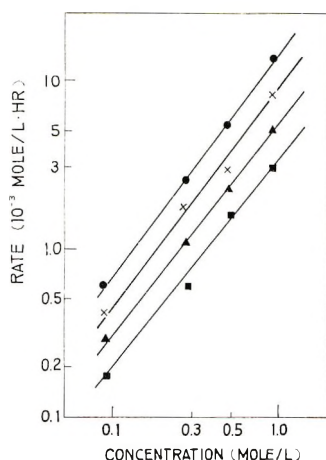


Fig. 13. Effect of complex concentration on polymerization rate: at various dose rates: (●) 1.5×10^4 r/hr.; (×) 0.78×10^4 r/hr.; (▲) 0.35×10^4 r/hr.; (■) 0.15×10^4 r/hr. $[\text{Ag}^+]/[\text{isoprene}] = 4$; temperature, 30°C .

Infrared Spectra of Polymer

The infrared spectrum of the polyisoprene product (containing silver nitrate) was obtained by the KBr disk method, as it is impossible to separate silver nitrate completely from the polymer which is crosslinked, insoluble, and nonmelting one. Figure 14 shows the infrared spectra of

TABLE II
Structural Composition of Various Polyisoprenes

	Polyisoprene conditions			
	1,2, %	<i>cis</i> -1,4, %	<i>trans</i> -1,4, %	3,4, %
This experiment	41.9	20.0	34.1	4.7
Radical catalyst ¹²	6	22	65	7
Hevea ¹²	2-6	94-98	0	0
Na catalyst ¹²	5	27	52	16

polyisoprene prepared in this experiment and various other kinds of polyisoprene which were obtained by Richardson et al.¹¹

The structural composition of the polyisoprene obtained, determined on the basis of the extinction coefficients for each structure obtained by Richardson et al., are shown in Table II with values of other polyisoprenes.¹²

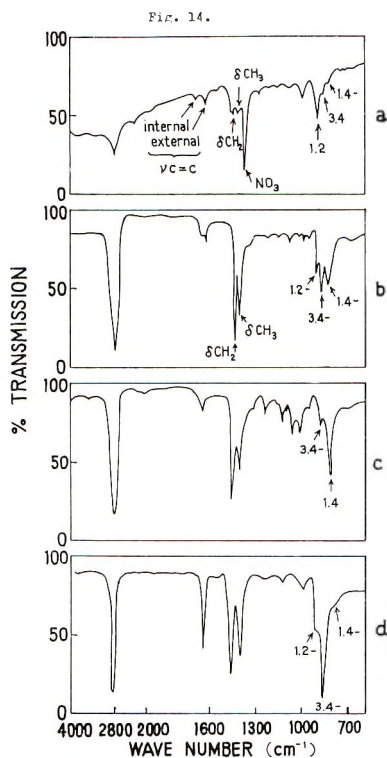


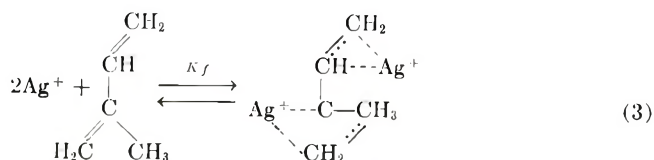
Fig. 14. Infrared spectra of various polyisoprenes: (a) polyisoprene obtained in this experiment; (b) polymerized by radical catalyst; (c) hevea; (d) polymerized by Na catalyst.

It should be pointed out that the 1,2-structure is present in the product of this experiment in greater proportion than any other polyisoprene structure, and this is different from the case with other polyisoprenes.

DISCUSSION

On the basis of these results, we may now discuss the polymerization mechanism.

The rate of polymerization is so fast that it seems reasonable to assume that complex, which consists of one isoprene molecule and two silver ions, takes part in the propagation reaction, as shown in eq. (3).



This complex polymerizes as the monomer by attacking of a free radical.

The relationship between the concentration of complex and the initial concentration of isoprene and silver nitrate is as follows. In this polymerization system, the following relationship is always established: $[\text{Ag}^+]_0 \gg [\text{B}]$. Therefore, the concentration of complex is given by eq. (4):

$$[\text{Ag}_2^+\text{B}] = K_f[\text{Ag}^+]_0^2[\text{B}]_0 / (1 + K_f[\text{Ag}^+]_0^2) \quad (4)$$

In a system with a high concentration of silver nitrate, it is reasonable to assume $K_f[\text{Ag}^+]_0^2 \gg 1$, so that eq. (4) becomes

$$[\text{Ag}_2^+\text{B}] \doteq [\text{B}]_0 \quad (5)$$

Equation (5) shows that the concentration of complex is almost equal to the initial concentration of isoprene, and therefore, the rate of polymerization is a function of the isoprene concentration. This is confirmed by Figure 12.

At high concentrations of isoprene, it is obvious that eq. (5) is inapplicable, so that the rate of polymerization is to be written as a function of the concentration of the complex. If it is assumed that the primary radicals are generated in the radiolysis of both H_2O and complex and the stationary-state treatment is applicable to the system, the overall reaction rate becomes:

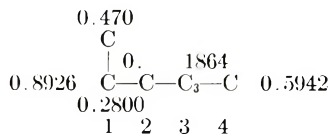
$$R_p = k_p/k_t^{-0.5} I^{0.5} (\phi[\text{Ag}_2^+\text{B}] + \phi'[\text{H}_2\text{O}])^{0.5} [\text{Ag}_2^+\text{B}] \quad (6)$$

where k_p and k_t are the rate constants of propagation and termination, respectively, I is radiation dose rate, and ϕ , ϕ' are the rate constant of free radical formation in complex and H_2O , respectively.

Equation (6) shows that the rate of polymerization should be proportional to the concentration of the complex to the 1.0–1.5 power. The experimental results indicate that the rate of polymerization is proportional to the complex concentration to the power of 1.3, which represents a good agreement between eq. (6) and the experimental results.

We will now consider why the 1,2 structure is more abundant than any other structures in the polyisoprene obtained in this experiment. It is likely that 1,4 structure would be more abundant than any other structures if isoprene and Ag^+ complex were to have a 1:1 structure. This assumption is based on the fact that the 1,4 structure predominates over 1,2 structure in polybutadiene–sulfone prepared by the alternative copolymerization of butadiene and sulfur dioxide.¹³ The complex in the present experiment, however, consists of one isoprene molecule and two Ag^+ ; it is, therefore, probable that 1,2 or 3,4 structures may be more abundant than 1,4 structure in polyisoprene obtained.

The equilibrium constant K_f which was obtained consists of both the equilibrium constant $K_{f(1,2)}$ between Ag^+ and the 1,2 double bond and $K_{f(3,4)}$ between Ag^+ and the 3,4-double bond. Hayashi et al.¹³ calculated the frontier electron density of isoprene as follows:



The total electron density for C_1 and C_2 is more than that for C_3 and C_4 , so that the 1,2 double bond is larger has a greater capacity for forming a complex than the 3,4 double bond, with Ag^+ that is:

$$K_{f(1,2)} > K_{f(3,4)}$$

The above discussion agrees with the experimental fact that the proportion of 1,2 structure is very large in polyisoprene obtained.

The authors thank Prof. Okamura for his encouragement through this work, Dr. Ph. Teyssié for many helpful discussions, and Mr. Nukushima for permission to publish the results.

References

1. G. Bier, G. Messwarb, E. Nölken, M. Lederer, W. Eichlern, and L. Hofmann, *Angew. Chem.*, **74**, 977 (1962).
2. S. Rösinger and St. Müllner, paper presented at Conference on the Application of Large Radiation Sources in Industry, Salzburg, Germany, May 1963.
3. R. N. Keller, *Chem. Rev.*, **28**, 299 (1941).
4. K. Ohdan, K. Kayashi, and S. Okamura, *Ann. Rept. Japan Assoc. Radiation Res. Polymers*, **2**, 95 (1960).
5. H. Sumitomo, K. Kobayashi, and Y. Hachihama, *Kogyo Kagaku Zasshi*, **67**, 1659 (1964).
6. I. Yamashita, J. Furukawa, T. Saegusa, and K. Kawasaki, *Kogyo Kagaku Zasshi*, **65**, 239 (1962).
7. J. W. Kraus and E. W. Stern, *J. Am. Chem. Soc.*, **84**, 2893 (1962).
8. C. D. Buckley and L. Seed, French Pat. 1,062,004 (1954); Brit. Pat. 778,225 (1954).
9. E. R. Garrett and R. L. Guile, *J. Am. Chem. Soc.*, **75**, 3958 (1953).
10. R. M. Kiefer and L. J. Andrews, *J. Am. Chem. Soc.*, **72**, 4677 (1950); *ibid.*, **75**, 3776 (1953).
11. W. S. Richardson and A. Sacher, *J. Polymer Sci.*, **10**, 353 (1953).
12. R. S. Stearns and L. E. Forman, *J. Polymer Sci.*, **41**, 381 (1959).
13. S. Fujioka, Y. Shinohara, and K. Hayashi, *Kogyo Kagaku Zasshi*, **69**, 330 (1966).

Received May 23, 1967

Revised July 5, 1967

Physicochemical and Macromolecular Properties of Sodium Amylose Xanthate in Dilute Solution

A. G. PRAMANIK and P. K. CHOUDHURY, *Department of Applied Chemistry, Calcutta University, Calcutta, India*

Synopsis

Sodium amylose xanthate has been studied in dilute solution. Potato starch was fractionated for this purpose into amylose and amylopectin fractions. Amylose was xanthated in solution under alkaline conditions and the Na amylose xanthate was then characterized by reaction with I_2 solution and ultraviolet spectra of the xanthate groups determined. Stability of the xanthate in alkaline condition under both oxygen and nitrogen atmospheres was also investigated. From light scattering measurements of dilute salt solutions of Na amylose xanthate, the weight-average molecular weight \bar{M}_w as well as the molecular dimensions were determined. In 0.11M NaCl, which conforms to the Θ solvent, Na amylose xanthate molecules appear to have a random-coil configuration. Two other configurational parameters, such as the effective bond length b , and the steric factor σ , i.e., $(R_0^2)^{1/2}/(\bar{R}_f^2)^{1/2}$, where $(R_0^2)^{1/2}$ is the Root-mean-square end-to-end distance in the unperturbed state and $(\bar{R}_f^2)^{1/2}$ is the unperturbed value calculated on the assumption of free rotation about each intermonomer C-O bond of the amylose chain) were also calculated and found to be 6.24 and 1.020, respectively. It is thus concluded that the amylose chain in Na amylose xanthate behaves as a typical flexible coil in dilute salt solution.

INTRODUCTION

Amylose, a 1,4-*cis* polysaccharide, is one of the two fractions of starch. Chemically, amylose resembles cellulose but the two differ structurally, the difference being similar to that between isotactic and syndiotactic polymers of the same monomer. Cellulose and cellulose derivatives are technically important products and their physicochemical and macromolecular properties have therefore been extensively studied; however, similar investigations on amylose and its derivatives have been comparatively few. This is mainly due to the fact that, unlike cellulose which can be readily obtained in a very pure form, it is rather difficult to get pure amylose for such investigations; also, amylose and its derivatives are not yet technically so important.

Recently, however, some studies on physicochemical and macromolecular properties of various esters and ethers of amylose have been undertaken. Stavermann et al.¹ prepared the hydroxyethyl ether of amylose and characterized it by its degree of modification (M.S.), intrinsic viscosity, and iodine absorption value. Cowie² performed light-scattering and vis-

cosity measurements on fractionated samples of amylose acetate in chloroform and nitromethane, and important parameters like the linear expansion factor α and the effective bond length b were determined. The Kratky-Porod chain model was found to be most suitable in describing the hydrodynamic behavior, and this indicated that the molecule is much stiffer than the vinyl polymers but more flexible than the cellulose ester chains. Further studies³ on the fractions of amylose acetate in various solvent-nonsolvent mixtures revealed that Flory's hydrodynamic theory was not applicable in this case, while the Kurata and Ptitsyn theories were in good agreement with the observed data.

All the above observations were made on amylose acetate. Other important amylose derivatives, such as amylose xanthate, were hardly used for such investigations. In fact, except for some work on the distribution of xanthate groups in partially substituted starch xanthate⁴ it appears that there has been practically no work done on the physicochemical and macromolecular properties of amylose xanthate in solution. We therefore decided to concentrate on the above study, particularly elucidation of the macromolecular properties of amylose xanthate by viscosity and light scattering and determination of other important configurational parameters.

EXPERIMENTAL

Preparation of Pure Amylose

Potato starch was chosen as the raw material. About 10 g. of completely ground air-dry starch was refluxed in a Soxhlet apparatus for about 8 hr. with methanol as the solvent for the fatty materials. The solvent was then evaporated off and the residue dried in air. Separation of amylose and amylopectin from the starch solution was carried out by the standard method,⁵ butanol being used as the complexing agent. The purity of the amylose fraction was tested by potentiometric titration⁶ of the sample with I_2 solution. The iodine absorption value was found to be 16%. The crude amylose fraction was therefore further purified by recrystallization; the iodine absorption value was then found to be 18.2%, indicating the sample to be almost pure amylose.

Xanthate Reaction

A 5 g. portion of amylose⁷ was added to 125 cc. of 8% caustic soda solution in a closed bottle and stirred mechanically until dissolution was complete. Then about 2 cc. of CS_2 (48% by weight of amylose) was added to the mixture in two stages at a 1/2-hr. interval, and stirring was continued for another 3 hr. The reaction mixture was then stored in an atmosphere of N_2 below 0°C. It had the characteristic carrot color similar to that of cellulose xanthate solution (viscose).

Pure Na amylose xanthate (NaAX) was separated from its associated byproduct by precipitation with methanol following the technique of

Ghosh et al.⁸ The precipitate was successively washed with methanol until it was completely free from alkali. It was finally dried in vacuum. Pure NaAX had a characteristic light-green color similar to that of Na cellulose xanthate (NaCX).

Characterization of Sodium Amylose Xanthate (NaAX)

Determination of Degree of Substitution in Sodium Amylose Xanthate by Reaction with I₂. As in the case of Na cellulose xanthate,⁹ the reaction of I₂ solution with the xanthate group was utilized for the determination of the DS.

The xanthate solution containing 0.1–0.3% polymer was made by dissolving the vacuum-dried pure sample in ice-cooled doubly distilled water. A 5 cc. portion of this solution was taken in a 250-cc. stoppered Erlenmeyer flask and diluted to about 100 ml. with ice-cooled doubly distilled water. Then 10 cc. of standard I₂ solution (*N*/40) was added to it, followed by the addition of 10 ml. of 10% acetic acid solution. The resulting solution was then left in the dark for about 15 min. to allow sufficient time for complete reaction. The excess I₂ was back-titrated with standard thio-sulfate solution, aqueous starch solution being used as the indicator. The degree of substitution was found to lie between 0.4 and 0.5 (using 48% CS₂ by weight of amylose).

Ultraviolet Spectra of the Xanthate Group. In the ultraviolet region, the xanthate group has maximum absorption at 3020 Å.^{10,11} Very recently, Elmgren¹² found two absorption maxima for the xanthate group of NaCX in 1*M* NaOH, one at 2250 Å. and the other at 3020 Å.

The optical density (OD) of pure NaAX in doubly distilled water was measured with a Beckman DU spectrophotometer between the wave lengths of 2100 and 4000 Å. The results are shown in Figure 1. It is found that the xanthate group has two absorption maxima, one around 2100 Å. and the other at 3020 Å., the latter being characteristic of the xanthate group.

Polyelectrolyte Behavior of NaAX in Aqueous and Salt Solutions. The anomalous viscosity behavior of polyelectrolytes can be attributed to changes in the volume of the polymer–solvent complex and to a change in the coiling of the polymer molecules, which in turn, is due to changes in the repulsion between charged groups on the polymer chain. With dilution the screening effect of electrolytes is diminished, and the repulsion between polymer charges increases.

Early work^{8,13} on viscosity measurements of dilute solutions of Na cellulose xanthate showed marked changes in reduced viscosity in aqueous, caustic soda, and salt solutions and it was apparent that the charged xanthate groups were playing an important role in the viscosity effects in these solutions. Accordingly, work was undertaken to determine the extent of their contribution in Na amylose xanthate in aqueous and NaCl solutions.

Viscometric readings on aqueous solution of NaAX were taken in a constant temperature bath at 30 ± 0.1°C., with an Ostwald viscometer

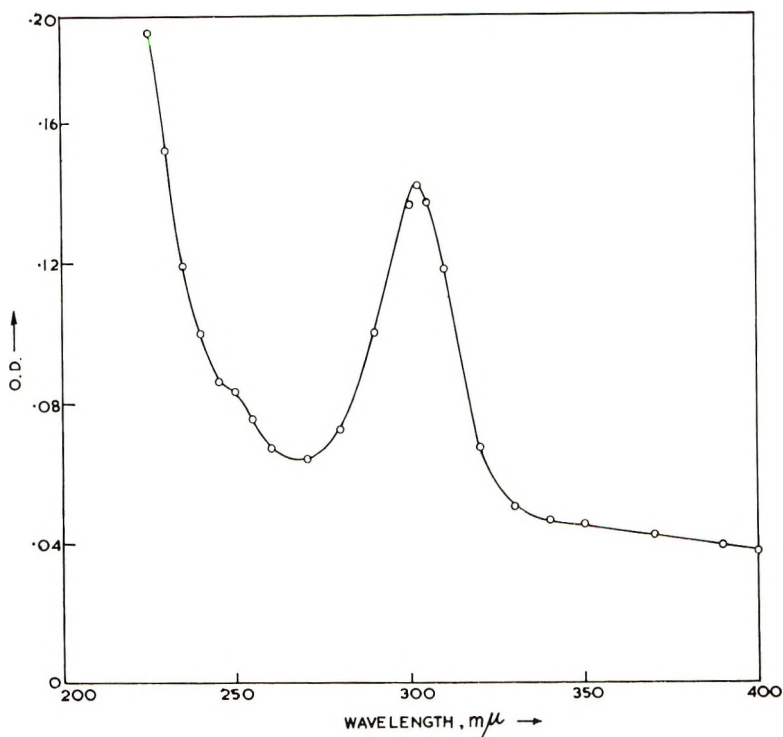


Fig. 1. Ultraviolet spectrum of Na amylose xanthate in water.

having a flow time of 106.2 sec. with respect to water. Results are shown in Table I.

Plots of η_{sp}/c versus c are given in Figure 2; these gave a curve typical for a polyelectrolyte. The values of η_{sp}/c decreased continuously with decreasing c up to a concentration of 0.24 and then rose abruptly, giving continuously higher values of η_{sp}/c with decrease in the concentration of the polymer, a phenomenon common for all polyelectrolytes. On applying Fuoss's equation for a polyelectrolyte $\eta_{sp}/c = (1 + B\sqrt{c})$, the plot of

TABLE I
Viscosity of Na Amylose Xanthate in Aqueous Solution

No.	Concn. c , g./100 cc.	η_{sp}/c	\sqrt{c}	$(\eta_{sp}/c)^{-1}$
1	0.3772	2.520	0.6142	0.3968
2	0.3018	2.505	0.5494	0.3992
3	0.2414	2.517	0.4914	0.3973
4	0.1690	2.584	0.4111	0.3870
5	0.1014	2.714	0.3184	0.3684
6	0.0608	2.933	0.2467	0.3410
7	0.0365	3.087	0.1911	0.3239
8	0.0219	3.002	0.1480	0.3332

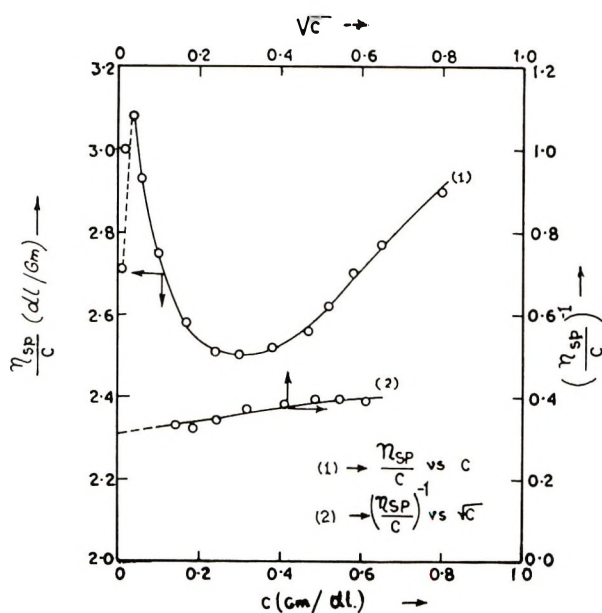


Fig. 2. Viscosity behavior of Na amylose xanthate in water.

$(\eta_{sp}/c)^{-1}$ against \sqrt{c} gave a straight line (Fig. 2) which agreed with the above equation. The extrapolated value of $(\eta_{sp}/c)_{c \rightarrow 0}^{-1}$ gave the value of $1/A$, the inverse of which gave the value of (η) , the intrinsic viscosity of NaAX in aqueous solution. Simultaneously, the quantity, $B\sqrt{c}$ which is a function of the dielectric constant of the solvent, gave a measure of the extent of the electrostatic interactions between polyions and dissociated counterions.

The effect of various concentrations of NaCl on the viscosity behavior of NaAX is shown in Figure 3. Even 0.1M NaCl was not able to suppress the ionization of the polyelectrolyte completely. The optimum concentration of salt solution which could just suppress this behavior was found to lie between 0.1 and 0.2M of NaCl. Further increase in the concentration of NaCl up to 1.5M continued to decrease the intrinsic viscosity values but did not bring about flocculation or gelation of the NaAX, although a much lower concentration of NaCl (about 0.35M NaCl) caused gelation of the NaCX.¹⁴ The peculiar behavior of these two xanthates towards salt solution may possibly be due to differences in the structure of the monomer of the two parent polymers. The hydrophilic nature of NaCX is solely due to its solubilizing factor, the CSSNa group, the cellulose chain being hydrophobic in character. For NaAX, however, in addition to its solubilizing CSSNa group, the amylose chain itself is hydrophilic. Flocculation of the hydrophilic solution will occur only when both of its two stability factors, i.e., capillary electric charge and hydration factors, are sufficiently suppressed. Thus flocculation or gelation of NaCX in salt solution can be explained as being due to its pronounced hydrophobic character in the

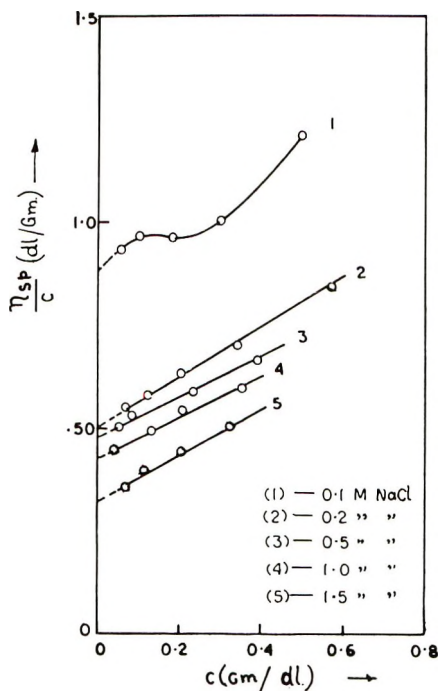


Fig. 3. Effect of electrolyte (NaCl) on viscosity behavior of aqueous Na amylose xanthate solution.

medium, only capillary electric charges being responsible for its stability. On the other hand, for NaAX, apart from the presence of NaCl which suppresses the electric charges, the hydration factor plays a strong role in its stability, the addition of dehydrating agents such as methanol or acetone thus being necessary to bring about its flocculation.

Stability of the Compound in Alkaline Solution. Ordinarily, NaAX in 4% NaOH solution is not stable. In contrast to the behavior of NaCX in alkali, which undergoes only decomposition of xanthate groups at room temperature, NaAX undergoes decomposition of the xanthate groups along with the degradation of the amylose chain. The process of degradation is marked in the presence of atmospheric oxygen but can be retarded if the alkaline solution is stored under N_2 . The alkaline solution of NaAX was therefore stored under N_2 below $0^\circ C$. to minimize both decomposition of xanthate groups and degradation of the chain.

Molecular Weight and Dimensions from Light-Scattering Experiments in Salt Solutions. Zimm¹⁴ has shown that in the case of large molecules, the turbidity due to concentration fluctuations is related to the molecular weight of the solute by the equation:

$$Hc/\tau = [1/MP(\theta)] + 2Bc \quad (0 < \theta < 180) \quad (1)$$

where $P(\theta)$ is a particle scattering factor which corrects for the effects of internal interference and is related to the form and dimensions of the solute molecules, and the other symbols have the usual significance. The determination of the value of constant H requires the value of the refractive index increment, dn/dc , which must be accurately determined.

To determine the value of dn/dc , the Brice-Phoenix differential refractometer was used. For dilute xanthate solution, the values of Δn were determined at $546\text{ m}\mu$ at five different concentrations and the values were treated in the usual manner to get the dn/dc values. The values of dn/dc in different concentrations of salt solutions are shown in Table II.

TABLE II
 dn/dc Values of NaAX in Varying Concentrations of
Salt Solutions at $546\text{ m}\mu$ at 25°C .

NaCl concn., M	dn/dc , ml./g.
0.1	-0.1460
0.25	-0.1480
0.50	-0.1555
1.0	-0.1741

The turbidity τ , molecular weight $\bar{M}w$, and dissymmetry (Z) of dilute NaAX solutions were determined by means of a Brice-Phoenix universal light-scattering photometer equipped with a spotlight galvanometer. For scattering ratio and dissymmetry measurements, a 15-ml. capacity circular cell of Witnauer-Scherr type¹⁵ was used. Scattering ratios for the determination of turbidity were determined by recording the galvanometer deflections at 90° and 0° . For the determination of dissymmetry, scattering intensities at 45° and 135° were also measured. Dilutions were made within the circular cell with perfectly clean pipets. In all the cases, the

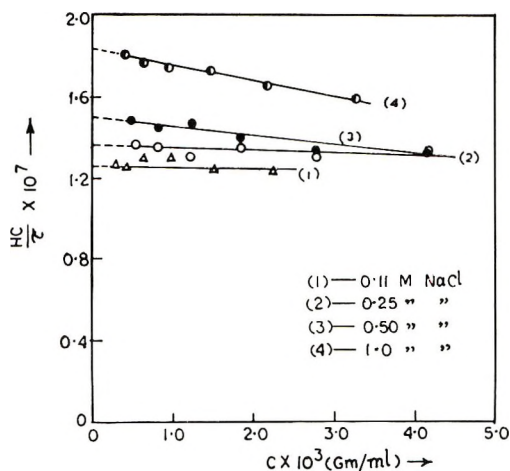


Fig. 4. Molecular weight ($\bar{M}w$) of Na amylose xanthate in salt solutions.

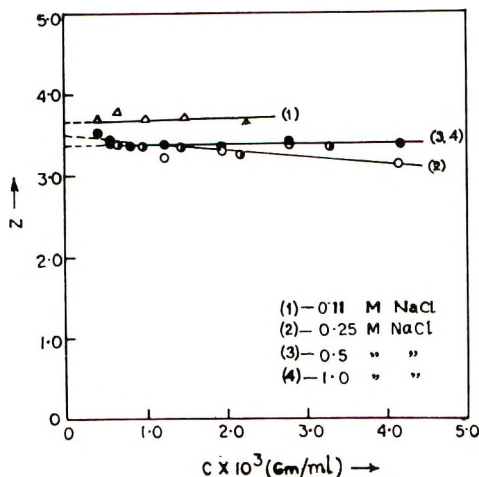


Fig. 5. Dissymmetry of Na amylose xanthate in salt solutions.

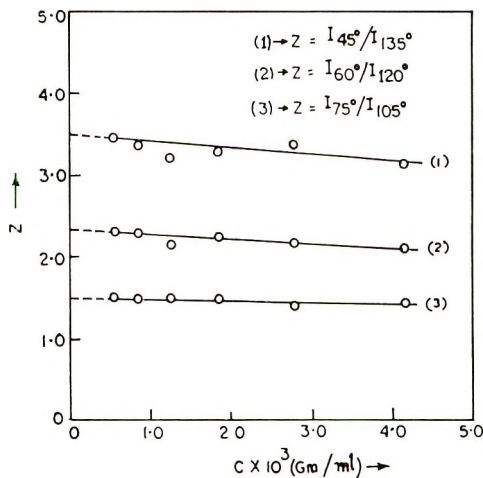


Fig. 6. Dissymmetry of Na amylose xanthate with variation of dissymmetry angles in 0.25M NaCl.

turbidity of the solvent was subtracted from that of the solution to get absolute turbidity. All solvents used were centrifuged at 18,000 rpm in a Servall angle centrifuge and filtered through a sintered glass filter, grade 5 (average pore size 1.7μ) three times before scattering measurements were undertaken. Solutions were made in clarified solvents and then the solutions were further clarified by filtering through Pyrex sintered glass filter (grade 4), until it appeared to be optically clear by visual inspection. The data were treated by plotting separately Hc/τ against concentration (c) and also dissymmetry against concentration; these plots are shown in Figures 4 and 5.

Before calculating the actual molecular weight, it was necessary to determine the shape of NaAX molecules in salt solutions. We can express

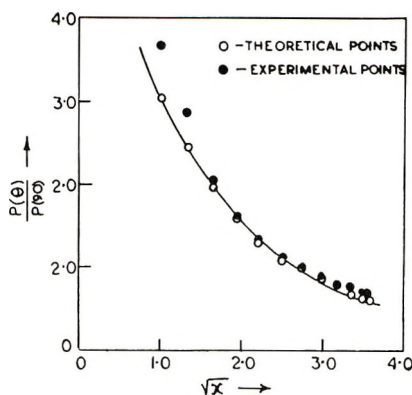


Fig. 7. Shape of Na amylose xanthate in 0.25*M* NaCl (assumption of polydispersed random coil).

the difference between the dissymmetry $I_{\theta}/I_{180-\theta}$ (which is the ratio of the intensity of light scattered at some forward angle θ to that scattered at its supplementary angle $(180 - \theta)$ and unity for particles which are not too big (small L/λ^1) by the appropriate formula:¹⁶

$$I_{\theta}/I_{180-\theta} - 1 = K(L/\lambda^1)^2 \cos \theta \quad (2)$$

where K is a constant, its value being dependent on the shape of the molecules. Equation (2) shows that for a polymer molecule conforming to a particular shape, we should obtain a constant value of L/λ^1 for all angles. Thus, solutions of NaAX in 0.25*M* NaCl gave dissymmetry values of 3.50, 2.35, and 1.50 (Fig. 6) for θ equal at 45° , 60° , and 75° , respectively. All these results are consistent with a value of $L/\lambda^1 = 0.695$ found from idealized curves¹⁶ for random coil plotted for $I_{\theta}/I_{180-\theta}$ against L/λ^1 for various values of θ . This result was further confirmed by another experimental method as described by Moulik et al.¹⁷

The intensities of scattered light were measured at several angles from 30° to 135° and each intensity value was multiplied by the factor $\sin\theta/(1 + \cos^2 \theta)$, where the denominator takes account of the horizontal component of the unpolarized incident light, and the $\sin \theta$ term is included to correct for the change in the volume "seen" by the photomultiplier at angles removed from 90° . The corrected ratios, $P(\theta)/P(90)$, also equal to the ratio of the intensity of scattering at any angle θ to that at 90° , were calculated. For a Gaussian coil, the particle scattering factor $P(\theta)$, is related to the form and dimensions of the solute molecules by the expression,

$$P(\theta) = (2/x^2)[e^{-x} - (1 - x)]$$

where x , the characteristic dimension for the polycoid system, is given by $x = (8/3)\lambda^2 \sin^2(\theta/2)(L/\lambda^1)^2\lambda^1$ being the wavelength of light in the solution and L being the root mean square of the distance between ends of the random coil. The value of L/λ^1 was obtained corresponding to the value of the dissymmetry Z from the standard curve, and then values of x were

obtained for various values of θ . Theoretical $P(\theta)$ values were next obtained corresponding to \sqrt{x} for the random coil system with the help of the theoretical curve, (theoretical values of $P(\theta)$ plotted against \sqrt{x}). The theoretical $P(\theta)/P(90)$ values were then obtained. Both experimental and theoretical $P(\theta)/P(90)$ values were plotted separately against \sqrt{x} and these are shown in Figure 7. It was found that the experimental $P(\theta)/P(90)$ values for NaAX in 0.25M salt solution are in sufficient coincidence with the theoretical curve. Other molecular models such as spheres, rods, etc. have been tried, but the experimental points deviate too much from the theoretical curves. The weight-average molecular weight, along with other parameters of Na amylose xanthate in NaCl solutions are shown in Table III.

TABLE III
Parameters of Na Amylose Xanthate in Salt Solutions

NaCl concn., M	$\bar{M}_w \times 10^{-7}$	B , ml.-mole/g. ²	$[\eta]$	$(\bar{R}^2)^{1/2}$, A.
0.1	3.8486	0	3.650	3274
0.25	3.3335	-0.600×10^{-6}	3.500	3068
0.50	2.9336	-2.222×10^{-6}	3.375	2859
1.0	2.3496	-3.667×10^{-6}	3.375	2859

The slope of the line in Figure 4 for a particular solvent-solute system is a measure of the second virial coefficient B . The light-scattering data for NaAX in salt solutions showed B to be effectively zero for 0.11M and 0.25M NaCl solutions, respectively. B is related to the linear expansion coefficient, α , by the Flory-Orofino equation:¹⁸

$$B = \frac{16\pi}{3^{3/2}} \cdot \frac{N(\bar{\rho}_0^2)^{3/2}}{M^2} \cdot \ln \left[1 + \frac{\pi^{1/2}}{2} (\alpha^2 - 1) \right] \quad (3)$$

Since B is effectively zero for the first two concentrations of salt solutions studied (0.11 and 0.25M NaCl), α must be equal to unity for the above two solvent systems. The magnitude of B thus proved that aqueous salt solutions are thermodynamically ideal solvents for NaAX near about 25°C. Hence the values of the root-mean-square end-to-end distance $(\bar{R}^2)^{1/2}$ given in the last column of Table III are also the unperturbed values, i.e., $(\bar{R}_0^2)^{1/2}$. In this connection it should be borne in mind that according to the findings of Banks and Greenwood,¹⁹ aqueous KCl (0.33M) is also a thermodynamically ideal solvent for amylose. The very small negative values of second virial coefficients in salt solutions greater than 0.25M NaCl can be interpreted according to Timasheff et al.²⁰ by using the theory of Kirkwood and Shumaker;²¹ this predicts a long-range, intermolecular attractive force for the solute molecules in the solvent since solute-solute interaction is favored over the solute-solvent interaction, resulting in a negative excess chemical potential. Such negative values of second virial coefficients have also

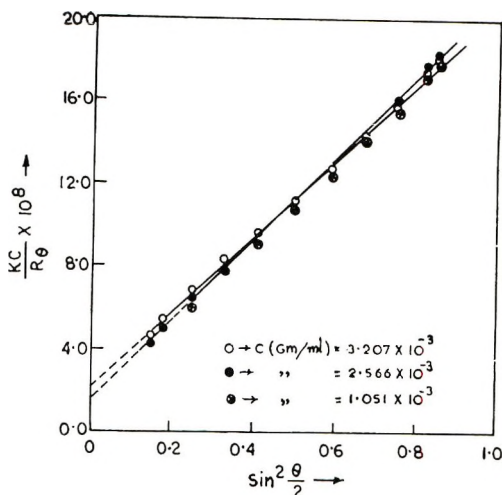


Fig. 8. Plot of Kc/R_θ vs. $\sin^2(\theta/2)$ for Na amylose xanthate in 0.25M NaCl.

been obtained for other systems.²²⁻²⁴ The slight increase in the intercepts of the Hc/τ versus c plots in Figure 4 with increase in the salt concentration resulting in the slight decrease in molecular weights can be explained by considering the systems to be three-component ones²⁵ and assuming that in these solvents NaAX molecules show a preference for the water molecules, and so the optical properties in the immediate neighborhood of the solute molecules are not representative of the medium as a whole. Strauss and Ander,²⁶ in their studies on lithium polyphosphates in LiBr solution, found the same trend towards decrease in molecular weights with increase in LiBr-concentration. However, the effect of salt concentrations on the molecular dimensions of NaAX is small, as can be seen from the data in Table III.

In order to derive configurational parameters from light-scattering data, the appropriate distribution of molecular weights, i.e., the relations among the number-average, weight-average, and Z -average molecular weights must be determined. This was achieved from a plot of Kc/R_θ^0 against $\sin^2(\theta/2)$ obtained from light-scattering experiments, the terms K , c , and R_θ having the usual significance. In practice, Kc/R_θ values were plotted against $\sin^2(\theta/2)$ for three different values of concentration c , as shown in Figure 8. The extrapolation of these values to $\theta = 0$ is said to depend on the molecular model assumed and the polymer heterogeneity.²⁷ However, for random coils with a molecular distribution characterized by $\bar{M}_w/\bar{M}_n = 2$, this plot should extrapolate linearly to $\theta = 0$ and this is actually the case for the system studied (Fig. 8). This is not surprising in view of the fact that for many other condensation polymers a similar distribution has been observed. Thus cellulose studied in solvent Cadoxen²⁸ has been shown to possess a distribution of molecular weights of this type. The corresponding Zimm plot for an unfractionated sample of NaAX in 0.25M NaCl is

shown in Figure 9. The weight-average molecular weight \bar{M}_w and end-to-end distance obtained from this plot were 4×10^7 and 3602 Å., respectively, as against 3.33×10^7 and 3068 Å. obtained from the dissymmetry method. However, the constancy in the values of the intercepts of Figure 8 at different concentrations may be explained due to the θ conditions of 0.25M NaCl solution.

Important parameters for characterizing a given polymer chain in solution are the effective bond length b and also the steric factor σ , where $\sigma = (\bar{R}_0^2)^{1/2}/(\bar{R}_f^2)^{1/2}$, the ratio of unperturbed root-mean-square end-to-end distance calculated for the hypothetical case of free rotation about each

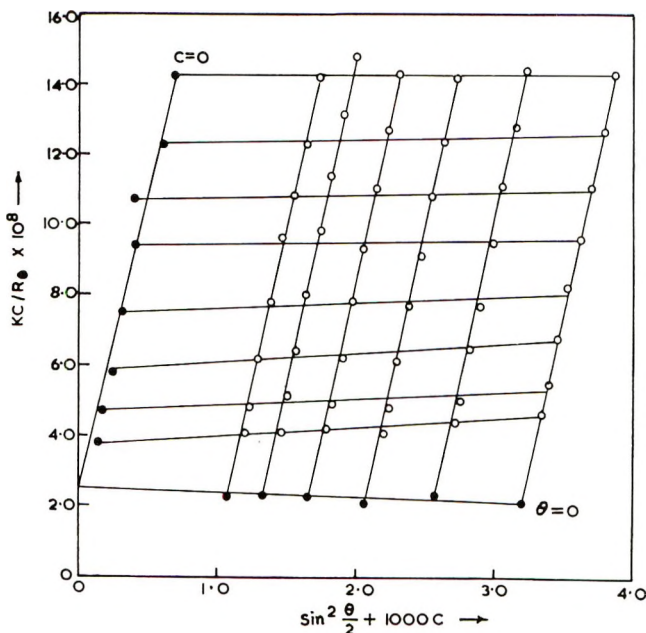


Fig. 9. Zimm plot for Na amylose xanthate in 0.25M NaCl.

bond in the amylose chain. For the amylose chain, using the value of 5.15 Å. for the length of each monomer unit (anhydroglucose unit) and 100° for the oxygen-valence angle, $(\bar{R}_f^2)^{1/2}$ can be related to the \overline{DP}^{29} by eq. (4):

$$(\bar{R}_f^2)^{1/2} = 6.144(\overline{DP})^{0.5} \quad (4)$$

The values of b and σ are found to be 6.24 and 1.02, respectively, which are characteristics for a flexible polymer chain.

The two parameters, b and σ of NaAX in 0.11 M NaCl solution have been compared with NaCX in alkali along with certain other polymeric chains and are shown in Table IV.

That the two parameters of amylose chain calculated from our results are somewhat smaller in magnitude than those found for amylose in 0.33M

KCl may be due to higher chain length^{33,34} in our case. But the similarity between our data and those found for Na polyphosphates is very striking. It may be that, because of the oxygen with its wide valence angle, in a polyphosphate chain, there seems to be less steric hindrance and hence greater flexibility in a polyphosphate chain. However, the magnitude of

TABLE IV
Comparison between the Effective Bond Length b and the Steric Factor σ of NaAX in 0.11M NaCl and Other Polymeric Chains in Appropriate Solvents

System	b , A.	$(\overline{R}_0^2)^{1/2}/(\overline{R}_f^2)^{1/2}$	References
NaAX in 0.11M NaCl (θ -solvent)	6.2	1.02	Present work
NaCX in 1M NaOH	28.9	3.70	30
Amylose in 0.33M KCl (θ -solvent)	10.95	2.38	19
Polystyrene in Toluene	7.25	—	31
Na polyphosphates in 0.415M NaBr (θ -solvent)	6.2	1.68	32

effective bond length and steric factor given in Table IV reveals that the Na cellulose xanthate molecule in 1M NaOH is stiffer than the Na amylose xanthate molecule in NaCl solution and that this difference may be due to the difference in their steric configurations.

CONCLUSIONS

Chemical reactions of Na amylose xanthate are basically similar to those of Na cellulose xanthate. Their physical properties which are primarily due to their xanthate groups are also similar, but in contrast to the stability of NaCX molecules in alkali, Na amylose xanthate undergoes degradation under alkaline condition. This degradation occurs primarily due to the oxidative breakdown of the 1-4 α -glucosidic linkages of the amylose chain and thus can be prevented if the alkaline solution is stored under N₂.

The results of light-scattering studies reveal that 0.11M and 0.25M NaCl solutions, particularly the former, conform to the θ solvent conditions in the neighborhood of 25°C. for sodium amylose xanthate. It is also known that 0.33M KCl solution is a θ solvent for amylose at about 25°C. It may possibly be that the alkali metals may have some specific interaction with the —OH groups of the amylose chain. Further studies of hydrodynamic properties on fractionated NaAX samples over a wide molecular weight range in θ solvent will be of great interest and will be taken up shortly as a part of our program of work.

Thanks are due to Mr. B. Das and Mr. P. K. Sengupta for assistance in the light-scattering study. The authors also express their gratitude to the University Grants Commission, New Delhi for the award of a research fellowship to one of them (A.G.P.).

References

1. A. J. Staverman et al., *J. Polymer Sci.*, **55**, 657 (1961).
2. J. M. G. Cowie, *J. Polymer Sci.*, **49**, 455 (1961).
3. R. S. Patel and R. D. Patel, *J. Polymer Sci. A*, **3**, 2123 (1965).
4. E. G. Adamek and C. B. Purves, *Can. J. Chem.*, **38**, 2425 (1960).
5. T. J. Schoch, *Advan. Carbohydrate Chem.*, Academic Press, New York, 1945, Vol. I, p. 259.
6. F. L. Bates et al. *J. Am. Chem. Soc.*, **65**, 142 (1943).
7. R. W. Kerr, *Chemistry and Industry of Starch*, Academic Press, New York, 1950; p. 305.
8. K. K. Ghosh, Thesis, Calcutta University, India.
9. C. Doree, *Methods of Cellulose Chemistry*, Chapman and Hall, London, 2nd Ed., 1950.
10. E. Schauenstein and E. Treiber, *Melliand Textilber.*, **32**, 43 (1951).
11. J. P. Dux and L. H. Phifer, *Anal. Chem.*, **29**, 1842 (1957).
12. E. Elmgren, *Arkiv Kemi*, **24**, 250 (1965).
13. C. W. Tait, R. J. Vetter et al., *J. Poly. Sci.*, **7**, 261 (1951).
14. B. H. Zimm, *J. Chem. Phys.*, **16**, 1093 (1948).
15. L. P. Witnauer and H. J. Scherr, *Rev. Sci. Instr.*, **23**, 99 (1952).
16. G. Oster and A. W. Pollister, *Physical Techniques in Biological Research*, Academic Press, New York, 1955, Vol. I, p. 57.
17. S. P. Mouluk, B. N. Ghosh et al., *J. Indian Chem. Soc.*, **40**, 607 (1963).
18. P. J. Flory and T. A. Orofino, *J. Chem. Phys.*, **26**, 1067 (1957).
19. C. T. Greenwood et al., *Makromol. Chem.*, **67**, 49 (1963).
20. S. N. Timasheff, B. D. Coleman and J. G. Kirkwood, paper presented at 125th Meeting of the American Chemical Society, March 1954.
21. J. G. Kirkwood and J. B. Shumaker, *Proc. Natl. Acad. Sci. U.S.A.*, **58**, 863 (1952).
22. W. B. Dandlikar, *J. Am. Chem. Soc.*, **76**, 6036 (1954).
23. R. S. J. Manley and A. Bengtsson, *Svensk Papperstidn.*, **61**, **15**, 471 (1958).
24. K. K. Ghosh and P. K. Choudhury, *Makromol. Chem.*, **102**, 217 (1967).
25. R. H. Ewart, C. P. Roe, P. Debye, and J. R. McCarthey, *J. Chem. Phys.*, **14**, 687 (1946).
26. U. P. Strauss et al., *J. Phys. Chem.*, **66**, 2235 (1962).
27. H. Benoit, *J. Polymer Sci.*, **11**, 507 (1953).
28. D. Henley, *Arkiv Kemi*, **18**, 327 (1962).
29. H. Benoit, *J. Polymer Sci.*, **3**, 376 (1948).
30. B. Das and P. K. Choudhury, *J. Polymer Sci. A-1*, **5**, 769 (1967).
31. C. E. H. Bawn, T. B. Grimley, and M. A. Wajid, *Trans. Faraday Soc.*, **46**, 1112 (1950).
32. U. P. Strauss and P. L. Winemann, *J. Am. Chem. Soc.*, **80**, 2366 (1958).
33. A. Peterlin, *J. Polymer Sci.*, **5**, 473 (1950).
34. R. Badger and R. H. Blaker, *J. Phys. Colloid Chem.*, **53**, 1056 (1949).

Received June 28, 1967

Revised September 6, 1967

Hyperelectronic Polarization in Macromolecular Solids

ROGER D. HARTMAN* and HERBERT A. POHL,
*Department of Physics, Oklahoma State University, Stillwater,
Oklahoma 74074*

Synopsis

Hyperelectronic polarization may be viewed as the electrical polarization in external fields due to the pliant interaction with the charge pairs of excitons, in which the charges are molecularly separated and range over molecularly limited domains. It is particularly pronounced in molecular solids composed of long polymeric molecules having extensive regions of electronic orbital delocalization. Hyperelectronic polarization is regarded as the principal contributor to the high polarizabilities of the following five macromolecular solids: four polyacene quinone radical polymers formed by condensation of aromatic hydrocarbon derivatives with aromatic acids and poly(Cu(II)-*N,N'*-dimethyl rubeanate). The first four polymers at 100 hz had dielectric constants of 1800-2400, decreasing to about 58-100 at 100,000 hz, with relaxation times of 10^{-3} to 10^{-4} sec. A sixth polymer, a Schiff-base condensate of 1,4-naphthaquinone and *p*-toluene diisocyanate, however, showed little hyperelectronic polarization, displaying a dielectric constant of 10, constant over 100-100,000 hz. By simple arguments it is shown that the relaxation times and the frequency response of conduction are consonant with the proposed model of charges roaming over long molecular domains (up to 4000 Å.) but restricted by molecular boundaries.

INTRODUCTION

Investigations of the electrical behavior of organic compounds date back to the turn of the century, but it was some forty years later that investigators began seriously to study organic solids. Recent studies of the electrical properties of polymeric solids have led to unexpected results, in that many such solids, normally considered insulators, have now been classified as semiconductors, and certain types, moreover, have unusually high dielectric constants.

That the latter result is surprising should be evident from the fact that these highly purified polymers are hydrocarbon derivatives, i.e. conjugated organic solids. Typical values of the dielectric constants of most types of pure polymer lie in the range of 2-10;^{1,2} however, we recently have found a polymer that exhibits a dielectric constant of 20,000 when measured at elevated pressures and temperatures.

* NSF Science Faculty Fellow during major part of this research period. Present address: Department of Physics, University of Tulsa, Tulsa, Oklahoma.

Initial measurements of extraordinarily high dielectric constants were reported by Pohl and Rosen^{3,4} in 1965. They reported dielectric constants of up to 900 at 300 hz and 85°C. for three polymers, each belonging to the polyacene quinone radical (PAQR) class. Since that time Hartman and Pohl^{5,6} have reported findings of additional polymers with dielectric constants of 2000 at room temperature; most of them are of the PAQR type, but one is a copper-complexed polyrubeanate polymer.

Certain characteristics of the electrical properties of polymeric semi-conductors with high dielectric constants have been observed.

First, it is noted that the resistivity ρ is strongly pressure-dependent and temperature-dependent³⁻⁷ and moderately sensitive to the magnitude of, and weakly dependent on, the frequency of the applied electric field. Pohl et al.⁷ have developed a theory, using transition-state formalism to describe this behavior.

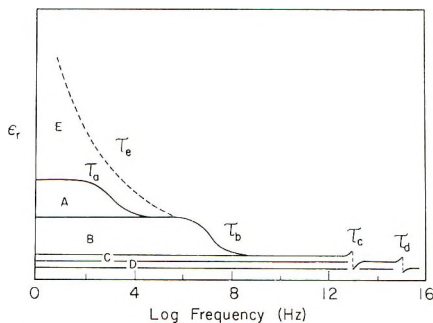


Fig. 1. Schematic diagram of electrical polarization mechanisms and their frequency responses. The region in which each mechanism predominates, along with the associated relaxation time is as follows: (A) interfacial or surface (Maxwell-Wagner) polarization; (B) dipolar polarization; (C) atomic polarization; (D) electrical polarization; (E) hyper-electronic polarization.

Second, the dielectric constant is observed to be strongly pressure-dependent and temperature-dependent, increasing with either or both parameters, but inversely dependent upon the magnitude and frequency of the applied electric field. Regarding the high dielectric constant effect, Pohl and Rosen³ first suggested a new type of polarization mechanism, called *hyper-electronic polarization*. Hyper-electronic polarization differs from ordinary electronic polarization in the following ways (Fig. 1).

(1) Normal electronic polarization^{1,2,3,9} is considered to be due to a slight shift of the centers of positive and negative charge in *atoms* when an external electric field is applied. This type of polarization usually results in a bulk polarizability, which is linearly proportional to the applied electric field for a wide range of field strengths. With respect to dispersion, this polarization mechanism exhibits relaxation at a frequency $\nu \approx 10^{15}$ hz, or a relaxation time $\tau \approx 10^{-15}$ sec. The behavior of nonpolar and normal dipolar polymers is well described by Smyth.¹

(2) Hyperelectronic polarization may be considered due to the pliant interaction of charge pairs of excitons, localized temporarily on long, highly polarizable molecules, with an external electric field (Fig. 2). These carriers, which are thermally produced by exciting intermolecular ionization levels of long conjugated molecules ($L \approx 4000 \text{ \AA.}$), are molecularly separated and range over molecularly limited domains. When an external electric field is applied, these highly mobile carriers, spending most of their time in extraordinarily long regions of near-zero resistance, form a collection of highly polarizable monopoles and therefore exhibit a very high bulk polarizability. Hyperelectronic polarization is observed to be nonlinearly dependent upon the applied electric field and exhibits dispersive relaxation at a frequency $\nu \approx 10^3 \text{ hz}$, or a relaxation time $\tau \approx 10^{-3} \text{ sec}$.

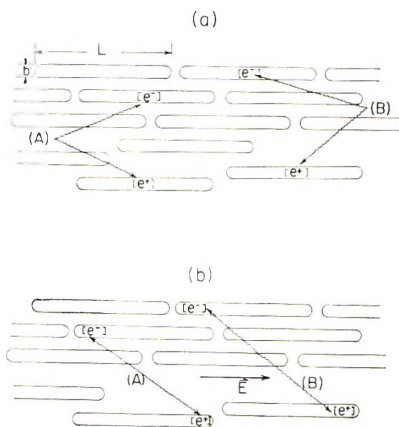


Fig. 2. Schematic diagram of monopole (exciton and ion) formation in long, conjugated polymers. Charge pairs thermally formed at regions (A) and (B) migrate to distant molecules of dimension $L \times b$. When the electric field is off (a), there is a certain amount of delocalization of the carriers, indicated by the brackets around the charges, but the net polarization is zero. With the field on (b) a large polarization results from the long domains in which the carriers may move.

Since, as is shown in Figure 1, the polarization effects in this frequency region are generally attributed to Maxwell-Wagner surface polarization,^{1,8} and since, in fact, the polymers studied are not single-crystalline but, rather, polycrystalline in nature, one must establish that, indeed, hyper-electronic polarization, rather than surface polarization, is what has been observed in these investigations.

It is the purpose of this paper to establish the mechanism of hyper-electronic polarization as being the principal contributor to the high polarizabilities observed in a number of macromolecular solids. This is accomplished by showing that numerous physical characteristics and, especially, the relaxation times and frequency response of electrical conductivity, as observed, are consistent with the proposed model of charges roaming over long domains, restricted by molecular boundaries.

We suggest that hyperelectronic polarization may be looked upon as a Maxwell-Wagner type of polarization^{1,8} observed on a molecular scale, in which the grain boundary is replaced by the molecule-to-molecule gap itself.

EXPERIMENTAL PROCEDURES

Sample Preparation

Each of the pure, dry polymers studied was a fine-grained, black, insoluble powder, with the exception of EHE102, which was more coarsely grained and was deep brown in color. They were prepared and highly purified in a manner similar to that described by Pohl and Engelhardt.¹⁰ After formation the powders were purified by continued extraction with aqueous hydrochloric acid, with hot water, with ethanol, and finally with toluene in a Soxhlet apparatus. The resultant materials were then dried and stored for use. The procedure for the preparation of each polymer follows; the composition of each is shown in Table I.

Polymers JM77B and JM85B, both PAQR's, were formed by mixing 1:1 mole ratios of anthracene with pyromellitic dianhydride (PMA) and of phenothiazine with mellitic trianhydride, respectively. The mixtures were heated at 295°C. for a period of 24 hr. under nitrogen ambient temperature¹¹ with zinc chloride as catalyst.

Polymer DP1A, also a PAQR, was prepared by mixing a 1:1 mole ratio of anthraquinone with PMA, with zinc chloride as catalyst. The mixture was heated 24 hr. at 300°C.⁴⁻⁶ Neutron activation analyses have shown that the purified polymer contains less than 5 ppm Zn.

Polymer SK3A, a copper coordination polymer, was prepared by mixing a 1:1 mole ratio of *N,N'*-dimethyl dithiooxamide with copper sulfate in a hot ethanol-water solution.^{12,13} The polymeric precipitate was purified by extraction.

Polymer EHE59, a PAQR polymer, was formed by mixing 1:1 mole ratios of fluoranthene with PMA, with 2 parts ZnCl₂ as catalyst. It was heated to 306°C. for 24 hr.¹⁰ and then purified as for the PAQR polymers.

TABLE I
Composition of Polymers

Polymer	Type	Composition	Ref.
DP1A	PAQR ^a	Anthraquinone PMA ^b	4-6
JM77B	PAQR	Anthracene PMA ^b	11
JM85B	PAQR	Phenothiazine MTA ^c	11
EHE59	PAQR	Fluoranthene PMA ^b	10
EHE102	Schiff's base	1,4-Naphthaquinone- <i>p</i> -TODI ^d	10
SK3A	metallo-	Cu(II)- <i>N,N'</i> -dimethyl rubeanate	12,13

^a Polyacene quinone radical polymer.

^b Pyromellitic dianhydride.

^c Mellitic trianhydride.

^d Toluene diisocyanate.

Polymer EHE102, a Schiff base, was prepared by heating 1:1 mole ratios of 1,4-naphthaquinone with *p*-toluene diisocyanate to 300°C. in the absence of air¹⁰ and then was purified as the PAQR polymers were.

Dielectric Constant Measurements

The dielectric constants and resistivities were determined in the frequency range of 100 hz to 100 khz by measuring the parallel capacitance and resistance of the samples in a Bridgman opposed-anvil high-pressure cell. The cell has been described elsewhere.⁴ A General Radio 716C capacitance bridge, modified into a comparison bridge of the type proposed by Koops,¹⁴ was employed for measuring these properties. This bridge has the advantage over most bridges that it yields the parallel capacitance C_p and parallel resistance R_p of the unknown directly.

The test cell was carefully checked with blanks of mica, Teflon, polyethylene, and polystyrene, substituted for the sample for determination of the contribution of the cell to the capacitance measured. During actual measurements of capacitance a bridge balance was determined, first with the unknown sample and then with a standard mica capacitor in series with the unknown sample. This produced two balances, from which the actual capacitance contribution of the sample could be computed free from background.

Equivalent capacitance circuits of the systems are shown in Figure 3. The initial bridge balance C_1 is given by

$$C_1 = C_B + C_x \quad (1)$$

where C_B is the background capacitance due to the leads and stray capacitance, and C_x is the capacitance of the sample in the cell. The second bridge balance with the mica in series yields a new value, C_2 , given by

$$C_2 = C_B + (C_x C_m)/(C_x + C_m) \quad (2)$$

where C_m is the capacitance of the mica standard.

By subtracting eq. (2) from eq. (1) and solving for C_x one obtains

$$C_x = \{ \Delta C \pm [(\Delta C)^2 + 4\Delta C C_m]^{1/2} \} / 2 \quad (3)$$

where $\Delta C = C_1 - C_2$. The negative sign is to be avoided, since it is not physically permissible. This can be seen by choosing $\Delta C \gg C_m$. In the limit, as $C_x \rightarrow 0$, from eq. (2) we have $C_2 = C_B$ and then $\Delta C = C_x$. For eq. (3) to give the correct value one must take the plus sign only.

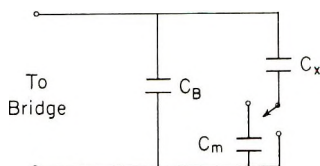


Fig. 3. Schematic diagram of the circuit measuring dielectric constant.

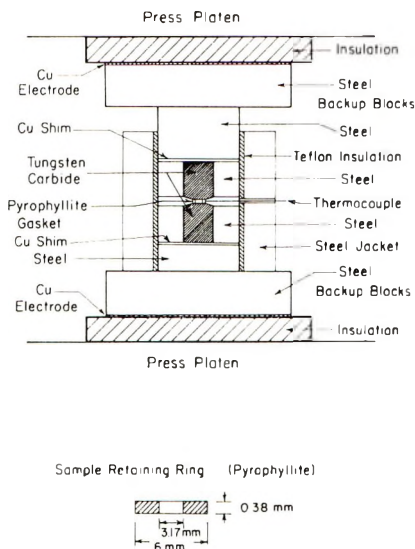


Fig. 4. Section view diagram of the anvil apparatus for obtaining extreme pressure.

Since in some cases the in-place resistance of the sample may be quite low (100 ohms), one must take care that the effective capacitance is being measured correctly. To make certain that such was the case, standard resistors (1%) mounted in parallel with standard mica capacitors, whose nominal R_p and C_p values corresponded to the respective values measured for the sample, were frequently substituted into the unknown arm of the bridge. The balance obtained agreed with the standard values to within 5% at 1 khz. Below 1 khz the reliability drops, whereas it is improved at frequencies above 1 khz.

Before electrical measurements were made, each thoroughly dried sample, which was initially polycrystalline in form, was premolded under high pressures (up to 20 kbars). The resulting dense pellet was then placed in the high-pressure cell, and measurements were made at a pressure of 1.37 kbars. A Pasadena Hydraulics Model SB-230C press (50 tons) provided uniaxial pressure on the specimen.

Exceptions to these procedures are the procedures for polymer DP1A whose data were taken at 15 kbars and on polymer SK3A, whose data were taken at 7.85 kbars; the initial pressure cell would not allow the high pressures to be attained. For the measurements in these instances the cell shown in Figure 4 was used, the specimen being contained in a pyrophyllite retaining ring.

RESULTS AND DISCUSSION

The observed variations in resistivity (or conductivity) and permittivity of the samples appear to be consistent in all respects with the proposed model of hyperelectronic polarization.⁴ They include the electrical

response of the polymers to temperature, pressure, electric field strength, and frequency of applied field. In what follows we shall enlarge upon these observed effects and thereby show the consistency of the data with the proposed model. The theory and behavior of conventional nonpolar and dipolar polymers with dielectric constants ranging from 2 to 10 have been presented elsewhere.^{1,2,15-17}

Our model of the phenomenon of hyperelectronic polarization is as follows. In this type of electrical polarization one observes the response to an external electric field of an assembly of highly mobile charges lying individually in extended regions of near-zero resistance (i.e., in extraordinarily long sequences of associated π orbitals) but limited in path ultimately by the molecular boundary. The initial charge separation is that due to the formation of normal and easily thermally excited intermolecular excitons and ions in long, conjugated molecules. This dissociation of charge pairs creates what is in effect an assembly of highly field-sensitive monopoles.

In the absence of an external field the monopoles will mutually interact, forming domains of spiralled and cyclized links of polarization. The collection of domains will exhibit a near-zero overall moment, which is easily perturbed by external fields. The field response will be nonlinear, for it is to be expected from the model (nearly free charges each situated on a very long domain) that small fields will already produce a large displacement of the charge and a large net dipole per charge pair. Because of the kinetic and transitory nature of the individual monopoles a finite rate of domain reorganization is expected, leading to noticeable field dependence, the low frequencies being the most effective. Furthermore, the formation, recombination, and intermolecular transfer rate of the excitons and ions and, hence, of the monopoles are obviously temperature-dependent and pressure-dependent, as is known from conduction studies of the eka-conjugated^{7,18-20} polymers. Accordingly, one expects the degree of hyperelectronic polarization to be both temperature-dependent and pressure-dependent.

The postulated hyperelectronic polarization fits the observed behavior in five respects, as was shown earlier.⁴ The model correctly fits (1) the unusually high dielectric constants now observed for hydrocarbon derivatives ($\epsilon_r = 50-20,000$, compared to $\epsilon_r = 2-7$, normally observed for hydrocarbon derivatives), (2) the observed field dependence, both as to sign and magnitude, (3) the observed temperature dependence, (4) the observed pressure dependence, and (5) the observed frequency dependence of the dielectric constant. The present discussion will emphasize these five aspects to fit with respect to further recent data and then develop a strong further argument for the concept of hyperelectronic polarization which is based upon the relaxation times of polarization and conduction and upon sample morphology.

Figures 5 and 6 display the variation of the relative dielectric constant and conductivity with frequency for sample DP1A. The data on the other samples have been reported,^{5,6} so here no actual curves are shown for them; however, the electrical properties of all six samples are tabulated in Table II.

TABLE II
Electrical Properties of Polymers, Measured at a Pressure of 1.37 kbars and Room Temperature (300°K.)

Polymer	Resistivity ρ , ohm-cm.					Relative dielectric constant, ϵ_r				
	100 Hz	1 kHz	10 kHz	100 kHz	100 Hz	1 kHz	10 kHz	100 kHz	10 kHz	100 kHz
EHE102	10^9	10^9	10^9	10^9	12	10	10	10	10	10
EHE59	3.5×10^{10}					60	34	27 ^b		
JM77B	1.7×10^8	1.6×10^6	1.5×10^6		100	58	40			
DP1A	2.7×10^4	2.7×10^4	2.6×10^4	2.4×10^4	680	480	305	178		
SK3A ^b		2.3×10^4	2.1×10^4	1.4×10^4		1,520	300	200		
JM85B	930 ^c	930	930		2,400 ^c	1,800	1,000			
DP1A ^d	500	500	500	490	14,000	13,000	10,800	6,500		

^a Taken from Pohl and Engelhardt,¹⁰ measured at D.C.

^b Pressure of 7.85 kbars.

^c Measured at 300 Hz.

^d Pressure of 15 kbars.

These data represent the properties of the respective polymers at a pressure of 1.37 kbars, at room temperature (300°K.), and at the frequencies indicated, unless otherwise noted.

As one examines Figures 5 and 6 and Table II, two things become apparent. First, the dielectric constant decreases rapidly at a frequency in the range of

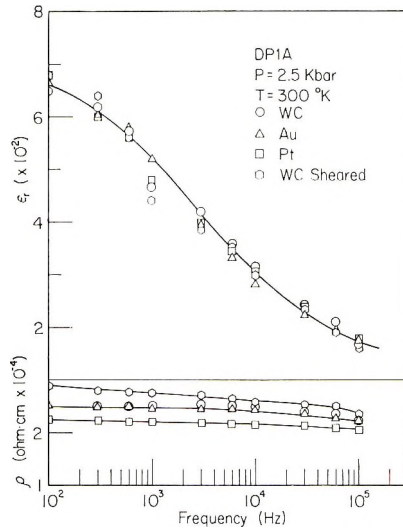


Fig. 5. The observed frequency dependence of the relative dielectric constant and the specific resistance of polymer DP-1A with varied electrodes or shearing.

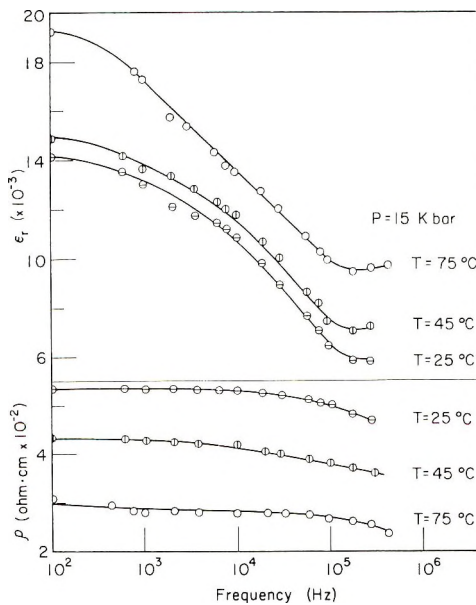


Fig. 6. The observed frequency dependence of relative dielectric constant and specific resistance of polymer DP-1A at 15 kbars and several temperatures.

1–10 khz, while the resistivity exhibits little or, at best, slight relaxation in this range. Exceptions to this generalization are the resistivity of SK3A, which tends to relax near 10 khz, and the dielectric constant of LHE102, which does not exhibit noticeable relaxation. When the samples exhibit high (hyperelectronic) polarizability, then the following behavior is in accord with the proposed model.

In comparing Figures 5 and 6 one also observes a pressure effect on the measured dielectric constant. Although it is not the purpose of this paper to discuss the pressure effect in detail, it should be mentioned that we find the dielectric constant ϵ_r pressure-dependent in the following way:

$$\epsilon_r \propto \exp \{b'P^{1/2}\} \quad (4)$$

where P is the external pressure applied to the sample. Hence, a log plot of ϵ_r versus $P^{1/2}$ yields a straight line.

It has been established⁷ that the effective resistivity of a molecular solid is pressure-dependent approximately in the following way:

$$\rho \propto \exp \{-bP^{1/2}\} \quad (5)$$

Since the resistivity is inversely proportional to the number of carriers per unit volume, n , one concludes that

$$n \propto \exp \{bP^{1/2}\} \quad (6)$$

It may be noted that the mobility also varies with pressure, but less strongly.⁷ If hyperelectronic polarization is to be observed, it should be dependent on pressure as given by eq. (6), since the number of carriers present on the molecular domains determine the amount of polarization observed. This type of pressure response is observed and is in agreement with the model proposed.

Concerning the temperature effect on the dielectric constant, it may be seen from Figure 6 that, as one increases the temperature, the dielectric constant increases. This is in agreement with earlier work by Rosen and Pohl⁴ and with the model proposed. The model suggests that the carriers, which form the monopoles necessary for the effect of hyperelectronic polarization to occur, are formed by an activation process. Hence, one should expect the dielectric constant to exhibit rather strong temperature dependencies. This effect is being studied in more detail at the present time and will be reported upon later.

Regarding the electric field dependence of the dielectric constant, it was observed³⁻⁶ that the dielectric constant drops off roughly as the inverse of the applied electric field strength. This should again be expected from the model, since it should take only a slight field to displace the highly mobile carriers within the molecular domain of near-zero resistance. As the field strength is decreased, a hopping of the carrier from one molecule to another, rather than an oscillation of the carrier within its respective domain, will predominate. This is readily seen, since the carrier will be given enough energy from the field change over the long (about 4000 Å.) length of the

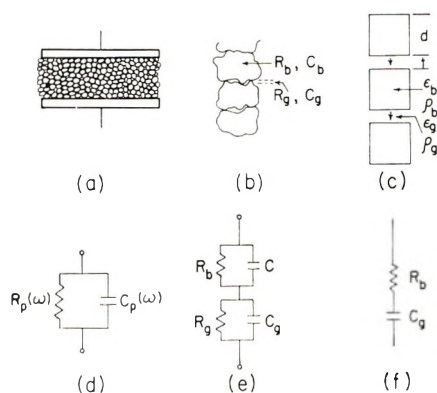


Fig. 7. Resistance-capacitance network configurations: (a) representation of a polycrystalline sample between parallel capacitor plates; (b) enlarged view of the voids between grains; (c) idealized polycrystalline solid, composed of cubes of dimension d , separated by air gaps of dimension t ; (d-f) various ways of representing polycrystalline sample in lumped-circuit equivalents.

molecular domain to *hop* the energy barrier at the end of the domain. After hopping, the motion of the carriers will no longer be in phase with the oscillations of carriers still localized on distant molecular domains, and thus the hyperelectronic polarization effect eventually disappears, as the field is increased without limit.

Convincing evidence of hyperelectronic polarization in macromolecules may be seen in the frequency response of the dielectric constant and resistivity. It has already been mentioned that for the samples studied we observed a strong dispersion in the dielectric constant near a frequency of 1–10 khz.

The question is raised whether this dispersion frequency, indicating a relaxation time of the order of 10^{-3} to 10^{-4} sec, is consistent with what one should expect from a simple treatment of a polycrystalline sample, in which one observes a Maxwell-Wagner type of polarization.^{1,2,14}

In dealing with ceramic or other polyphase materials one may choose a method of characterizing the sample's electrical behavior from a number of equivalent circuit configurations. Figure 7 displays several such configurations. In each case, if the grain-boundary properties are related to the gap properties, such that $R_b \ll R_g$ and $C_b \ll C_g$, where R_b and C_b are the parallel resistance and parallel capacitance of the bulk grain boundaries, and R_g and C_g are the same parameters for the gap, then the resistance R_p and capacitance C_p and, hence, resistivity and dielectric constants will exhibit dispersion, as shown in Figure 8.^{1,2,14,21-24} Considering the simplest circuit (Fig. 7f) as the equivalent configuration for the macromolecular solids, we proceed to estimate the order of magnitude of the relaxation times one should expect.

To arrive at an order-of-magnitude estimate of the relaxation time, we shall temporarily consider the sample to be composed of a one-dimensional

array of cubic bulk grains of dimension d , separated by air gaps of dimension l . For such a case the Maxwell-Wagner relaxation time is given by

$$\tau_{MW} = R_b C'_g = (\rho_b d/A)(\epsilon_g \epsilon_0 dA/l) = \rho_b \epsilon_g \epsilon_0 d^2/l \tag{7}$$

where A is the cross section of the grain and gap, ϵ_g and ϵ_b are the relative dielectric constant of the gap and resistivity of the bulk grain, respectively, and ϵ_0 is the permittivity of free space. We now estimate the order of magnitude of τ_{MW} for such a system by assigning reasonable values to these parameters.

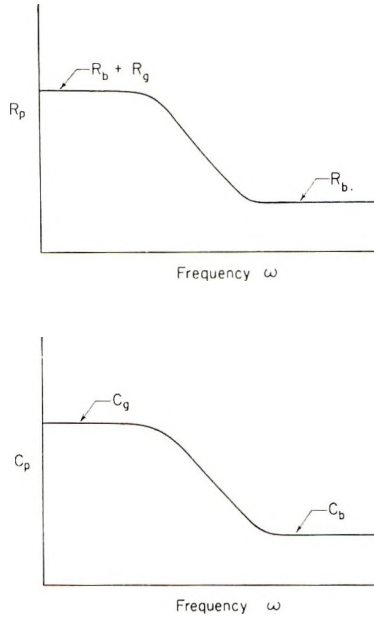


Fig. 8. Change of effective parallel resistance R_p and parallel capacitance C_p with frequency for simple bulk-gap models of a two-phase dielectric as implied from equivalent-circuit calculation.

Consider, for example, sample DP1A. We estimate that a bulk resistivity and dielectric constant of $\rho_b \approx 10^2$ ohm-cm. and $\epsilon_b \approx 10$, a gap resistivity and dielectric constant of $\rho_g \approx 10^{20}$ ohm-cm. and $\epsilon_g \approx 1$, a grain size of $d \approx 10 \mu$, and a gap of $l \approx 1000$ A. are reasonable parameters for the sample. From these values one calculates the relaxation time from eq. (7) to be

$$\tau_{MW} \approx (1 \text{ ohm-m.})(1)(8.85 \times 10^{-12} Fd/M)[(10 \times 10^{-6} M)/ (100 \times 10^{-10} M)]$$

$$\tau_{MW} \approx 10^{-9} \text{ sec.}$$

This value of τ is far removed from the value observed ($\tau_{obs} \approx 10^{-3}$ sec.).

One may choose to use a more elegant Maxwell-Wagner model for computing the relaxation times, in hopes of obtaining better agreement with the

observed τ_{obs} . For example, Takashima²⁴ has developed an expression for τ for dielectric particles dispersed in a continuous medium:

$$\tau_T = (2\epsilon_1 + \epsilon_2)/4\Pi(2\sigma_1 + \sigma_2) \quad (8)$$

where ϵ_1 and σ_1 are the dielectric constant and conductivity of the particles and ϵ_2 and σ_2 are the dielectric constant and conductivity of the medium. Note that here ϵ is not the relative dielectric constant as used before. We therefore must multiply eq. (8) by ϵ_0 .

Taking the same values for sample DP1A as used above in the calculation of τ_{MW} , we find

$$\begin{aligned} \tau_T &= [2(10) + 1](8.85 \times 10^{-12}Fd/M)/4\Pi[2(1) + 10^{-20}(\text{ohm-m.})^{-1}] \\ \tau_T &\approx 10^{-11} \text{ sec.} \end{aligned}$$

This τ does not agree as well with τ_{obs} as does the simple model that was first chosen. This anomaly may be removed, however, if one uses the hyper-electronic polarization model, in which the *molecule* is considered to be quite elongated and is treated as the bulk *grain*.

Pollak²⁵ has pointed out, in an analysis of Takashima's approach²⁴ to calculating relaxation times for DNA, that eq. (8) is not applicable in cases of highly elongated molecules. He developed an expression for τ that is appropriate to the case of a Maxwell-Wagner mechanism for highly elongated molecules. For elongated molecules of length L and diameter b , with $b \ll L$, Pollak's relaxation time τ_P is given by two forms, one representing polarization along the long dimension and the other along the short dimension:

$$\tau_L = 2L^2\epsilon/(Cb^2\sigma_L) \quad (9a)$$

$$\tau_b = 2\epsilon/\sigma_b \quad (9b)$$

where $C = 2 \ln(4L^2/b^2)$, ϵ is an average dielectric constant of the medium and the molecules, and σ_L and σ_b are the conductivities in the respective directions within the molecule.

Since the large domain is dominant for observing hyper-electronic polarization, we are concerned only with eq. (9a). Further, since we are interested in an order-of-magnitude calculation only, we replace eq. (9a) with

$$\tau_P \approx \epsilon_0\epsilon_b\rho_b(L/b)^2 \quad (10)$$

according to Pollak's suggestion.²⁶ Again, using the parameters chosen for sample DP1A and, in addition, using for L the value of 4000 Å., as suggested by Pohl and Rosen,³ and for b the average chain diameter distance of 4 Å., one computes τ_P :

$$\begin{aligned} \tau_P &\approx 10(8.85 \times 10^{-12})(Fd/M)(1 \text{ ohm-m.})[(4000 \text{ Å.})/(4 \text{ Å.})] \\ \tau_P &\approx 10^{-4} \text{ sec.} \end{aligned}$$

This calculated τ_P agrees well with the observed τ_{obs} and lends strong support to the interpretation that the high dielectric constants observed are due to hyper-electronic polarization, as postulated earlier.

Table III lists estimated parameters for the six polymers investigated in this study, and Table IV lists the relaxation times computed by the formulae used for sample DP1A. It is seen that in all cases the Pollak relaxation time closely agrees with the observed relaxation time.

Hence, from an analysis of the relaxation times we see that the results indicate that normal macroscopic Maxwell-Wagner polarization cannot account for the observed results; however, hyperelectronic polarization, or Maxwell-Wagner polarization on the molecular scale, can reconcile the anomaly in relaxation times.

TABLE III
Estimated Parameters for Polymers

Polymer	Bulk properties					Gap properties		
	ϵ_b	ρ_b , ohm-cm.	d , μ	L , A.	b , A.	ϵ_g	ρ_g , ohm-cm.	t , A.
EHE102	10	10^6	1000	4000	4	1	10^{20}	10^4
EHE59	10	10^3	100	4000	4	1	10^{20}	10^3
JM77B	10	10^3	10	4000	4	1	10^{20}	10^3
DP1A	10	10^2	10	4000	4	1	10^{20}	10^3
SK3A	10	10^3	10	4000	4	1	10^{20}	10^3
JM85B	10	10^2	10	4000	4	1	10^{20}	10^3

TABLE IV
Relaxation Times of Macromolecular Solids

Polymer	Relaxation time, sec.			
	τ_{obs}^a	τ_{MW}^b	τ_T^c	τ_P^d
EHE102	$>10^{-2}$	10^{-4}	10^{-7}	1
EHE59	10^{-4}	10^{-7}	10^{-10}	10^{-3}
JM77B	10^{-3}	10^{-8}	10^{-10}	10^{-3}
DP1A	10^{-3} to 10^{-4}	10^{-9}	10^{-11}	10^{-4}
SK3A	10^{-4}	10^{-8}	10^{-10}	10^{-3}
JM85B	10^{-3}	10^{-9}	10^{-11}	10^{-4}

^a Observed relaxation time.

^b Relaxation time as calculated from Maxwell-Wagner effects, eq. (7).

^c Relaxation time as calculated by Takashima's method, eq. (8).

^d Relaxation time as calculated by Pollak's method, eq. (10).

It is well known that macroscopic-scale Maxwell-Wagner (interfacial) polarization depends sensitively upon the morphology of the materials present. Typical assemblies of materials exhibiting such Maxwell-Wagner polarization are alternant sheets of metal and insulator, or dispersions of metallic spheres in an insulator matrix,² and compactions of conducting oxide grains, surrounded by thin layers or pellicles of less conductive materials or by voids.^{14,21-23} The observed frequency response of the effective dielectric constant and in-place resistance of these macroscopically in-

homogeneous materials can be simulated "theoretically" by curve-fitting with the use of lumped-circuit equivalents with a complex of virtual resistors and capacitors in various series and parallel arrays (von Hippel, Chap. 26,² and others).^{14, 21, 23-24} The method of lumped-circuit equivalents is a powerful means of giving an *engineering* description of practically any dielectric, even, as von Hippel² showed, of water or chlorinated hydrocarbons, which are certainly single-phase systems. The fact that a given dielectric behavior can practically always be expressed in terms of lumped-circuit equivalents has led some to the erroneous belief that a successful matching of the dielectric characteristics by lumped-circuit equivalents then implies that the material is displaying macroscopic-scale Maxwell-Wagner or interfacial polarization. Such a conclusion is unwarranted, as von Hippel showed in the cases of water and the chlorinated hydrocarbons. In the present case of polymers that exhibit very high dielectric constants one could construct a lumped-circuit equivalent made of virtual capacitors and resistors in some array that would give an excellent engineering description of a given polymer but that type of analysis would present no evidence, pro or con, of the fundamental nature of the polarization processes actually present. An analysis by lumped-circuit equivalents cannot in itself distinguish between macroscopic-scale Maxwell-Wagner (interfacial) polarization and molecular-scale Maxwell-Wagner (hyperelectronic) polarization.

How, then, can one distinguish between, on the one hand, interfacial polarization, which always involves at least two phases of materials, and, on the other, those polarizations which are molecular in their scale of origin? In particular, what evidence can be adduced that in the polymers under discussion here the polarization is hyperelectronic and of some other molecular-scale type rather than macroscopic and interfacial?

To begin with, we make the three following points.

First, these polymers are single and highly purified materials.

Second, under the conditions of measurement (temperatures up to 150°C., pressures up to 20,000 atm, or 300,000 psi) the samples must be void-free, for the pressures are about 10 times greater than the compressive or tensile strengths of known organic polymers.²⁷ The polymers cannot, therefore, be giving rise to an interfacial polarization of a particle-void-particle type, for the dielectric properties vary smoothly with pressure and temperature over all ranges. The dielectric constant, for example, increases steadily with pressure, even at the extreme pressures, and does not show sign of the collapse at extreme pressures that might be expected of voids in soft materials.

Third, it might be argued that the polymers, here found to have high dielectric constants, have some special gross morphology capable of showing interfacial polarization, such as conductive particles surrounded by thin pellicles of poorly conductive polymer. This argument is very hard to refute, for its proponent can always suppose "insulating monolayers" and the like, which no techniques known to us could show to be positively absent. However, we consider the following evidence to constitute con-

siderable grounds for believing that no such polymer phases cause the observed high polarization.

First, the pure polymer SK3A, which is Cu(II)-*N,N'*-dimethyl rubeanate polymer, is very soft and flows like butter under the pressures given. Under high magnification molded samples show no evidence of physical inhomogeneity. It is furthermore very difficult to conceive that this single substance of high dielectric constant (≈ 1600) can maintain a two-phase nature, as in, for example, the ceramic or oxide compacts,²¹⁻²³ which have a thin, poorly conducting layer, always surrounding a conducting region (if conducting regions gain contact across the sample, they "shunt out" the interfacial polarization) throughout the pressure range and temperature range of the experiment. We conclude that the Cu(II)-*N,N'*-dimethyl rubeanate polymer is a macroscopically homogeneous polymer displaying hyperelectronic polarization.

Second, if a polymer sample is indeed an assembly of conductive grains, each wrapped in a layer of poorly conductive substance, one should expect that harsh physical treatment, such as intense and long-continued shearing, would bring about notable changes in the grain-to-layer distribution and, therefore, in the interfacial polarization. But exposure of the polymer even to drastic shear produces no particularly significant change, as one can see by inspection of the data of Table V. The sheared sample, premolded at 20 kbar, was subject to 3° of shear ten times while under 2.5 kbar of uniaxial pressure and in a layer 0.25 mm. thick. The dielectric constants for the sheared and unsheared samples agree to within $\pm 10\%$, the precision of measurement. We conclude, then, from the knowledge that these polymers are single substances, from the evidence of microscopic examination, from the observation of high (1600) dielectric constant on a polymer that is physically weak and waxy, and from the unchanging dielectric behavior

TABLE V
Dielectric Constant for Polymer DP1A at Room Temperature (300°K.) as Function of Several Sample Thicknesses, Electrode Materials, and Pressure-Shear Treatments^a

Pres- sure, kbar	Mechanical treatment	Electrode material	Sample thickness <i>t</i> , mm.	ϵ_r			
				100 hz	1 khz	10 khz	100 khz
2.8	Unsheared	WC	0.33	590	451	336	—
1.2	"	WC	0.25	600	470	342	—
2.5	"	WC	0.24	750	490	260	172
2.5	"	WC	0.16	732	485	303	171
2.5	"	WC	0.13	565	425	336	155
1.5	"	Pt	0.33	680	480	305	178
2.5	"	Au	0.24	666	520	280	176
2.5	Sheared (60° at 2.5 kbars)	WC	0.14	680	445	300	162

^a All except the first two entries were premolded at 20 kbars; they were premolded at lower pressure. *E* field ≈ 7 to 10 v./cm. on each sample.

despite drastic shear, that the observed high polarizability here is *not* due to the presence of two phases (interfacial polarization).

Fourth there remains the possibility that the observed effective high dielectric constants of these polymers is due to a surface-layer effect between the sample and the contacting electrodes of the measuring cell. If this were the case, it should show up on a change of sample thickness or of electrode materials. As may be seen from the data of Table V, the measured dielectric constant is not a function of sample thickness. From the data of Table V and Figure 5 we see also that the electrode material has no visible effect. We conclude, therefore, that surface polarization effects are absent or so small as to be within experimental error. They certainly cannot account for the observed high dielectric constants of these polymers.

In addition, in the case of normal Maxwell-Wagner polarization both the dielectric constant and the resistivity should exhibit dispersive effects at or near the same frequency. In general, our samples did not show a resistivity dispersion in the range of frequencies studied (100 hz to 100 khz).

CONCLUSION

Hyperelectronic polarization appears to be the primary cause of extremely large dielectric constants in certain macromolecular solids that are composed of long polymeric molecules.

It is seen from an examination of the relaxation times of the dielectric constants that one could not be observing normal, surface grain-boundary polarization of the Maxwell-Wagner type. However, if one assumes the hyperelectronic model to be applicable, whereby (1) the grain boundary is replaced by the molecule itself and (2) the relaxation time is modified by the product of the square of the ratio of the molecular length to molecular diameter, as suggested by Pollak,^{25,26} one then finds that the calculated relaxation time is in agreement with the observed relaxation time. Thus, hyperelectronic polarization may be looked upon as Maxwell-Wagner polarization occurring on a molecular scale.

We have shown that surface polarization does not contribute to the polarization observed by noting that the observed dielectric constant does not change either with sample thickness or with the electrode material used. We have shown also that interfacial polarization or normal, surface grain-boundary polarization of the Maxwell-Wagner type, such as is caused by the presence of two interspersed phases of differing conductance, is very unlikely in these polymers, for they (1) are single, pure substances, (2) are free from voids, (3) possess high dielectric constants (1600) even when very soft, (4) are homogeneous even at high magnification, and (5) display a dielectric constant unaffected by violent mechanical shear.

Other results that support the hyperelectronic-polarization model include an inverse electric field dependence and direct temperature and pressure dependence as observed for the dielectric constant. This is to be expected for a material composed of highly elongated molecules on which charge carriers produced by activation processes are temporarily localized.

Hence, we conclude that hyperelectronic polarization is the principal contribution to the high polarizabilities of long, polymeric, eka-conjugated,^{4,10,18} macromolecular solids.

The authors wish to thank Michael Pollak for his helpful discussions and suggestions during the development of this paper. They also wish to express their thanks to James W. Mason, Seiichi Kanda, Douglas Pohl, and Eugene H. Engelhardt for the synthesis of polymers bearing their respective initials. They acknowledge with thanks the support of the Research Foundation of Oklahoma State University during this study. In addition, one of us (R. D. H.) wishes to acknowledge financial support from the National Science Foundation in the form of a Science Faculty Fellowship.

Work submitted in partial fulfillment of the requirements for the Doctor of Philosophy in Physics at Oklahoma State University.

References

1. C. P. Smyth, *Dielectric Behavior and Structure*, McGraw-Hill, New York, 1955.
2. A. von Hippel, *Dielectric Materials and Applications*, Wiley, New York, 1956.
3. H. A. Pohl and R. Rosen, *Bull. Am. Phys. Soc.*, **10**, 396 (1965).
4. R. Rosen and H. A. Pohl, *J. Polymer Sci. A-1*, **4**, 1135 (1966).
5. R. D. Hartman and H. A. Pohl, paper presented at Am. Phys. Soc. Meeting, Chicago, March 27-30, 1967; cf. *Bull. Am. Phys. Soc.*, **12**, 409 (1967).
6. R. D. Hartman, *Proc. Oklahoma Acad. Sci.*, **47**, in press.
7. H. A. Pohl, A. Rembaum, and A. Henry, *J. Am. Chem. Soc.*, **84**, 2699 (1962).
8. A. von Hippel, Ed., *Dielectrics and Waves*, Wiley, New York, 1954.
9. H. Frölich, *Theory of Dielectrics*, Oxford Press, London, 1949.
10. H. A. Pohl and E. H. Engelhardt, *J. Phys. Chem.*, **66**, 2085 (1962).
11. J. W. Mason, H. A. Pohl, and R. D. Hartman, in *Electrical Conduction Properties of Polymers*, (*J. Polymer Sci. C*, **17**), A. Rembaum and R. F. Landel, Eds., p. 187, 1967.
12. R. D. Hartman, S. Kanda, and H. A. Pohl, *Proc. Oklahoma Acad. Sci.*, **47**, in press.
13. S. Kanda, *J. Chem. Phys.*, **34**, 1070 (1961).
14. C. G. Koops, *Phys. Rev.*, **83**, 121 (1951).
15. H. Frölich, *Proc. Roy. Soc. (London)*, **185A**, 399 (1946).
16. R. M. Fuoss, in *The Chemistry of Large Molecules*, Ch. VI., R. E. Burk and O. Grummitt, Ed., Interscience, New York, 1943.
17. R. M. Fuoss, *J. Am. Chem. Soc.*, **63**, 2401, 2410 (1941).
18. H. A. Pohl, in *Electrical Conduction Properties of Polymers*, (*J. Polymer Sci. C*, **17**) A. Rembaum and R. F. Landel, Eds., p. 13 (1967).
19. F. Gutmann and L. E. Lyons, *Organic Semiconductors*, Wiley, New York, 1967, p. 481.
20. A. Rembaum and J. Moacanin, *Polymeric Semiconductors*, Jet Propulsion Laboratory, Pasadena, Calif., 1964.
21. L. G. Van Uitert, *Proc. IRE*, **44**, 1294 (1956).
22. E. J. W. Verwey, *Semiconducting Materials*, Butterworths, London, 1951, p. 151.
23. H. E. Matthews, Jr., *Proc. Oklahoma Acad. Sci.*, **45**, 138 (1965).
24. S. Takashima, *J. Mol. Biol.*, **7**, 455 (1963).
25. M. Pollak, *J. Chem. Phys.*, **43**, 908 (1965).
26. M. Pollak, private communication.
27. N. Lange, *Handbook of Chemistry*, McGraw-Hill, New York, 1967, p. 868.

Received August 25, 1967

Anion Radicals of Polyphenylsiloxanes*

D. H. EARGLE, JR., *University of Illinois at Chicago Circle, Chicago, Illinois 60680*, and W. B. MONIZ, *U.S. Naval Research Laboratory, Washington, D.C. 20390*

Synopsis

The anion radicals of a number of siloxanes bearing phenyl and methyl substituents have been prepared by metal reduction. The cleavage and reaction mechanisms of these radicals have been studied by ESR, and interpretations have been made regarding the structures of the radicals.

Introduction

The effect of substituting phenyl groups for methyl in polysiloxanes of similar chain length is an enhancement of the thermal^{1,2} and oxidative³ stability of the molecule. An increase of the phenyl/methyl ratio of these compounds will lessen destructive effects.⁴ At elevated temperatures the most common degradative processes are cyclization of the linear chains into trimers and tetramers (lowering viscosity), and crosslinking (leading to gels). An effort has been made in this research to discover a mechanism whereby the aromatic phenyl groups improve the stability of the molecules. The technique chosen was that of metal reduction in ethereal solvents, which normally results in the production of free radicals, especially if aromatic groups are present in the molecule. The strong electron affinity of aromatic rings, as opposed to saturated molecular structures, is well known.⁵ The initial hypothesis to be tested was that a large number of phenyl groups to be found in several polysiloxanes should stabilize an odd electron more readily than a compound of very low phenyl/methyl ratio.

Experimental Results

Electron paramagnetic resonance (EPR) was used for detecting the presence of the radicals formed in the reduction of polymers. A definite trend was found toward increased ease of radical formation with increasing phenyl/methyl ratio; the results are tabulated in Table I. In those compounds which were reducible the paramagnetic material detected by EPR was orange-brown with a greenish tinge. The EPR spectrum of the phenyl-methyl compounds was in almost every case observed, 20-28 lines with a "hole" in the middle (Table II) indicating interaction of the

* Presented in part at the 151st National Meeting of the American Chemical Society, Pittsburgh, Pennsylvania, April 1966.

TABLE I
 Reduction of Siloxane Fluids

Compound ^a	Av. mol. wt.	Si atoms (approx.)	Ratio phenyl to methyl ^b	Direction of increasing		
				Therm. stabil.	Oxidat. stabil.	Reductibility (free-rad.)
D.C. 200	458	6	0.0	→	→	←
D.C. 510	—	—	0.1	→	→	←
D.C. 258	2000	22	0.3	→	→	←
G.E. 1032	2000	22	0.3	→	→	←
D.C. 550	—	—	0.5	→	→	←
D.C. 702	530	5 to 6	0.7	→	→	←
G.E. 1033	530	5 to 6	0.7	→	→	←
D.C. 704	484	4 to 5	1.0	→	→	←
D.C. 710	2600	20	1.0	→	→	←

^a D.-C., Dow-Corning siloxane fluid number; G.E., General Electric siloxane fluid number.

^b A measure of the independent phenyl groups with respect to methyl groups on the central silicon atoms of linear polysiloxanes, the trimethyl silyl endgroups remaining unchanged.

TABLE II
Radicals of $\phi_2\text{Si}-\text{O}$ —Type of Molecule

	Initial hyperfine splitting			Final hyperfine splitting	
	lines/ a_1	lines/ a_2	ΔH	lines/ a_1	ΔH (if different)
$(\phi_2\text{SiO})_3$ (cyclic trimer)	2/8.4	6/3.1	21.5	5/4.1	21.5
	6/3.7	—	—	4-5/4	—
$(\phi_2\text{SiO})_4$ (cyclic tetramer) G.E. 1032 ^b	2/8.9	6/3.1	21.5	5/4.1	21.5 ^a
	2/4.9	$\approx 5/.84$	18.8	9/1.9	18
		(one set of quintets noted in each wing)			
G.E. 1033 ^c	2/5.4	8/1.6	ca. 14.5	—	—
	9/1.72	—	—	9/1.44	17.6
$[\phi_2\text{SO}_2]_{\phi_2}$	9/2.37				
	9/2.65				
$\phi_2\text{SiH}_2$ $\phi_2\text{Si}(\text{OH})_2$ [actually, $\phi_2\text{Si}(\text{OK})_2$]	2/9 (MeTHF)	5?/1.9	23.5	biphenyl! (in DME)	
	overlays cyclic tetramer			overlays tetramer	

^a The B set is apparently covered by the very broad lines of the A set.

^b $\text{Me}_2\text{SiO}(\phi_2\text{SiO})_n(\text{Me}_2\text{SiO})_m\text{SiMe}_3$, $n + m \approx 22$.

^c In this, $n + m \approx 6$.

electron with an odd number of protons. The envelope shape was of two large sets of lines, indicating primary splitting of a single proton. The total width of a spectrum was only about 18 Gauss, an indication that the odd electron is not widely delocalized; the sharpness and narrowness of the lines indicate that the radicals are not rapidly exchanging spin with unreduced material or with neighboring aryl portions of the molecule.

Table I, then, shows that an increase in the phenyl/methyl ratio created increasingly favorable conditions for the metal-reductive production of an anion radical. Evidence of reducibility was in part an observable development of color in the sample tube and in part observation of the development of an EPR signal. The first color noticeable was a light peach color (not paramagnetic); it was followed by a darkening of the solution and increasing strength of the EPR signal. The all-methyl siloxane, Dow-Corning 200 fluid, exhibited no tendency whatsoever to react or to form an anion radical. Its resistance to reduction prompted several other experiments catalogued in Table III. Number 200 continued unamenable to treatment with potassium alone (no solvent) and to biphenyl anion radical generated in its presence.

The latter experiment settled one other question: the products observed by EPR with other siloxanes probably were not the result of attacks upon the chain itself by any anion radicals of an aromatic-anion radical nature.

It was apparent from the EPR spectra (see the Discussion) that some cleavage must have occurred after the initial radical formation. An effort was made to determine the types of cleavage that might reasonably be expected from the reduction of a siloxane similar in nature but much simpler than the polymers. Such a compound was found in diphenyltetramethyl disiloxane. Complete reduction *in vacuo* followed by admission of air and analysis of products via ether-aqueous extraction and infrared

TABLE III
Treatment of Dow-Corning 200

Components	Treatment, °C. and time	Results
200 + DME + K	-70 to +60 (up to several weeks)	negative; enhanced solvation of K in DME
200 + K	-70 to +60 (1 week)	negative
200 + (C ₆ H ₅) ₂ + DME + K	-70 to room temp.	production of biphenyl negative ion; no reaction with 200, even after 1 week of contact
200 + (C ₆ H ₅) ₂	400 (1½ days) (1½ weeks)	production of broad EPR signal lessening of EPR signal; no gel formation; terminal methyl groups evident in infrared spectrum

spectroscopy showed that in addition to regenerated starting material the only material recoverable in any measureable quantity was a silanol of a structure resembling that of the starting material. This material is presumably dimethylphenyl silanol. No biphenyl (from coupled phenyl fragments) or methylene absorption (infrared spectra) was found in the neutral products, indicating that cleavage must have occurred only at the Si—O bond.

NOTE: This result is not paralleled in recent infrared studies of thermal cleavage of Dow-Corning fluids at this laboratory (USNRL), in which considerable Si—C bond cleavage was observed.

In all the reductions studied the g value was not noted to vary significantly from that of the biphenyl anion radical. A careful measurement was made of the g value of diphenyltetramethyl disiloxane against biphenyl anion radical. The deviation from the biphenyl anion radical g value was <0.0001 , a value which is insignificant compared to standard g value measurements. Moreover, ^{29}Si , of spin $1/2$, has a relative abundance of

TABLE IV
Radicals of the $\phi\text{—}\overset{\text{Me}}{\underset{\text{Me}}{\text{Si}}}\text{—O—}$ Type of Molecule

Compound	Phenyl/methyl	Comments
D.C. 702	0.7	20-line spectrum, "hole" in center with secondary splittings ≈ 0.84 G.; $a_1 \approx 7.0$ G.; $\Delta H = 18$ G.
D.C. 258	0.3	pattern similar to that of D.C. 702, $a_1 \approx 8.85$ G.
D.C. 510	0.1	spectrum identical with that of D.-C. 702
D.C. 550	0.5	spectrum identical with that of 702 but much less well resolved
D.C. 704	1.0	11-line spectrum, strong line in center, hyperfine splittings ≈ 1.6 G.; $\Delta H \approx 17.8$, same spectrum in dimethoxyethane and methyl tetrahydrofuran
D.C. 710	1.0	spectrum identical with that of D.-C. 702
$\begin{array}{c} \text{Me} \\ \\ (\phi\text{—Si—O—})_2 \\ \\ \text{Me} \end{array}$	(1.0)	spectrum a poorly resolved 20 lines, very similar to that of D.-C. 702
$\begin{array}{c} (\phi\text{—Si—O—})_3 \\ \\ \text{Me} \end{array}$	(cyclic trimer)	spectra of both trimer and tetramer almost overlay spectrum of D.-C. 258; very slight difference in hyperfine splittings and intensities
$\begin{array}{c} (\phi\text{—Si—O—})_4 \\ \\ \text{Me} \end{array}$	(cyclic tetramer)	

TABLE V
Results with Other Small ϕ -Si Molecules

$\phi_3\text{SiOH}$	pattern very similar to that of $\phi_2\text{Si}(\text{OH})_2$, but ΔH more compact by 2 G.
$\phi_4\text{Si}$	spectrum identical with published spectrum (M. G. Townsend, <i>J. Chem. Soc.</i> , 51 , 1962.)
$(\phi\text{CH}_2)_3\text{SiH}$	diamagnetic, brilliant blue, probably metal complex
$\phi_3\text{SiMe}$	signal less well resolved, but similar to that of $\phi_4\text{Si}$

only 4.70%. These observations indicate that very little spin in the reduced radical is dwelling upon the silicon atom; it does not mean, however, that the silicon atom is not acting as a conjugation agent, possibly coupling spin from a methyl group to a phenyl group.

It is not likely, either, that potassium is involved in the major sets of splittings. Some very weak potassium splitting was noted at -95° with Dow-Corning 710.

Initial studies of the reduction of the ϕMeSiO type of compound (Table IV) prompted a study of the $\phi_2\text{SiO}$ type of compound, both large and small molecules (Tables II and V). This study was necessary in order to determine the extent to which siloxane groups participate in conjugation between the groups attached to them.

Notes

1. D.-C. (Dow-Corning) 200 seemed to enhance solvation of the potassium in dimethoxyethane, as seen by the rapid development of the characteristic blue color.

2. D.-C. 510 took more than 10 min. in the cold to develop color on reduction. The more highly phenylated the other materials, the shorter the time needed; the limit was less than 1 sec. for D.-C. 704 and 710.

3. Most materials retained strong radical activity a week or more if left in the cold. Storage at room temperature frequently resulted in loss of signal and a concomitant development of a gelled brown material.

4. D.-C. 258 stabilized with cerium³ gave results identical with those of the unstabilized material in time of reduction and clarity of spectrum.

5. Overmodulation (200–300 db.) of the strong 20-line spectrum (D.-C. 258) showed a definite primary 2-line spectrum (major splitting from a single proton).

6. A thermal stability test of D.-C. 200 plus two phenyls gave a spectrum with a rather high g value and a total width of about 80 Gauss; no hyperfine splitting was observed, and there was only one strong derivative curve.

7. In D.-C. 710 and 704 oils the development of color and EPR signal was practically instantaneous. Therefore, an attempt to slow down the reaction was made by using a "poorer" solvent and a less reactive cation (sodium in methyl tetrahydrofuran), but it was unsuccessful, the reaction still being practically instantaneous; however, the spectra were less well resolved.

8. Concentration ranges are given in molarity of reducible groups for $\phi_2\text{SiO}$ (MW 198) and ϕMeSiO (MW 136), since the total molecular weights vary from 200 to 20,000:

Molecular weight	Concentration range
198	1.6×10^{-4} to $7.5^* \times 10^{-6} M$
136	2.3×10^{-4} to $1.1 \times 10^{-5} M$

Most of the samples were observed in the more concentrated state, where better resolution (without apparent line-broadening) could be obtained.

9. All the spectra were measured in dimethoxyethane with potassium metal at -50 to -85° unless otherwise specified.

10. Exhaustive reduction produced a deep-green material, whose spectra were of 4 or 5 very broad, asymmetric lines, showing that a large mixture of radicals was present.

11. The spectra were obtained from V-4501A Varian 100 kc./sec. and JES-3BS-X JEOLCO 100 kc./sec. instruments.

Discussion

The interpretation of the EPR spectra of the anion radicals met with substantial difficulties from several directions: temperature and concentration dependencies, inability to obtain good resolution, overlapping spectra, and other gross effects that might be expected from multiple reduction sites within a single polymer molecule. Since all groups of the species examined have similar structures, an effort was made to find some pattern common to all of the spectra within a group.

In almost all the siloxanes studied the EPR patterns appear to indicate two overlapping sets of spectra, apparently one each from cleaved and uncleaved molecules. Results from the Table II spectra indicate two sets of spectra (called A and B): one in which only a phenyl group

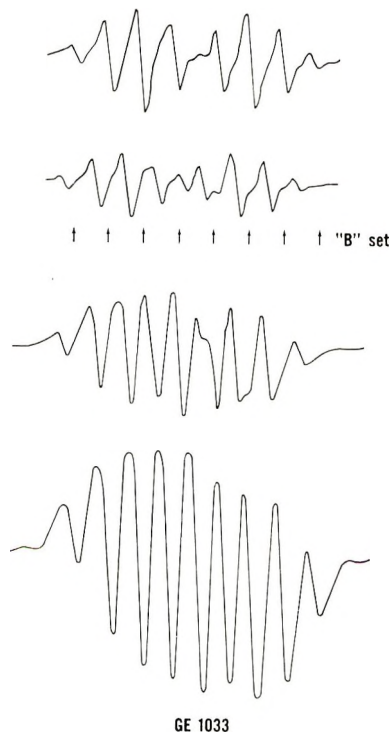


Fig. 1. EPR spectrum of anion radical of G.E. 1033: (bottom) A set; (top) B set appears upon further reduction.

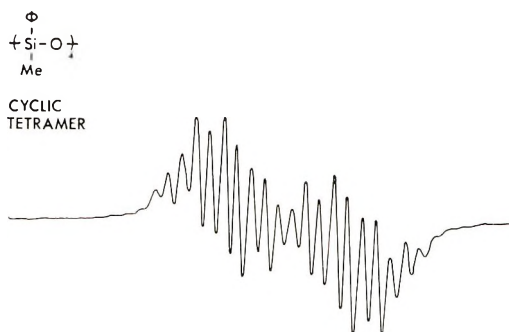


Fig. 2. EPR spectrum of $(\text{Si}-\text{O})_4$ anion radical (cyclic tetramer).

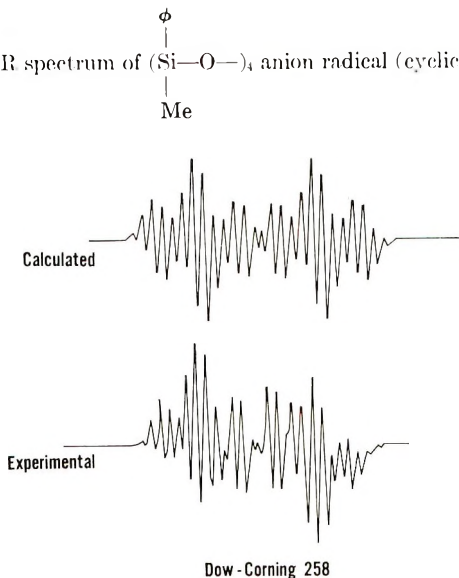


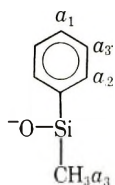
Fig. 3. EPR spectra of D.C. 25S anion radical: (top) calculated; (bottom) experimental.

participates, that is, the free electron resides only upon the phenyl group, and one in which conjugation across the Si atom takes place. This effect may be seen in GE 1033 (Fig. 1), in which there is a primary splitting of the *para* proton (5.4 G.) followed by a secondary splitting of three lines each assigned to the two *ortho* protons. No further hyperfine splitting was observed, indicating isolation (no conjugation) of the phenyl group. Upon continued reduction a second set of lines (B arrows) becomes predominant: a 9-line set, which is not unlike diphenyl sulfone and biphenyl anion radicals (see inset in Table II). This pattern would indicate conjugation between two phenyl groups through the Si atom and probably would result from some change in molecular structure (chain cleavage).

Since the spectra of the cyclic compounds of Tables II and IV overlay those of the linear compounds (as in the cyclic tetramer, Fig. 2), it is evident that the terminal methyl groups present in the linear compounds do

not participate in the hyperfine splittings and, therefore, there is no perturbation of one reducible system by an adjacent system.

Results in the Table II compounds do, in one or two instances, give some evidence of a second very weak set of splittings, but these disappear rapidly and have not been interpretable. In this series the "cleaved" material seems to predominate. The spectra (with the exception of the anomalous D.-C. 704, which, for reasons unknown, appears to approximate the A group of Table II) indicate a large primary splitting from a single proton (the phenyl para), followed by lines too great in number and too varied in intensity to be ascribed to simple *ortho* and *meta* splittings of the phenyl group. The spectrum of D.-C. 258 shown in Figure 3 (a ϕ MeSiO type of molecule) has been carefully analyzed and compared with a theoretical spectrum obtained with the following constants:

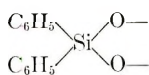


$$\begin{aligned} 1\text{H, } a_1 &= 8.85 \\ 2\text{H, } a_2 &= 3.04 \\ 5\text{H, } a_3 &= 0.76 \end{aligned}$$

It may be seen from a comparison of the experimental and theoretical spectra that the two lines to the right and left of the center are slightly more intense in the experimental spectrum. We must attribute this additional intensity to a contribution from some other cleavage product; however, its contribution is slight. It may be concluded that the methyl group participates to a large extent in conjugation with the phenyl group. If the two systems of Tables II and IV are to be considered analogous, then the spectra of the compounds of Table IV are probably derived from a structurally altered (cleaved) material.

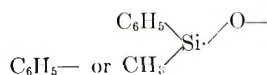
Assuming that *d*-orbital overlap of the Si—O orbital may be likened to that in sulfone and sulfoxide structures,⁶ it can be seen that the silicon atom may participate directly in spin exchange with the orbitals of the phenyl ring, or it may serve, through its *d* orbitals, to transmit spin from the phenyl ring to another phenyl or a methyl group.⁷⁻¹⁰ Schematically, the results may be demonstrated as follows:

Uncleaved moiety:

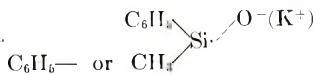


Conjugation not observed;
free electron confined to phenyl group;
yellow in color

Cleaved moiety:



or



Conjugation observed
between groups; green
or brown in color

It is unclear why the structure of the uncleaved material inhibits electron conjugation, as it apparently does. The inclusion of at least one oxygen, shown on the cleaved material, has an experimental basis in that the $(C_6H_5)_2Si(OK)_2$ spectrum is almost identical to the final cleavage product of the cyclic tetramer $[(C_6H_5)_2SiO]_4$.

Several smaller molecules (Table V) were investigated in an attempt to procure spectra of sharper splittings than those from the larger molecules, but most of them immediately decomposed, giving spectra similar to those of the decomposition products of the larger linear and cyclic materials.

In spite of the uncertainties involved in translating some of their spectra it is obvious that the phenyl siloxanes form anion radicals in the cold with ease and that regeneration of the parent compound may be accomplished with little decomposition, provided exhaustive reduction and chain scission have not been allowed to occur.

From the behavior of the anion radicals of polysiloxanes it is reasonable to conjecture that the observed thermal and oxidative stability of phenylated siloxanes may be due to the action of the aromatic moieties as free-radical traps. Such a mechanism would involve a highly transient complex, probably of a nature somewhat similar to that of the metal-aromatic ion pair of reductive processes. The complex would serve as a radical deactivator, possibly allowing the radical fragments to re-form rather than to attack another part of the molecule.

We are indebted to Roy W. King and Graham Underwood, of Iowa State University, for generating the theoretical spectrum of D.-C. 258 and G.E. 1033 and for furnishing the splitting constants of these spectra.

This research was performed at the United States Naval Research Laboratory, Washington, D.C.

References

1. W. Patnode and D. F. Wilcock, *J. Am. Chem. Soc.*, **68**, 358 (1946).
2. M. J. Hunter, J. F. Hyde, E. L. Warick, and H. J. Fletcher, *J. Am. Chem. Soc.*, **68**, 667 (1946).
3. H. R. Baker, J. G. O'Rear, P. J. Sniegoski, and R. E. Kagarise, *U.S. Naval Res. Lab. Rept.*, **6156**, Jan. 8, 1965.
4. R. C. Gunderson and A. W. Hart, *Synthetic Lubricants*, Reinhold, New York, 1962, Ch. 7.
5. J. Hoijtink, E. deBoer, P. H. van der Mey, and W. P. Weijland, *Rec. Trav. Chim.*, **75**, 487 (1956).
6. H. P. Koch and W. E. Moffitt, *Trans. Faraday Soc.*, **47**, 7 (1951).
7. M. D. Curtis and A. L. Allred, *J. Am. Chem. Soc.*, **87**, 2554 (1965).
8. R. D. Cowell, G. Urry, and S. I. Weissman, *J. Am. Chem. Soc.*, **85**, 822 (1963).
9. J. Chatt and A. A. Williams, *J. Chem. Soc.*, 1954, 4403.
10. L. Goodman, A. H. Konstam, and L. H. Sommer, *J. Am. Chem. Soc.*, **87**, 1012 (1965).

Received August 14, 1967

Studies of Polymers from Cyclic Dienes.

IV. Determination of the Structure of Polycyclopentadiene*

CHUJI ASO, TOYOKI KUNITAKE, and YOSHIKAZU ISHIMOTO,
*Department of Organic Synthesis, Faculty of Engineering, Kyushu
 University, Fukuoka, Japan*

Synopsis

3,4- and 3,5-Dimethylcyclopentenes were prepared as model compounds of the structural unit in polycyclopentadiene. These two isomers give characteristic NMR spectra. The assignment based on the 60 Mc./sec. spectrum was further confirmed by decoupling experiments on the 100 Mc./sec. spectrum of 3,5-dimethylcyclopentene. By comparing the NMR spectra of these compounds with that of polycyclopentadiene methods were developed for estimating the polymer structure from the relative peak area of the methine-methylene and olefinic protons. Polycyclopentadiene obtained with Friedel-Crafts catalysts at lower temperatures was shown to be composed mostly of the 1,4 and 1,2 structures. Polycyclopentadiene obtained with several Ziegler-type catalysts possessed comparable amounts of both structures, contrary to the earlier proposals.

Since the earlier study of Staudinger and Bruson¹ cyclopentadiene has been polymerized with various catalytic systems. Many structures of the polymer obtained from cyclopentadiene are possible. Two basic structural units of the polymer are shown:



For both of these structures there exist *cis* and *trans* isomers and, furthermore, stereoisomerism is possible for the 1,2 and *trans*-1,4 structures. Double-bond migration and branching give rise to further complications, as shown by the polymer obtained by Upadhyay et al.² This complex situation is quite similar to those of polybutadiene and of polyisoprene. Apart from the stereochemical problems, the determination of the 1,2 or 1,4 structure of polycyclopentadiene has been attempted by chemical and physical methods. For example, Gaylord and Mark obtained polycyclo-

* Contribution No. 119 from the Department of Organic Synthesis, Faculty of Engineering, Kyushu University, Japan. A note on this work is given in *J. Polymer Sci. B*, **4**, 701 (1966).

pentadiene with $\text{LiAlH}_4\text{-TiCl}_4$ catalyst and considered its structure to be mainly of the 1,2 type, according to chemical evidence.³ NMR spectroscopy has been utilized for the determinations by several workers. Yen concluded that the polymer with a Ziegler catalyst was of the 1,4 structure,⁴ and Bonin et al.⁵ and Momiyama et al.⁶ proposed somewhat different assignments for the cationically obtained polymer.

Since it was considered interesting to establish the structure of polycyclopentadiene obtained with various catalytic systems, 3,4- and 3,5-dimethylcyclopentenes, (I) and (II), were prepared as model compounds,

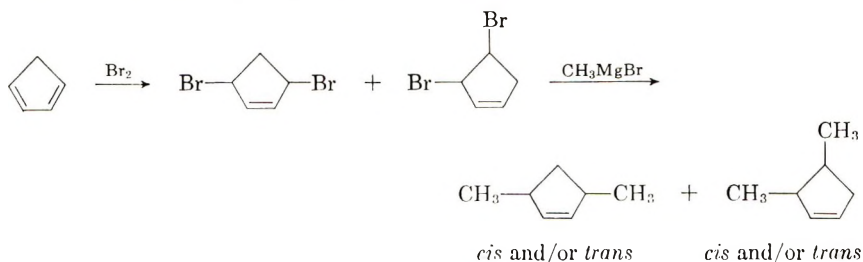


and the structural determination of polycyclopentadiene was carried out with their spectroscopic data.

EXPERIMENTAL

Preparation of Model Compounds

3,4- and 3,5-Dimethylcyclopentenes were prepared by Grignard coupling of dibromocyclopentene with methylmagnesium bromide:



According to Young et al.,⁷ dibromocyclopentene was obtained from addition of 0.5 mole of bromine to 1 mole of cyclopentadiene at -10 to -30°C . in chloroform.

When the Grignard coupling was carried out in tetrahydrofuran, the product could not be separated from the solvent. In diethyl ether the yield of the dimethylcyclopentene fraction was only 10%.⁸ However, the coupling product was obtained in a fairly high yield in di-*n*-butyl ether as follows. Methylmagnesium bromide was prepared from 17.2 g. (0.7 mole) of magnesium and 67.1 g. (0.7 mole) of methyl bromide in 300 ml. of di-*n*-butyl ether. The reaction mixture was cooled with an ice-salt bath during addition of methyl bromide and then stirred at room temperature for 1 hr. To the methylmagnesium bromide solution thus formed was added dropwise a 50 vol.-% solution of dibromocyclopentene (40 g., 0.18 mole) in di-*n*-butyl ether. The coupling temperature was

50–60°C. After the addition was completed, the reaction mixture was further stirred for 20–30 hr. at room temperature and then poured into ice. The resulting gel-like material was decomposed with dilute acetic acid. The organic layer was separated, washed with dilute alkali and water, dried with calcium chloride, and distilled. A fraction boiling at 77–90°C was obtained in 65% yield; $n_D^{20.6}$ 1.4212. This fraction gave four peaks on a gas chromatogram (column: PEG 600 and PEG 1000, 30°C.). Only two major components (A and B) could be recovered as liquid, and they occupied 70–80% and 10–20% of the total area, respectively. Some physical properties of these components are given in Table I.

TABLE I
Some Physical Properties of Dimethylcyclopentene Isomers

Component:	A	S
Structure:	3,5-dimethyl- cyclopentene	3,4-dimethyl- cyclopentene
Purity:	98.8%	85.4%
$n_D^{20.6}$:	1.4185	1.4269
$d_4^{20.6}$:	0.7517	0.7748
Elemental analysis ^a	C, 86.65 H, 12.84	C, 86.46 H, 12.45

^a Calcd. for C₇H₁₂: C 87.42%, H 12.58%.

The purity of each component was determined from the peak areas of the analytical gas chromatogram. The contaminants for components A and B were B and A, respectively. The somewhat lower carbon contents of the elemental analyses are probably due to water deposited in the cold trap during recovery. As described below, the structures of components A and B were determined as 3,5-dimethylcyclopentene and 3,4-dimethylcyclopentene, respectively.

Materials for Polymerization

Cyclopentadiene was obtained by degradative distillation of dicyclopentadiene (courtesy of Yawata Chemical Co. Ltd.), dried with molecular sieve 3A, and redistilled before use in nitrogen atmosphere. Since cyclopentadiene dimerizes quite rapidly, it was kept at low temperature. Toluene was washed with sulfuric acid, water, dilute alkali, and water, dried over calcium chloride, refluxed over metallic sodium, and distilled. Aluminum bromide was prepared from aluminum and bromine. Boron trifluoride-etherate and tin tetrachloride were distilled before use. Titanium tetrachloride was refluxed over copper powder and distilled. Trichloroacetic acid was purified by distillation. Methylene chloride was washed with dilute alkali, dried over calcium chloride, refluxed over phosphorous pentoxide, and distilled. Commercial triisobutylaluminum and titanium trichloride were used without further purification.

Polymerization Procedures

Schlenk-type glass ampules were used as polymerization vessels. The addition of reagents and the polymerization were carried out under nitrogen, which was dried by being passed through phosphorus pentoxide. After a given period of time polymerization was stopped by adding pyridine or ethanol, and the reaction mixture was added dropwise under nitrogen to excess methanol containing a small amount of 2,6-di-*t*-butyl-*p*-cresol. The precipitate was filtered with a glass filter in a nitrogen box and dried *in vacuo*. When necessary, the polymer was purified by reprecipitating from toluene and methanol.

Measurements

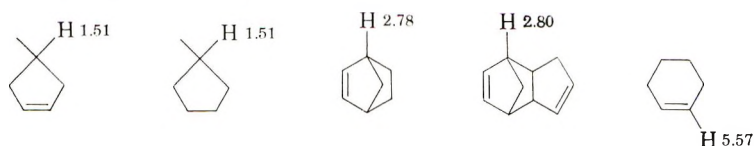
Viscosities were measured in benzene at 30°C. with Ubbelohde viscometers. NMR spectra were taken with a Varian A60 spectrometer. All the polymer spectra were obtained in carbon tetrachloride as solutions of approximately 1 mole (mer unit) per liter at 37°C. Infrared spectra were obtained with a Nippon Bunko DS301 spectrometer.

RESULTS AND DISCUSSION

Structural Determination of Model Compounds

In Figure 1 are shown NMR spectra (60 Mc./sec.) of components A and B. The spectrum of component A consists of a multiplet at about $\delta = 1.0$ ppm, a triplet centered at $\delta = 1.60$ ppm, a broad multiplet at about $\delta = 2.7$ ppm, and a doublet at $\delta = 5.54$ ppm. These peak groups may be reasonably assigned to protons of 3,5-dimethylcyclopentenes as six methyl protons, two β -methylene protons, two α -methine protons, and two olefinic protons, respectively, and the area ratio of the methyl, methylene-methine, and olefin protons is approximately 3:2:1. The smaller peaks found at $\delta = 2.0$ to 2.5 ppm cannot be given a reasonable assignment and are most probably due to impurities.

The chemical shifts of similar protons⁹ agree well with those of 3,5-dimethylcyclopentenes as shown below:



Thus the chemical shift of the β -methylene protons (1.60 ppm) is close to that of the β -methylene proton in cyclopentene and that of the methylene proton in cyclopentane (1.51 ppm), and the α -methine chemical shift (2.7 ppm) can be compared to the α -methine shift of norbornene (2.78 ppm) and of dicyclopentadiene (2.80 ppm). Furthermore, the olefinic proton (5.54 ppm) appears at the same position as that of cyclohexene

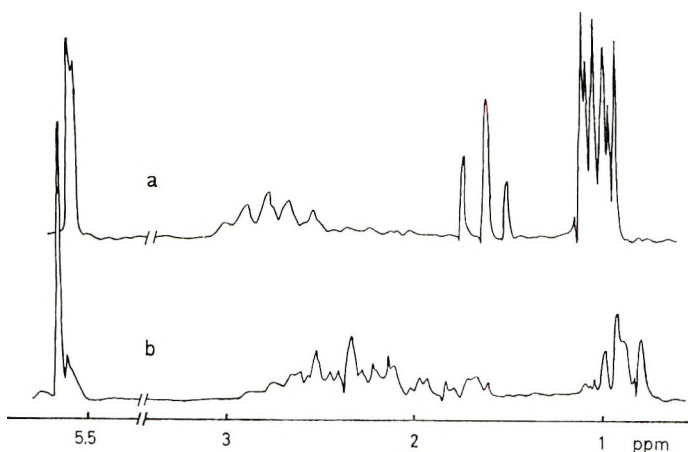


Fig. 1. NMR spectra of (a) 3,5-dimethylcyclopentene and (b) 3,4-dimethylcyclopentene; CCl_4 solution; internal standard, tetramethyl silane.

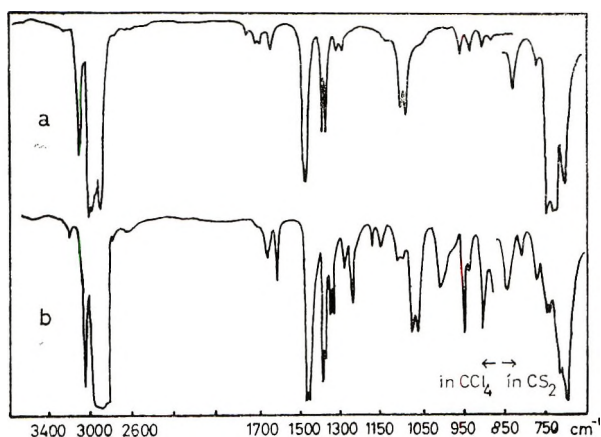


Fig. 2. Infrared spectra of (a) 3,5-dimethylcyclopentene and (b) 3,4-dimethylcyclopentene.

(5.57 ppm) within the experimental uncertainty. The unsymmetrical doublet of the olefinic protons indicates that this component contains both *cis* and *trans* isomers. The methine protons are quite complex, probably because of spin-spin coupling with both β -methylene and methyl protons. The β -methylene proton gives a triplet ($J = 6$ cps) by the coupling with two methine protons. The methyl peaks of the *cis* and *trans* isomers seem to have different chemical shifts and to be made complex through the spin-spin coupling with the methine protons.

The spectrum for component B (Fig. 1b) contains a multiplet at about $\delta = 0.90$ ppm, a very complex multiplet from 1.7 to 2.8 ppm, and a singlet at 5.60 ppm. The spectrum may be attributed to 3,4-dimethylcyclopentene. The multiplet at $\delta = 0.9$ ppm and the singlet at $\delta = 5.60$ ppm may be readily assigned to methyl and olefin protons, respectively. How-

ever, the methine-methylene protons are extensively coupled, and simple assignment is impossible. Whether this sample contains both or either of the *cis* and *trans* isomers of 3,4-dimethylcyclopentene is not clear from the present NMR spectrum. Although there is a small olefinic peak at $\delta = 5.54$ ppm, this peak may be due to 3,5-dimethylcyclopentenes and other impurities.

The infrared spectra of 3,5- and 3,4-dimethylcyclopentenes are given in Figure 2. Both spectra show peaks for olefinic C—H stretching at 3070 cm.^{-1} and peaks for methyl groups at 1370 to 1380 cm.^{-1} . Peak shapes from 700 to 750 cm.^{-1} are characteristic of each isomer: 3,4-dimethylcyclopentene gives a strong peak at 710 cm.^{-1} and the 3,5 isomer gives stronger peaks at 730 to 750 cm.^{-1} . Some of the weaker peaks from 830 to 950 cm.^{-1} are also different between these two isomers.

100 Mc./sec. NMR Spectrum of 3,5-Dimethylcyclopentene

In Figure 3 are shown decoupled NMR spectra of 3,5-dimethylcyclopentene at 100 Mc./sec. (in benzene). Decoupling of the methine proton (Fig. 3a) converted the methylene peak to a singlet and the methyl peak to an unsymmetrical doublet. The olefinic proton peak did not change. A decoupled spectrum at the β -methylene region shown in Figure 3b gives somewhat simplified methine peaks. Figure 3c is a decoupled spectrum at the methyl peak. The β -methylene and olefin region do not change. The methine region now seems to consist of two sets of overlapped triplets ($J = 6$ cps).

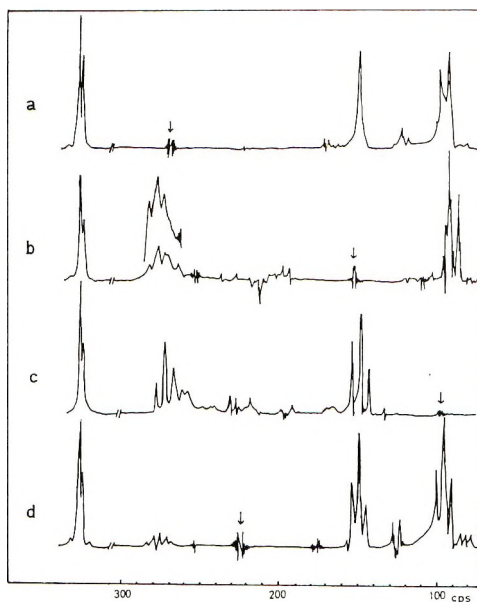


Fig. 3. Decoupled NMR spectra of 3,5-dimethylcyclopentene (100 Mc./sec.); Decoupled positions are indicated by arrows.

These results clearly support the assignment based on the 60 Mc./sec. spectrum. Thus, both the β -methylene and the methyl protons are independently coupled to the methine proton with coupling constants of 6 and 4 cps, respectively. The unsymmetrical doublets of the olefinic and methyl protons (Fig. 3a) may be attributed to the presence of the *cis* and *trans* isomers. Seemingly overlapped triplets in the methine region (Fig. 3c) would correspond to the *cis* and *trans* isomers, though the presence of impurity prevented a clear-cut analysis. When decoupling was carried out for the olefinic proton (spectrum not shown), only the methyl region was somewhat simplified. Irradiation at 2634 cps (oscillator frequency) simplified the methyl region into a triplet, of which the central peak had a shoulder at a higher field (Fig. 3d).

In addition to the expected peaks, these spectra show smaller peaks at about 2634 cps (irradiated, Fig. 3d) and at both sides of the methyl peaks. All these smaller peaks and some of the methyl peaks are probably due to impurities, including isomeric cyclopentene derivatives, since the decoupled spectra were taken a few months after the gas chromatographic separation.

Structural Assignment of Polycyclopentadiene

Examples of the NMR spectra of polycyclopentadiene obtained by cationic polymerization are given in Figure 4. A fairly sharp peak at $\delta = 5.6$ ppm may be assigned to olefinic protons, and three broad peaks ranging from $\delta = 1.5$ to 3.0 ppm are due to the methine and methylene protons.

Although polycyclopentadiene obtained by gamma-ray irradiation in methylene chloride was reported to have multiple olefinic peaks,⁵ a single olefinic peak was always obtained with cationic and complex metal catalysts. When the polymer spectrum is compared with those of the model compounds, the olefinic proton peaks appear at about the same position, and the broad methine-methylene peaks of the polymer spectrum correspond

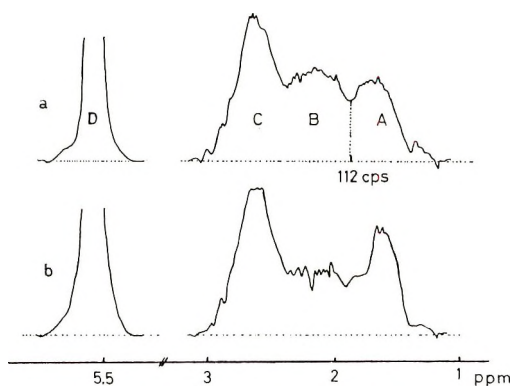


Fig. 4. Examples of spectra of polycyclopentadiene: (a) obtained at -50°C . in toluene with TiCl_4 -trichloroacetic acid; (b) obtained at -50°C . in toluene with $\text{BF}_3\text{-OEt}_2$.

to the methine and methylene peaks of the 3,5- and 3,4-dimethylcyclopentene.

As is clear from a comparison of the two spectra in Figure 1, the most remarkable difference between the methine-methylene regions of the NMR spectra of these model compounds is the presence of the β -methylene triplet in the former. Since the chemical shift of the triplet is similar to the peak A in the polymer spectrum, peak A may be considered to be mainly due to the β -methylene protons in polymer. Peaks B and C will be due to the remaining methine-methylene protons and are difficult to assign separately. The number of protons that may be attributed to the respective NMR peaks for each structural unit in polymer is given in Table II.

TABLE II
Number of Protons (Three Types) in Each Structural Unit

NMR peak:	A	B + C	D
Type of proton:	β -methylene	The rest of the methine-methylene protons	Olefinic
Number of protons in 1,4 structure:	2	2	2
Number of protons in 1,2 structure:	0	4	2

On the basis of these assignments the structure 1,2 or 1,4 of polycyclopentadiene may be estimated from the relative peak areas (*A*, *B*, *C*, and *D*) as follows:

Method 1:

$$(1,2 \text{ structure})/(1,4 \text{ structure}) = [(B + C) - A]/2A$$

$$\therefore (1,2 \text{ structure}) (\%) = [(B + C) - A]/[A + (B + C)] \times 100$$

Method 2:

$$(1,4 \text{ structure})/[(1,4 \text{ structure}) + (1,2 \text{ structure})] = A/D$$

$$\therefore (1,2 \text{ structure}) (\%) = (1 - A/D) \times 100$$

As shown in Figure 4, peaks A and B were separated at 112 cps, which is calibrated with the chloroform peak at $\delta = 7.25$ ppm (436 cps from tetramethylsilane). A smooth curve was drawn along the peaks, and the peak areas were determined by weighing pieces of paper that had been cut along the smooth peak shape and the baseline.

The assignment of the polymer peaks by direct comparison with those of the model compounds may not be very precise, since the β -methylene peak in 3,5-dimethylcyclopentene somewhat overlaps the methine-meth-

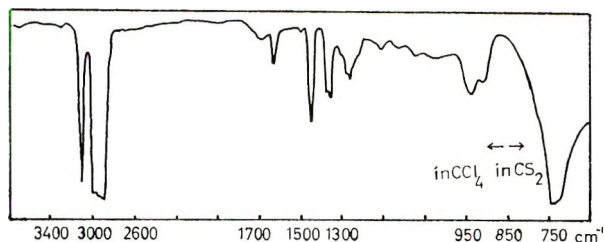


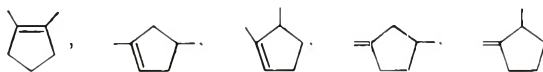
Fig. 5. Infrared spectrum of polycyclopentadiene obtained at -78°C . in toluene with SnCl_4 .

ylene peaks in the 3,4 isomer, and the broad polymer peaks cannot be fully resolved. However, the methine-methylene peak area at less than $\delta = 1.8$ ppm (i.e., area overlapping the β -methylene peak of the 3,5 isomer) is about 10% of the total methine-methylene area of the 3,4 isomer. And the error in the calculated content of the 1,2 structure arising from the overlapping would be a few per cent. When the ratio of the peak area $(B + C)/A$ or D/A is taken as an index of the polymer structure, the relative variation of these ratios will be more reliable, since the peak area ratios are reproducible within 2 to 3%, and uncertainty concerning the peak separation is no longer a problem.

The infrared spectrum of polycyclopentadiene (Fig. 5) shows a strong, broad peak at 750 cm^{-1} . From the difference between the spectra of the model compounds this peak was expected to be correlated with polymer structure. However, it was almost invariant among the polymers obtained under different polymerization conditions. The relative absorption of the peaks at 910 and 940 cm^{-1} were variable to some extent, but correlation with the polymer structure was not successful.

Structure of Polycyclopentadiene Obtained with Friedel-Crafts Catalyst

In Table III is shown the result of a structure determination of some polycyclopentadienes obtained with Friedel-Crafts catalysts. For polymers obtained at -78°C . the content of the 1,2 structure ranges from 40 to 60%, and the contents calculated by two different methods agree within a few per cent. In the last column are shown the $D/(A + B + C)$ values, which are the ratios of olefinic protons to total methine-methylene protons. If the monomer unit in polycyclopentadiene is composed only of the 1,4 and 1,2 structures, this ratio should be invariably 0.5. The $D/(A + B + C)$ values for polymer obtained at -78°C . are from 0.47 to 0.50, disproving the presence of isomerized units such as those shown below:



Furthermore, a comparison of experiments 26 and 27 and of experiment 22 before and after additional reprecipitation shows that the present

TABLE III
 Cationic Polymerization of Cyclopentadiene in Toluene

Expt. no.	Catalyst	Temp., °C.	[Cat.]/[M], %	[M], mole/l.	Time, min.	Convsn., %	$[\eta]_{C_6H_6}^{30^\circ}$	1,2 structure, %		$D/(A+B+C)$
								Meth. 1	Meth. 2	
13	TiCl ₄	-78	0.8	0.8	21	75	0.24	52	51	0.49
14	TiCl ₄ ^a	-78	0.2	1.2	7	73	0.36	57	55	0.48
5	AlBr ₃	-78	0.5	0.4	21	75	0.24	48	45	0.47
22	SnCl ₄ ^a	-78	0.8	1.2	6	65	0.34	46	43	0.47
26	BF ₃ OEt ₂	-78	0.8	1.2	97	8	1.13	(46) ^b	(47) ^b	(0.51) ^b
27	BF ₃ OEt ₂	-78	0.8	1.2	204	5	1.7	43	43	0.50
1	AlBr ₃	0	0.6	0.4	16	100	0.10	43	40	0.47
7	TiCl ₄	0	0.8	1.2	233	84	0.17	55	41	0.38
16	SnCl ₄	0	0.8	1.2	220	68	0.18	50	41	0.43
23	BF ₃ OEt ₂	0	0.8	1.2	191	97	0.59	41	38	0.47

^a Trichloroacetic acid used as cocatalyst.

^b Value in parentheses obtained after additional reprecipitation.

TABLE IV
Ziegler-Type Polymerization of Cyclopentadiene at 0°C. in Toluene

Expt. no.	Catalyst	[Al]/[Ti]	[Ti]/[M], %	[M], mole/l.	Time, min.	Convsn., %	$[\eta]_{\text{C}_6\text{H}_6}^{30^\circ}$	1,2 structure, %		$D/(A + B + C)$
								Meth. 1	Meth. 2	
1	Al- <i>i</i> Bu ₃ -TiCl ₄	1.2	—	—	—	—	—	40	30	0.43
2	LiAlH ₄ -TiCl ₄	1.0	0.8	—	40	>90	—	38 ^a	—	—
3	AlEt ₃ -TiCl ₄	3.0	1.0	—	180	≈60	—	46 ^a	—	—
4	Al <i>i</i> Bu ₃ -TiCl ₄	1.1	0.72	1.26	5.5	90 ^b	0.51	40	30	0.43
5	Al <i>i</i> Bu ₃ -TiCl ₃	1.0	2.1	1.14	6	68 ^b	0.78	47	37	0.42

^a Method 2 was not applicable, since the spectra were obtained in tetrachloroethane at 100°C.

^b About 10% of insoluble fraction present.

method of structure estimation is quite reproducible. Thus, the variation of the polymer structure with catalysts is well beyond the experimental uncertainty and suggests that the nature of the propagating ion affects the polymer structure. This problem will be discussed in a subsequent paper.

Cationic polymerization at 0°C. gives somewhat different results. The $D/(A + B + C)$ values for polymers obtained with $AlBr_3$ and $TiCl_4$ are much lower than 0.50. This is considered to be due to the presence of isomerized units in polymer. Although further discussion will be postponed to another paper, it is to be noted that highly active catalysts tend to give isomerized polymers (compare experiments 1 and 7 with experiments 16 and 23).

Structure of Polycyclopentadiene Obtained with Complex Metal Catalysts

A few polymerization results with complex metal catalysts are given in Table IV. The structures of polycyclopentadiene obtained with complex metal catalysts were considered to be mainly of the 1,2 type³ or the 1,4 type.⁴ However, these results indicate the presence of comparable amounts of both structures and a lack of regular structures, contrary to the suggestion made before.

We are especially grateful to Prof. T. Matsuo of this department for cooperation in the measurement of 60 Mc./sec. NMR spectra and to Uetsuki of the Kurashiki Rayon Co. for the 100 Mc./sec. NMR spectra. The generous donation of dicyclopentadiene from Yawata Chemical Co. is also acknowledged.

References

1. H. Staudinger and H. A. Bruson, *Ann.*, **447**, 97 (1926).
2. J. Upadhyay, P. Gaston, A. A. Levy, and A. Wassermann, *J. Chem. Soc.*, **1965**, 3252.
3. N. G. Gaylord and H. F. Mark, *Polymerization and Polycondensation Processes*, American Chemical Society, Washington, D.C., 1962, p. 134.
4. S. P. S. Yen, papers presented at the 145th Meeting of the American Chemical Society, Sept. 1963; *Polymer Preprints*, p. 82.
5. M. A. Bonin, W. R. Busler, and E. Williams, *J. Am. Chem. Soc.*, **87**, 199 (1965).
6. Z. Momiyama, Y. Imanishi, and T. Higashimura, *Chem. High Polymers, Tokyo*, **23**, 56 (1966).
7. W. G. Young, S. Winstein, and H. K. Hall, *J. Am. Chem. Soc.*, **78**, 4338 (1956).
8. K. Ito, Master's Thesis, Kyushu University, 1965.
9. S. Fujiwara, N. Nakagawa and H. Shimizu, *High-Resolution NMR Spectroscopy*, Maruzen, Tokyo, 1962, p. 355.

Received June 19, 1967

Studies of Polymers from Cyclic Dienes.
V. Cationic Polymerization of Cyclopentadiene,
Influence of Polymerization Conditions on the
Polymer Structure*

CHUJI ASO, TOYOKI KUNITAKE, and YOSHIKAZU ISHIMOTO,
Department of Organic Synthesis, Faculty of Engineering, Kyushu
University, Fukuoka, Japan

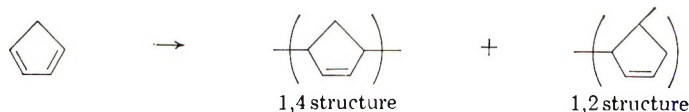
Synopsis

Cationic polymerization of cyclopentadiene was studied with several Friedel-Crafts catalysts, and the influence of polymerization conditions on the polymer structure was investigated. Polycyclopentadiene contained higher amounts of the 1,2 structure when a stronger catalyst and a more polar solvent were used. This fact is discussed in terms of the tightness of the growing ion pair. The polymer structure did not vary with polymerization temperature in toluene solvent. In methylene chloride at around 0°C. the structural variation with catalysts was much smaller, suggesting a freer nature of the growing ion pair. The viscosity data also support the change in the structure of the ion pair under similar conditions. The use of aliphatic hydrocarbon solvents gave the highest contents of the 1,2 structure. This result was ascribed to the lack of solvation, considering the dependence of the polymer structure on the monomer concentration, which was found only in this solvent. Furthermore, isomerization during propagation was observed in polar solvents at higher temperature.

The nature of the propagating ion in cationic polymerization of vinyl compounds remains much to be clarified in spite of the effort of many investigators. Among the reasons for this are the difficulty of identifying the propagating cation, owing to its instability and the presence of complex ion-solvent and ion-monomer interactions, unlike in anionic polymerization systems. Relative reactivities, such as reactivity ratios in copolymerization and steric courses in propagation, have been utilized to collect information on the property of the propagation ion. Conjugated diene monomers give various structures on polymerization. The structural variation of the diene polymer has been discussed in connection with the nature of the growing species in anionic polymerization.¹ In the cationic polymerization of butadiene and isoprene, however, extensive cyclization occurs in addition to propagation, rendering a similar discussion impossible.

* Contribution No. 120 from Department of Organic Synthesis, Faculty of Engineering, Kyushu University. Presented in part at the Annual Meeting of the Chemical Society of Japan, Tokyo, April, 1966.

As shown in the preceding paper,² the 1,2 or 1,4 structure of polycyclopentadiene can be estimated from its NMR spectrum:



Thus, it was hoped that variation of the polymer structure with polymerization conditions (catalytic species, solvents, etc.) would yield information concerning the nature of the propagation cation.

In this paper the cationic polymerization of cyclopentadiene with several Friedel-Crafts catalysts is described, and the structural variation of the polymer is discussed in terms of the nature of the growing ion pair.

EXPERIMENTAL

The materials, polymerization procedures, and polymer characterizations have been described.²

RESULTS

In Table I are given polymerization results with several Friedel-Crafts catalysts in toluene. The data given in the preceding paper are also included. The temperature range of polymerization was 0 to -78°C ., except in one case, in which the polymerization was carried out at -100°C . The latter temperature was maintained by adding liquid nitrogen into a petroleum ether bath. Polymerization is generally fast. Since a gel is readily formed with stronger catalysts (AlBr_3 and TiCl_4), lower monomer concentrations were used correspondingly. The polymer structures were calculated by the two different methods already described, and the ratio of the olefinic protons to the aliphatic protons, $D/(A + B + C)$ is given in the last column. The contents of the 1,2 structure calculated by these two methods agree quite well when the ratio of the olefinic to methine-methylene protons is close to the theoretical value (i.e., 0.5). However, the latter ratio tends to be smaller than 0.5 when stronger catalysts or higher temperature, or both, are used. This indicates that the polymer contains structural units other than the 1,2 and 1,4 types.

In several instances the ratio is larger than 0.5. There is no adequate explanation available for this abnormal result at the moment. Poor resolution of the NMR spectra is the most probable reason. As mentioned briefly in the preceding paper,² repeated measurements of NMR spectra of one polymer sample showed good reproducibility, the calculated contents of the 1,2 structure agreeing within 2 to 3% between measurements. On the other hand, reproducibility of the structure of different polymer samples obtained under the same polymerization condition is somewhat worse, being approximately within $\pm 3\%$. The intrinsic

viscosities of polycyclopentadiene varied from 0.1 to 1.7, and higher values were obtained when weaker catalysts were used at lower temperatures.

The addition of cocatalysts (trichloroacetic acid or water) accelerated polymerization appreciably, but the structural variation of the polymer was small (Nos. 25, 26, and 27).

The polymerization results with methylene chloride are summarized in Table II. Since the tendency of gel formation was much greater in this solvent, smaller monomer concentrations were used than in toluene solvent. The polymers obtained in methylene chloride contained more isomerized units than in toluene, as indicated by the lower $D/(A + B + C)$ values. Thus the contents of the 1,2 structure estimated by the two methods are inconsistent in many cases.

Cationic polymerization of cyclopentadiene was further carried out in several nonpolar solvents, and the results are shown in Table III. The solvents selected are carbon tetrachloride, cyclohexane, and methylcyclohexane. The rate of polymerization was much smaller than in other solvent systems. The extents of isomerization of the polymer were generally small except for a few cases. Polymerization results in chloroform and chlorobenzene are also included in Table III.

Two of the polymer samples obtained in toluene were further treated with Friedel-Crafts catalysts at 0°C. The results given in Table IV show that the changes in the polymer structure caused by the TiCl_4 treatment are comparable to the experimental uncertainty, the extent of isomerization being much smaller than observed during polymerization under similar conditions. In spite of the increase in viscosity for the first example the change in the polymer structure was small.

DISCUSSION

The use of monomer reactivity ratios as a measure of the nature of the propagating ion pair elucidated many aspects of propagation in cationic polymerization. For instance, the solvation of the growing ion pair by monomer was found to affect reactivity ratios, and the polarity of solvent had an influence on the stability of the cation which, in turn, controlled the reactivity ratio.^{3,4} On the other hand, the possibility of block polymer formation always obscured the discussion based on the reactivity ratio. The propagation step in copolymerization systems is, therefore, affected by too many factors to give a straightforward interpretation. Thus it becomes desirable to utilize simple competitive reactions to monitor the nature of the propagating ion pair. The cyclization constant in the cyclopolymerization of *o*-divinylbenzene varies with the catalysts, and this result was interpreted in terms of the structure of the growing ion pair.⁵ Cationic polymerization of cyclopentadiene has advantages over other competitive reactions, because the polymer possesses only the 1,2 and 1,4 structure, and their ratio, as estimated from the NMR spectrum, was found to vary with the polymerization condition.²

TABLE I
 Cationic Polymerization of Cyclopentadiene in Toluene

No.	Temp., °C.	[Cat.]/[M], %	[M], mole/l.	Time, min.	Convsn., %	$[\eta]_{\text{C}_6\text{H}_6}^{30^\circ}$	1,2 structure, %		$D/(A + B + C)$
							Meth. 1	Meth. 2	
AIBN ₃									
1	0	0.58	0.41	16	100	0.10	55	41	0.38
2 ^a	0	0.7	0.57	24	46	0.06	48	39	0.43
3	-50	0.66	0.41	29	100	0.20	52	48	0.47
4 ^a	-50	0.7	0.57	38	60	0.19	49	48	0.49
5	-78	0.54	0.41	21	75	0.24	48	45	0.47
6 ^a	-78	0.7	0.57	25	100	0.28	49	48	0.50
TiCl ₄									
7	0	0.77	1.16	233	84	0.17	50	41	0.43
8	0	0.75	0.82	51	20	0.15	57	54	0.46
9 ^a	0	0.19	1.21	18	70	0.16	55	58	0.54
10 ^a	-50	1.67	0.61	43	65	0.15	57	56	0.49
11 ^a	-50	0.19	1.21	7	72	0.33	54	53	0.49
12 ^b	-50	<0.38	1.19	4	45	0.23	54	54	0.50
13	-78	0.75	0.82	21	75	0.24	52	51	0.49
14 ^a	-78	0.19	1.21	7	73	0.36	57	55	0.48
15 ^c	-100	0.75	1.19	272	100	0.36	55	49	0.44

SnCl ₄																						
16	0	1.6	0.43	354	5	—	45	46	0.51													
17	0	1.6	0.43	1870	9	—	45	41	0.47													
18 ^a	0	0.8	1.12	17	72	0.20	45	53	0.59													
19 ^a	0	0.75	1.17	2	83	0.18	41	38	0.47													
20	0	0.77	1.16	220	68	0.18	48	44	0.47													
21	0	0.4	2.27	1870	13	—	50	52	0.53													
22	0	0.36	2.27	318	13	—	44	43	0.49													
23	0	0.4	2.27	174	6	—	42	42	0.50													
24	0	0.31	2.55	324	12	—	45	42	0.47													
25	-50	0.75	1.19	545	12	0.26	45	46	0.51													
26 ^b	-50	<0.75	1.17	528	21	0.28	46	47	0.51													
27 ^a	-50	0.75	1.17	5	83	0.32	44	43	0.49													
28 ^a	-78	0.75	1.17	6	65	0.34	46(46) ^d	43(47) ^d	0.47(0.50) ^d													
BF ₃ OEt ₂																						
29	0	0.77	1.16	191	97	0.59	43	41	0.48													
30	0	0.77	1.16	12	100	0.64	46	50	0.54													
31	-50	0.77	1.16	20	65	1.05	43	47	0.54													
32	-78	0.75	1.19	97	8	1.13	43	43	0.50													
33	-78	0.77	1.16	204	5	1.7	43	40	0.47													

^a Cocatalyst, trichloroacetic acid.^b Cocatalyst, H₂O.^c Catalyst solution, 0.5 mole/l. in *n*-hexane.^d Data in parentheses obtained on additional reprecipitation.

TABLE II
 Cationic Polymerization of Cyclopentadiene in Methylene Chloride

No.	Temp., °C.	[Cat.]/[M], %	[M], mole/l.	Time, min.	Convsn., %	$[\eta]_{\text{C}_6\text{H}_6}^{30^\circ}$	1,2 structure, %		$D/(A + B + C)$
							Meth. 1	Meth. 2	
AlBr ₃									
1	0	0.34	0.41	29	82	0.30	53	41	0.40
2	-50	0.40	0.14	6	51	0.30	57	47	0.41
3	-78	0.40	0.14	2	51	--	53	41	0.41
TiCl ₄									
4	0	0.80	0.77	146	78	0.26	59	55	0.45
5	-50	0.77	0.42	4	89	--	52	42	0.41
6	-50	0.09	0.17	11	12	0.15	55	48	0.43
7	-78	0.75	0.17	1	83	--	58	49	0.41
8	-78	0.75	0.16	0.8	65	0.36	56	51	0.45
SnCl ₄									
9	+10	0.73	0.44	7	68	0.16	56	47	0.42
10	0	0.80	0.77	71	90	0.43	59	53	0.43
11	0	0.8	0.30	15	85	0.20	57	41	0.37
12 ^a	0	0.8	0.30	9	66	0.16	53	43	0.42
13	-11	0.73	0.44	14	73	0.26	56	48	0.42

14	-22	0.76	0.42	20	73	0.29	47	37	0.42
15	-50	0.40	0.42	22	36	—	49	47	0.48
16	-50	0.66	0.62	10	—	0.24	—	—	—
17	-50	0.72	0.44	5	35	0.85	—	—	—
18	-50	0.72	0.44	8.5	30	1.15	—	—	—
19	-78	0.75	0.43	13	36	—	46	37	0.43
20	-78	0.93	0.43	105	16	—	51	41	0.41
21	-78	0.72	0.44	6.5	32	1.14	—	—	—
22	-78	0.72	0.44	7.3	33	1.00	—	—	—
23	-100	0.75	0.43	126	35	—	49	50	0.51
BF ₃ OEt ₂									
24	+10	0.73	0.44	18	78	0.34	53	40	0.43
25	+10	0.73	0.44	—	77	0.29	51	41	0.42
26	0	0.80	0.59	43	93	1.0	55	55	0.50
27	0	0.8	0.30	7	77	0.31	56	58	0.53
28	-10	0.73	0.44	10	78	0.51	52	44	0.43
29	-22	0.76	0.42	11	72	0.74	44	32	0.41
30	-50	0.77	0.61	5	57	—	45	44	0.50
31	-50	0.77	0.42	6	2	1.0	—	—	—
32	-78	0.75	0.43	531	2	—	45	46	0.51

^a Cocatalyst, trichloroacetic acid.

TABLE III
 Cationic Polymerization of Cyclopentadiene in Other Solvents

No.	Solvent	Temp., °C.	[Cat.]/[M], %	[M], mole/l.	Time, hr.	Convsn., %	$[\eta]_{C_6H_6}^{30^\circ}$	1,2 structure, %		D/(A + B + C)
								Meth. 1	Meth. 2	
TiCl ₄										
1	C ₆ H ₁₂	0	0.8	1.12	10.4	10	—	57	55	0.48
2	"	0	0.82	1.2	3.2	2	—	53	45	0.42
3	"	0	0.8	1.12	5.9	3	—	56	54	0.48
AlBr ₃										
4 ^a	C ₇ H ₁₄	0	1.8	0.58	14.9	6	—	62	64	0.52
TiCl ₄										
5	"	0	0.8	1.12	19.5	10	0.15	56	53	0.47
6	"	0	0.8	1.12	24.3	14	—	55	52	0.47
SnCl ₄										
7	"	0	1.6	0.43	30.8	trace	—	—	—	—
8 ^b	"	0	0.92	0.63	1.3	46	—	54	53	0.49
9	"	0	0.8	1.12	19.4	3	—	53	45	0.43
10	"	0	0.8	1.12	24.2	4	—	57	54	0.46

11	"	0	0.72	1.24	25.0	1	—	52	47	0.45
12 ^b	"	0	0.76	1.24	2.6	74	0.22	50	44	0.44
13	"	0	0.40	2.27	30.8	2	—	47	38	0.43
14	"	0	0.36	2.27	47.5	1	—	43	31	0.42
15	"	0	0.36	2.27	25.0	1	—	—	—	—
16 ^b	"	0	0.38	2.27	2.5	57	0.26	51	54	0.53
17 ^b	"	-20	0.76	1.24	14.3	84	0.21	53	51	0.48
18	CCl ₄	0	0.8	0.58	5.2	15	—	52	42	0.42
19	"	0	0.4	1.12	3.0	21	0.18	50	44	0.45
20	"	0	0.2	2.24	0.8	10	0.17	46	37	0.44
21	CHCl ₃	-22	0.76	0.62	35	27	0.20	46	38	0.43
22	C ₆ H ₅ Cl	-50	0.72	0.66	53	11	—	42	40	0.49
23	"	-50	0.74	0.64	144	12	—	50	43	0.44
BF ₃ OEt ₂										
24 ^c	C ₇ H ₁₄	0	<0.8	1.12	24.6	35	0.69	49	44	0.45
25 ^c	"	0	<0.8	1.12	29.3	25	0.67	45	39	0.45
26	C ₆ H ₅ Cl	-50	0.72	0.66	28	35	—	43	38	0.46

^a AIBr₃ is insoluble in methylcyclohexane.

^b Cocatalyst, trichloroacetic acid.

^c A saturated solution of BF₃OEt₂ in methylcyclohexane was used.

TABLE IV
Treatment of Polycyclopentadiene with TiCl_4

No.	Polymer	Solvent	Reaction condition						Recovery, %	Color of system
			Temp., °C.	[Cat.]/[Mer], %	[Mer], mole/l.	Time, hr.	I,2 structure, %			
1	Table I, No. 11	CH_2Cl_2	0	1.9	0.58	1.0	83	red-brown		
2	Table I, No. 17	$\text{C}_6\text{H}_5\text{CH}_3$	0	1.0	0.24	0.5	90	brown		
Structural Change										
Before treatment										
No.	I,2 structure, %		$D/(A + B + C)$	$[\eta]_{\text{C}_6\text{H}_6}^{30^\circ}$	After treatment			$D/(A + B + C)$	$[\eta]_{\text{C}_6\text{H}_6}^{30^\circ}$	
	Meth. 1	Meth. 2			Meth. 1	Meth. 2	+ B + C			
1	54	53	0.49	0.33	51	47	0.46	0.58		
2	41	38	0.47	0.18	40	38	0.48	0.18		

These advantages were made use of in the interpretation of the polymerization results of cyclopentadiene with Friedel-Crafts catalysts as follows.

Effect of Polymerization Temperature

In Figure 1 is shown the 1,2 type content versus polymerization temperature for polymers obtained in toluene. Although experimental results under a given condition are somewhat scattered at several places, the reproducibility becomes better if the data with the more isomerized structure [lower $D/(A + B + C)$ value, indicated by arrow] are eliminated. The structure of polycyclopentadiene can be considered temperature-independent, as indicated by straight lines drawn for the respective catalyst systems. This result may be related to the fact that the activation energy of propagation in cationic polymerization is rather small ($E_p = 6$ kcal./mole is given for the iodine-catalyzed polymerization of styrene in ethylene dichloride.⁶ In that case the difference in activation energies between competitive propagations of the same type will be much smaller. In fact, the ratio of the two structures is close to 1 under the polymerization conditions studied, implying that the two types of propagation are quite similar energetically.

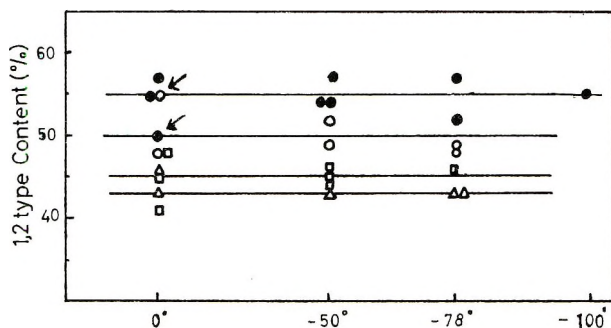


Fig. 1. Structure of polycyclopentadiene obtained in toluene. Catalyst: (●) TiCl_4 ; (○) AlBr_3 ; (□) SnCl_4 ; (△) BF_3OEt_2 .

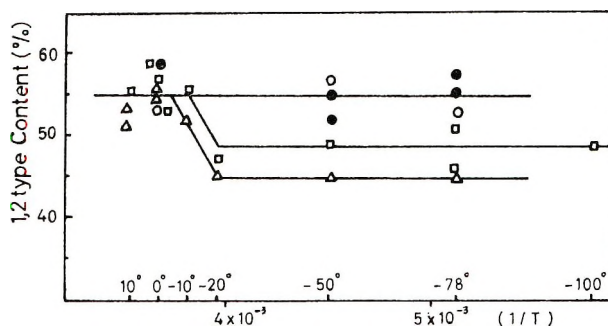


Fig. 2. Structure of polycyclopentadiene obtained in methylene chloride. Catalyst: (●) TiCl_4 ; (○) AlBr_3 ; (□) SnCl_4 ; (△) BF_3OEt_2 .

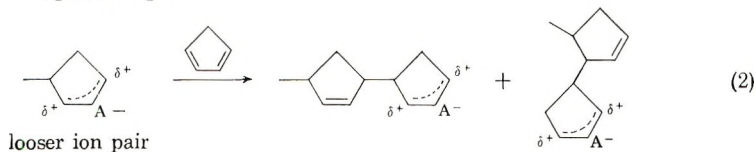
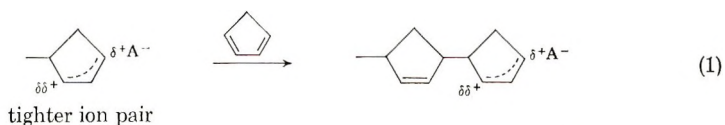
In cationic polymerization, however, the presence of the gegenion and also the difference in solvation state exert a strong influence on the structure of the growing ion pair. In the present system the polymer structure varied with solvents and catalysts, indicating the variation of the nature of the growing cation with gegenanions and solvents. The constancy of the content of the 1,2 structure over the wide range of temperature, therefore, suggests that the structure of the propagating ion pair, including its solvation state (and propagation thereof), is not sensitive to temperature variation in toluene. Polymerization results in methylene chloride also show the temperature independency of the polymer structure below -10°C . (see Fig. 2).

The temperature effect would be observed for competition between two reactions of a greater energetic difference. For example, in cationic cyclopolymerization of *o*-divinylbenzene (BF_3OEt_2 catalyst, toluene solvent) the activation energy for intramolecular cyclization was higher by 5.3 kcal./mole than that for intermolecular propagation.⁷ This greater difference may be ascribed to the unfavorable energetic situation of cyclization as compared with propagation, rather than to the change in the ion pair structure with temperature. A temperature dependence was also found for the steric structure in the cationic polymerization of α -methylstyrene.⁸

Effect of Catalyst

The difference in the structure of polycyclopentadiene with the catalyst is apparent from Figure 1. The content of the 1,2 structure varies with catalyst: $\text{TiCl}_4 > \text{AlBr}_3 > \text{SnCl}_4 > \text{BF}_3\text{OEt}_2$. There are several examples of the effect of the catalyst on the polymer structure in the cationic polymerization of vinyl compounds. Variations of monomer reactivity ratios,⁹ of molecular weights,¹⁰ and of steric structures⁸ have been already noted. As reported from this laboratory, the extent of cyclization in the cationic polymerization of *o*-divinylbenzene varies in the order of $\text{AlCl}_3 > \text{SnCl}_4 > \text{TiCl}_4 > \text{FeCl}_3 > \text{BF}_3\text{OEt}_2 > \text{ZnCl}_2$.⁵ Since the observed order of influence of catalysts on polymer structures coincides generally (but not necessarily) with the known order of potencies of Friedel-Crafts catalysts^{11,12} and with the strength of coordination of these Lewis acids to carbonyl groups,¹³ the observed structural variation of polycyclopentadiene may be explained in terms of the tightness of the growing ion pair. A more acidic catalyst is considered to give an ion pair of weaker interaction and a less acidic catalyst to give one of stronger interaction. The gegenanion would interact with the cation more strongly in a tighter ion pair, causing localization of the positive charge, while in a looser ion pair the positive charge of the growing ion pair would tend to be more delocalized for want of the stronger interaction.

In the following are schematically shown these two kinds of ion pairs and their propagation reactions.



A weak Friedel-Crafts catalyst (e.g., BF_3OEt_2) gave a higher 1,4 structure content. Therefore, the positive charge in a higher ion pair will be more localized at the 4 position, when an assumption is made that the monomer attacks at the more positive carbon atom. The positive charge in a looser ion pair would be more delocalized, making the monomer attack less selective, as shown in eq. (2).

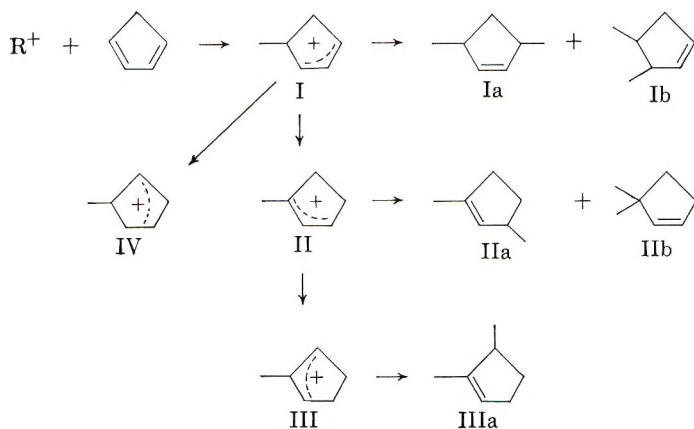
The variation of the cyclization constant in the cationic polymerization of *o*-divinylbenzene was similarly interpreted in terms of the nature of the growing ion pair.⁵

Isomerization during Polymerization

The ratios of olefinic protons to methine-methylene protons in polymer [$D/(A + B + C)$ values] are generally close to 0.5 for polymers obtained in toluene, agreeing with the assumption that the polymer consists mostly of the 1,2 and 1,4 structures. When the values are examined more closely, however, a tendency becomes apparent that the lower values are obtained in general at higher temperatures and with stronger catalysts (i.e., AlBr_3 or TiCl_4 rather than SnCl_4 or BF_3OEt_2). These results indicate the decrease of the olefinic proton in polymer and suggest isomerization of the cyclopentene unit. In cationic polymerization of cyclopentadiene with trichloroacetic acid, Davies and Wassermann obtained a highly isomerized (branching and double bond migration) polymer.¹⁴ The NMR spectrum of this polymer clearly shows the decrease of olefinic protons.

A question arises whether the decrease in the amount of olefinic protons in the present system occurred during propagation as reported for cationic polymerization of 3-methyl-1-butene,¹⁵ or whether migration of hydrogen was induced by the action of Friedel-Crafts catalysts on the internal double bond in the polymer. The results given in Table IV indicate that treatment of polycyclopentadiene with the catalyst causes only a little change in the structure of polymer, although polycyclopentadiene obtained by polymerization with TiCl_4 at 0°C. showed a larger decrease in olefinic protons. Therefore, most of the isomerized units must have been formed during propagation.

The cationic propagation of cyclopentadiene without isomerization gives structures (Ia), 1,4 structure, and (Ib), 1,2 structure, via an allylic carbonium ion intermediate (I):



Hydride transfer may convert (I) into (II) and (IV). Repeated hydride transfer can yield (III) from (II). Among the three isomerized intermediates, (IV) is the same as (I) and need not be considered further as far as the polymer structure is concerned. Propagation of the intermediates (II) and (III) would give structural units (IIa) and (IIb), and (IIIa), respectively.

As mentioned above, the criterion for isomerization was the decrease in the amount of the olefinic proton in polymer. This criterion will be reasonable, since exclusive formation of (IIb) from (II) would be improbable. It cannot be decided from the NMR spectroscopic data which of (IIa), (IIb), and (IIIa) is predominant in the isomerized units in polymer. However, since the alkyl group on the terminal carbon rather than on the central carbon stabilizes an allylic carbonium ion more effectively, the intermediate (III) may be less important than (II). Furthermore, formation of (IIa) might be favored over (IIb) because of steric effects. Thus, (IIa) would be the most probable candidate for the isomerized units, and the driving force for isomerization would be the higher stability of (II) as compared with (I).

The isomerization as estimated from decrease of the amount of the olefinic proton occurs more readily with stronger catalysts, in more polar solvents, and at higher temperatures. This fact suggests that the case of hydride transfer is particularly remarkable with the growing carbonium ion of increased reactivity (i.e., the looser the growing ion pair, the greater the extent of isomerization). For example, the polymer obtained with $AlBr_3$ at $0^\circ C$. in toluene showed $D/(A + B + C)$ values of about 0.4. On lowering of the polymerization temperature the value becomes much closer to 0.5. In methylene chloride the values were invariably much lower than 0.5 with $AlBr_3$ catalyst, in spite of the use of lower temperatures. $BF_3 \cdot OEt_2$ catalyst, however, tends to give the normal product in methylene chloride even at $0^\circ C$.

In Figure 2 are plotted the contents of the 1,2 structure with varying catalysts and temperature in methylene chloride. As is apparent from

Table II, the extent of isomerization is higher in this solvent. The estimated amounts of the 1,2 structure will, therefore, be less reliable than those in toluene. The presence of the isomerized units as shown above would decrease the amount of the olefinic proton and increase the amount of the β -methylene proton, since the β -methylene group is present in all of the isomerized units (IIa), (IIb), and (IIIa).

Thus, isomerization lowers the calculated amount of the 1,2 structure, and this influence will be much greater when the content is calculated from the amounts of the β -methylene (A) and olefinic (D) protons (method 2) than from method 1 (see Table II). This is actually reflected in the discrepancies of the 1,2 structure contents obtained by two methods (always higher when calculated by method 1). Therefore, the 1,2 structure contents calculated by method 1 were plotted in Figure 2.

When (IIa) is assumed to be the only isomerized unit, the influence of isomerization on the calculation of the 1,2 structure content can be estimated. With the $D/(A + B + C)$ value of 0.40 the content of (IIa) in polymer is 28.6% [the remaining units were assumed to consist only of (Ia) and (Ib)]. The β -methylene peak of (IIa) is supposed to appear in a region similar to that of peak A, and the α -methine and α -methylene peak for (IIa) will be contained in peaks B and C. Then, the corrected content of the 1,2 structure becomes 49.5%, as against the uncorrected content of 52.8%. With the $D/(A + B + C)$ value of 0.45 a similar calculation leads to 13.8% of (IIa) and a corrected content of 47.8% against the uncorrected value of 49.5%. Therefore, if (IIa) is the predominant isomerized unit, the uncorrected 1,2 structure contents given in the tables are, when calculated by method 1, close to the true values, since the $D/(A + B + C)$ values are over 0.40 in most cases.

Effect of Solvent

In spite of the above-mentioned limitation in the structural assignment, several conclusions can be drawn from polymerization in methylene chloride. First, the polymer structure does not vary with temperature for a given catalyst below -10°C ., and the amount of the 1,2 structure increases as $\text{TiCl}_4 \approx \text{AlBr}_3 > \text{SnCl}_4 > \text{BF}_3\text{OEt}_2$, which order is the same as in toluene. Thus the effects of temperature and catalysts as already described for toluene solvent are similarly observed in this solvent: the structure of the growing ion pair is not temperature-dependent, and the gegenanion is an important factor in determining the polymer structure.

Second, the amounts of 1,2 structure are higher in methylene chloride than in toluene for a given catalyst by several per cent (but not so for TiCl_4). Apparently, the growing ion pair is better solvated with polar methylene chloride than with toluene, resulting in a weaker interaction of the ion pair and a higher 1,2 structure content.

The most remarkable phenomenon in methylene chloride is that the polymer structure tends to converge at around 0°C . The amounts of the

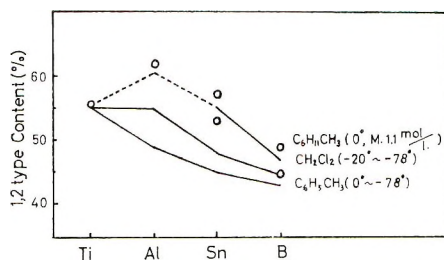


Fig. 3. Variation of polymer structure with catalyst and solvent. The data for methylcyclohexane were obtained at 0°C. with monomer concentrations of 1.1 mole/l. ($TiCl_4$, $SnCl_4$, and BF_3OEt_2) and 0.6 mole/l. ($AlBr_3$). Since the polymer structure varies with monomer concentration in methylcyclohexane, the line drawn for this solvent at $AlBr_3$ is tentative.

1,2 structure obtained with $SnCl_4$ and BF_3OEt_2 at $-20^\circ C$. are comparable to those at lower temperatures, while at -10 to $+10^\circ C$. the 1,2 structure contents increase to 53 or 55% from about 50% ($SnCl_4$) and 45% (BF_3OEt_2) at lower temperatures. Since all the catalysts gave similar polymer structures, the natures of the growing cations should be quite analogous above $-10^\circ C$. in methylene chloride, irrespective of the gegenanion. This result can be interpreted as either that the influence of the gegenanion becomes too weak to be differentiated or even that the growing cation is free from the gegenanion. Although it cannot be determined at present whether free ions or ion pairs exist in this polymerization system, this is a quite interesting problem for future research.

In Figure 3 are plotted the variation of the 1,2 structure content with solvents and catalysts. The plots for methylene chloride and toluene are average values at the temperature range indicated.

It was already mentioned that polar methylene chloride yields higher contents of the 1,2 structure through better solvation of the growing ion pair. This is clearly shown for all the catalytic systems except $TiCl_4$. The polymerization results with other solvents, such as chlorobenzene and chloroform, give plots between toluene and methylene chloride. The difference in the polymer structure between toluene and methylene chloride solvent will be, therefore, due to the solvent polarity.

When methylcyclohexane and cyclohexane are used as solvent, the polymer contains larger amounts of the 1,2 structure than in other solvents (Fig. 3). This result is in conflict with the discussion just described: less polar methylcyclohexane should give less 1,2 structure. This contradictory result requires either that the solvent polarity is actually not a factor that decided the polymer structure or that the aliphatic hydrocarbons bring about different types of solvation state from other solvents. We prefer to adopt the latter possibility, since the influence of the polymerization solvent such as toluene, methylene chloride, and chloroform on the polymer structure could be satisfactorily interpreted in terms of polarity and solvation capacities of these solvents. It is possible that very poor

solvating power of methylocyclohexane makes the nature of the growing ion pair quite different from those in other solvent systems. The poor solvation by methylocyclohexane and cyclohexane (and, to some extent, carbon tetrachloride) can be inferred also from the effect of monomer concentration in these solvents, as discussed below. As another possibility, the abnormal results in methylocyclohexane can be explained by assuming formation of ion aggregates, which include the growing ion pair. Then the surroundings of the growing ion pair would be quite different in methylocyclohexane from the more polar solvents, and the higher content of the 1,2 structure and the influence of monomer concentration may be rationalized.

From Figure 3 it is apparent that the structure of the polymer with TiCl_4 catalyst is not subject to solvent effect. Since TiCl_4 gives the highest content of the 1,2 structure among the catalysts used, the growing ion pair derived from TiCl_4 will be the loosest and may be affected least by surrounding solvents. Another possibility is that the ion pair derived from TiCl_4 possesses particularly strong interaction with monomer, owing to some kind of *d*-orbital participation, thereby minimizing the influence of the surroundings. A deactivation of TiCl_4 catalyst due to formation of a titanocene compound was already proposed.¹⁸

Effect of Monomer Concentration

In Figure 4 is shown the relationship of the polymer structure to monomer concentration with SnCl_4 catalyst at 0°C . The amount of 1,2 structure does not change with monomer concentration in toluene, implying that the solvation state of the growing ion pair is not affected by variation of the cyclopentadiene concentration in this solvent. On the other hand, the 1,2 structure content seems to decrease with monomer concentration in carbon tetrachloride and in methylocyclohexane. When trichloroacetic acid was used as cocatalyst in methylocyclohexane, however, the polymer structure was independent of monomer concentration at about 52% of the 1,2 structure. Since the addition of cocatalyst did not change the polymer structure in other solvents, this again indicates the sensitive nature of the growing ion pair in methylocyclohexane. At higher monomer concentra-

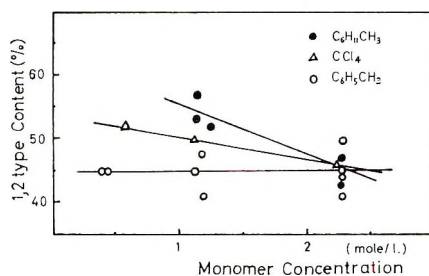


Fig. 4. Effect of monomer concentration on polymer structure. Polymerization at 0°C . with SnCl_4 catalyst.

tions (about 2.2 mole/l.) in these solvents the amount of the 1,2 structure becomes quite close to that in toluene. These results may be interpreted as follows.

At lower monomer concentrations in carbon tetrachloride and in methylcyclohexane the growing ion pair will be very poorly solvated (i.e., surrounded more by carbon tetrachloride or by methylcyclohexane), giving rise to higher amounts of the 1,2 structure, possibly for the above-mentioned reasons. With increasing monomer concentrations the ion pair becomes solvated more fully by cyclopentadiene molecules, and its solvation state would become similar to that in toluene solvent, as may be presumed from the structure of the resulting polymer. The fact that the polymer structure does not depend on monomer concentration in toluene can be explained by considering the better solvating capacity of toluene, which must be greater than, or at least similar to, that of cyclopentadiene. That is, the solvation state of the ion pair in toluene must be invariant in spite of different monomer concentrations. A similar situation will be encountered in methylene chloride. As methylene chloride is more polar than toluene, it is expected to solvate the ion pair better than toluene. Thus, the polymer structure will be independent of the monomer concentration in methylene chloride. Although lower monomer concentrations were used for polymerization in methylene chloride because the tendency to form a gel was great, it is this consideration that justifies the direct comparison of the polymer structure obtained in toluene and in methylene chloride in spite of different monomer concentrations.

Variation of Molecular Weight

The variation of intrinsic viscosities of polycyclopentadiene with polymerization conditions is given in Figure 5 for toluene solvent. The molecular

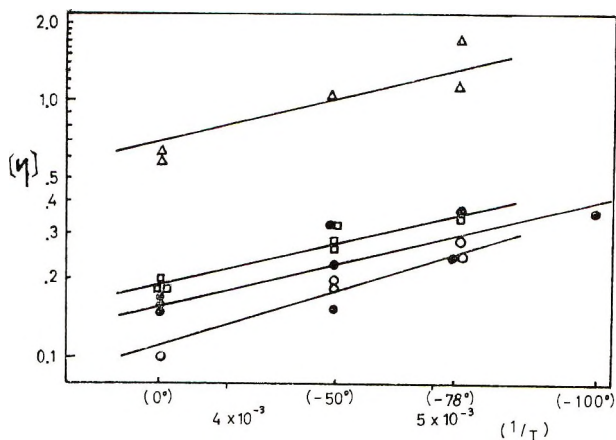


Fig. 5. Variation of intrinsic viscosity with polymerization conditions for polycyclopentadiene obtained in toluene. Catalyst: (●) TiCl_4 ; (○) AlBr_3 ; (□) SnCl_4 ; (Δ) $\text{BF}_3 \cdot \text{OEt}_2$.

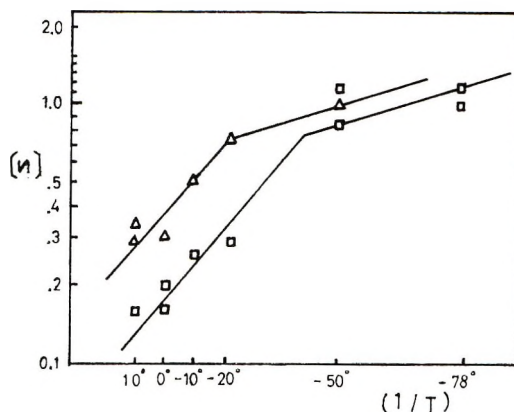


Fig. 6. Variation of intrinsic viscosity with polymerization conditions for polycyclopentadiene obtained in methylene chloride. Catalyst: (□) SnCl₄; (Δ) BF₃OEt₂.

weight increases with decrease in polymerization temperature. The monomer concentrations were 1.2 mole/l., except for AlBr₃ catalyst, with which lower monomer concentrations (0.4 and 0.6 mole/l.) were used because of faster polymerization. The viscosities are highest for BF₃OEt₂ catalyst, and there were smaller differences between the other three catalyst systems. The data for TiCl₄ are somewhat scattered.

The molecular weight of polycyclopentadiene obtained in toluene decreases with potency of the catalyst used. It was reported that k_p/k_t (the ratio of rate of propagation to rate of transfer) is greater for stronger catalysts in the cationic polymerization of styrene.¹⁰ The same may be said for the present case. The AlBr₃-TiCl₄ reversal must be due to the smaller monomer concentrations used for AlBr₃ catalyst. Similar effects of the catalyst on molecular weights were also found for the polymerization of substituted cyclopentadienes, such as allylcyclopentadiene¹⁶ and methylcyclopentadiene.¹⁷

On the basis of the temperature independence of the polymer structure, the structure of the growing ion pair in toluene was assumed not sensitive to temperature change. The linearity of $\log [\eta]$ with $1/T$, therefore, seems to support the lack of the structural change of the growing ion pair with temperature, and the difference in activation energies between propagation and termination ($E_p - E_t$) can be calculated from the slope. Interestingly, the slopes for the different catalytic systems are all similar. With the value, given by Achon et al.,¹⁹ of $\alpha = 0.5$ in $[\eta] = K[M]^\alpha$ the difference in activation energies becomes -1.7 kcal./mole. These similar slopes would suggest that the influence of the counteranion on molecular weight is related to the entropy difference between propagation and termination rather than to the corresponding enthalpy difference.

The intrinsic viscosity of some polymers obtained in methylene chloride is plotted against $1/T$ in Figure 6. As systematic viscosity data for TiCl₄ and AlBr₃ catalysts were not obtained, plots are given only for the

data from BF_3OEt_2 and SnCl_4 catalysts. Apparently, these plots are divided into two linear portions with a steeper slope at higher temperatures. Thus, the activation energy differences between propagation and termination (-1.7 kcal./mole) are similar at lower temperatures to those in toluene but greater (-4.3 kcal./mole) at higher temperatures.

The difference in viscosity data between these two solvents (Fig. 5 versus Fig. 6) is particularly noteworthy when its parallelism with the variation of the polymer structure is considered. It was mentioned that the growing ion pair in methylene chloride undergoes a structural change at about -10°C ., becoming looser at higher temperatures. The viscosity data of Figure 6 may be also understood by considering the similar structural change. Since the slope at lower temperatures is similar to those of Figure 5, the structure of the growing ion pair must be similar and the ($E_p - E_t$) value is affected much neither by solvent nor by temperature in this range. At higher temperatures, however, the ion pair structure may become loose to a considerable extent; hence, a higher value of $E_p - E_t$.

The authors are indebted very much to Prof. T. Matsuo for cooperation in numerous NMR measurements. The generous donation of dicyclopentadiene by Yawata Chemical is also acknowledged.

References

1. R. G. Stearns and L. E. Forman, *J. Polymer Sci.*, **41**, 381 (1959).
2. C. Aso, T. Kunitake, K. Ito, and Y. Ishimoto, *J. Polymer Sci. B*, **4**, 701 (1966); C. Aso, T. Kunitake, and Y. Ishimoto, *J. Polymer Sci. A-1*, **6**, 1163 (1968).
3. Y. Imanishi, T. Higashimura, and S. Okamura, *J. Polymer Sci. A*, **3**, 2455 (1965).
4. C. G. Overberger and V. G. Kamath, *J. Am. Chem. Soc.*, **85**, 446 (1963).
5. C. Aso, T. Kunitake, and R. Kita, *Makromol. Chem.*, **97**, 31 (1966).
6. N. Kanoh, T. Higashimura and S. Okamura, *Makromol. Chem.*, **56**, 65 (1962).
7. C. Aso and R. Kita, *Kogyo Kagaku Zasshi*, **68**, 707 (1965).
8. Y. Ohsumi, T. Higashimura, and S. Okamura, *J. Polymer Sci. A-1*, **4**, 923 (1966).
9. A. V. Tobolsky and R. J. Boudreau, *J. Polymer Sci.*, **51**, S53 (1961).
10. H. Sakurada, T. Higashimura, and S. Okamura, *Kogyo Kagaku Zasshi*, **61**, 1640 (1958).
11. I. F. Fieser and M. Fieser, *Advanced Organic Chemistry*, Reinhold, New York, N.Y., 1961, p. 659.
12. O. C. Dermer, D. M. Wilson, F. M. Johnson, and V. H. Dermer, *J. Am. Chem. Soc.*, **63**, 2881 (1951).
13. B. P. Susz, *Chem. Eng. News*, May 31, 1965, p. 97.
14. A. G. Davies and A. Wassermann, *J. Polymer Sci. A-1*, **4**, 1887 (1966).
15. J. P. Kennedy, W. W. Schultz, R. G. Squires, and R. M. Thomas, *Polymer*, **6**, 287 (1965).
16. C. Aso and O. Ohara, *Chem. High Polymers (Tokyo)*, **23**, 895 (1966).
17. C. Aso and O. Ohara, *Makromol. Chem.*, **109**, 161 (1967).
18. S. Kikutani, T. Yamane, Y. Imanishi, T. Higashimura, and S. Okamura, The 15th Discussion Meeting of the Society of Polymer Science, Osaka, Japan, 1966, *Preprints*, p. 323.
19. M. A. Achon, M. I. Garcia Banon, J. L. Matates, and J. L. Ynfesta, *Anales Real Soc. Espan. Fis. Quim. (Madrid)*, **57**, 309 (1961); *C. A.*, **56**, 3609 (1962).

Received June 19, 1967

Room-Temperature Polycondensation of β -Amino Acid Derivatives. I. Polyamide from Amino Alcohols and Acrylates

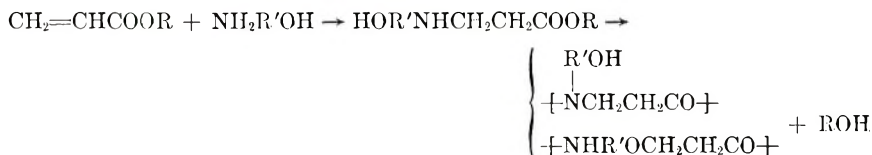
KOHEI SANUI, TOMOHIKO ASAHARA,* and NAOYA OGATA,†
Chemistry Department, Sophia University, Chiyoda-Ku, Tokyo, Japan

Synopsis

Acrylates, such as ethyl acrylate, add with amino alcohol to form *N*-(hydroxyalkyl) β -alanine ester and room-temperature polycondensation follows, forming polyamide in the presence of a basic catalyst, such as alkali metal alkoxide. The reaction medium has an influence on the course of the polycondensation; that is, *N*-(hydroxyalkyl) polyamide is formed in methanol solution and polyamide ether in other solvents, such as tetrahydrofuran. These two courses of the room-temperature polycondensation have been studied, and the reaction mechanism is discussed in this paper.

INTRODUCTION

It was previously shown^{1,2} that acrylates, such as ethyl acrylate, add with amino alcohol and then room-temperature polycondensation follows in the presence of an alkoxide, to form polyamide as described below:



The reaction medium has an influence on the course of the polycondensation. *N*-(Hydroxyalkyl) polyamide is mainly formed in methanol solution, and polyamide ether is obtained in other polar solvents, such as tetrahydrofuran. In this work extensive studies of the room-temperature polycondensation of amino alcohol and acrylate were carried out and the reaction mechanism is discussed in this paper.

RESULTS

Simultaneous Polycondensation of Amino Alcohol and Acrylate

The rates of acrylate consumption and alcohol liberation in tetrahydrofuran solution are shown in Figures 1 and 2. The catalytic activity of alkox-

* Present address: Basic Research Laboratories, Toyo Rayon Co., Ltd., Tebiro, Kamakura, Japan.

† To whom all inquiries should be addressed.

TABLE I
Room-Temperature Polycondensation of Ethanolamine and Acrylate

Solv.	Mono- mer concn., mole/l.	Catalyst	Catalyst concn., mole-%	Temp., °C.	Time, days	Polymer						
						Yield, %	Yield, %	m.p., °C.	m.w.			
Methyl None	1	CH ₃ OLi	5	30	10	1.5	160	925	98	grease	530	
		CH ₃ ON ^a	5	30	13	15	160	810	75	grease	450	
CH ₃ OH	1	CH ₃ OK	5	30	0.5	77	170	850	12	grease	500	
		K	5	-78	7	0	—	—	100	grease	510	
		K	5	0	7	5.6	160	900	95	grease	500	
		K	5	25	5	62	160	925	38	grease	500	
		K	5	64	1	1	—	—	—	92	grease	—
		KOH	5	30	10	2.3	—	—	—	98	grease	—

	Na	5	25	5	22	160	810	78	grease	450
	Na	5	64	0.5	0	—	—	100	grease	400
	Triton-B	5	25	2	0	—	—	100	grease	532
	Triton-B	5	25	13	0	—	—	100	grease	—
	CH ₃ OK	5	25	1	0	—	—	100	grease	—
<i>t</i> -BuOH	Na	5	25	9	0	—	—	100	grease	450
	Na	5	84	1	0	—	—	100	grease	—
THF	CH ₃ OK	5	25	8	0	—	—	100	grease	400
	CH ₃ ONa	5	25	9	0	—	—	100	grease	—
DMF	CH ₃ OK	5	25	8	0	—	—	100	grease	—
Heptane	AlEt ₃	0.6	20	6	41	204	—	43	grease	—
Ethyl										
CH ₃ OH	K	5	30	6	23	180	860	75	grease	450
THF	ZnEt ₂	4	20	1	100	245	—	0	—	—
Butyl										
CH ₃ OH	K	5	30	7	27	180	903	1	30	520
Phenyl										
DMF	CH ₃ OK	5	25	1	0	—	—	100	grease	450

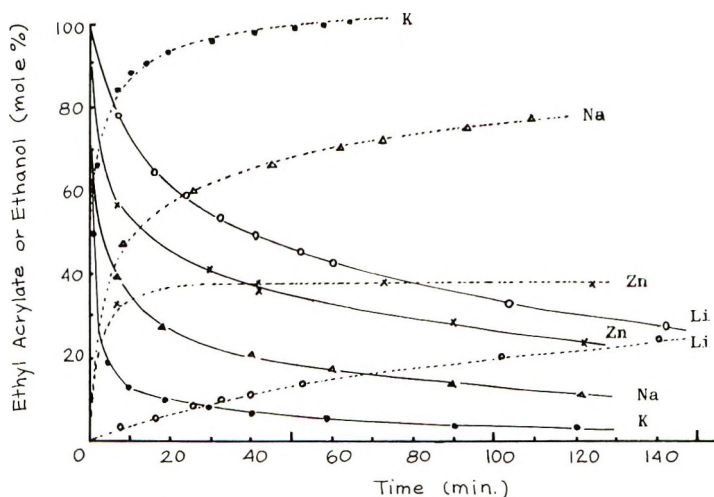


Fig. 1. Rate of reaction of ethanolamine and ethyl acrylate in presence of basic catalysts (concn., 1 mole/l. in THF at 20°C.; catalyst concn., 5 mole-%): (—) ethyl acrylate; (---) ethanol.

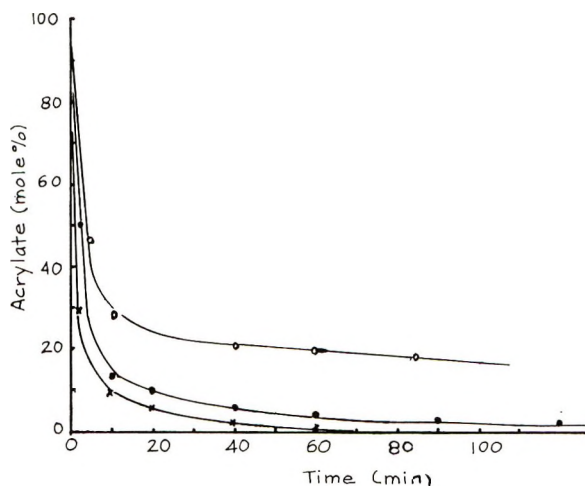


Fig. 2. Rate of reaction of ethanolamine and acrylate (concn., 1 mole/l. in THF at 20°C.; catalyst, $K = 5$ mole-%): (O) butyl ester; (●), ethyl ester; (×) methyl ester.

ide decreases in the order of $K > Na > Zn > Li$ and the reactivity of acrylic ester in the order $-\text{CH}_3 > -\text{C}_2\text{H}_5 > -\text{C}_4\text{H}_9$. The properties of the polymers are summarized in Table I.

The yields of polymers in various solvents are almost quantitative and most of them are soluble in methanol and water. The rate of the formation of the alcohol-insoluble polymer in methanol is shown in Figure 3.

The alcohol-insoluble polymer has a melting point of 160–180°C., and its molecular weight is in the range of 800 and 1000, while the alcohol-soluble polymer is a grease with a molecular weight of about 400. Infrared

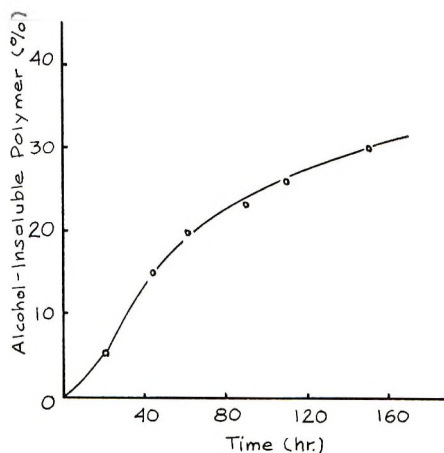


Fig. 3. Rate of formation of alcohol-insoluble polymer from ethanolamine and methyl acrylate (concn., 1 mole/l, in methanol at 25°C., $K = 5$ mole-%).

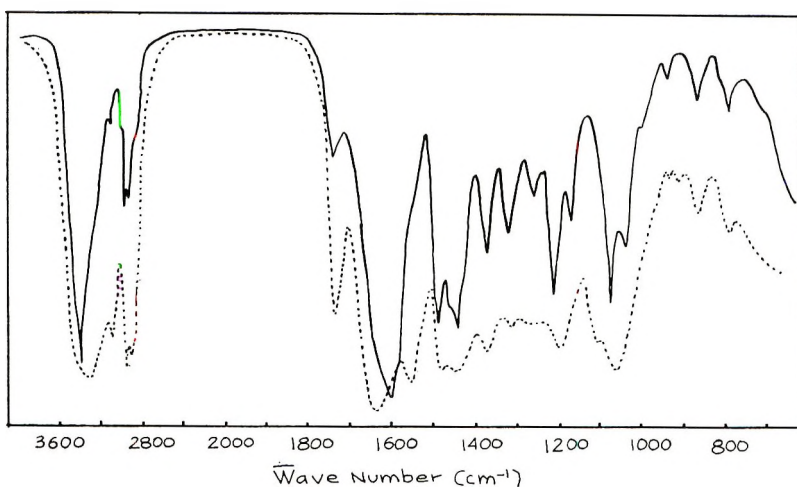


Fig. 4. Infrared spectra of polymers of ethanolamine and acrylate, KBr: (···) alcohol-soluble polymer; (—) alcohol-insoluble polymer.

spectra of alcohol-soluble and alcohol-insoluble polymers are shown in Figure 4, in which the alcohol-soluble polymer indicates absorptions owing to secondary amide and ether groups, and the alcohol-insoluble polymer shows peaks of tertiary amide. Acetylation of the alcohol-insoluble polymer resulted in the disappearance of 3440 cm.^{-1} absorption, owing to hydroxyl group, and a new absorption appeared at 1750 cm.^{-1} , which could be assigned to the ester carbonyl absorption.¹ Paper chromatograms of the hydrolyzed product of the alcohol-soluble and insoluble polymers showed ninhydrin-positive spots of $R_f = 0.10$ and 0.40 , respectively, by developing with a mixed solution of *n*-butanol and ammonia of 80:20. The R_f value of ethanolamine (0.53) was not consistent with those values, and they

corresponded to R_f values of the hydrolyzed product of $\text{CH}_3\text{CONHCH}_2\text{-CH}_2\text{OCH}_2\text{CH}_2\text{COOR}$ and $\text{HOCH}_2\text{CH}_2\text{NHCH}_2\text{CH}_2\text{COOR}$, respectively. Therefore, it is assumed that the alcohol-soluble polymer had the structure of polyamide ether and the alcohol-insoluble polymer was *N*-(hydroxyethyl) poly- β -alanine.

Room-Temperature Polycondensation of *N*-(Hydroxyalkyl) β -Alanine Esters

N-(Hydroxyalkyl) β -alanine esters were dissolved in a solvent in the concentration of 1 mole/l. in the presence of alkali metal catalyst. Polycondensation took place immediately at room temperature, and alcohol was eliminated in the solution. The rates of the polycondensation of various β -alanine esters in tetrahydrofuran solution are shown in Figure 5. Generally, polycondensation proceeds in such a course that alcohol is eliminated immediately after the addition of potassium alkoxide and then the amount of alcohol decreases gradually to an equilibrium. Polycondensation of *N*-(hydroxyhexyl) β -alanine ester proceeds in a different way from that of other esters, resulting in a gradual increase of the amount of alcohol to an equilibrium as in the case of the simultaneous polycondensation of acrylate and amino alcohol.

The polymers produced are alcohol-soluble with a molecular weight of about 500, and their infrared spectra indicate the structure of polyamide ether. This result suggests that a rearrangement might take place, forming polyamide ether in tetrahydrofuran solution.

When methanol was used as a solvent for the polycondensation of *N*-(hydroxyethyl) β -alanine ester, a white polymer precipitated gradually, which had the same structure as that obtained by the simultaneous polycondensation of ethanolamine and methyl acrylate in methanol. The

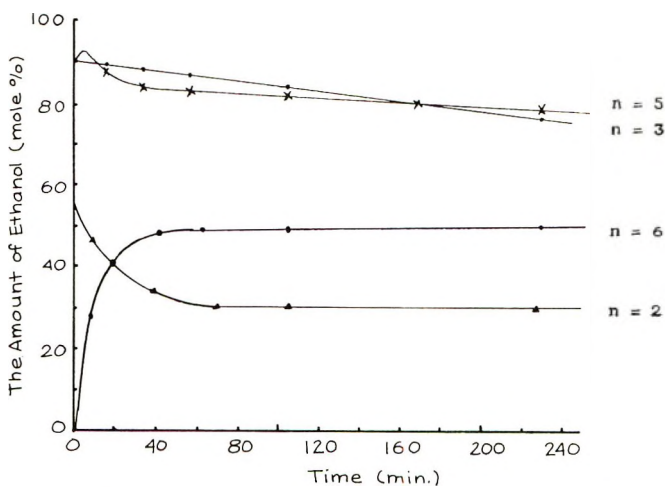


Fig. 5. Rate of polycondensation of *N*-(hydroxyalkyl) β -alanine ethyl esters $\text{HO-(CH}_2)_n\text{-NHCH}_2\text{CH}_2\text{COOEt}$ (concn., 1 mole/l. in THF at 20°C., $K = 5$ mole-%).

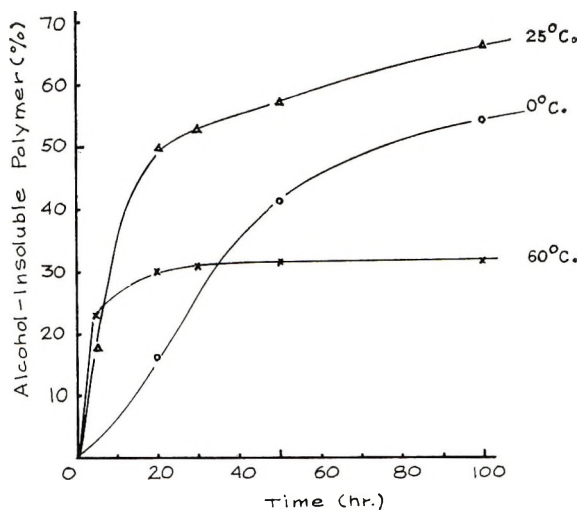


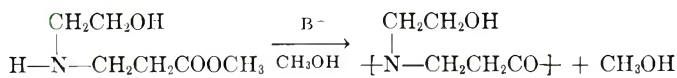
Fig. 6. Rate of formation of alcohol-insoluble polymer of *N*-(hydroxyethyl) β -alanine ester in presence of sodium catalyst (monomer concn., 1 mole/l. in methanol, sodium = 5 mole-%).

rates of the formation of the alcohol-insoluble polymer from *N*-(hydroxyethyl) β -alanine ester were measured in methanol at various temperatures. The results are shown in Figure 6. Compared with Figure 3, the rate is much faster than that of the simultaneous polycondensation of ethanolamine and acrylate. The properties of the polymer are summarized in Table II.

TABLE II
Polycondensation of *N*-(Hydroxyethyl) β -Alanine Methyl Ester in Methanol (Concn., 1 mole/l.)

Catalyst	Temp., °C.	Time, hr.	Yield, %	m.p., °C.	m.w.
K, 5 mole-%	0	100	56.3	180-190	1760
K, 5 mole-%	25	100	70.0	185-195	2000
K, 5 mole-%	60	50	32.0	185-195	2500
K, 5 mole-%	60	100	32.0	193-203	2700

The molecular weight is higher with increasing temperature and the polymer becomes insoluble even in water as the molecular weight reaches more than 2000.



The rate of formation of the alcohol-insoluble polymer was determined in methanol in the presence of various alkali metal alkoxides, as shown in Figure 7. It is seen in this figure that the formation rate decreases in the order $\text{Li} > \text{Na} > \text{K} > \text{Cs}$, which is the reverse of the order of simultaneous polycondensation of ethanolamine and acrylate.

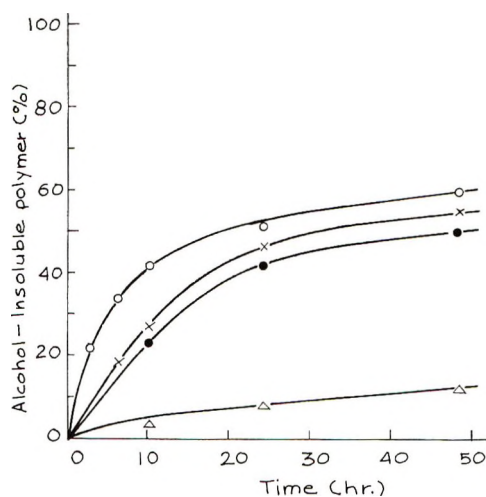


Fig. 7. Rate of polycondensation of *N*-(hydroxyethyl) β -alanine methyl ester in presence of alkali metal methoxide (concn., 1 mole/l. in CH_3OH at 30°C .; catalyst concn., 5 mole-%): (O) Li; (X) Na; (●) K; (Δ) Cs.

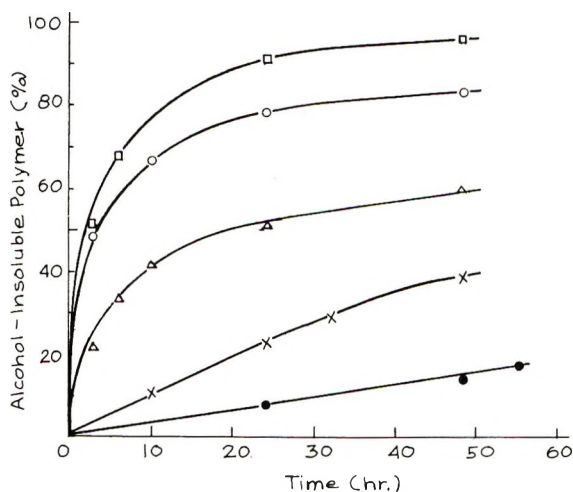


Fig. 8. Effect of monomer concentration on polycondensation of *N*-(hydroxyethyl) β -alanine methyl ester (catalyst, 5 mole-% Li, in CH_3OH at 30°C .). Monomer concn. (mole/l.): (●) 0.30; (X) 0.60; (Δ) 1.00; (O) 2.00; (\square) bulk.

The effects of the monomer concentration in methanol are shown in Figure 8, where it is seen that increasing monomer concentration results in increase of the polycondensation rate and the polymer yield. However, the molecular weight of the polymer decreases with increasing monomer content in the solution, as seen in Table III.

TABLE III
Effect of Monomer Concentration on Polycondensation^a of
N-(Hydroxyethyl) β -Alanine Methyl Ester

Concn. of monomer, mole/l.	Yield, %	m. w.
0.30	12.8	2200
0.60	38.1	1850
1.00	50.0	1320
2.00	81.7	1350
bulk ^b	91.3	1140

^a Catalyst: 5 mole-% Li in CH₃OH at 30°C. Time, 48 hr.

^b 24 hr.

Thermal Polycondensation of *N*-(Hydroxyethyl) β -Alanine Ester

N-(Hydroxyethyl) β -alanine ethyl ester was heated at various temperatures in vacuum in the presence of 1 mole-% of basic or acidic catalysts. The results are shown in Table IV. Basic catalysts gave a water-soluble polymer having a molecular weight of around 2000, whereas acidic catalysts gave insoluble and infusible polymer, which had a crosslinked structure. The thermal polycondensation did not give a high molecular weight polymer.

TABLE IV
Thermal Polycondensation of *N*-(Hydroxyethyl) β -Alanine Ester
(Catalyst Concn., 1 mole-%)

Catalyst	Temp., °C.	Time, hr.	Yield, %	η_{inh}^a	m. w.	M. p., °C.
None	100	8	90	0.03	—	90–100
K	153	5	100	—	1700	235–238
CH ₃ OK	100	8	100	0.08	1400	210–220
CH ₃ OK	153	5	100	0.07	—	180–188
SnCl ₂	100	8	95	0.06	—	120–130
SnCl ₄	153	5	90	—	1400	255–260
TiCl ₄	100	8	90	0.09	—	159–161
TiCl ₄	153	5	91	—	900	300
ZnCl ₂	153	5	92	—	850	290–300
AlCl ₃	153	5	90	—	1000	260–265
BF ₃ OEt ₂	100	8	95	0.05	—	100–110
BF ₃ OEt ₂	153	5	93	—	—	55–65
Sb(OEt) ₃	153	5	95	—	—	160–170
H ₃ PO ₄	153	5	90	—	2500	230–240

^a 1.0 g./100 ml. in water at 25°C.

DISCUSSION

It was previously reported¹ that the rate of the addition of alkoxide ion with acrylate was much faster than that of amine. Therefore, it is expected that amino alcohol adds to acrylate at the hydroxyl group in the presence

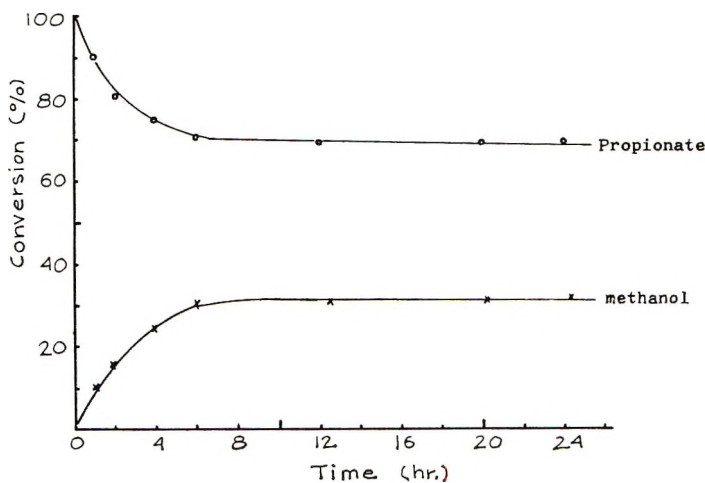


Fig. 9. Rate of exchange reaction between β -methoxy methyl propionate and ethanolamine in THF (concn., 1 mole/l., at 25°C.).

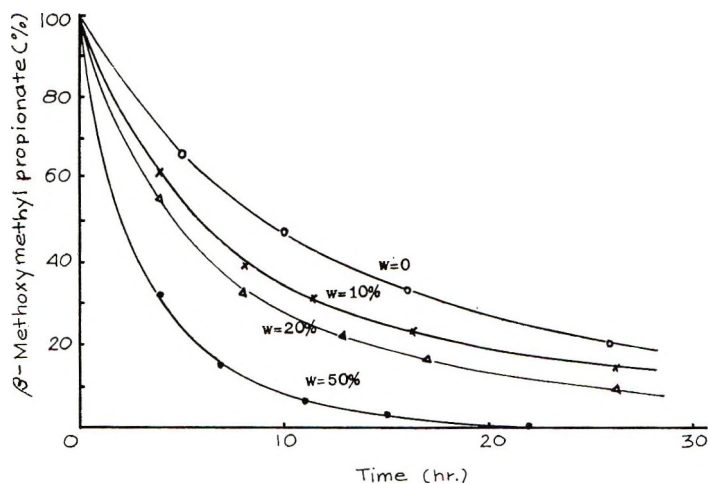
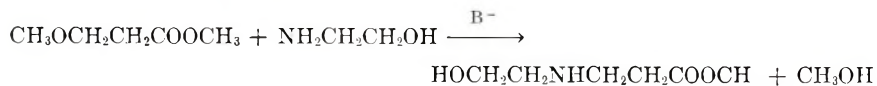


Fig. 10. Rate of exchange reaction between β -methoxy methyl propionate and ethanolamine in aqueous methanol (concn., 1 mole/l., 25°C.; W = water content).

of an alkoxide catalyst. However, *N*-(hydroxyalkyl) polyamide is formed in methanol solution. This result suggests that amino alcohol reacts with acrylate at the amino group in methanol even in the presence of alkali metal alkoxide. The previous results,³ that methanol accelerates the addition of amine with acrylate, might give an explanation for this curious reaction. If ethanolamine is more nucleophilic than methoxide ion in methanol, an exchange reaction might take place between β -methoxy methyl propionate and ethanolamine as shown below:



Therefore the following experiment was carried out. β -Methoxy methyl propionate, which was synthesized from methyl acrylate and methanol, was mixed in equimolar amount with ethanolamine, each in the concentration of 1 mole/l. in tetrahydrofuran or methanol in the presence of 1 mole-% of potassium methoxide. The change of the amount of the propionate was determined by gas chromatography. Figures 9 and 10 show that the amount of β -methoxy methyl propionate and ethanolamine decreased gradually to an equilibrium.

The reaction product was distilled under vacuum, and a product of the same boiling point and the same structure as *N*-(hydroxyethyl) β -alanine methyl ester was obtained. Therefore, it is confirmed that an exchange reaction took place between the propionate and ethanolamine. In tetrahydrofuran solution 30 mole-% of methanol was eliminated immediately after the addition of potassium methoxide, and 30 mole-% of the propionate disappeared in the solution. Polar solvents cause a shift of the equilibrium toward exchange, and water has an accelerating effect on the exchange, as may be seen in Figure 10.

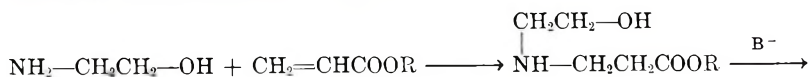
Therefore, it is presumed that the amino group of ethanolamine is more nucleophilic than methoxide ion in methanol solution. These results might also explain that the room-temperature polycondensation of *N*-(hydroxyethyl) β -alanine ester takes place to form polyamide, since the amine hydrogen is activated in methanol solution.

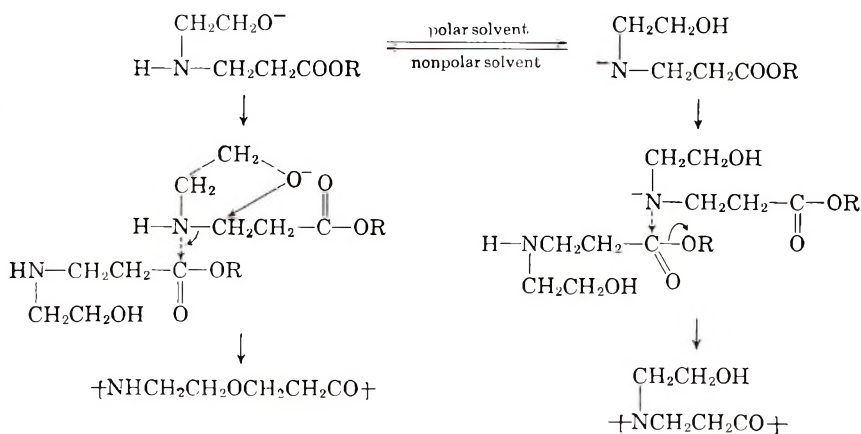
In the polycondensation of *N*-(hydroxyalkyl) β -alanine esters in tetrahydrofuran solution the eliminated alcohol was gradually consumed, as may be seen in Figure 5. This behavior, which seems to be quite curious, might be related to the above-mentioned exchange reaction. In methanol solution polymer was precipitated gradually, to remove it from participation in the exchange reaction.

The apparent reverse order of the catalytic activity of alkali metal in the simultaneous polycondensation of ethanolamine and acrylate might be explained that the addition reaction of ethanolamine to acrylate is accelerated with a more basic catalyst.

N-Alkyl β -alanine ester did not polymerize at all under the same reaction condition as that of *N*-(hydroxyethyl) β -alanine ester, and it is assumed that the hydroxyl group has an important role on the room-temperature polycondensation. When an equimolar amount of methanol was added to a tetrahydrofuran solution of *N*-butyl β -alanine methyl ester in the presence of potassium methoxide, the amount of methanol in the solution increased up to 20%, suggesting that condensation takes place. The residual product after evaporation of the solution had a molecular weight of 200. Therefore, the intramolecular effect of the hydroxyl group of β -alanine ester may have an important role on the room-temperature polycondensation.

A tentative reaction scheme is postulated:



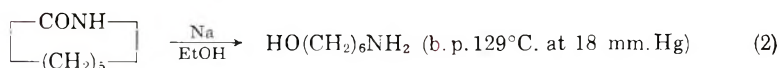
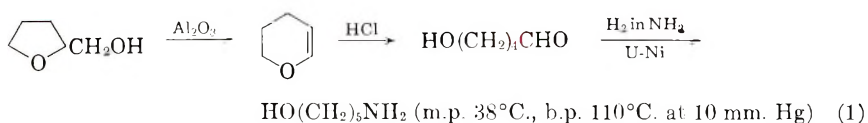


The detailed studies of each step of the room-temperature polycondensation will be reported later.

EXPERIMENTAL

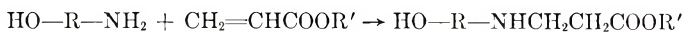
Synthesis of Amino Alcohols

Commercial ethanolamine and propanolamine were purified by a fractional distillation, and the following amino alcohols were synthesized as shown below:



Synthesis of *N*-(Hydroxyalkyl) β-Alanine Esters

Amino alcohol and acrylate were mixed together in tetrahydrofuran, each in the concentration of 1 mole/l., keeping the solution temperature at 25°C. for 24 hr., and then the contents were distilled in vacuum. The yield of the β-alanine esters was almost quantitative.



R	R'	b.p., °C.
—(CH ₂)—	—CH ₃	107/3 mm. Hg
—(CH ₂)—	—C ₂ H ₅	135/3
—(CH ₂)—	—C ₄ H ₉	116/1
—(CH ₂) ₃ —	—CH ₃	102/2
—(CH ₂) ₃ —	—C ₂ H ₅	137/3
—(CH ₂) ₅ —	—C ₂ H ₅	140/2
—(CH ₂) ₆ —	—C ₂ H ₅	145/2

Room-Temperature Polycondensation of β -Alanine Esters

N-(Hydroxyalkyl) β -alanine esters were dissolved in a solvent, each in the concentration of 1 mole/l., and then a given amount of alkali metal was added to the solution. The amount of alcohol eliminated by polycondensation was determined in a given period by gas chromatography with a DOP column. When equal moles of amino alcohol and acrylate are mixed together in a solvent, amino alcohol adds to acrylate at the amino group, giving *N*-(hydroxyalkyl) β -alanine ester quantitatively, and polycondensation does not occur further. However, when a strong base, such as an alkali metal alkoxide, is present in the solution, polycondensation takes place with the addition reaction, and alcohol is eliminated in the solution. A white polymer precipitated gradually on standing at 25°C. within a day, when methyl acrylate reacted with ethanolamine, each in the concentration of 1 mole/l. in methanol in the presence of 1 mole-% of potassium methoxide.

The characterization of the polymer was done by elementary and infrared analyses, and the molecular weight was determined by a vapor-pressure osmometer or endgroup titration. The elementary analyses of alcohol-soluble and alcohol-insoluble polymers gave the following results:

	C, %	H, %	N, %
Alcohol-soluble polymer:	49.8	8.5	11.9
Alcohol-insoluble polymer:	49.0	8.3	11.5

References

1. N. Ogata and T. Asahara, *Bull. Chem. Soc. Japan*, **39**, 1486 (1966).
2. N. Ogata and T. Asahara, *J. Polymer Sci. B*, **4**, 273 (1966).
3. N. Ogata and K. Sanui, *Bull. Chem. Soc. Japan*, **40**, 1727 (1967).

Received February 10, 1966

Revised September 10, 1967

Infrared Studies of Stereoregular Polymerization of Methyl Methacrylate and Methacrylonitrile by Organometallic Compounds

TAKETOSHI FUJIMOTO,* NARIYOSHI KAWABATA, and JUNJI FURUKAWA, *Department of Synthetic Chemistry, Kyoto University, Kyoto, Japan*

Synopsis

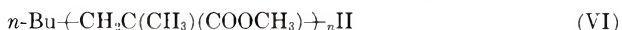
Infrared spectra of reaction mixtures of methyl methacrylate or methacrylonitrile with an equimolar amount of organometallic compounds were investigated in relation to the stereoregulating ability of the catalysts in polymerization. It was found that the carbonyl or nitrile stretching frequency correlated with the stereoregularity of polymers prepared with the corresponding catalysts; i.e., the higher the frequency, the higher the isotacticity. From these results a mechanism of isotactic polymer formation was proposed, in which catalyst counterion was located near the carbonyl group in polymer terminal and that of monomer to be reacted, and consequently the isotactic polymerization is facilitated.

INTRODUCTION

The stereoregular polymerization of acrylates and methacrylates by organometallic compounds has been investigated by many workers,¹ and various mechanisms have been proposed.^{1,2} The stereoregular polymerization of acrylic nitriles by anionic mechanisms has also been investigated in detail.³ In general, the organometallic catalyst was supposed to play an important role in polymerization through the stereospecific location of counterion in the transition state. In this concept the interaction of catalyst with polymer-end or with monomer is assumed to be associated with the stereoregulating ability of the catalyst.⁴ The present work was aimed at estimating the interaction between catalyst and polymer end from infrared spectra of the reaction mixture of methyl methacrylate or methacrylonitrile and organometallic compound.

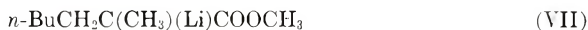
Previously one of the writers (N.K.) made a systematic study of elementary reactions of metal alkyl in the anionic polymerization of acrylic monomers.⁵⁻⁸ In the reaction mixture of methyl methacrylate and *n*-butyllithium were detected, after hydrolysis, the following reaction products:⁵

* Present address: Sumitomo Chemical Co., Kikumoto Works, Niihama, Ehime, Japan.



Similar products were also detected in the reaction mixtures of methyl methacrylate with Grignard reagent⁸ and with lithium aluminum hydride.⁷ Among the reaction products the compounds (IV), (V), and (VI) are related to the polymerization reaction.

It is already established that the reaction of methyl methacrylate with such organometallic compounds as lithium alkyl, Grignard reagent, and lithium aluminum hydride is very rapid at room temperature.⁵⁻⁸ When methyl methacrylate reacts with an equimolar amount of one of these compounds, the monomer is thoroughly consumed within a short time, and there remains no monomer intact. Among the reaction products *n*-butane, (II), and (III) do not show the infrared absorption in the region of 1700 to 1800 cm^{-1} . When methyl methacrylate reacts with an equimolar amount of organometallic compound, a product such as (IV) is in greatest amount among the products having a carbonyl group. Therefore, the writers tried to investigate the infrared spectra of the reaction mixture of equimolar amounts of methyl methacrylate and organometallic compound before hydrolysis. In the region of 1700–1800 cm^{-1} of the spectra will appear the carbonyl absorption of the adduct (VII), and the spectra may show, depending upon the kind of counterion, an interaction between catalyst and polymer end.



A similar situation was also observed in the reaction of methacrylonitrile with each of these organometallic compounds,^{6,8} and the authors also investigated the reaction mixture by infrared spectroscopy.

EXPERIMENTAL

Reagents

Commercial samples of methyl methacrylate and methacrylonitrile were purified by the usual method.⁹ The purity of these monomers was checked by vapor-phase chromatography. Grignard reagents were prepared from alkyl halides and metallic magnesium in diethyl ether. Lithium aluminum triethyl-*n*-butyl was prepared from triethylaluminum and *n*-butyllithium.¹⁰ Lithium zinc *n*-butyldiethyl and dilithium zinc di-*n*-butyldiethyl were prepared from *n*-butyllithium and diethylzinc.¹⁰ Commercially available lithium aluminum hydride, lithium borohydride, diethylzinc, triethylaluminum, and diisobutylmagnesium were used without further purification.

The concentrations of these anionic initiators were estimated by the usual alkalimetry or iodometry. Toluene and diethyl ether were purified by the usual methods.¹¹ Nitrogen was purified by being passed through a tube containing copper turnings in a furnace at 170°C. and then dried. The other chemicals were commercial products and were used without further purification.

Polymerization Procedure

The polymerizations were carried out under a nitrogen atmosphere in sealed Pyrex test tubes. The polymers were recovered by adding methanol containing hydrochloric acid to the reaction mixture and were dried to a constant weight *in vacuo*. Poly(methyl methacrylate) was purified by reprecipitation from the methanol-benzene system and then dried.

NMR Spectra of Polymers

Proton magnetic resonance spectra of poly(methyl methacrylate) and polymethacrylonitrile were obtained with a Japan Electron Optics Lab. Model 4H-100 high-resolution spectrometer at 70°C. Deuteriochloroform and trifluoroacetic acid were used as solvents for poly(methyl methacrylate) and polymethacrylonitrile, respectively. Tetramethylsilane or hexamethyldisilane was used as internal standard for poly(methyl methacrylate) and polymethacrylonitrile. The tacticities of poly(methyl methacrylate)¹² and polymethacrylonitrile¹³ were determined as previously reported.

IR Spectra of Mixtures of Monomers and Organometallic Compounds

A nearly equal amount of methyl methacrylate or methacrylonitrile was added to a solution of an organometallic compound at -78°C. under a nitrogen atmosphere. The reaction mixture was kept at 20°C. for several minutes, to complete the reaction. The infrared spectra of the reaction mixture in a sealed cell were obtained with a Perkin-Elmer Model PE-521 double-beam spectrophotometer or with a Hitachi EPI-S₂ double-beam spectrophotometer at room temperature.

RESULTS AND DISCUSSION

Infrared spectra of reaction mixture of methyl methacrylate with an equimolar amount of one of various organometallic compounds in diethyl ether at room temperature were obtained. The stretching vibration of the carbonyl group was observed in the region of 1724-1732 cm.⁻¹. The stretching frequencies are listed in Table I; they depend on the nature of the catalyst employed. The reaction mixture involves no methyl methacrylate monomer, because of the rapid reaction of the monomer with the organometallic compound.⁵⁻⁸ Among various types of reaction products having a carbonyl group the product (IV) is predominant in the case in which nearly equimolar amounts of methyl methacrylate and an organometallic compound reacted.⁵⁻⁸ Therefore, the absorption in the region of

TABLE I
 Carbonyl Stretching Frequency of Reaction Mixtures of Methyl Methacrylate and Organometallic Compounds and Tacticity of Poly(methyl methacrylate) Prepared with the Organometallic Compounds^a

Organometallic compounds	$\nu_{\text{C=O}}$, cm.^{-1}	Tacticity of poly(methyl methacrylate), % ^b				
		<i>i</i>	<i>s</i>	<i>I</i>	<i>H</i>	<i>S</i>
LiAlH ₄	1732	91	9	85	12	3
LiBH ₄	1728	63	37	43	41	16
<i>n</i> -BuLi	1730.5	71	29	58	26	16
LiAlBuEt ₃	1724	50	50	25	51	24
EtMgCl	1728	47	53	35	25	40
<i>n</i> -BuMgCl	1728	51	49	39	24	37
<i>n</i> -BuMgBr	1728	67	33	55	23	22
C ₆ H ₅ MgBr	1728	69	31	61	16	23

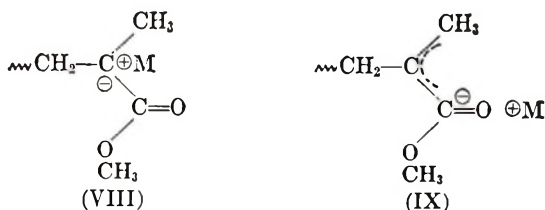
^a Infrared spectral measurements were made in diethyl ether at room temperature. Polymerizations were carried out in diethyl ether at room temperature for 48 hr. with 1 mole-% of initiators.

^b *i* and *s* are isotactic and syndiotactic structure in the diad and *I*, *S*, and *H* are isotactic, syndiotactic, and heterotactic ones in the triad, respectively.

1724–1732 cm.^{-1} was ascribed mainly to the carbonyl group of the adduct (VII).

Methyl methacrylate was polymerized at room temperature in diethyl ether with the same organometallic compounds as the catalysts. The tacticity of the polymer was determined by the proton magnetic resonance spectra. In Figure 1 is plotted the carbonyl stretching frequency against the diad isotacticity of the polymer prepared by the corresponding catalyst. As the figure shows, there seems to be some correlation between the tacticity and the carbonyl stretching frequency; i.e., the higher the frequency, the higher the isotacticity.

The adduct (VII) may be a resonance hybrid of the structures (VIII) and (IX):



Because of extremely low tendency of the adduct to dissociation¹⁴ the carbonyl absorption may not be ascribable to free ions but to the undissociated ion pairs.

The magnitude of the carbonyl absorption shift to higher frequency may indicate the degree of the contribution of the structure (IX), which can be explained by assuming the electron occupation of the antibonding orbitals of the carbonyl group. In other words, we may conclude that the higher

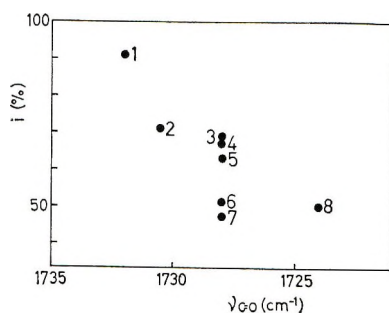


Fig. 1. Plot of $\nu_{C=O}$ versus diad isotacticity: (1) LiAlH_4 ; (2) $n\text{-BuLi}$; (3) $\text{C}_6\text{H}_5\text{MgBr}$; (4) $n\text{-BuMgBr}$; (5) LiBH_4 ; (6) $n\text{-BuMgCl}$; (7) EtMgCl ; (8) LiAlBuEt_3 .

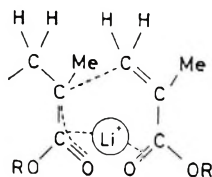


Fig. 2. A mechanism of isotactic polymerization.

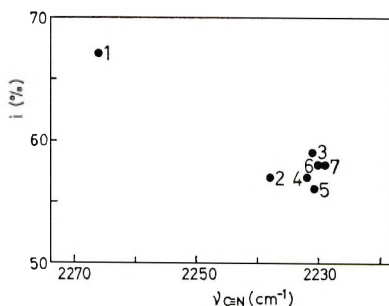


Fig. 3. Plot of $\nu_{C\equiv N}$ versus diad isotacticity: (1) LiAlBuEt_3 ; (2) LiAlH_4 ; (3) $n\text{-BuLi}$; (4) $i\text{-Bu}_2\text{Mg}$; (5) LiBH_4 ; (6) ZnEt_2 , LiZnBuEt_2 , and $\text{Li}_2\text{ZnBu}_2\text{Et}_2$; (7) $\text{C}_6\text{H}_5\text{MgBr}$.

the stretching frequency, the nearer stands the counterion to the carbonyl group of the polymer end, a fact that results in a higher isotacticity. In the transition state the reaction center, i.e., the carbanion of the terminal unit in the growing polymer chain, may locate near to the reaction center of the monomer β -carbon. The rotation around the axis through these two centers may be much restricted when the counterion is in the vicinity of carbonyl groups in the polymer end and in the monomer, and in this way isotactic stereocontrol may be enhanced. Figure 2 affords illustrations of this mechanism.

A similar correlation was also seen between the nitrile stretching frequency of the reaction mixture of equimolar amounts of methacrylonitrile and various organometallic compounds, as is shown in Table II and Figure 3.

TABLE II
Nitrile Stretching Frequency of Reaction Mixtures of Methacrylonitrile and Organometallic Compounds and Tacticity of Polymethacrylonitrile Prepared with the Organometallic Compounds^a

Organometallic compounds	$\nu_{\text{C}=\text{N}}$, cm. ⁻¹	Tacticity of polymethacrylonitrile, %	
		<i>i</i>	<i>s</i>
LiAlH ₄	2238	57	43
LiBH ₄	2231	56	44
C ₆ H ₅ MgBr	2229	58	42
<i>i</i> -Bu ₂ Mg	2232	57	43
<i>n</i> -BuLi	2231	59	41
Et ₂ Zn	2230	58	42
LiZnBuEt ₂	2230	58	42
Li ₂ ZnBu ₂ Et ₂	2230	58	42
LiAlBuEt ₃	2266	67	33

^a Polymerizations were carried out at 70°C. for 7 hr. with 5 mole-% of initiators. Infrared spectra were obtained in toluene at room temperature.

References

- (a) M. C. Miller and C. E. Rauhut, *J. Am. Chem. Soc.*, **80**, 4115 (1958); (b) T. G. Fox, B. S. Garret, W. E. Goods, S. Cratch, J. F. Kincaid, A. Spell, and J. D. Stroupe, *ibid.*, **80**, 1768 (1958); (c) J. D. Stroupe and R. E. Hughes, *ibid.*, **80**, 2341 (1958); (d) A. A. Korotkov, S. P. Mitsengendler, N. V. Krasulina, and L. A. Wolkowa, *Vysokomolekul. Soedin.*, **1**, 1319 (1958); (e) R. K. Graham, D. L. Dunkelberger, and E. S. Cohn, *J. Polymer Sci.*, **42**, 501 (1960); (f) F. A. Bovey and B. V. D. Tiers, *ibid.*, **44**, 173 (1960); (g) F. A. Bovey, *ibid.*, **46**, 59 (1960); (h) W. E. Goode, F. H. Owens, R. P. Fellmann, W. H. Snyder, and J. E. Moore, *ibid.*, **46**, 317 (1960); (i) A. Nishioka, H. Watanabe, K. Abe, and Y. Sono, *ibid.*, **48**, 241 (1960); (j) J. Furukawa, T. Tsuruta, and T. Makimoto, *Makromol. Chem.*, **42**, 165 (1960); (k) D. L. Glusker, E. Stiles, and B. Yonkoskie, *J. Polymer Sci.*, **49**, 297 (1961); (l) D. L. Glusker, L. Lysloff, and E. Stiles, *ibid.*, **49**, 315 (1961); (m) A. A. Korotkov, S. P. Mitsengendler, and V. N. Krasulina, *ibid.*, **53**, 217 (1961); (n) T. Makimoto, T. Tsuruta, and J. Furukawa, *Makromol. Chem.*, **50**, 116 (1961); (o) T. G. Fox and H. W. Schnecks, *Polymer*, **3**, 575 (1962); (p) D. M. Wiles and S. Bywater, *ibid.*, **3**, 175 (1962); (q) Z. A. Azimov, S. P. Mitsengendler, and A. A. Korotkov, *Vysokomolekul. Soedin.*, **4**, 835 (1962); (r) D. Braun, M. Herner, U. Johnson, and W. Kern, *Makromol. Chem.*, **51**, 15 (1962); (s) D. L. Glusker and R. A. Evans, *J. Am. Chem. Soc.*, **86**, 187 (1964); (t) H. Abe, K. Imai, and M. Matsumoto, *J. Polymer Sci. B*, **3**, 1053 (1965); (u) T. Tsuruta, T. Makimoto, and Y. Nakayama, *Makromol. Chem.*, **90**, 12 (1966); (v) T. Tsuruta, T. Makimoto, and H. Kanai, *J. Makromol. Chem.*, **1**, 31 (1966); (w) J. Furukawa, N. Kawabata, and H. Oda, paper presented at 15th Annual Meeting of the Society of Polymer Science, Japan, May 1966.
- (a) D. J. Cram and K. R. Kopecky, *J. Am. Chem. Soc.*, **81**, 2748 (1959); (b) J. Furukawa, *Polymer*, **3**, 487 (1962); (c) C. E. H. Bawn and A. Ledwith, *Quart. Rev.*, **16**, 361 (1962).
- (a) M. Frankel, A. Ottolenghi, M. Albeck, and A. Zilkha, *J. Chem. Soc.*, **1959**, 3858; (b) J. Furukawa, T. Tsuruta, K. Ito, I. Kashiuchi, and A. Kawasaki, *Kogyo Kagaku Zasshi*, **63**, 640 (1960); (c) M. L. Miller, *J. Polymer Sci.*, **56**, 203 (1962); (d) A. Zilkha and Y. Katz, *ibid.*, **62**, 153 (1962); (e) A. Ottolenghi, S. Barzakay, and A. Zilkha, *ibid. A*, **1**, 3643 (1963); (f) A. Ottolenghi and A. Zilkha, *ibid.*, **A**, **1**, 687 (1963).
- N. Kawabata and J. Furukawa, *Kogyo Kagaku Zasshi*, **70**, 1423 (1967).
- N. Kawabata and T. Tsuruta, *Makromol. Chem.*, **86**, 231 (1965).

6. N. Kawabata and T. Tsuruta, *Makromol. Chem.*, **98**, 262 (1966).
7. T. Tsuruta, N. Kawabata, and K. Yamamoto, *Kogyo Kagaku Zasshi*, **69**, 125 (1966).
8. Y. Yasuda, N. Kawabata, and T. Tsuruta, *J. Macromol. Sci. (Chem.)* **A1** (4), 669 (1967).
9. E. R. Blout and H. Mark, *Monomers*, Interscience, New York, 1957.
10. J. Furukawa, T. Tsuruta, K. Ito, I. Kashiuchi, and A. Kawasaki, *Kogyo Kagaku Zasshi*, **63**, 640 (1960).
11. A. Weisserberger, E. S. Proskauer, J. A. Riddick, and E. E. Toops, Jr., *Organic Solvents*, Interscience, New York, 1965.
12. F. A. Bovey and G. V. D. Tiers, *J. Polymer Sci.*, **44**, 173 (1960).
13. F. Ciampelli and G. Dall'Asta, *J. Polymer Sci. B*, **4**, 633 (1966).
14. W. Fowells, C. Schuerch, F. A. Bovey, and F. P. Hood, *J. Am. Chem. Soc.*, **89**, 1396 (1967).

Received August 21, 1967

Contribution to the Study of the Mechanism of Curing of Unsaturated Polyester Resins

PAUL FIJOLKA and YOUSIF SHAHAB, *Institut für Kunststoffe of the German Academy of Sciences, Berlin-Adlershof, Germany*

Synopsis

The mechanism of copolymerization of monomethyl and dimethyl maleates and fumarates with styrene was studied by analysis of the conformation of the acid units of the resulting copolymers. The absorption bands for C=O stretching and OH stretching in the spectra of the copolymers are fully identical. They are quite different from the spectra of the copolymers obtained from maleic anhydride and styrene that are subsequently treated with absolute methanol to give the monoester which is then esterified with diazomethane to give the diester. The acid units of the copolymers derived from maleic anhydride exist in a *gauche* configuration; copolymers derived from fumaric units exist in a *trans* conformation. The identity of copolymers derived from maleic units with those derived from fumaric units but not with those derived from maleic anhydride indicates that the first step in the copolymerization of the maleic units is an isomerization to fumaric units, which are actually the genuine comonomers.

During the esterification of unsaturated polyester a great amount of the maleic anhydride used as the unsaturated component undergoes isomerization to fumaric acid. It was observed that the degree of curing of polyester increases with increasing degree of isomerization, and this has been the subject of numerous publications.¹ Although much information about the dependence of the properties and degree of curing of cured polyester upon the isomerization of the related polyester has been obtained, less work has been done on the cause of the difference in behavior of maleic and fumaric units of polyester. Obviously, the reactivity of the maleic and fumaric units of polyester in copolymerizing with styrene is a matter of the specific structure of these units.

The unsaturated dicarboxylic acids exist as esters in the center of the chain and as half-esters at the ends. Thus it is convenient to study the mechanism of the copolymerization of monomethyl and dimethyl fumarates and maleates with styrene.

Mayo et al.² investigated the copolymerization of diethyl and monoethyl fumarates and maleates with styrene and other vinyl monomers some time before the influence of isomerization upon the curing of the polyester was ascertained. They found that diethyl fumarate is 40 times more reactive than diethyl maleate. Monoethyl fumarate and maleate ex-

hibited no difference and were nearly as reactive as diethyl fumarate. This behavior has been ascribed to steric inhibition of resonance. The intermediate free radical of the monomers can be stabilized through resonance only, if the oxygen atoms of the carbonyl groups lie in the same plane as the atoms attached to the doubly bound carbon atoms.

Consideration of models shows that in the case of dialkyl maleate the interference of the two substituents in the *cis* position is great: it is impossible to have the two carbonyl groups in the same plane of the doubly bound carbon atoms and to have one of them coplanar is not probable. The substituents of the fumaric units do not interfere with each other and

TABLE I
Copolymers Investigated

Copolymer	Composition	Acid number	Ratio acid unit per styrene
1	styrene + maleic anhydride	—	1:1
1a	copolymer 1 heated with absolute methanol	228.2	1:1
1b	copolymer 1a esterified by diazomethane	—	1:1
2	styrene + dimethylmaleate	—	1:2,2
2a	copolymer 2 partially hydrolyzed	61	1:2,2
3	styrene + monomethyl maleate	221	1:1
3a	copolymer 3 esterified with diazomethane	—	1:1
4	styrene + dimethyl fumarate	—	1:1
4a	copolymer 4 partially hydrolyzed	216	1:1
5	styrene-monomethyl fumarate	2.18	1:1
5a	copolymer 5 esterified by diazomethane	—	1:1

coplanarity of both, or at least one, of the two carbonyl groups with the double bond is possible. Maleic half-esters can form a ring structure through a hydrogen bond between the proton of the acid and the carbonyl group of the ester and thus possess the same reactivity as the fumaric units.

Price³ has considered the steric effect to be the main factor influencing the reactivity of the monomers concerned.

A report by Shahat⁴ on the determination of the molecular structure of maleic acid has focused our attention on another probable reason for the difference in reactivity of the monomers. The distance between the doubly bound carbon atoms of maleic acid is 1.43 Å; this is characteristic of a

single rather than a double bond. Accordingly, it is reasonable to assume that the maleic units are not capable of copolymerizing. However, in this condition, the heat released in the homopolymerization of the comonomer is great enough to isomerize the maleic units and these isomerized units are the real comonomers. The reactivity of the half-esters could be caused by a low activation energy of isomerization to the fumaric form. It was observed in our laboratory that maleic half-esters tend to form a precipitate at room temperature, which was identified polarographically as mainly fumaric units.

It seemed appropriate to approach the problem by investigating the spatial arrangement of the two substituents of the acid units of several copolymers prepared from styrene and the reference monomers.

RESULTS

Table I contains a list of the copolymers prepared. A 0.5% solution of these copolymers in chloroform or dioxane was measured by infrared spectroscopy.

Copolymers 2, 4, and 1b (Fig. 1). In this case only the C=O stretching mode is of interest. This mode appears as a strong band at 1730 cm.^{-1}

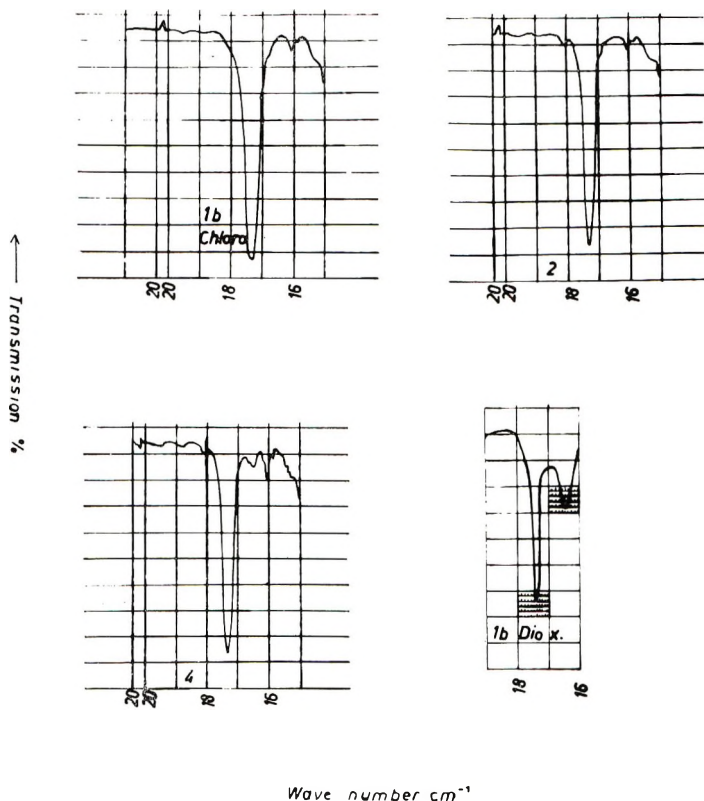


Fig. 1. Infrared spectra of copolymers 2, 4, and 1b.

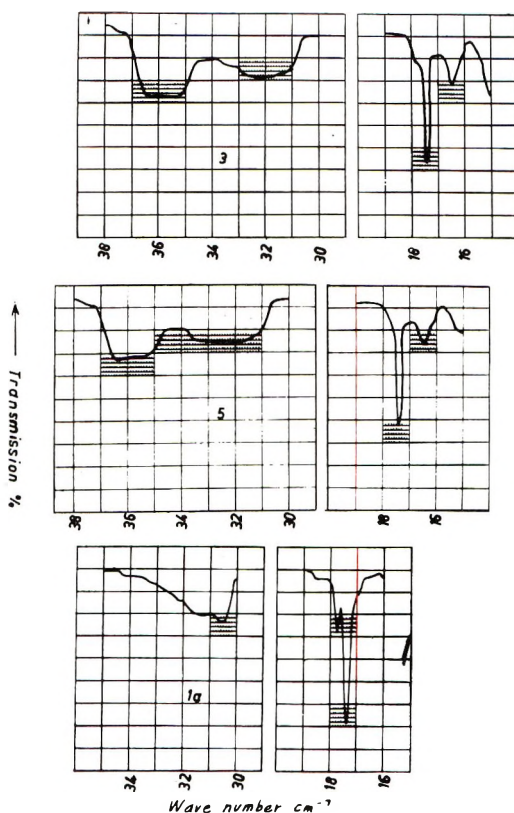


Fig. 2. Infrared spectra of copolymers 3, 5, and 1a.

in the spectra of the three copolymers in chloroform solution. The bands of copolymers 2 and 4 are similar in shape. The band of copolymer 1b is broadened and intensified. In a solution of dioxane two bands appear, one at 1745 cm^{-1} and the other at 1650 cm^{-1} . Figures 1-4 show only the spectra of copolymers 2 and 1b in this solvent. The spectrum of copolymer 4 is similar to that of copolymer 2. The band of copolymer 1b at 1650 cm^{-1} is broadened and intensified.

Copolymers 3, 5, and 1a (Fig. 2). The C=O stretching and the OH stretching modes are of interest. The spectra are obtained from a 0.5% solution of the copolymers in dioxane. The spectra of copolymers 3 and 5 are identical. Two bands appear, at 1650 and 1745 cm^{-1} , which can both be assigned to the C=O stretching mode. The absorption between 3060 and 3720 cm^{-1} is caused by the OH stretching mode of the acid groups of the copolymers. It seems that the protons partially build hydrogen bonds with the oxygen atoms of the solvent (dioxane), which shifts the absorption to a lower frequency. The spectrum of copolymer 1a is considerably different. The band at 1645 cm^{-1} disappears, and the band at 1740 cm^{-1} is intensified, broadened, and split into two coupled

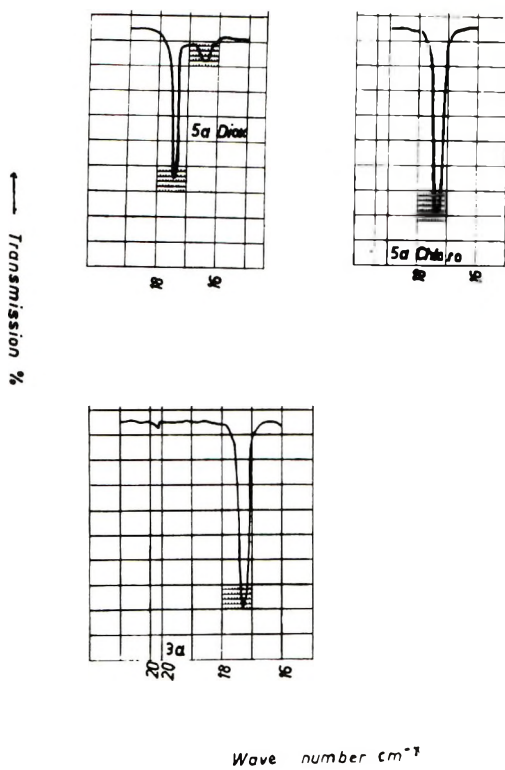


Fig. 3. Infrared spectra of copolymers 3a and 5a.

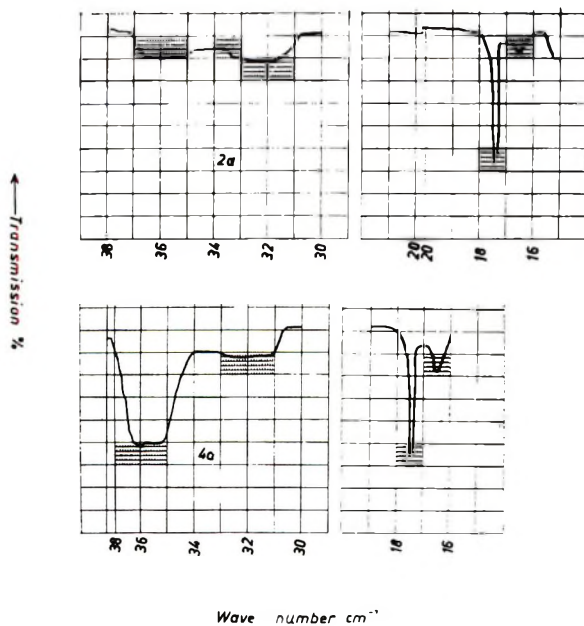


Fig. 4. Infrared spectra of copolymers 2a and 4a.

bands. The absorption of the OH stretching mode is further shifted toward a lower frequency and weakened, which indicates the occurrence of an internal hydrogen bond.

Copolymers 3a and 5a (Fig. 3). These have the same spectra as copolymers 2 and 4.

Copolymers 2a and 4a (Fig. 4). These have the same spectra as copolymers 3 and 5.

DISCUSSION

To elucidate the spectra of the copolymers it is first necessary to consider the conformation of the diester and half-ester units of the copolymers. The two substituents in the reference units can have either the *gauche* or the *trans* form. The activation energy needed to transfer the one form into the other is great enough to prevent any change in the conformation of the mentioned units. The reasons for this are the following.

(1) The attraction and repulsion forces are great because of the strong dipole nature of the ester and acid groups.

(2) The free rotation about the C—C bond of the chain is restricted, owing to the high moment of inertia, to rotation caused by the length of the chain attached to the carbon atoms and the bulky phenyl groups of the comonomer.

(3) In concentrated solutions or in the glassy state the intermolecular forces impair free rotation about the C—C bonds of the chain.

(4) The formation of the hydrogen bond in the case of monoester units makes free rotation somewhat difficult.

It is to be expected that free rotation about the bonds of the chain could occur only in dilute solutions and at elevated temperatures. Under moderate conditions, dealt with in this work, it is probable that the carbon of the chain carries out torsional vibrations without jumping past the energy barrier separating the different rotational isomers. Surely, it is possible for some units situated toward the ends of the chains to change their conformation but the number of these units is negligible. The conformation of the substituents of the acid units of the copolymers derived from maleic anhydride and styrene must have the *gauche* form, whereas all the copolymers derived from fumaric units and styrene must have the *trans* form. The conformation of the two substituents of the acid units of the copolymers derived from maleic units and styrene depends upon the way in which these units copolymerize with styrene. If the copolymerization occurs by formation of a radical from maleic units, the conformation of the acid units of the chain might be the same as in the copolymers derived from maleic anhydride and styrene. If the isomerization to fumaric units represents the first step of the copolymerization, the conformation of the units might be similar to those derived from fumaric units. A consideration of the spectra shows that copolymers 3 and 5 are similar. These are derived from monomethyl maleate and styrene and from monomethyl

fumarate and styrene, respectively. The absorption of the OH stretching mode is not essentially shifted, which is in agreement with the assumed *trans* conformation of the acid and ester groups of the monoester units.

The spectrum of copolymer 1a, prepared from copolymerizing maleic anhydride with styrene and heating the latter in a solution of absolute methanol at 50°C., is quite different. The OH stretching band indicates the occurrence of an internal hydrogen bond, which is in conformity with the proposed *gauche* arrangement. Furthermore, the band at 1650 cm.^{-1} disappears, and the band at 1745 cm.^{-1} becomes larger and splits into two coupled bands. The spectra of copolymers 2 and 4 are also identical. We obtain the same spectra of the two copolymers if we esterify the acid groups of copolymers 3 and 5 by means of diazomethane (copolymers 3a and 5a). It is obvious that the acid units of copolymers 2 and 4 possess the same conformation as the acid units of copolymers 3 and 5, i.e. the *trans* configuration. The C=O stretching band of the spectra of copolymer 1b, gained from esterification of copolymer 1a by means of diazomethane, is broadened and intensified compared with those from copolymers 2 and 4. The spectra of copolymers 2, 4, 1b, 3a, and 5a, measured in a solution of dioxane, shows two bands for the C=O stretching mode, at 1650 and 1745 cm.^{-1} . The two bands are similar in the spectra of copolymers 2, 4, 3a, and 5a (in Figs. 1-4 only the spectrum of copolymer 5a is shown). The band at 1650 cm.^{-1} is enlarged and intensified in the spectrum of copolymer 1b. The question of the appearance of two C=O stretching bands in a solution of dioxane and only one in a solution of chloroform seems to be quite interesting but is beyond the scope of the present work. Unfortunately, the copolymers with free carboxyl groups that were investigated are insoluble in chloroform; thus, we cannot answer the question whether only one band exists for C=O stretching in this solvent, as in the totally esterified copolymers. The broadening of the band of copolymer 1b (in chloroform) at 1745 cm.^{-1} , the band of the same copolymer in dioxane at 1650 cm.^{-1} , and the band of copolymer 1a at 1740 cm.^{-1} and the splitting of this band into two coupled bands could be ascribed to a quick change of the position of the carbonyl group. Hence the group is sometimes in the plane of the molecule and sometimes twisted out of the plane of the molecule owing to steric interference of the two bulky groups possessing the *gauche* conformation. The spectra of copolymers 2a and 4a, produced from partial hydrolyzation of copolymers 2 and 4, are identical with those of copolymers 3 and 5. This constitutes additional evidence of a *trans* arrangement of the substituents of the acid units of copolymers 2 and 4.

EXPERIMENTAL

Monomers

Commercial grade styrene was purified by distillation under reduced pressure by means of a black apparatus, $n_D^{20} = 1.5469$. Maleic anhydride,

dimethyl maleate, and dimethyl fumarate were also commercial grade and were purified by recrystallization. Monomethyl maleate was obtained by treating maleic anhydride with sodium methylate and neutralizing the resulting sodium salt. Monomethyl fumarate was prepared through partial hydrolysis of dimethyl fumarate by means of methanolic KOH.

Preparation of Copolymers 1, 2, 3, 4, and 5

Equimolar amounts of styrene and maleic anhydride were weighed into a Pyrex tube. A 0.1% solution of benzoylperoxide was used as catalyst. The tube was frozen in solid carbon dioxide, evacuated, and sealed. The copolymerization was carried out in a water bath at 80°C. for 10 hr. The other copolymers were prepared in the same manner but maleic anhydride was replaced with dimethyl maleate, monomethyl maleate, dimethyl fumarate, or monomethyl fumarate. The copolymers were dissolved in acetone and precipitated by adding ether as nonsolvent.

Preparation of Copolymer 1a

Copolymer 1 was heated with absolute methanol for 3 hr. at 50°C. The product was precipitated from the solution by adding ether.

Preparation of Copolymers 1b, 3a, and 5a

These are obtained by esterification of copolymers 1a, 3, and 5 by means of diazomethane. The copolymers were dissolved in acetone, and an ethereal solution of diazomethane was added to it until the solution became yellow. It was necessary to add occasionally some acetone to the solution in order to keep the copolymer soluble. After 48 hr. the resulting copolymers were precipitated by adding ether.

Preparation of Copolymers 2a and 4a

The copolymers were obtained by hydrolyzing copolymers 2 and 4 with NaOH solution. Acetone was used as solvent. The free acids were gained from the salts by neutralization with hydrochloric acid.

Measurement of Infrared Spectra

All the spectra were measured in a 0.5% solution of the copolymers in dioxane or chloroform with an infrared spectroscope UR 10 VEB, Carl Zeiss, Jena. Copolymers 1a, 2a, 3, 4a, and 5 are insoluble in chloroform and were measured only in dioxane. The other copolymers were measured in solutions of dioxane and chloroform.

The authors wish to express sincere thanks to Günther Kretschmar and the Misses Jutta Bautz and Barbara Engmann, from the Institut für Fettchemie, of the German Academy of Sciences, for obtaining the infrared spectra, and to Mrs. Gerlinde Schneider for technical assistance.

References

1. W. Funke and H. Janssen, *Makromol. Chem.*, **50**, 188 (1961).
2. F. R. Mayo, F. M. Lewis, and C. Walling, *Discussions Faraday Soc.*, **2**, 285 (1947).
3. C. C. Price, *J. Polymer Sci.*, **1**, 83 (1946).
4. M. Shahat, *Acta Cryst.*, 763 (1952).

Received February 10, 1966

Revised September 10, 1967

Water-Absorption Properties of an Acetal Copolymer

M. BRADEN, *The London Hospital Medical College,
University of London, England*

Synopsis

The kinetics of sorption from the liquid phase to equilibrium and desorption were studied over the temperature range 0–80°C. Equilibrium uptake was found to increase linearly with concentration in this range. Sorption-desorption kinetics showed the diffusion coefficients to decrease with increasing concentration, although the extent of this dependence did not appear in itself to be temperature-dependent. The apparent diffusion coefficient obeyed the law $D = D_0 \exp \{-E/RT\}$ over the temperature range studied, giving $E = 9.9$ kcal./mole and $D_0 = 0.45$ cm.² sec.⁻¹. These values are compared with corresponding values for other polymers.

The absorption of water by polymers has been shown to be a diffusion process. In many cases the diffusion coefficient D is a function of concentration in the sense that D decreases with C .¹⁻³ This article shows the acetal copolymer to conform to this general pattern of behavior; comparisons are made between it and other polymers with respect to entropies and energies of activation. Data on the equilibrium uptake of water from the liquid phase are given.

Experimental

Specimens of acetal copolymer* $7 \times 2.5 \times 0.311$ cm. were immersed in water at a controlled temperature and weighed at convenient intervals until equilibrium uptake was achieved. The specimen was then transferred to an air oven containing a desiccant at the same temperature, and weighings were continued until the desorption was complete. This cycle was repeated a number of times so that the variability of the sorption and desorption processes could be examined. Such measurements were carried out at temperatures in the range 2–80°C. (measurements at 2°C. were carried out in a refrigerator, desorption being in closed tubes containing desiccant).

Apparent diffusion coefficients for the sorption and desorption processes, D_s and D_d respectively, were calculated from the equation

$$M_t/M_\infty = 2(Dt/\pi l^2)^{1/2} \quad (1)$$

* Acetal copolymer of Imperial Chemical Industries, U.K.

where M_t is the mass uptake (or loss during desorption) after a time t , M_∞ is the uptake of equilibrium, and l is half the specimen thickness.

The appropriate D value is readily calculated from the slope of M_t/M_∞ versus $t^{1/2}$ (Fig. 1). The diffusion coefficients thus calculated have been

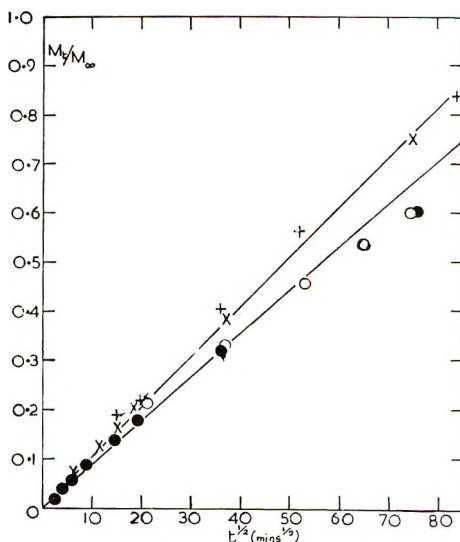


Fig. 1. Plot of M_t/M_∞ vs. $t^{1/2}$ at 25°C.: (●, ○) repeated sorption data; (×, +) repeated desorption data.

termed "apparent" because in eq. (1), which is derived from classical diffusion theory, D is not a function of concentration.⁴ The actual sorption and desorption data were plotted and compared with the theoretical uptake predicted by classical diffusion theory,⁴ with D_d or D_s , as appropriate:

$$M_t/M_\infty = 1 - 8/\pi^2 \sum_{n=0}^{\infty} 1/(2n+1)^2 \exp \left\{ -\pi^2(2n+1)^2 Dt/4l^2 \right\} \quad (2)$$

Results

Typical plots corresponding to eqs. (1) and (2) are given in Figures 1 and 2. Since diffusion coefficients usually conform to the relationship

$$D = D_0 \exp \left\{ -E/RT \right\} \quad (3)$$

TABLE I

Polymer	D_0 , cm. ² sec. ⁻¹	E , kcal./mole
Acetal copolymer	0.45	9.9
Rubber hydrochloride	6.98	14.0
Polyethylene terephthalate	0.153	10.4
Ethyl cellulose	0.0212	6.6
Polyethylene	5.15×10^3	14.2
Polypropylene	2.18×10^6	16.4

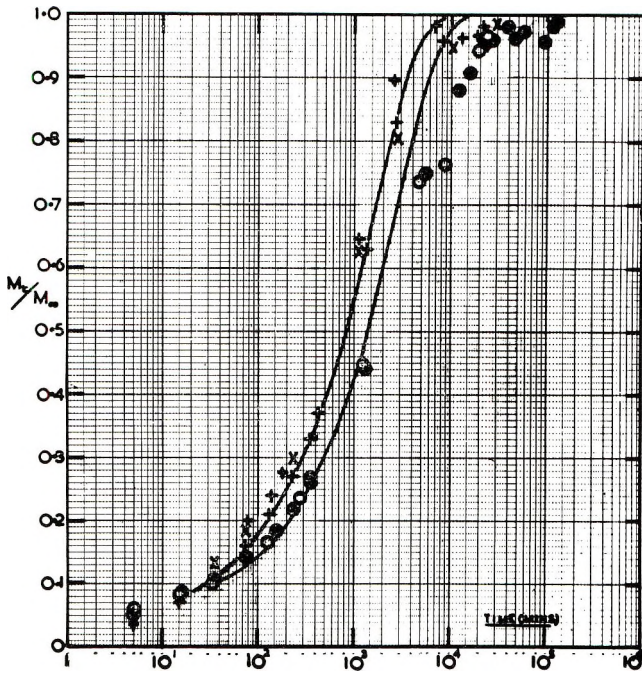


Fig. 2. Plot of M_t/M_∞ vs. t (logarithmic scale) at 37°C .: (\bullet , \circ) repeated sorption data; (\times , $+$) repeated desorption data.

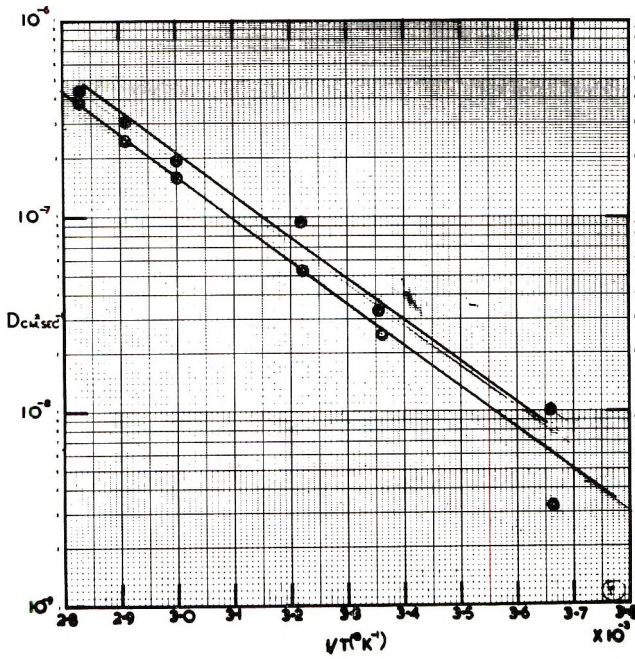


Fig. 3. Plot of $\log D$ vs. $1/T$: (\circ) D_s ; (\bullet) D_d .

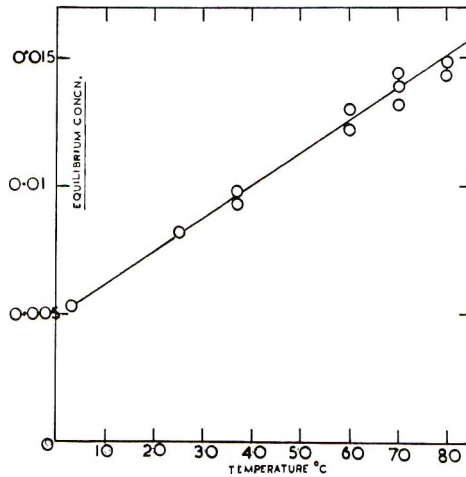


Fig. 4. Equilibrium uptake (gram per gram) as a function of temperature.

D_s and D_d were plotted in the form of $\log D$ versus $1/T$ (Fig. 3). E is the activation energy and R the universal gas constant. D_0 and E are tabulated in Table I together with published data⁵ for other polymers.

The equilibrium uptake is plotted as a function of temperature in Figure 4.

Discussion

Figure 1 shows the linearity of the plots of M_t/M_∞ versus $t^{1/2}$. However, the slope during desorption is greater than that during sorption, showing⁶ that D decreases with C . Moreover, departures from linearity

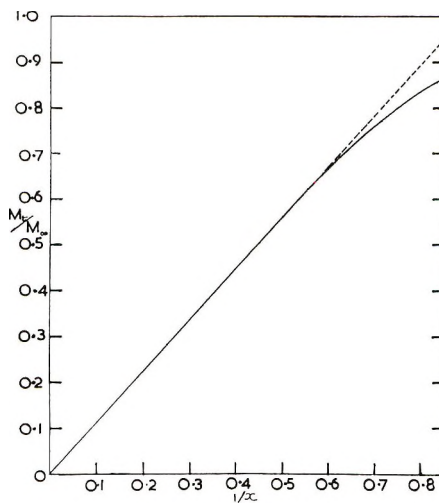


Fig. 5. Plot of eq. (4).

occur at $M_t/M_\infty \approx 0.5$ during sorption, yet during desorption linearity obtains for M_t/M_∞ at least up to 0.8; classically, such departures should occur at $M_t/M_\infty \approx 0.65$, as may be readily shown by plotting M_t/M_∞ against $X = D_t/l$ (Fig. 5), according to (4) the following equation:

$$M_t/M_\infty = 2(Dt/l^2)^{1/2} \left\{ 1/\pi^{1/2} + 2 \sum_{n=1}^{\infty} (-1)^n \operatorname{erf}(nl/Dt)^{1/2} \right\} \quad (4)$$

As may be seen in Figure 1, sorption and desorption cycles are reversible and are indeed reversible for more than the two cycles shown.

Figure 2 shows that D_a , on the basis of classical theory, predicts the desorption process to equilibrium quite well; the later stages of sorption, however, are very much slower than the values that D_s predict. This is again in accord with D 's being a decreasing function of C , the value of D becoming much smaller as the specimen approaches saturation.

The features so far discussed were apparent at all the temperatures studied.

Figure 3 shows the variation of D_s and D_a with temperature to be in reasonable accord with the Arrhenius type of relationship. Since the slopes for D_s and D_a are approximately equal, then, if the dependence of D on C is of the form

$$D = D_{c=0} f(C/C_0) \quad (5)$$

$f(C/C_0)$ would seem to be sensibly independent of temperature, even though the equilibrium concentration C_0 itself varies with temperature (*vide infra*).

D_0 is related to the entropy of activation, ΔS^\ddagger , by the relationship

$$D_0 = (RT/R)\lambda^2 \exp \{ \Delta S^\ddagger/R \} \quad (6)$$

Since, however, there is some uncertainty about the value which should be ascribed to the "jump distance" λ , D_0 will be used as a comparison index for ΔS^\ddagger . In Table I the acetal copolymer is seen to have properties very similar to those of polyethylene terephthalate. The difference in the D_0 values corresponds to a difference of 2.2 e.u. in the ΔS^\ddagger values; if the value for the terephthalate polymer is taken as 7.9 e.u., this difference is not large.

References

1. P. Rouse, *J. Am. Chem. Soc.*, **69**, 1068 (1947).
2. R. M. Barrer and J. A. Barrie, *J. Polymer Sci.*, **28**, 377 (1958).
3. M. Braden, *Trans. Plastics Inst.*, **8**, 83 (1963).
4. J. Crank, in *The Mathematics of Diffusion*, 1st ed., Oxford Univ. Press, 1957, p. 45.
5. H. Yasuda and V. Stannett, *J. Polymer Sci.*, **57**, 907 (1962).
6. J. Crank, in *The Mathematics of Diffusion*, 1st ed., Oxford Univ. Press, 1957, p. 280.

Received September 19, 1967

Investigation of Reactions in Carboxyl-Terminated Polybutadiene and Tris-[1-(2-methyl)aziridinyl] Phosphine Oxide*

R. A. STRECKER and A. S. TOMPA,
*Research and Development Department,
Naval Ordnance Station, Indian Head, Maryland 20640*

Synopsis

The functionalities of a series of carboxyl-terminated polybutadiene samples (CTPB) were calculated from an infrared spectroscopic study of the samples reacting to the gel point with tris-[1-(2-methyl)aziridinyl] phosphine oxide (MAPO), Epon X801, and glycerol. Identical functionalities were calculated when Epon X801 and glycerol were used as curing agents. Higher functionalities for CTPB with MAPO were due to additional reactions that MAPO underwent with hydroxyl groups and water, present in carboxyl-terminated polybutadiene, and with itself (homopolymerization). Rate constants were calculated for the homopolymerization of MAPO in Nujol, in nonfunctional polybutadiene, and in CTPB. The homopolymerization resulted in an increase and then a gradual decrease in MAPO functionality, which was in agreement with that predicted from theoretical considerations.

Introduction

Tris-[1-(2-methyl)aziridinyl] phosphine oxide (MAPO) is a trifunctional derivative of phosphorous oxychloride and propylene imine. Owing to its high functionality and reactivity, MAPO can be used as a crosslinking agent with polymers that contain active hydrogens such as carboxyl-terminated polybutadiene (CTPB).

An infrared technique was developed to follow to the gel point the course of the CTPB-MAPO curing reaction. The functionalities of the reactants were calculated according to a method previously described.¹

Material

MAPO was obtained from Interchemical Corporation and was triply distilled before use. The CTPB samples were obtained from various manufacturers, and one lot was purified by dissolving in benzene and then precipitating with acetone. This process was repeated three times. The

* Presented before the Division of Polymer Chemistry at the 153rd National Meeting of the American Chemical Society, Miami Beach, Fla., April 1967.

sample was dried over phosphorous pentoxide in a rotator evaporator, until Karl Fisher reagent indicated that no water was present.

Experimental

The reactants were mixed mechanically and heated at 105°C. in a constant-temperature bath until the gel point was reached. Gel points were determined with a Brookfield Synchro-lectric viscometer. Samples were withdrawn periodically and immediately run as a film between potassium bromide windows on a Model 421 Perkin-Elmer infrared spectrophotometer.

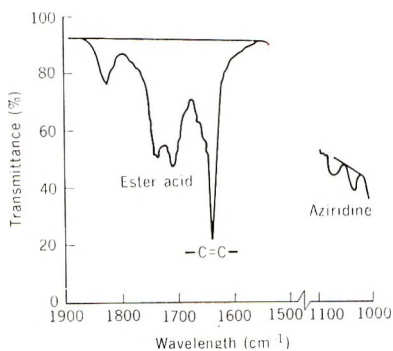


Fig. 1. Transmittance of CTPB and MAPO after 90 min. at 105°C.

The course of the reaction was followed by observing the decrease in absorbance of the aziridine (MAPO) ring frequency at 1040 cm^{-1} . The ring opens in an acidic medium and reacts with the carboxyl group of CTPB, which results in a decrease in intensity of carboxyl absorption at 1708 cm^{-1} and an increase in intensity of ester absorption at 1738 cm^{-1} . The —C=C— stretching frequency at 1638 cm^{-1} was used as an internal standard to compensate for varying film thickness (Fig. 1). In the homopolymerization study of MAPO in Nujol the CH_3 frequency at 1375 cm^{-1} served as the internal standard. The precision of the MAPO determination was $\pm 3\%$. The hydroxyl groups in CTPB were determined by the acetic anhydride method,² after the carboxyl groups were esterified with diazomethane.

Discussion

Table I shows the functionalities obtained for a series of CTPB samples when MAPO, Epon X801, and glycerol were employed as curing agents. Nearly identical functionalities for CTPB were obtained with Epon X801 and glycerol, but apparently anomalously high results were obtained with MAPO. Two possible explanations of this anomaly are that CTPB contains additional functional groups, which react only with MAPO and not

TABLE I
Functionalities of CTPB With Various Curing Agents

Lot no.	Functionality ^a		
	f_{PM}	f_{PE}	f_{PG}
Telagen A	2.71	2.40	2.40
Telagen B	2.79	2.37	2.38
Telagen C	3.52	2.95	2.97
Hycar A	2.62	2.38	2.38
Hycar B	2.51	2.29	2.29
Hycar C	2.52	2.24	2.22
Butarez A	2.98	2.42	2.46
Butarez B	2.62	2.18	2.22

^a Functionality: f_{PM} , of polymer in MAPO reaction; f_{PE} , of polymer in epoxide reaction; f_{PG} , of polymer in glycerol reaction.

with epoxides and alcohols, and that MAPO undergoes homopolymerization, which creates a change in its functionality. Evidence supporting these assumptions may be seen in Figure 2, where the percentage of functional groups that have reacted are plotted against time. The conversion of aziridinyl groups is much greater than the disappearance of carboxyl groups in CTPB. This means that MAPO reacts not only with COOH groups but also with some other groups.

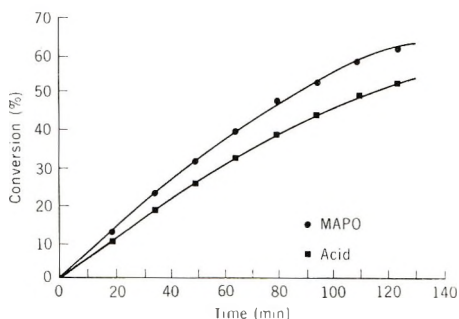


Fig. 2. Conversion of functional groups in reaction between CTPB and MAPO.

MAPO-Water Reaction

It is known³ that MAPO can react readily with water under acidic conditions. The pH of the CTPB samples ranges from about 4 to 6, and the water content is usually between 0.03 and 0.07%. It was, therefore, of interest to see whether a reaction between MAPO and water occurs under these conditions. Water was added to a precipitated and dried sample of CTPB until the water content was brought to 0.1 and 0.3%; the mixture then reacted with MAPO. In Figure 3 the difference in per cent reacting (MAPO — acid) versus time is plotted. It can be seen clearly that MAPO is reacting with water under these conditions, because as the water content

increases, the percentage of MAPO reacting also increases. In addition it may be noted that, even when no water is present in CTPB, more aziridine groups are reacting than COOH groups. This indicates that the cause of the high functionality of CTPB with respect to MAPO cannot be attributed solely to water in the mixture. The presence of water in CTPB causes the functionality of MAPO to be less than 3 because of

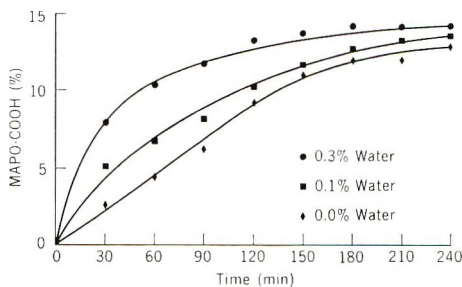


Fig. 3. Reaction of MAPO with water in CTPB.

the water-aziridine reaction and, consequently, the calculated functionality of CTPB is higher, because it is based on a MAPO functionality of 3. According to the equation of Stockmayer,⁴

$$f_E = 1/P^2(g_E - 1) + 1$$

where P is the percentage of reactants that have reacted at the gel point, and f_E and g_E are the functionalities (i.e. number of reactive groups per mole) of polymer and curing agent, respectively. Thus f_E and g_E are inversely proportional to each other.

MAPO-Alcohol Reaction

CTPB was found to contain from 0.02 to 0.07% hydroxyl groups. To demonstrate that MAPO reacts with hydroxyl groups an experiment

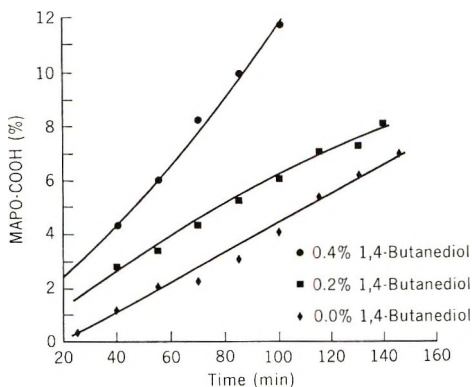


Fig. 4. Reaction of MAPO with 1,4-butanediol in CTPB.

similar to that between MAPO and water in CTPB was carried out. To precipitated and dried CTPB 0.2 and 0.4% 1,4-butanediol was added and the mixture was reacted with MAPO. Figure 4 shows that the percentage reacting (MAPO - CTPB) increases as the concentration of alcohol increases and proves that MAPO reacts with hydroxyl groups. The presence of hydroxyl groups in CTPB increases its functionality with respect to MAPO but not with respect to epoxides, which do not react with hydroxyl groups under such conditions.

Polymer Functionalities

In Table II the f_{PM} and f_{PE} are the functionalities of CTPB polymer when MAPO and Epon XS01 were employed as curing agents. The hydroxyl functionality may be calculated from its concentration and the molecular weight of the CTPB polymer. If one makes the assumption that the rate of reaction between MAPO-OH and MAPO-COOH groups is about the same, then by adding the functionality of CTPB obtained in the epoxide reaction to the calculated hydroxyl functionality one should obtain the total functionality of CTPB with respect to MAPO. However, the calculated total functionality was always found to be smaller than the functionality observed with MAPO as curing agent. This indicates that another side reaction, such as homopolymerization of MAPO, occurs in the CTPB-MAPO reaction, which is responsible for the difference in functionalities.

TABLE II
Functionalities of Various CTPB Samples

Sample No.	Functionality, ^a		OH, %	f_{PH}	$f_{PE} + f_{PH}$
	f_{PM}	f_{PE}			
Butarez A	2.98	2.42	0.072	0.24	2.66
Butarez B	2.62	2.18	0.060	0.21	2.39
Butarez C	2.35	2.14	0.025	0.09	2.23
Telagen A	2.71	2.40	0.036	0.10	2.50
Telagen B	3.52	2.95	0.043	0.21	3.16
Telagen C	2.79	2.37	0.041	0.16	2.53

^a Functionality: f_{PM} , of polymer in MAPO reaction; f_{PE} , of polymer in epoxide reaction; f_{PH} , hydroxyl functionality of polymer.

Homopolymerization of MAPO

It is known^{3,5-8} that MAPO and other imine compounds are capable of homopolymerization. To study this homopolymerization MAPO was added to Nujol and nonfunctional polybutadiene in the same concentration ratio and at the same temperature as in the CTPB reaction. Figure 5 shows the percentage of MAPO reacting as a function of time, in Nujol, polybutadiene, and CTPB (values of per cent reacted, MAPO - COOH).

The homopolymerization reaction of MAPO was found to be second-order. The data are shown in Figure 6, in which values of the second-order rate expression $(C_0/C) - 1$ versus time are plotted. The aziridine concentration expressed in equivalents per gram was obtained from the relative absorption A_{1040}/A_{1638} , the subscripts indicating frequency. The reaction rates were obtained from the slopes of the curves.

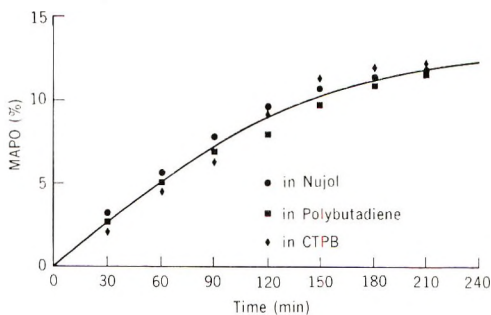


Fig. 5. Homopolymerization of MAPO at 105°C.

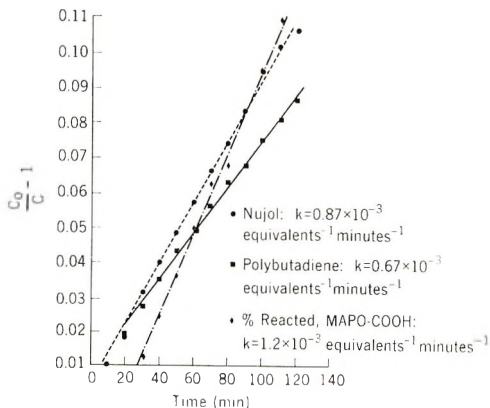


Fig. 6. Homopolymerization of MAPO at 105°C.

It is seen that the rates of homopolymerization in Nujol and nonfunctional polybutadiene are equivalent, within experimental error, namely 0.9 and $0.7 \times 10^{-3} \text{ eq.}^{-1} \text{ min.}^{-1}$, respectively. Equivalent amounts of CTPB and MAPO reacted, and values of the percentage reacting (MAPO — CTPB) were used to obtain the rate of homopolymerization of MAPO in CTPB. It is known that the aziridine ring is more reactive in an acidic medium. This observation was confirmed in this study, since a homopolymerization rate of $1.2 \times 10^{-3} \text{ eq.}^{-1} \text{ min.}^{-1}$ was found.

Effect of MAPO Homopolymerization on its Functionality

The influence of the homopolymerization of MAPO on its functionality was investigated. This may be seen from the following theoretical con-

TABLE III
Functionalities of CTPB

Sample	Gel time, min.	PM ^a	f_{PM}	f_{PE}	OH, %	f_{PH}	$f_{PE} + f_{PH}$	f_M
Hycar A	18	0.581	2.48	2.44	0.025	0.07	2.51	2.96
Hycar B	22	0.617	2.32	2.26	0.020	0.06	2.32	3.00
Telagen A	62	0.540	2.71	2.40	0.036	0.10	2.50	3.28
Telagen B	72	0.446	3.52	2.95	0.043	0.21	3.16	3.32
HC434-A	96	0.556	2.62	2.38	0.014	0.03	2.41	3.30
HC434-B	93	0.576	2.51	2.29	0.030	0.06	2.35	3.24
HC434-C	112	0.573	2.52	2.22	0.024	0.06	2.28	3.38
Butarez A	109	0.504	2.98	2.42	0.072	0.24	2.66	3.38
Butarez B	146	0.555	2.62	2.18	0.060	0.21	2.39	3.34
Butarez C	171	0.610	2.35	2.14	0.025	0.09	2.23	3.18
Butarez D	126	0.518	2.86	2.40	0.051	0.16	2.56	3.38
Butarez E	139	0.503	2.99	2.51	0.050	0.17	2.68	3.35

^a Functionality: for symbols see Tables I and II. PM, conversion of carboxyl groups in MAPO reaction. f_M , functionality of MAPO.

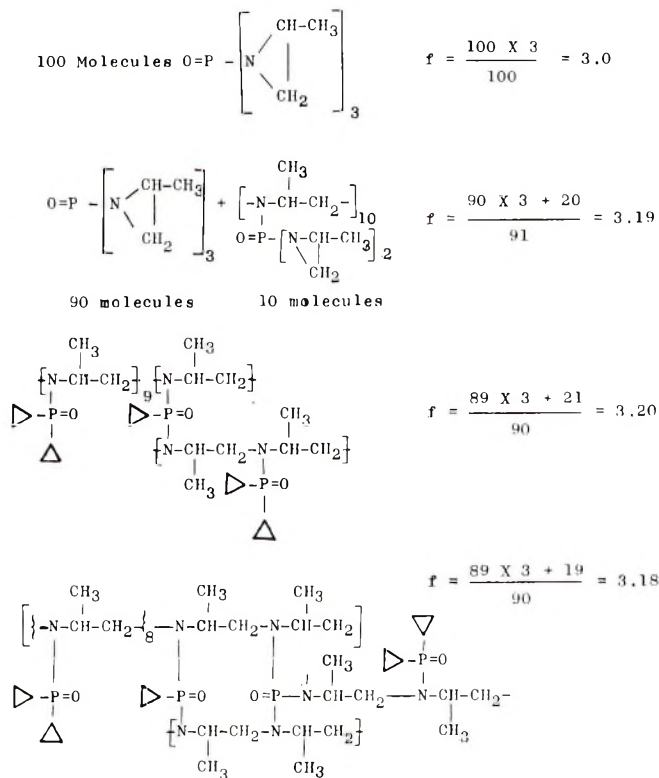


Fig. 7. Theoretical dependence of functionality on homopolymerization.

siderations, shown in Figure 7. If one starts with 100 molecules of MAPO with a functionality of 3, then after the homopolymerization of 10 molecules one obtains an average functionality of 3.19. If the next step is the polymerization of an additional molecule to a side chain, the average functionality becomes 3.20. However, if two adjacent imine rings react with each other, the functionality decreases. This means that as homopolymerization proceeds, a three-dimensional network of MAPO molecules is built up, and the functionality decreases steadily. This behavior of the functionality must, therefore, be time-dependent.

Table III shows the functionalities of a series of CTPB samples with various gel times in the reaction with MAPO. The total functionality of CTPB with respect to MAPO was determined by the addition of the COOH functionality, obtained in the epoxide reaction, and the calculated hydroxyl functionality. The functionality of MAPO was determined from the total CTPB functionality and, as seen in the last column in Table III, the MAPO functionality is not constant but varies between 2.96 and 3.38. Figure 8 shows the time dependence of MAPO functionality, which is in agreement with the predicted increase and subsequent decrease in MAPO functionality as the homopolymerization proceeds. The purity of MAPO was 98%, which corresponds to a functionality of 2.94.

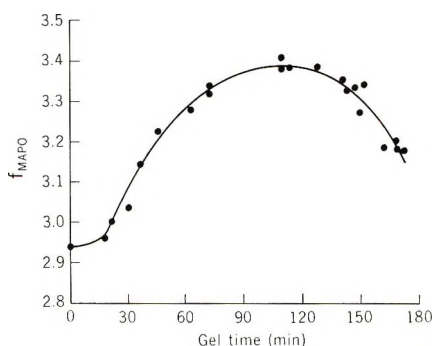


Fig. 8. Dependence of functionality of MAPO on time at 105°C.

Thus, the apparently high functionality of CTPB with respect to MAPO may be attributed to the increase in functionality of MAPO owing to homopolymerization, since in the reaction with MAPO a functionality of 3 for MAPO was taken for the calculation of the functionality of CTPB.

Johnson et al.⁸ found that the ester product formed between MAPO and acetic acid can rearrange to form dimethyloxazolines. However, the formation of addition products has no effect on the determination of functionality.

Conclusion

It was found that through homopolymerization of MAPO a chain-like polymer is formed, and the average functionality increases. As homopolymerization proceeds, a three-dimensional network is formed, and the functionality decreases again. The homopolymerization of MAPO is the main reason for the higher functionalities for CTPB. In addition, hydroxyl groups and moisture influence the determination of CTPB functionality when MAPO is used as the curing agent.

This work was funded under the Standards Laboratory Program of the Naval Ordnance Systems Command.

References

1. R. Strecker and D. French, *Am. Chem. Soc. Polymer Preprints*, **7**, 952 (1966).
2. S. Siggia, *Quantitative Organic Analysis via Functional Groups*, Wiley, New York, 1949, p. 4.
3. Interchemical Corporation, unpublished results.
4. W. H. Stockmayer, *J. Polymer Sci.*, **9**, 1, 69 (1952).
5. U.S. Pat. 2,318,730 (1943).
6. Ger. Pat. 665,791 (1938).
7. W. Kern and E. Brenneisen, *J. Prakt. Chem.*, **159**, 193 (1941).
8. D. E. Johnson, R. S. Bruenner, and A. J. Di Milo, *Ind. Eng. Chem., Prod. Res. Develop.*, **5**, 53 (1966).

Received September 25, 1967

Revised October 25, 1967

The Thermal Degradation of Acrylic Acid-Ethylene Polymers

M. C. McGAUGH and SHERMAN KOTTLE, *Polyolefin Research Department, The Dow Chemical Company, Freeport, Texas 77541*

Synopsis

A study of the thermal degradation of a copolymer of ethylene and acrylic acid is presented. The degradation mechanism of the acrylic acid portion of the polymer was found to be dehydration of the acid, forming anhydride, and decarboxylation of the anhydride, forming unsaturation. The resultant unsaturation reduces the copolymer's stability to both thermal and oxidative degradation.

Acrylic acid-ethylene (AA-E) copolymers exhibit less oxidative and thermal stability than does polyethylene, and they are not stabilized by free-radical inhibitors to the same extent as is polyethylene. This investigation was begun to determine what differences existed between the degradation mechanisms of the two polymers.

EXPERIMENTAL

Polymer

An experimental acrylic acid-ethylene copolymer containing 16.8 wt.-% acrylic acid was used in this investigation. The resin was synthesized by free-radical polymerization and was additive-free.

Thermogravimetric Analysis (TGA)

Thermogravimetric analysis was performed with a du Pont Model 950 TGA instrument. The temperature range investigated was from room temperature to 500°C.; the atmospheres were of air and helium. In runs in which the temperature was varied a heating rate of 15°C./min. was used.

Infrared Analysis

Infrared spectra were obtained with a Beckman IR-9. Anhydride standardization was performed with acetic anhydride. The molar extinction coefficient was used to calculate the concentration of anhydride in the polymer as acrylic anhydride. All samples were in the form of thin films.

Oxygen-Uptake Analysis

Oxygen-uptake analysis was performed with an apparatus similar to that of Grieveson et al.¹ The polymer specimen was molded into a film 0.625 mm. (0.025 in.) in thickness. A sample 5 × 75 mm. was introduced into the apparatus, and the system was evacuated. A heater block at the test temperature (135°C.) was positioned over the sample tube. After 2 min. of heating, oxygen was admitted to a pressure of 1 atm. Pressure was recorded as a function of time; the induction period was taken as the time required for a pressure drop of 2 mm. of mercury. Duplicate determinations were in agreement within ±1.0 min.

Thermal Volatilization Analysis

TVA curves were produced with an apparatus similar to that of McNeill.² Samples (20–500 mg.) were evacuated to 20 μ and heated at a programmed rate (10°C./min.) from 35 to 500°C. Pressures of the volatile products produced during the heating period were measured by means of a vacuum gage and plotted against temperature.

RESULTS AND DISCUSSION

A series of ethylene-acrylic acid samples was prepared by vacuum-heating the copolymer for various periods of time at 275°C. The results are given in Table I. The data in Table I show that the acrylic anhydride concentration is proportional to the heating time. Melt index measurements, also shown in Table I, indicate that the copolymer is rapidly becoming crosslinked.

TABLE I
Anhydride Formation in AA-E Copolymer (Pellets), 16.8% AA

Heating time at 275°C., hr.	Acrylic anhydride, %	Melt index ^a
0	none detectable	17.1
1	0.35	3.1
2	0.38	0.3
3	0.90	<0.02
4	1.55	<0.02
5	1.61	<0.02

^a ASTM D-1238.

Upon detection of anhydride formation in the copolymer, as suggested by previous work with polyacrylic acid,³ it was decided to determine whether the anhydride was subject to anhydride-type reactions, mainly that of hydration. Film samples from the vacuum-heating experiments were boiled in water for 1.5 hr. Infrared analysis showed a reduction in anhydride concentration of 87 to 91% (Table II).

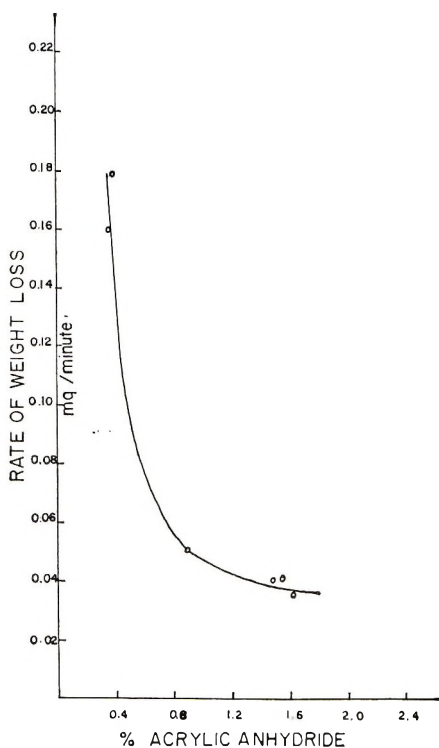


Fig. 1. Rate of weight loss vs. per cent acrylic anhydride data for 16% acrylic acid-ethylene polymer. Sample weight 27-30 mg.

Hydration of the anhydride suggested experiments to determine whether other polymer properties were also being returned to their original values. Sufficient vacuum-heated samples for melt index and stability measurements were boiled in water for 14 hr. and examined (Table III). Not only did the polymer's melt index return to approximately 50% of the original value, but also the polymer's stability to oxidation improved. It is thought that chain scission or reactions other than anhydride formation took place during heat treatment; thus, 100% return of the original properties was not attained.

TABLE II
Reversibility of Anhydride Formation (2-mil film), 16.8% AA-E Polymer

Sample no.	Heating time at 275°C., hr.	Acrylic anhydride, %	Acrylic anhydride after 1.5 hr. in boiling H ₂ O, %	Acrylic anhydride hydrolyzed, %
1	0	0.00	—	—
2	2	0.72	0.062	91
3	1.5	0.61	0.082	87

TABLE III
Reversibility of Anhydride Formation as Shown by Crosslinking (Pellets),
16.8% AA-E Polymer

Sample	Acrylic anhydride, %	Melt index	Induction period at 135°C., min.
Blank	none detectable	17.1	15.0
Blank after 2 hr. heating at 275°C.	0.98	<0.02	3.5
Blank after 2 hr. heating at 275°C. and 14 hr. in boiling water	none detectable	8.69	6.0

Further evidence of the dehydration reaction was obtained from TGA measurements. Figure 1 shows a plot of per cent anhydride versus rate of weight loss from the TGA measurements made in air. The rate measurements were obtained in the region of 275–300°C. of the TGA curve. When the anhydride concentration was the greatest, the rate of reduction in weight was least. This was to be expected, since the rate of dehydration should depend on the concentration of the remaining acid groups.

The decarboxylation reaction of acrylic anhydride, forming unsaturation, could not be followed by infrared spectroscopy, which was used for polyacrylic acid,³ since infrared could not detect unsaturation in the degraded polymer, owing to interference. The unsaturation band could not be resolved in the region of 850–950 cm^{-1} , because of intense acrylic acid absorption and because of much carbonyl absorption in the 1650 cm^{-1} region.

Figure 2 shows a TVA curve for a 16% acrylic acid-ethylene polymer and an ethylene homopolymer.

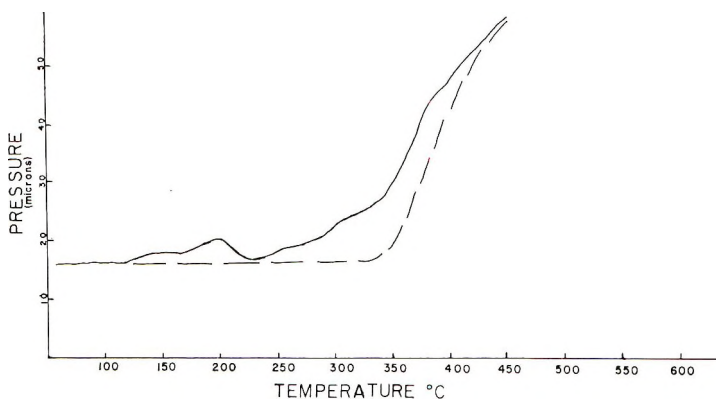


Fig. 2. Pressure-temperature data on 16% acrylic acid-ethylene polymer and polyethylene: (—) copolymer; (---) ethylene homopolymer.

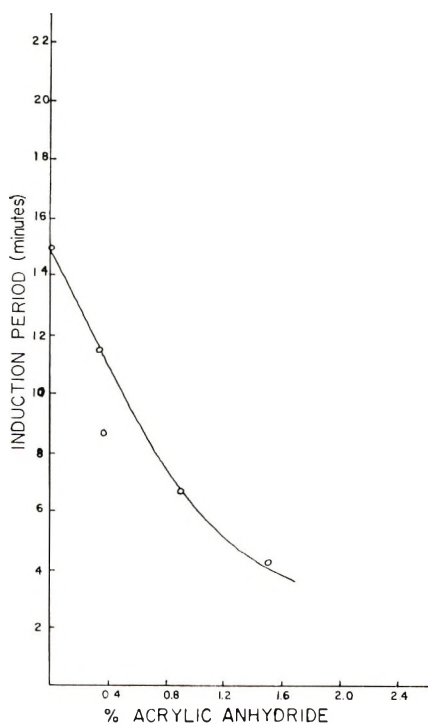


Fig. 3. Induction period (minutes at 135°C.) vs. per cent acrylic anhydride data for 16% acrylic acid-ethylene polymer.

The small peak for the copolymer between 150 and 200°C. corresponds to the dehydration reaction discussed for polyacrylic acid. Figure 2 also shows a broad peak for the copolymer starting at 225°C. and continuing until complete polymer degradation at 460°C. TVA curves for polyacrylic acid show the decarboxylation peak for 225–325°C. Therefore it is thought that the decarboxylation peak for the copolymer is included in the broad peak in Figure 2. The decarboxylation peak of the copolymer was not resolved, because of the presence of the ethylenic part of the molecule. Mass spectrographic analysis of the volatile products produced during vacuum pyrolysis at 225–325°C. showed CO₂ to be the major constituent.

Stability

Figure 3 shows that increasing the anhydride concentration decreases the resin's stability to oxidation. This decrease in oxidative stability is believed to be due to the resulting unsaturation formed by decarboxylation of the anhydride as heat treatment is increased. The decrease in oxidative stability may also be attributed to thermal degradation of the ethylene portion of the polymer, since these polymers were subjected to severe heat treatment. Since acrylic acid-ethylene polymers are less stable to

oxidation than ethylene homopolymers, it is felt that the dehydration-decarboxylation scheme of the formation of unsaturation is a contributing factor in the copolymer's degree of stability.

References

1. B. M. Grieveson, R. Haward, and B. Wright, *SCI Monograph No. 13*, 1961, p. 413.
2. I. C. McNeill, *J. Polymer Sci. A-1*, **4**, 2479 (1966).
3. M. C. McGaugh and S. Kottle, *J. Polymer Sci. B*, **5**, 817 (1967).

Received August 16, 1967

Revised October 31, 1967

Catalytically Active Form of Ferric Acetate Hydroxide for the Insertion Polymerization of Propylene Oxide

M. OSGAN,* *Mellon Institute, Pittsburgh, Pennsylvania*

Synopsis

Hydrated ferric oxides prepared in the presence of acetate ions show substantially higher catalytic activity over that of ordinary hydrated ferric oxide (for the polymerization of propylene oxide). The maximum in activity is reached at a ratio of acetate to iron of 2. It is suggested that the active species are formed through the trinuclear μ -acetato-ferric complex. This would imply that the insertion mechanism requires a particular geometry with probably a minimum of three coordination centers.

INTRODUCTION

Catalysts capable of polymerizing propylene oxide to high molecular weight partly isotactic polymer, with relatively high polymerization rates, are distinguished by a common feature: they appear to contain in their structure some kind of a bridged bi- or polynuclear species, generally in the form of metal-oxygen-metal groupings. Thus the reaction products of ferric chloride with propylene oxide, at complete exclusion of water, were shown to be a poor catalyst, unless the third chloride on iron was hydrolyzed to give structures containing Fe-O-Fe species.^{1,2} Similarly ferric alcoholates by partial hydrolysis with water were claimed to give active catalysts.³ Partial hydrolysis products of dialkylmagnesium and trialkylaluminum were found to be very efficient polymerization catalysts.^{4,5} Dialkylzinc, as such was nearly inactive; a highly active catalyst was obtained on the other hand, when it was used with certain cocatalysts capable of providing Zn-O-Zn species.⁶⁻⁸

In all the above examples the formation of an active catalyst includes a step in which the catalyst precursor is treated in an organic solvent with an appropriate oxygen donor. In this paper, we present an alternative route for the formation of active species. First, polynuclear water-soluble μ -acetato complexes of ferric ions have been prepared in aqueous solution; then, by adjusting conditions favorable to hydrolysis of the bridging acetato ligands, ferric acetate hydroxide (FAH) has been allowed to precipitate from this solution. The FAH catalysts obtained by this way were found to give about sevenfold higher rates of polymerization of propylene oxide than ferric hydroxide catalyst obtained by direct hydrolysis of ferric ion.

* Present address: Laboratoire de Chimie Macromoléculaire, Institut Français du Pétrole, Hauts de Seine, France.

EXPERIMENTAL

Materials

Propylene oxide (Distillation Products, Eastman Kodak Co.) was refluxed over potassium hydroxide pellets, rectified, refluxed over freshly powdered calcium hydride, and finally distilled over calcium hydride under nitrogen.

n-Heptane was purified by treatment first with concentrated sulfuric acid and then with an acidic, concentrated solution of potassium permanganate and distilled.

The final drying and distillation was done in the same manner as for propylene oxide.

Ferric chloride hexahydrate (A.R., lumps, low phosphorus, Mallinckrodt), sodium acetate trihydrate (A.R., Baker), hexamethylenetetramine (Baker) were used without further purification.

Acetone, benzene, and toluene were Fisher Certified Reagent grade, used as received.

Water used for catalyst preparation was distilled water, passed subsequently over ion-exchange columns.

Nitrogen was H.P. grade dry nitrogen (Linde) used as received.

Analyses

Elemental analyses were by Schwarzkopf Microanalytical Laboratory, Woodside, New York.

General Handling Techniques

The catalyst, the monomer, and the polymerization solvent, once subjected to the final drying, were kept in previously purged screw-cap bottles fitted with self-sealing gaskets under 8–15 psig nitrogen. Liquids, including slurries, were transferred by the usual hypodermic and syringe techniques, the solids were handled in polyethylene bags, all of which were prepurged with nitrogen just before utilization.

Preparation of the Catalysts

An aqueous, concentrated sodium acetate solution (in the given molar proportion) was added at room temperature to a 1*M* aqueous ferric chloride solution (100 ml.) and left to stand for overnight. The basic ferric acetate was then precipitated quantitatively by addition of this ferric acetate solution to 1300–1330 ml. of water at 80–85°C. containing 10 g. of hexamethylenetetramine, under vigorous stirring. The gellike precipitate was washed with 0.2*N* aqueous sodium acetate until it becomes practically free from chloride, then once with water. For highly active catalysts, the precipitate was a chocolate-colored powder with a violet-blue hue on reflected light. The filtered precipitate was first predried to a loose powder

and subsequently it was subjected to a final drying *in vacuo* at 100°C. over phosphorus pentoxide.

ANAL. Calcd. for $2\text{Fe}_2\text{O}_3 \cdot \text{FeOOH} \cdot \text{FeOOAc}$: C, 4.30%; H, 1.07%; Fe, 60.22%. Found for a FAH sample prepared from an acetate ratio of (acetate/Fe) = 0.25: C, 4.72, 4.54%; H, 1.35, 1.13%; Fe, 60.88 (titrimetric), 60.71, 61.13%. Found for acetate/Fe = 2.0: C, 4.92, 5.04%; H, 1.14, 1.40%; Fe, 60.45 (titrimetric), 60.93, 60.76%.

All the samples of FAH were amorphous by x-ray.

The dried FAH catalysts were slurried in *n*-heptane and ball-milled (Pyrex beads) just until a fine suspension was obtained that could be handled through a 20 g. hypodermic needle (about 0.9 mm.) at 0.1 g./ml. solids content.

Polymerization Techniques

Polymerization studies were carried out in sealed Pyrex tubes. Nitrogen-filled tubes were charged with the catalyst (suspended in heptane) through a serum stopple, cooled in Dry Ice-alcohol, and the monomer was added. The tubes were then quickly transferred to an all glass vacuum line under nitrogen, and sealed under vacuum. The sealed tubes were placed on a rocking rack immersed in an oil bath maintained at $70 \pm 0.5^\circ\text{C}$. After a given polymerization time the contents of the tube were frozen in Dry Ice-alcohol, the tube was broken, and the polymer was quickly chopped while frozen. The crude polymer was then shaken with a mixture of aqueous phosphoric acid (20% by volume) and toluene until the brown color of the catalyst disappeared completely. The toluene solution of the polymer was washed subsequently with fresh aqueous phosphoric acid, water, dilute sodium bicarbonate solution, and water. After addition of 5–25 mg. of Tenox BHT butylated hydroxytoluene (food grade) of Eastman Chemical Products, Kingsport, Tennessee as antioxidant (estimated to obtain 0.2–0.5% antioxidant in the polymer), the polymer solution was (portionwise) poured into aluminum trays placed in a hood and was left to dry by removing the volatiles by a sweeping current of fresh air at room temperature. Usually after 20–48 hr. they attained constant weight, and the polymer was then obtained as a colorless, tough film not exceeding 0.5 mm. in thickness. This drying procedure was found by parallel tests to be as efficient as the technique of freeze-drying from a benzene solution.

Separation of Acetone-Insoluble Fraction of Poly(propylene Oxide)

An accurately weighted, 1 g. sample of unfractionated polymer was dissolved in a pressure bottle at 80–90°C. in about 80 ml. of acetone containing 10 mg. of antioxidant. The solution was quantitatively transferred into a 250 ml. centrifuge bottle, bringing it to a final dilution of 150 ml. It was then placed at -5 to -8°C . for at least 30 hr., after which time it was centrifuged at -5 to -8°C . for 3–4 hr.

The precipitate was then reprecipitated from an acetone solution in a similar manner, the second soluble portion, which contained less than 1% solids, being discarded. The acetone-insoluble portion thus obtained was finally dissolved in a small volume of toluene and dried as described above. The per cent acetone-insoluble material was calculated from the weights of unfractionated polymer and its acetone-insoluble fraction thus obtained.

Determination of Viscosities

The intrinsic viscosities of various polymer samples were determined in benzene solution at $30 \pm 0.1^\circ\text{C}$. by using an Ubbelohde viscometer by dilution method. The solutions of the crude polymer and of the acetone-insoluble fraction were prepared by direct weighing of the samples in volumetric flasks and dissolving to the final volume at room temperature. The concentrations were so adjusted as to have relative viscosities between 1.8 and 1.2 dl./g.

For the acetone-soluble fractions it was found more convenient to convert the acetone solution of the polymer to a benzene solution of the same by repeated distillations on a water bath. Once the concentration of this latter was adjusted to obtain a relative viscosity of 1.8–1.7 dl./g., a suitable volume of an aliquot was dried to obtain the concentration.

RESULTS

Table I shows the activities of a series of ferric acetate hydroxide (FAH) catalysts, expressed as time required to convert propylene oxide to 50% polymer and the intrinsic viscosities of the products at this conversion.

TABLE I
Effect of Acetate/Iron (III) mole Ratio in the FAH Catalyst Preparation on the Polymerization Rates of Propylene Oxide and on Product Viscosities^a

Acetate ratio (acetate/Fe)	Time required for 50% conversion to polymer, min.	[η], dl./g. ^b		
		Unfractionated polymer	Acetone-soluble fraction	Acetone-insoluble fraction
0	1500	1.6	0.8	4.4
0.25	440	4.3	2.5	7.6
1.0	340	5.0	3.0	7.8
1.2	230	4.8	2.8	7.5
2.0	200	4.8	3.0	7.5
3.2	230	5.0	3.5	7.5
6.6	1700	5.5	3.5	7.6
6.6 ^c	12000 ^d	—	3.9	6.5

^a Polymerization conditions: 0.5 g. catalyst in 5.0 ml. *n*-heptane and 5.8 g. propylene oxide at 70°C .

^b In benzene at 30°C .

^c FAH precipitate aged for 20 hr. in contact with 0.6M NaOAc at room temperature.

^d Time required for 10% conversion.

TABLE II
Effect of Monomer/Catalyst Ratio on Product Viscosities and of Acetone Insolubles^a

Catalyst		PO, g.	Polymerization time, hr.	Polymer, g.	[η], dl./g.			
Wt., g.	Acetate ratio				Unfractionated polymer	Acetone-soluble fraction	Acetone-insoluble fraction	Acetone insolubles, %
0.5	1.0	2.9	5	2.41	1.7	0.8	4.7	22
0.5	1.0	5.8	3/4	0.61	0.7 ₅	0.3 ₇	2.1	16
0.5	1.0	5.8	5	3.23	2.7	1.9	6.6	29
0.2	1.0	5.8	5	1.45	2.9	1.6	6.0	27
0.2	1.0	11.6	15	3.36	4.9	3.2	8.0	32
0.5	2.0	5.8	2	1.82	4.3	1.8	6.5	28
0.2	2.0	11.6	10	3.20	6.5	4.8	8.5	41
0.2	2.0	11.6	30	7.93	6.9	5.2	9.0	44

^a Polymerization at 70°C.

The catalysts were prepared, by precipitation, from an aqueous solution containing sodium acetate and ferric chloride in varying mole ratios, but otherwise under rigorously fixed conditions. The first sample, which is included for a comparison, was prepared in the absence of acetate, hence it is a ferric hydroxide. Its catalytic activity compares favorably with that reported previously,⁸ though our sample was prepared under somewhat different conditions.

Elemental analysis of two different FAH catalyst samples, of acetate ratios 0.25 and 2.0 indicate nearly the same composition for both samples.* For these samples, the best agreement with analysis is obtained for a formulation such as $2 \text{ Fe}_2\text{O}_3 \cdot \text{FeOOH} \cdot \text{FeOOAc}$.

The dependence of viscosities on monomer/catalyst ratio (Table II) and conversion (Table III) indicate a stepwise increase of molecular weight. In addition a rough calculation shows that the relative number of chains increases with conversion, thus indicating some sort of chain transfer process with active sites.

TABLE III
Effect of Conversion on Product Viscosities
and Content of Acetone Insolubles^a

Polymerization time, hr.	Conversion, %	[η], dl./g.			
		Unfrac- tionated polymer	Acetone- soluble fraction	Acetone- insoluble fraction	Acetone insolubles, %
7	22	5.0	3.0	7.5	34
10	29	5.5	3.9	8.5	36
14 ¹ / ₂	43	6.3	4.6	9.0	39
20 ¹ / ₃	54	6.2	4.0	9.0	38
30	64	6.3	3.9	8.6	39

^a Polymerization conditions: 0.2 g. FAH catalyst (acetate ratio = 2) in 2.0 ml. *n*-heptane and 11.6 g. propylene oxide at 70°C.

The acetone-insoluble fraction increases both with conversion (Table III) and with increasing acetate ratios of catalyst (Table IV).

Since our fractionation procedure would separate only crystallizable chains of sufficiently high molecular weight, and thus the low molecular weight but crystallizable portion would be included in the acetone-soluble fraction, the increase of acetone-insoluble fraction with conversion is probably due to the increase of molecular weights for the early stage of polymerization. With catalysts prepared with an acetate ratio above two

* Since catalysts with almost same composition show varying activities in as a function of acetate to iron ratio in their preparation, catalysts have been characterized by this latter ratio (Table I, first column), denoted throughout briefly as "acetate ratio."

there is, however, a definite, though small, increase of acetone insolubles with increasing acetate ratio.

The infrared spectrum of unfractionated poly(propylene oxide) obtained with FAH catalysts was identical with the previously reported spectrum, except that there were additional absorption bands at 3420 cm.^{-1} (OH) and at 1740 cm.^{-1} (acetate). Thick films of acetone insoluble fraction

TABLE IV
Effect of Acetate Ratio in the Catalyst Preparation on Content of Acetone Insolubles^a

Acetate ratio	Acetone insolubles, %	Conversion to polymer, %
0	17	39
0.25	30	35
—	33	61
0.85	34	36
—	38	66
1.0	24	41
—	35	73
1.2	31	63
—	36	93
2.0	36	64
—	37	94
3.2	39	61
—	40	91
6.6	48	35

^a Polymerization conditions: 0.5 g. catalyst, 5.0 ml. *n*-heptane, 5.8 g. propylene oxide at 70°C .

again revealed this latter 1740 cm.^{-1} absorption band. The powder x-ray pattern of the acetone-insoluble fraction indicated that the crystalline fraction corresponded to isotactic poly(propylene oxide).*

DISCUSSION

In comparing catalytic activities of ferric hydroxide (acetate) catalysts prepared by hydrolysis of a ferric salt in the presence and in the absence of acetate ions, the most striking differences appear in the higher rates of polymerization of propylene oxide and substantially higher molecular weights of both amorphous and crystalline fractions of polymer produced, when the catalyst is prepared in presence of acetate ions. Since ferric ions form a highly stable, soluble μ -acetato-ferric hydroxide complex,⁹ $[\text{Fe}_3(\text{OAc})_6(\text{OH})_2]^+$, and since the maximum in catalytic activity corresponds to an acetate to iron ratio of two, which is the same for the above mentioned soluble complex, the formation of ferric acetate hydroxide in a catalytically active form (for the polymerization of propylene oxide) must be due to a hydrolysis through μ -acetato-ferric hydroxide species. The

* I am indebted to Dr. Pollack for this identification.

fact that the catalytic activity continues to increase with increasing acetate ratios up to two, while the chemical composition of the precipitate (ferric acetate hydroxide) remains nearly unchanged, brings further support to the hypothesis that the essential condition for the formation of active centers is related to the nature of species to be hydrolyzed (prehydrolytic species).

In our opinion, the overall pattern observed here, that is a substantial increase in both polymerization rates and molecular weights of the polymer, with catalysts obtained from a particular type of this prehydrolytic species, parallels similar observations, for example, for zinc-based catalysts; these are striking differences in catalytic activity between catalysts prepared by hydrolysis of zinc chloride¹⁰ and those obtained from zinc alkyls.^{6,11}

We ascribe the decrease in polymerization rates, while molecular weights of the products remain unchanged, for catalysts prepared with an acetate ratio above 2, to a decrease in the relative number of active sites on the catalysts by adsorption of acetate by these sites. This would imply that the active sites are electrophilic in nature, as previously suggested.¹² Additional support for this interpretation comes from the results of an experiment in which the ferric acetate hydroxide precipitate prepared with an acetate ratio of 6.6 was left to age in contact with 0.6*M* sodium acetate. In this latter case the polymerization rate decreased by a factor of one hundred with respect to the maximum rate observed, whereas the molecular weight of the product was comparable with the products obtained by most active catalysts.

The small increase of acetone-insoluble fraction of poly(propylene oxide) observed with catalysts of this latter type may be due to a decrease in the rate of catalyst site exchange of growing polymer chains as a consequence of the reduction of the number of active sites. This in turn would lead to an increase of the formation of long stereoregular sequences which would be found in the acetone-insoluble fraction.

The author wishes to thank Mr. Paul Kaufman who assisted him in the workup of polymers and carried out the viscosities. The gift of a sample of Tenox BHT by Eastman Chemical Products Co. is gratefully acknowledged.

References

1. G. Gee, W. C. E. Higginson, and J. B. Jackson, *Polymer*, **3**, 231 (1962).
2. A. B. Borkovec (to Dow Chemical Co.), U.S. Pat. 2,873,258 (February 10, 1959).
3. A. B. Borkovec (to Dow Chemical Co.), U.S. Pat. 2,861,962 (November 25, 1958).
4. E. J. Vandenberg (to Hercules Powder Co.), Belg. Pat. 579,074 (April 20, 1960); *J. Polymer Sci.*, **47**, 486 (1960).
5. R. O. Colclough, G. Gee, and A. H. Jagger, *J. Polymer Sci.*, **48**, 273 (1960).
6. R. Sakata, T. Tsuruta, T. Saegusa, and J. Furukawa, *Makromol. Chem.*, **40**, 64 (1960).
7. K. T. Garty, T. B. Gibb, Jr., and R. A. Clendenning, *J. Polymer Sci. A*, **1**, 85 (1963).
8. M. E. Pruitt, J. M. Baggett, R. J. Bloomfield, and J. H. Templeton (to Dow Chemical Co.), U.S. Pat. 2,706,182 (April 12, 1955).

9. D. D. Perrin, *J. Chem. Soc.*, **1959**, 1710.
10. Ph. E. Ebert and C. C. Price, *J. Polymer Sci.*, **46**, 455 (1960).
11. J. Furukawa, T. Tsuruta, R. Sakata, T. Saegusa, and A. Kawasaki, *Makromol. Chem.*, **32**, 90 (1959).
12. C. C. Price and M. Osgan, *J. Am. Chem. Soc.*, **78**, 4787 (1956).

Received June 8, 1967

Revised July 11, 1967

Polymers with Quinoxaline Units. III. Polymers with Quinoxaline and Thiazine Recurring Units*

MASAHIKO OKADA and C. S. MARVEL, *Department of Chemistry, University of Arizona, Tucson, Arizona 85721*

Synopsis

Six ladder or partly ladder polymers have been prepared by the condensation reactions of combinations of two diaminodithiophenols, 4,6-diamino-1,3-dithiophenol and 3,3'-dimercaptobenzidine, with three tetrachloroquinoxaline derivatives, 2,3,7,8-tetrachloro-1,4,6,9-tetraazaanthracene, 2,2',3,3'-tetrachloro-6,6'-bisquinoxaline, and 2,2',3,3'-tetrachloro-6,6'-diquinoxalyl ether, with the use of dimethylacetamide, hexamethylphosphoramide, and polyphosphoric acid as reaction media. The polymers thus obtained are highly colored, powdery materials which are slightly soluble in methanesulfonic acid and concentrated sulfuric acid. These polymers ($\eta_{inh} > 1$) show good thermal stability.

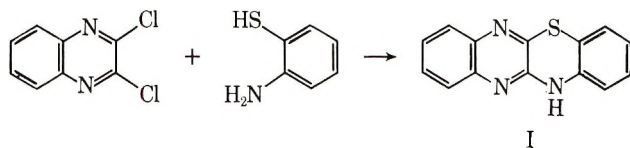
INTRODUCTION

Recent studies¹⁻⁷ have shown that polymers with quinoxaline recurring units exhibit good thermal stability and can be obtained as high molecular weight materials. Also, it has been established⁸⁻¹⁰ that aromatic ladder structures improve thermal properties over the other polyaromatic types. In the course of the investigations on the synthesis of thermally stable polymers of this type, the scope of the studies has been extended to the polymers which contain thiazine units in addition to quinoxaline units. This paper deals with the synthesis of thermally stable ladder or partly ladder polymers with quinoxaline and thiazine recurring units by the condensations of combinations of two diaminodithiophenols, 4,6-diamino-1,3-dithiophenol and 3,3'-dimercaptobenzidine, with three tetrachloroquinoxaline derivatives, 2,3,7,8-tetrachloro-1,4,6,9-tetraazaanthracene, 2,2',3,3'-tetrachloro-6,6'-bisquinoxaline, and 2,2',3,3'-tetrachloro-6,6'-diquinoxalyl ether.

DISCUSSION

The melt condensation of 2,3-dichloroquinoxaline with *o*-aminothiophenol to give quinoxalinobenzothiazine (I) has been reported.¹¹ This reaction seemed to offer a synthetic route for ladder-like polymers with quinoxaline and thiazine recurring units; hence it was reexamined under various reaction

* This work was presented in part at the Miami Beach meeting of the American Chemical Society in April 1967.



conditions to seek for an optimum reaction condition for the preparation of polymers. Experiments indicated that the condensed compound was obtained in an almost quantitative yield under proper control of the reaction by stirring the two reactants initially at room temperature for a few hours followed by raising the reaction temperature gradually up to 150°C. in dimethylacetamide or hexamethylphosphoramide or up to 250°C. in polyphosphoric acid. By the similar procedure, five model compounds have been successfully prepared. These are listed in Table I, together with ultraviolet data on them.

It was hoped that polymers with quinoxaline and thiazine recurring units could be obtained by the condensation of the corresponding tetrafunctional monomers under the similar reaction condition. Polymerization was generally carried out as follows: Equimolar amounts of a diaminothiophenol and a tetrachloroquinoxaline derivative were mixed in

TABLE I
Model Compounds with Quinoxaline and Thiazine Units

No.	Structure	λ_{\max} , $m\mu^a$		
I		243,	299,	318
II		261,	268,	311
III		253,	293,	302
IV		255,	276,	319
V		253,	291,	301

^a Ultraviolet spectra were taken in concentrated sulfuric acid.

dimethylacetamide or hexamethylphosphoramide at room temperature. After stirring for 1 or 2 hr., the reaction mixture was heated at 150°C. for 24 hr. During heating, a polymeric material precipitated out of the solution. It was separated from the reaction mixture by treating with dilute ammonium hydroxide solution and subsequently extracting with ethanol and benzene for several hours in a Soxhlet extractor. Since the polymers thus obtained seemed to have unclosed ring units to some extent and also to retain the solvent used in the polymerization, they were heated in a rotating flask at 330°C. for several hours under vacuum.

Condensation was performed also in polyphosphoric acid above 200°C. to give a polymer identical to that obtained in organic solvents. In this solvent tetrahydroxyquinoxaline derivatives also afforded a polymer by the condensation with diaminodithiophenol. The polymers obtained in polyphosphoric acid, however, retained some residues which were very difficult to remove.

The results on the preparation of polymers with quinoxaline and thiazine recurring units are summarized in Table II.

These polymers are highly colored, powdery materials and insoluble in common organic solvents. They are also very difficultly soluble in such solvents as hexamethylphosphoramide, dimethylformamide, and dimethyl sulfoxide, but slightly soluble in concentrated sulfuric acid and methanesulfonic acid. The nitrogen and the sulfur analyses of these polymers are fairly satisfactory but the carbon is nearly always low, presumably due to difficult combustion. This is a common trouble which is frequently

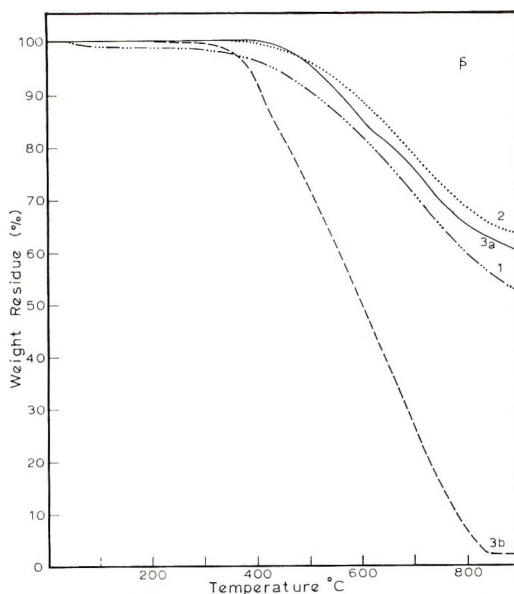
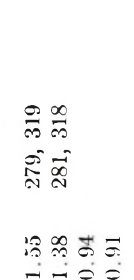
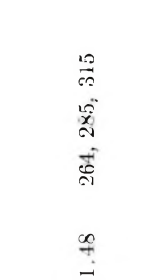
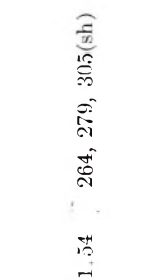


Fig. 1. TGA curves: (1) polymer I in nitrogen; (2) polymer II in nitrogen; (3a) polymer III in nitrogen; (3b) polymer III in air.

TABLE II
Polymers with Quinoxaline and Thiazine Recurring Units

No.	Structure	Reaction medium ^a	Appearance	η_{inh}^b	$\lambda_{max}, m\mu^c$
I		DMAC HMP PPA ^d	Black powder Dark brown powder Black powder	1.19 0.27 0.22	2.96, 317
II		DMAC	Dark brown powder	1.47	270, 306(sh)
III		DMAC	Black powder	1.25	255, 324

<p>IV</p> 	<p>DMAC HMP PPA PPA^d</p>	<p>Black powder Black powder Black powder Black powder</p>	<p>1.55 1.38 0.94 0.91</p>	<p>279, 319 281, 318</p>
<p>V</p> 	<p>DMAC</p>	<p>Brown powder</p>	<p>1.48</p>	<p>264, 285, 315</p>
<p>VI</p> 	<p>DMAC</p>	<p>Brown powder</p>	<p>1.54</p>	<p>264, 279, 305(sh)</p>

^a DMAC: dimethylacetamide; HMP: hexamethylphosphoramide; PPA: polyphosphoric acid.

^b Viscosities were taken in methanesulfonic acid (0.2% solution at 30°C.).

^c Ultraviolet spectra were taken in sulfuric acid.

^d 2,3,7,8-tetrahydroxy-1,4,9-tetraazaanthracene was used in place of the tetrachloro derivative.

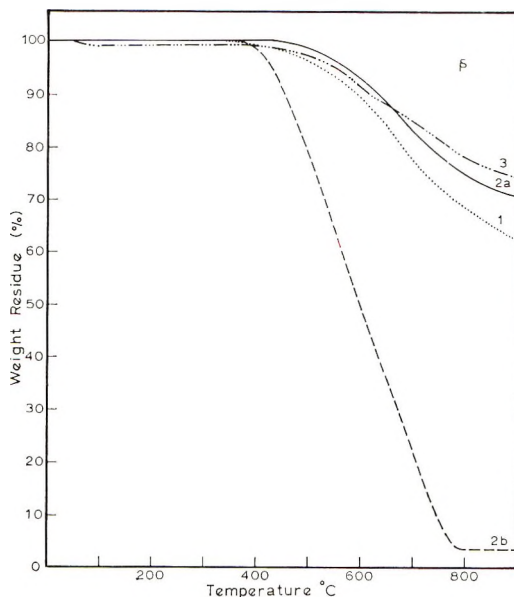


Fig. 2. TGA curves: (1) polymer IV in nitrogen; (2a) polymer V in nitrogen; (2b) polymer V in air; (3) polymer VI in nitrogen.

encountered in the analysis of thermally stable polymers with fused aromatic rings.

The thermal stability of these polymers was evaluated by thermogravimetric analysis which was run in nitrogen or air at the heating rate of 150°C./hr. Figures 1 and 2 show the thermogravimetric curves of the polymers. In most cases initial weight loss occurs at about 500°C. in nitrogen and about 400°C. in air. The unexpectedly poor thermal stability of polymer I which is supposed to have a fully ladder structure and should have the highest stability is believed to be due to incomplete ring closure. It might be difficult to achieve complete thiazine ring formation along the polymer backbone in the case of a polymer with such a rigid structure. However, it must be noted here that 4,6-diamino-1,3-dithiophenol is unstable even in the form of dihydrochloride and the purity of the monomer is somewhat in doubt. This, more than was anticipated, may be responsible for the poorer thermal stability of the polymer.

4,6-Diamino-1,3-dithiophenol was prepared by the thiocyanation method of Likhoshesterov and Petrov¹² followed by hydrolysis as described by Finzi and Grandolini.¹³ Since the literature directions are not too complete, we have described our synthesis in the experimental part of this paper.

EXPERIMENTAL

Monomers

4,6-Diamino-1,3-dithiophenol. A solution of freshly prepared dichloro-urea¹⁴ (17.5 g., 0.135 mole) in 220 ml. of acetic acid was added dropwise to

a mixture of *m*-phenylenediamine (14.5 g., 0.135 mole) and ammonium thiocyanate (20.5 g., 0.270 mole) in 220 ml. of acetic acid keeping the reaction temperature at 15–18°C. over 40 min. At the end of the addition, a white solid precipitated out of the solution. After the addition was completed, the reaction mixture was stirred for 20 min. after which it was poured into 3 liters of ice-water to yield a light gray solid. This was separated and washed with water until it was acid-free. Recrystallization twice from hot alcohol gave 13.5 g. of 4,6-diamino-1,3-dithiocyanobenzene as light brown crystals, m.p., 170–171°C. (decomp.), (lit.¹³ m.p. 170–172°C.).

4,6-Diamino-1,3-dithiocyanobenzene (4.4 g., 0.02 mole) thus obtained was added in portions to a solution of sodium disulfide (10.8 g., 0.045 mole) in 50 ml. of water at 50–55°C. under a nitrogen stream. The dithiocyano compound gradually dissolved into solution. After warming at the temperature for 30 min., the reaction mixture was filtered, and the ice-cooled filtrate was poured into 200 ml. of ice-cooled 50% aqueous acetic acid to give a yellow bulky solid. It was collected on a glass filter, washed with water thoroughly and finally with a small amount of cold methanol under a nitrogen stream, and dried. Careful recrystallization from ethanol under nitrogen gave 1.6 g. of 4,6-diamino-1,3-dithiophenol as yellow powder, m.p. 99–100°C. (decomp.), (lit.¹⁴ m.p. 99–101°C.).

ANAL. Calcd. for $C_6H_8N_2S_2$: C, 41.83%; H, 4.68%; N, 16.26%; S, 37.23%. Found: C, 41.42%; H, 4.47%; N, 16.46%; S, 37.01%.

Since this compound is highly sensitive to air oxidation, it was converted to the dihydrochloride and used as such.

3,3'-Dimercaptobenzidine Dihydrochloride. This compound was prepared¹⁵ by thiocyanation of benzidine with ammonium thiocyanate and bromine.

ANAL. Calcd. for $C_{12}H_{14}N_2S_2Cl_2$: C, 44.86%; H, 4.39%; N, 8.72%; S, 19.96%. Found: C, 44.67%; H, 4.50%; N, 8.80%; S, 19.62%.

2,3,7,8-Tetrachloro-1,4,6,9-tetraazaanthracene. This compound was prepared as described in the previous paper.¹

2,2',3,3'-Tetrachloro-6,6'-bisquinoxaline. This compound was prepared as described in the previous paper.¹

2,2',3,3'-Tetrachloro-6,6'-diquinoxalyl Ether. 3,3',4,4'-Tetraaminodiphenyl ether tetrahydrochloride (18.8 g., 0.05 mole) and oxalic acid dihydrate (12.6 g., 0.10 mole) were dissolved in 300 ml. of 4*N* hydrochloric acid and the solution was refluxed for 3 hr. A light yellow crystal precipitated out of the solution during refluxing. After cooling, the precipitate was collected, washed with water until it was acid-free and dried. The yield of 2,2',3,3'-tetrahydroxy-6,6'-diquinoxalyl ether was 96.3%.

A mixture of 2,2',3,3'-tetrahydroxy-6,6'-diquinoxalyl ether (10.1 g., 0.03 mole), phosphorus oxychloride (27.5 ml., 0.30 mole) and *N,N*-dimethylaniline (20 ml.) was refluxed for 3 hr. The dark brown viscous

solution was poured into an ice-hydrochloric acid mixture to give a yellow precipitate, which was collected, washed with hydrochloric acid and water, and dried. Extraction with boiling benzene gave 2,2',3,3'-tetrachloro-6,6'-diquinoxalyl ether in 72% yield, m.p. 219–220°C.

ANAL. Calcd. for $C_{16}H_6N_4OCl_4$: C, 46.63%; H, 1.47%; N, 13.60%; Cl, 34.42%. Found: C, 46.92%; H, 1.52%; N, 13.32%; Cl, 33.95%.

Model Compounds

Condensation of o-Aminothiophenol and 2,3-Dichloroquinoxaline

Model Compound I. Freshly distilled *o*-aminothiophenol (1.2540 g., 0.010 mole) was added to a solution of 2,3-dichloroquinoxaline (1.9920 g., 0.010 mole) in 20 ml. of hexamethylphosphoramide at room temperature. After stirring for 30 min., the solution was heated at 70°C. for 3 hr. under a nitrogen atmosphere. The reaction mixture was poured into 500 ml. of dilute ammonium hydroxide to precipitate a yellow solid. It was collected, washed with water and methanol, and dried. Quinoxalinobenzothiazine was obtained in 97.5% yield, m.p. 279–280°C. (lit.¹ m.p. 270°C.).

ANAL. Calcd. for $C_{11}H_9N_3S$: C, 66.91%; H, 3.61%; N, 16.72%; S, 12.76%. Found: C, 66.63%; H, 3.72%; N, 16.64%; S, 13.04%.

Condensation of 2,3,7,8-Tetrachloro-1,4,6,9-tetraazaanthracene and o-Aminothiophenol

Model Compound II. A solution of freshly distilled *o*-aminothiophenol (0.2518 g., 0.002 mole) in 10 ml. of dimethylacetamide was added to a suspension of 2,3,7,8-tetrachloro-1,4,6,9-tetraazaanthracene (0.3196 g., 0.001 mole) in 20 ml. of the same solvent at room temperature. The resulting dark red solution was stirred for 2 hr. under a nitrogen atmosphere and then heated at 150°C. for 18 hr. After cooling to room temperature, the reaction mixture was poured into dil. ammonium hydroxide to yield a dark red precipitate. It was separated, washed with water and methanol, and subsequently heated at 330°C. for 6 hr. under vacuum. The solid was then extracted with ethanol for 2 days and dried under reduced pressure. The yield of the dark brown solid was 85%, m.p. > 350°C.

ANAL. Calcd. for $C_{22}H_{12}N_6S_2$: C, 62.25%; H, 2.84%; N, 19.80%; S, 15.11%. Found: C, 60.59%; H, 3.16%; N, 19.37%; S, 15.03%.

Condensation of 2,2',3,3'-Tetrachloro-6,6'-bisquinoxaline and o-Aminothiophenol

Model Compound III. Freshly distilled *o*-aminothiophenol (0.2671 g., 0.002 mole) was added to a suspension of 2,2',3,3'-tetrachloro-6,6'-bisquinoxaline in 30 ml. of dimethylacetamide at room temperature. After stirring for 30 min. under nitrogen, the reaction temperature was raised

gradually to 70°C., when the orange-yellow turbid reaction mixture turned into a dark brown clear solution. It was then heated at 120°C. for 4 hr. An orange precipitate came out of the solution. The cooled reaction mixture was poured into 500 ml. of water containing 30 ml. of ammonium hydroxide solution with vigorous stirring to give an orange solid. It was collected, washed with water and ethanol, and subsequently heated at 230°C. for 3 hr. The tan solid thus obtained in an 86% yield dissolved in hexamethylphosphoramide, methanesulfonic acid, and concentrated sulfuric acid, m.p. > 350°C.

ANAL. Calcd. for $C_{28}H_{16}N_6S_2$: C, 67.18%; H, 3.22%; N, 16.79%; S, 12.81%. Found: C, 66.17%; H, 3.21%; N, 16.45%; S, 12.69%.

Condensation of 2,3-Dichloroquinoxaline and 3,3'-Dimercaptobenzidine

Model Compound IV. A solution of 3,3'-dimercaptobenzidine dihydrochloride (0.4818 g., 0.0015 mole) in 20 ml. of dimethylacetamide was added to a solution of 2,3-dichloroquinoxaline (0.5982 g., 0.0030 mole) in 20 ml. of the same solvent. The resulting solution was stirred at room temperature for 1 hr. and then heated at 70°C. for 4.5 hr. under a nitrogen atmosphere. The reaction mixture was poured into 500 ml. of 1% sodium hydroxide solution with vigorous stirring to give an orange-yellow precipitate. It was separated, washed with water and ethanol, and finally extracted with benzene for 24 hr. An orange-yellow residue weighed 0.77 g. (97%) after drying under reduced pressure. This compound was soluble in hexamethylphosphoramide, methanesulfonic acid, and sulfuric acid, m.p. > 350°C.

ANAL. Calcd. for $C_{28}H_{16}N_6S_2$: C, 67.18%; H, 3.22%; N, 16.79%; S, 12.81%. Found: C, 65.41%; H, 3.33%; N, 15.83%; S, 12.30%.

Condensation of 2,2',3,3'-Tetrachloro-6,6'-Diquinoxalyl Ether and o-Aminothiophenol

Model Compound V. Freshly distilled *o*-aminothiophenol (0.2547 g., 0.002 mole) was added to a suspension of 2,2',3,3'-tetrachloro-6,6'-diquinoxalyl ether (0.4133 g., 0.001 mole) in 30 ml. of dimethylacetamide. The resulting mixture was stirred at room temperature for 1 hr. under nitrogen and it turned gradually into a clear solution. The solution was then heated at 120°C. for 1.5 hr. After cooling, it was poured into 800 ml. of dilute ammonium hydroxide to give a yellow solid which was separated, washed with water, extracted with benzene and finally heated at 230°C. for 4 hr. The tan solid thus obtained in 85% yield dissolved in dimethylacetamide, hexamethylphosphoramide, methanesulfonic acid and sulfuric acid, m.p. 325°C. (decomp.).

ANAL. Calcd. for $C_{28}H_{16}N_6S_2O$: C, 65.10%; H, 3.12%; N, 16.27%; S, 12.41%. Found: C, 65.31%; H, 3.15%; N, 15.99%; S, 12.11%.

Polymers

Condensation of 2,3,7,8-Tetrachloro-1,4,6,9-tetraazaanthracene and 4,6-Diamino-1,3-dithiophenol; Polymer I: Poly(12H-pyrazino[2',3':6,7]quinoxalino[2,3-b][1,4]benzothiazine-2,2:9,10-tetrayl-10-imino-9-thio)

In Dimethylacetamide. A suspension of 2,3,7,8-tetrachloro-1,4,6,9-tetraazaanthracene (1.5996 g., 0.005 mole) in 60 ml. of dimethylacetamide was heated at 120°C. overnight to give a clear solution. After cooling to room temperature, freshly prepared 2,5-diamino-1,3-dithiophenol (0.8614 g., 0.005 mole) was added to the solution. The reaction mixture immediately turned to a dark brown solution. It was stirred at room temperature for 2 hr. and then at 150°C. for 24 hr. under a nitrogen atmosphere. The resulting black reaction mixture was poured into 1 liter of dilute ammonium hydroxide in a blender to yield a black solid. This was washed with water and methanol several times and dried under reduced pressure. This compound was heated at 300°C. for 4 hr. under vacuum (0.3 mm. Hg.). After cooling to room temperature, it was washed with dilute ammonium hydroxide, water and methanol successively and subsequently extracted with benzene for 24 hr. A black powdery polymer with an inherent viscosity of 1.19 (0.2% in methanesulfonic acid at 30°C.) was obtained in 89% yield.

ANAL. Calcd. for $(C_{16}H_6N_6S_2)_n$: C, 55.48%; H, 1.75%; N, 24.26%; S, 18.51%. Found: C, 53.49%; H, 2.71%; N, 21.90%; S, 16.19%; residue, 0.51%.

In Polyphosphoric Acid. 4,6-Diamino-1,3-dithiophenol dihydrochloride (1.2260 g., 0.005 mole) and 2,3,7,8-tetrahydroxy-1,4,6,9-tetraazaanthracene (1.2310 g., 0.005 mole) were mixed in polyphosphoric acid at room temperature under a nitrogen stream. The reaction temperature was slowly raised to 240°C. over 2 hr. and maintained for 18 hr. The resulting black viscous reaction mixture, while hot, was poured into 1 liter of dilute ammonium hydroxide in a blender to yield a black solid. It was treated with warm dilute ammonium hydroxide (50–60°C.) for 2 days, subsequently extracted with boiling water for 5 days and finally with ethanol overnight. The black powdery residue weighed 1.35 g. (78% yield) after drying at 60°C. under reduced pressure. The inherent viscosity was 0.22 (0.2% in methanesulfonic acid at 30°C.).

ANAL. Found: C, 53.20%; H, 2.79%; N, 22.76%; S, 18.10%.

Condensation of 2,2',3,3'-Tetrachloro-6,6'-bisquinoxaline and 4,6-Diamino-1,3-dithiophenol; Polymer II: Poly(15H,17H-quinoxalino[2,3-b]quinoxalino[2',3':5,6][1,4]thiazino[3,2-g][1,4]benzothiazine-3, 11-diyl)

To a suspension of 2,2',3,3'-tetrachloro-6,6'-bisquinoxaline (1.3059 g., 0.0033 mole) in 50 ml. of dimethylacetamide was added freshly prepared 4,6-diamino-1,3-dithiophenol (0.5685 g., 0.0033 mole) at room temperature.

After stirring for 4 hr., the reaction mixture was heated at 150°C. for 24 hr. under a nitrogen stream. The cooled reaction mixture was poured into 1 liter of dilute ammonium hydroxide in a blender to precipitate a dark red solid. It was separated, washed with water and ethanol, and subsequently heated at 320°C. for 5 hr. under vacuum. The dark brown solid was washed with dilute ammonium hydroxide and water, followed by extraction with ethanol and benzene for 24 hr., respectively. The product thus obtained in 93% yield had an inherent viscosity of 1.47 (0.2% in methanesulfonic acid at 30°C.).

ANAL. Calcd. for $(C_{22}H_{10}N_6S_2)_n$: C, 62.54%; H, 2.39%; N, 19.89%; S, 15.18%. Found: C, 61.00%; H, 2.89%; N, 19.19%; S, 14.82%; residue, 0.40%.

Condensation of 2,2',3,3'-Tetrachloro-6,6'-diquinoxalyl Ether and 4,6-Diamino-1,3-dithiophenol; Polymer III: Poly(15H,17H-quinoxalino-[2,3-b]quinoxalino[2',3':5,6][1,4]thiazino[3,2-g][1,4]benzothiazine-3,11-diyl-11-oxo)

To a suspension of 2,2',3,3'-tetrachloro-6,6'-diquinoxalyl ether (2.0595 g., 0.005 mole) was added freshly prepared 4,6-diamino-1,3-dithiophenol (0.8614 g., 0.005 mole) at room temperature and the resulting mixture was stirred for 2 hr. under a nitrogen atmosphere followed by heating at 150°C. for 24 hr. The brown-red reaction mixture, after cooling, was treated as described in the preparation of polymer II. The inherent viscosity of the brown powdery polymer obtained in 90% yield was 1.25 (0.2% in methanesulfonic acid at 30°C.).

ANAL. Calcd. for $(C_{22}H_{10}N_6S_2O)_n$: C, 60.26%; H, 2.28%; N, 19.16%; S, 14.65%. Found: C, 58.67%; H, 2.66%; N, 18.71%; S, 13.75%; residue, 0.33%.

Condensation of 2,3,7,8-Tetrachloro-1,4,6,9-tetraazaanthracene and 3,3'-Dimercaptobenzidine; Polymer IV: Poly(14H,18H-benzo[1'',2'':5,6;5'',-4'':5',6']dipyrazino[2,3-b:2',3'-b']bis[1,4]benzothiazine-3,11-diyl)

In Dimethylacetamide. To a solution of 2,3,7,8-tetrachloro-1,4,6,9-tetraazaanthracene (0.9588 g., 0.003 mole) in 80 ml. of dimethylacetamide was added 3,3'-dimercaptobenzidine dihydrochloride (0.9637 g., 0.003 mole) at room temperature, and the resulting mixture was treated as described in the preparation of polymer II. The yield of black powdery polymer with an inherent viscosity of 1.37 (0.2% in methanesulfonic acid at 30°C.) was 98%.

ANAL. Calcd. for $(C_{22}H_{10}N_6S_2)_n$: C, 62.54%; H, 2.39%; N, 19.89%; S, 15.18%. Found: C, 61.04%; H, 2.54%; N, 19.09%; S, 14.57%; residue, 0.86%.

In Polyphosphoric Acid. A sample of 3,3'-dimercaptobenzidine dihydrochloride (1.3367 g., 0.0042 mole) was added to 50 g. of polyphosphoric acid and the mixture was warmed up to 100°C. under nitrogen. After evolution of hydrogen chloride gas ceased, 2,3,7,8-tetrachloro-1,4,6,9-tetraazaanthracene (1.3300 g., 0.0042 mole) was added to the mixture. The color of the

mixture immediately turned to dark blue and hydrogen chloride gas began to generate as the reaction temperature was raised slowly to 200°C. The reaction mixture was heated at this temperature for 24 hr. The resulting very viscous reaction mixture, while hot, was poured into 1 liter of water with vigorous stirring and neutralized with ammonium carbonate. A black precipitate was separated, stirred in 10% ammonium hydroxide at 60°C. for 1 day, and then extracted with boiling water for 4 days and then with ethanol overnight. The residue, after it was dried under reduced pressure, weighed 1.90 g. (90% yield). The black powdery polymer thus obtained dissolved in concentrated sulfuric acid and methanesulfonic acid and had an inherent viscosity of 0.94 (0.2% in concentrated sulfuric acid at 30°C.).

ANAL. Found: C, 60.03%; H, 3.00%; N, 17.97%; S, 13.80%; residue, 1.27%.

Condensation of 2,2',3,3'-Tetrachloro-6,6'-bisquinoxaline and 3,3'-Dimercaptobenzidine; Polymer V: Poly(3,3'-bi-12H-quinoxalino-[2,3-b][1,4]benzothiazine-8,8'-diyl)

To a suspension of 2,2',3,3'-tetrachloro-6,6'-bisquinoxaline (6.7511 g., 0.0017 mole) in 190 ml. of dimethylacetamide was added 3,3'-dimercaptobenzidine dihydrochloride (5.4665 g., 0.017 mole) at room temperature and the resulting mixture was treated in a similar way as described in the preparation of polymer II. A brown powdery polymer was obtained in 88% yield. This polymer was soluble in concentrated sulfuric acid and had an inherent viscosity of 1.49 (0.2% in concentrated sulfuric acid at 30°C.).

ANAL. Calcd. for $(C_{28}H_{14}N_6S_2)_n$: C, 67.46%; H, 2.83%; N, 16.85%; S, 12.86%. Found: C, 66.45%; H, 3.36%; N, 16.39%; S, 12.85%.

Condensation of 2,2',3,3'-Tetrachloro-6,6'-diquinoxalyl Ether and 3,3'-Dimercaptobenzidine; Polymer VI: Poly(3,3'-bi-12H-quinoxalino-[2,3-b][1,4]benzothiazine-8,8'-diyl-8'-oxy)

To a suspension of 2,2',3,3'-tetrachloro-6,6'-diquinoxalyl ether (1.2357 g., 0.003 mole) in 75 ml. of dimethylacetamide was added 3,3'-dimercaptobenzidine dihydrochloride (0.9635 g., 0.003 mole) at room temperature. The yellow turbid reaction mixture turned into orange-red clear solution while stirring. The polymerization and workup was carried out as described in the preparation of polymer II. The brown powdery polymer was obtained in 84% yield. The inherent viscosity was 1.54 (0.2% in methanesulfonic acid at 30°C.).

ANAL. Calcd. for $(C_{28}H_{14}N_6OS_2)_n$: C, 65.36%; H, 2.74%; N, 16.33%; S, 12.46%. Found: C, 62.83%; H, 3.00%; N, 15.85%; S, 12.04%; residue, 1.74%.

This work was supported by the Air Force Materials Laboratory, Research and Technology Division, Air Force Systems Command, Wright-Patterson Air Force Base, Ohio.

We are indebted to Dr. G. Ehlers, Air Force Materials Laboratory, Wright-Patterson Air Force Base, for the thermogravimetric curves.

We are indebted to Chemical Abstracts Service for the names of our polymers. The names were supplied by Kurt L. Loening and are based on proposed nomenclature rules

developed by the Nomenclature Committee of the Division of Polymer Chemistry, American Chemical Society, chairman, Robert B. Fox, U.S. Naval Research Laboratory, Washington, D.C. 20390.

References

1. H. Jadamus, F. De Schryver, W. De Winter, and C. S. Marvel, *J. Polymer Sci. A-1*, **4**, 2831 (1966).
2. F. De Schryver and C. S. Marvel, *J. Polymer Sci. A-1*, **5**, 545 (1967).
3. J. K. Stille and J. R. Williamson, *J. Polymer Sci. A*, **2**, 3867 (1964).
4. J. K. Stille, J. R. Williamson, and F. E. Arnold, *J. Polymer Sci. A*, **3**, 1013 (1965).
5. J. K. Stille and F. E. Arnold, *J. Polymer Sci. A-1*, **4**, 551 (1966).
6. J. K. Stille and E. Mainen, *J. Polymer Sci. B*, **4**, 39 (1966).
7. G. P. de Gaudermaris and B. T. Sillion, *J. Polymer Sci. B*, **2**, 203 (1965).
8. M. M. Tessler, *J. Polymer Sci. A-1*, **4**, 2521 (1966).
9. J. F. Brown, Jr., in *First Biannual American Chemical Society Polymer Symposium* (*J. Polymer Sci. C*, **1**), H. W. Starkweather, Ed., Interscience, New York, 1963, p. 83.
10. W. De Winter and C. S. Marvel, *J. Polymer Sci. A*, **2**, 5123 (1964).
11. S. G. Walter, R. Hubsch, and H. Pollak, *Monatsh. Chem.*, **33**, 186 (1933).
12. M. V. Likhoshesterov and A. A. Petrov, *J. Gen. Chem. USSR*, **3**, 783 (1933); *Chem. Abstr.*, **28**, 1677^a (1934).
13. C. Finzi and G. Grandolini, *Gazz. Chim. Ital.*, **89**, 2543 (1959).
14. F. D. Chattaway, *Chem. News*, **98**, 285 (1908).
15. Houben-Weyl, *Methoden der Organischen Chemie*, E. Müller, Ed., Georg Thieme, Stuttgart, 1955, Vol. IX, p. 39.

Received July 14, 1967

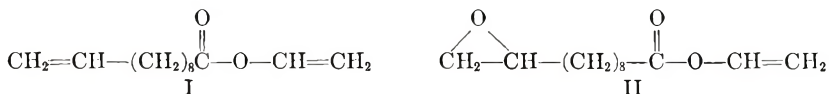
Preparation and Copolymerization of Vinyl 10,11-Epoxyundecanoate

ROBERTA C. L. CHOW and C. S. MARVEL,
Department of Chemistry, University of Arizona, Tucson, Arizona 85721

Synopsis

Vinyl 10,11-epoxyundecanoate has been copolymerized with vinyl chloride and vinyl acetate to give film-forming copolymers which are readily converted to insoluble materials.

It has been shown¹ that vinyl undecylenate (I) can be oxidized with peracetic acid to give vinyl 10,11-epoxyundecanoate (II).



The statement is made that such monomers polymerize normally for a vinyl ester, but no details are reported on the nature of the polymers or copolymers. Since undecylenic acid is readily available, and polymers and copolymers of the epoxy derivative are attractive because of the epoxy group, it was decided to reinvestigate this monomer (II).

Vinyl undecylenate was initially made available to us by Dr. T. H. Applewhite of the Western Utilization Research and Development Division, U.S. Department of Agriculture, and later some of the monomer was synthesized in our laboratory by transesterification of undecylenic acid by vinyl acetate.² Epoxidation of vinyl undecylenate³ with *m*-chloroperbenzoic acid in a weak basic medium gave a colorless liquid which analyzed satisfactorily for vinyl epoxyundecanoate. Isolation of the product was usually done by fractional distillation *in vacuo*. The oxirane content in the product which was determined by the hydrochloric acid-dioxane method⁴ was found to be 95-98% of the theory.

The presence of the epoxy grouping in the molecule was revealed by the appearance of an infrared absorption at 1257 cm.⁻¹, attributable to the C—O—C stretching frequency of epoxy ring^{5a} and chemically by the positive thiosulfate test. Some spectral data which lend support to the structure of vinyl 10,11-epoxyundecanoate are as follows. Infrared absorptions at 995 and 912 cm.⁻¹, presumably due to monoalkyl-substituted vinyl group, weakened considerably in going from the starting material to the

product, whereas absorptions at 953 and 874 cm^{-1} , due to the vinyl group bearing an acyloxy substituent, remained virtually unchanged.^{5b} Its NMR spectrum had among other things a quartet centered at 2.69 τ , integrated for one hydrogen which could be assigned to the vinylic hydrogen adjacent to the acyloxy group.⁶ These seemed to indicate that epoxidation had occurred across the $\text{C}_{10}=\text{C}_{11}$ double bond as one would expect.

Homopolymers of vinyl 10,11-epoxyundecanoate were prepared in emulsion systems. If the polymerization reaction is interrupted after about 2 hr. soluble polymers are obtained. Longer polymerization time gave insoluble material. If the soluble polymer is heated at 80°C. overnight it becomes insoluble. The infrared spectrum of the homopolymer showed absorption for the epoxy group at 1260 cm^{-1} .

Vinyl 10,11-epoxyundecanoate was copolymerized with vinyl chloride and vinyl acetate. Soluble copolymers of vinyl 10,11-epoxyundecanoate and vinyl chloride were easily obtained from a redox initiation system which consisted of ferrous sulfate, sodium pyrophosphate and benzoyl peroxide.⁷ Some examples of the copolymerization experiments are shown in Table I. These copolymers were stable at room temperature for a few days but became crosslinked when heated at elevated temperatures, treated with acids, or cured with amines.

Copolymers of vinyl 10,11-epoxyundecanoate and vinyl acetate which were prepared in an emulsion system with potassium persulfate or azobisisobutyronitrile as an initiator, were soluble in tetrahydrofuran and benzene when first isolated. These became crosslinked upon drying in air or *in vacuo*; they were then insoluble in *N,N*-dimethylformamide and did not melt below 210°C. Infrared spectra of the insoluble polymers had a weak absorption at 3630 cm^{-1} corresponding to O—H stretching

TABLE I
Copolymerization of Vinyl 10,11-Epoxyundecanoate (VEU) and Vinyl Chloride (VCl), with Redox Initiation^a

Run no.	Co-monomers charged		Time, hr.	Temp., °C.	Conversion, %	η_{inh}^b
	VEU, %	VCl, %				
COVEU-3	20	80	38.5	27	89	—
COVEU-3a	20	80	24	27	58	1.50
COVEU-4 ^c	10	90	35.5	27	70	1.14
COVEU-9	5	95	38.5	27	—	1.57

^a The redox recipe consisted of 1% ORR soap, 1% ferrous sulfate heptahydrate, 5% sodium pyrophosphate decahydrate, and 2% benzoyl peroxide.

^b Inherent viscosities were measured on 0.2% tetrahydrofuran solutions at 30°C.

^c The copolymer of run COVEU-4 was analyzed. Calcd. for 10.3% VEU and 89.7% VCl: C, 41.52%; H, 5.31%; Cl, 51.10%. Found: C, 41.95%; H, 5.60%; Cl, 51.70%.

TABLE II
Copolymerization of Vinyl 10,11-Epoxyundecanoate (VEU) with Vinyl Acetate (VAc)

Run no.	Comonomers Charged		Emulsifier ^a (1%)	Initiator ^b (1%)	Time hr.	Temp., °C.	Conversion, %	η_{inh}^c
	VEU, %	VAc, %						
COVEU-5	10	90	O	R	72	27	0	—
COVEU-20	5	95	S	P	2	60	59	1.89
COVEU-21	10	90	S	P	2	60	64	1.07
COVEU-22	20	80	S	P	2	60	54	—
COVEU-15	5	95	S	A	3	60	60	2.16
COVEU-23	10	90	S	A	2	60	54	1.75

^a O = ORR soap, S = Siponate DS-10.

^b R = redox system consisting of 1% ferrous sulfate heptahydrate, 5% sodium pyrophosphate decahydrate, and 2% benzoyl peroxide; P = potassium persulfate; A = azobisisobutyronitrile.

^c Inherent viscosities were measured on 0.2–0.7% tetrahydrofuran solutions at 30°C.

frequency which might be taken as evidence for the epoxy ring opening. A few examples of the copolymerization are listed in Table II.

Transparent films of soluble copolymers of both vinyl chloride and vinyl acetate were cast from tetrahydrofuran solutions. Those cast on glass plates peeled off readily whereas the ones cast on wood or copper sheets did not peel off. It was thought that epoxy polymers of the kind might be used as vehicles for paints.

EXPERIMENTAL

Preparation of Vinyl Undecylenate

In a 1-liter, three-necked, round-bottomed flask equipped with a stirrer and a condenser protected with a drying tube were placed 56 g. (0.283 mole) of undecenoic acid (Eastman Chemical, white label), 4 g. of mercuric acetate, 0.2 g. of copper resinate, and 700 ml. of freshly distilled vinyl acetate. The mixture was stirred until the solution had become homogeneous, when 0.5 ml. of concentrated sulfuric acid was added. The reaction was allowed to continue for 72 hr. at room temperature (ca. 27°C.). At the end of this period, 1.5 g. of sodium acetate was added to stop the reaction and the excess vinyl acetate and acetic acid which was generated in the reaction were distilled off under reduced pressure at temperatures below 50°C. The residue was taken up into 500 ml. of ether which was washed thoroughly with 2 liters of 2% sodium bicarbonate solution and water. After drying over anhydrous magnesium sulfate the solvent was removed on a Rotovap at room temperature. Vacuum distillation of the crude material in the presence of copper resinate through a 10-in. jacketed Vigreux column gave 42.6 g. (0.203 mole; 72%) of vinyl undecylenate which had a boiling point of 95–97°C./0.3 mm. and $n_D^{29} = 1.4440$ (lit.¹ b.p., 75–83°C./0.08 mm., $n_D^{30} = 1.4450$). Its infrared spectrum had the following characteristic absorptions: 3480w, 3120 (shoulder), 3070m, 2930s, 2860s, 2270w, 1765s, 1650s, 1460s, 1420m, 1360m, 1290m, 1230m, 1150s (broad), 995s, 953s, 912s, 874s, 724m, and 705w cm.^{-1} .

Epoxidation of Vinyl Undecylenate

In a 1-liter round-bottomed flask equipped with a magnetic stirrer and a dropping funnel protected with a drying tube were placed 20.5 g. (0.095 mole) of vinyl undecylenate, 25 g. of sodium bicarbonate, and 200 ml. of benzene. The mixture was stirred and maintained at 6–18°C. while a solution of 25 g. (0.145 mole) of *m*-chloroperbenzoic acid (FMC product) in 400 ml. of benzene was added dropwise over a period of ca. 80 min. The reaction was continued at room temperature for an additional 47 hr. Upon termination of the reaction, 10 g. of calcium hydroxide was introduced to neutralize the excess peracid, and the mixture was again stirred for a few hours. It was then filtered off the solid material, and the filtrate was washed with 2 liters of 2% sodium carbonate solution and water and

dried over magnesium sulfate. Removal of the solvent under reduced pressure left behind 19.1 g. (0.0845 mole; 89%) of vinyl 10,11-epoxyundecanoate which had $n_D^{30} = 1.4640$, oxirane oxygen being $98 \pm 0.5\%$ of theory. The epoxy oxygen content was determined by the hydrochloric acid-dioxane procedure;⁴ the endpoint was determined with a pH meter. For the use in copolymerization experiments vinyl 10,11-epoxyundecanoate was further purified by fractional distillation in the presence of copper resinate on a spinning band column *in vacuo*. A 35% yield was obtained because the remaining portion polymerized on heating to give insoluble polymers. The physical data of the distilled product varied slightly from run to run according to the oxirane oxygen content. For example, a typical sample containing $98.3 \pm 0.3\%$ of oxirane oxygen had a boiling point of $103^\circ\text{C./0.25 mm.}$ to $107^\circ\text{C./0.4 mm.}$, and $n_D^{30} = 1.4511$ (lit.:¹ b.p., $101^\circ\text{C./0.2 mm.}$, $n_D^{30} = 1.4509$, oxirane oxygen, 90%). The infrared spectrum of this sample was characterized by the following absorptions: 3480w, 3080w, 3040w, 1770s, 1650m, 1470m, 1420w, 1380w, 1350w, 1294w, 1257w, 1148s, 990w, 950s, 917w, 870s, 834w, and 723w cm.^{-1} . The NMR spectrum exhibited the following signals (τ): a quartet centered at 2.69 (1 H for $\text{CO}_2\text{—CH=}$), a multiplet at 5.30 (2 H, $\text{CO}_2\text{—CH=CH}_2$), a multiplet at 7.40 (3 H, the epoxy ring protons), a triplet at 7.70 (2 H, methylene protons adjacent to the ester function) and a singlet at 8.62 (14 H, for the rest of the methylene protons). A thin-layer chromatogram of the sample on alumina, eluted with carbon tetrachloride, showed a spot at $r_f = 0.70$ and a rather faint line at $r_f = 0.84$ which did not correspond to the starting material.

ANAL. Calcd. for $\text{C}_{13}\text{H}_{22}\text{O}_3$: C, 69.03%; H, 9.73%. Found: C, 69.00%; H, 9.79%.

Homopolymerization

In a typical run 0.02 g. of potassium persulfate, 0.02 g. of Siponate DS-10, 1.0 g. of vinyl 10,11-epoxyundecanoate and 5 ml. of buffer solution of pH 7 (Beckman Buffer Solution, 3501) were charged under nitrogen to a pressure tube (1 \times 4 in.) fitted with a bottle cap of neoprene rubber lining. The polymerization tube was tumbled end-over-end in a water bath at 60°C. for 2 hr. Upon termination of the reaction, the content was poured into a saturated sodium chloride solution to coagulate the suspended polymer. This was isolated and washed with water and methanol thoroughly and dissolved in 50 ml. of tetrahydrofuran (THF) which was then filtered. To the filtrate was added about 100 ml. of benzene to form an azeotropic mixture with water; these were then removed *in vacuo*. There was obtained 0.41 g. (41%) of the purified material whose inherent viscosity measured on a 0.2 g./100 ml. of THF solution at 30°C. was 0.31. Its infrared spectrum differed from that of the monomer in that absorptions at 3080, 1650, 950, and 870 cm.^{-1} , presumably due to the vinyl group, had disappeared or diminished considerably after the reaction. That the

epoxy group remained intact during the polymerization was revealed by the absorption at 1260 cm.^{-1} . The homopolymer was insolubilized upon heating at 80°C. overnight. In another experiment where azobisisobutyronitrile was used as an initiator, the polymerization was allowed to proceed to nearly completion which took 19 hr. at 60°C. ; the polymer thus obtained was partially insoluble in THF. The soluble fraction had an inherent viscosity of 0.16 in THF at 30°C.

ANAL. Calcd. for $(\text{C}_{13}\text{H}_{22}\text{O}_3)_n$: C, 69.03%; H, 9.73%. Found: C, 67.20%; H, 9.83%.

Copolymerization

The polymerization vessels were pressure tubes (1.5×7 in.) each fitted with a bottle cap lined with neoprene rubber.

Redox Initiation. As an example, copolymerization of vinyl 10,11-epoxyundecanoate and vinyl chloride was conducted as follows. Ferrous sulfate heptahydrate (0.04 g.), 0.04 g. of ORR soap (sodium stearate, sodium palmitate, and sodium oleate) and 0.2 g. of sodium pyrophosphate decahydrate were weighed into a pressure tube. Deaerated water (20 ml.) and 0.8 g. of vinyl 10,11-epoxyundecanoate were added subsequently, and the polymerization tube was chilled at -78°C. Vinyl chloride was trapped in excess and was allowed to boil down to 3.2 g., thus removing air from the vapor space. Benzoyl peroxide (0.08 g.) was introduced into the reaction mixture immediately before the tube was capped. The polymerization was conducted at room temperature with mechanical shaking for some 30 hr. At the end of the polymerization the contents were poured into a beaker of distilled water. It was filtered and washed thoroughly with water and methanol. The polymer was purified by reprecipitations from tetrahydrofuran and methanol and was dried in a vacuum oven at room temperature.

Radical Initiation. Copolymerization of vinyl acetate and vinyl 10,11-epoxyundecanoate was carried out in this same general manner. Vinyl acetate (3.8 g.), 0.2 g. of vinyl 10,11-epoxyundecanoate, 0.04 g. of α,α' -azobisisobutyronitrile, 0.04 g. of Saponate DS-10 (sodium dodecylbenzene sulfonate), and 20 ml. of oxygen-free buffer solution of pH 7 (Beckman pH solution, 3501) were charged under nitrogen in a polymerization tube which was capped and was tumbled end-over-end in a $60 \pm 1^\circ\text{C.}$ bath for 3 hr. The reaction mixture was frozen to coagulate the polymer which was then filtered and washed thoroughly with water. Attempted purification of the copolymer by reprecipitation from tetrahydrofuran and water, followed by drying in a vacuum oven at room temperature, led to cross-linking of the polymer. In another experiment, the polymer was dissolved in a large volume (ca. 400 ml.) of benzene, an azeotropic distillation *in vacuo* removed the last trace of water, and the polymer was then freeze-dried. Soluble polymers have been obtained by the freeze-drying technique when care was taken to maintain the temperature below 0°C. at all

times. The copolymers prepared with the initiation of potassium persulfate seemed to be even less stable; they became partially insoluble on freeze-drying.

This is a partial report of work done under contract with the Western and Southern Utilization Research and Development Divisions, Agricultural Research Service, U.S. Department of Agriculture, and authorized by the Research and Marketing Act of 1946. The contract is supervised by Dr. Glenn Fuller of the Western Division.

We are indebted to Dr. J. R. Sowa for his preliminary studies on the epoxidation of vinyl undecylenate.

References

1. F. C. Frostick, Jr., B. Phillips, and P. S. Starcher, *J. Am. Chem. Soc.*, **81**, 3350 (1959).
2. R. L. Adelman, *J. Org. Chem.*, **14**, 1057 (1949).
3. J. R. Sowa, private communication.
4. S. Siggia, *Quantitative Organic Analysis via Functional Groups*, 3rd Ed., Wiley, New York, 1963, p. 241.
5. L. J. Bellamy, *The Infrared Spectra of Complex Molecules*, 2nd Ed., Wiley, New York, 1964, (a) p. 118; (b) p. 49.
6. L. M. Jackman, *Applications of Nuclear Magnetic Resonance Spectroscopy in Organic Chemistry*, Pergamon Press, London, 1959, p. 61.
7. C. S. Marvel, R. Deanin, C. G. Overberger, and B. Kuhn, *J. Polymer Sci.*, **3**, 128 (1948).

Received June 30, 1967

Revised August 25, 1967

Polymers from the Vinyl Ester of Dehydroabiatic Acid

WAKICHI FUKUDA and C. S. MARVEL, *Department of Chemistry, University of Arizona, Tucson, Arizona 85721*

Synopsis

The vinyl ester of dehydrogenated abiatic acid has been homopolymerized, copolymerized with vinyl chloride, vinyl acetate, and butadiene and terpolymerized with styrene and acrylonitrile. Both in the homopolymerization and the copolymerization, the vinyl ester of dehydroabiatic acid has given lower molecular weight polymers than were obtained with the vinyl ester of tetrahydroabiatic acid. Polymers containing the vinyl ester of dehydroabiatic acid can be readily crosslinked with peroxide.

INTRODUCTION

In continuation of the studies on the preparation of polymers containing terpenes and various terpene derivatives,¹⁻⁸ vinyl dehydroabietate has been investigated and compared with vinyl tetrahydroabietate. Polymers containing the vinyl ester of tetrahydroabiatic acid were found to be readily crosslinked with peroxide.¹ As dehydroabiatic acid contains a substituted aromatic ring not present in tetrahydroabiatic acid, it is interesting to learn the effect this may have on the vinyl ester polymerization and the properties of polymers obtained as compared to those from vinyl tetrahydroabietate.

RESULTS AND DISCUSSION

Monomer

The dehydroabiatic acid was prepared by the dehydrogenation and disproportionation of commercial resin.⁹ The vinyl ester was prepared by vinyl interchange with vinyl acetate in the presence of mercuric sulfate as a catalyst.¹⁰

The vinyl ester of dehydroabiatic acid (VDA) was supplied as a water-clear, very viscous oil inhibited with copper resinate. This monomer solidified upon cooling and could be recrystallized from *n*-pentane and ethyl alcohol. It had the following physical constants: b.p. 149°C./0.08 mm. Hg, m.p. 44-45°C., and n_D^{20} 1.5345 (supercooled oil). Thin-layer chromatography of the vinyl ester on silica gel showed one spot with *n*-heptane containing 4% diethyl ether as an eluent. Infrared spectra showed absorption bands characteristic for vinyl dehydroabietate at 3040, 3010, 1610, 1495, 1090, 820, 720, and 625 cm.⁻¹. The monomer has a good

shelf life under nitrogen at room temperature. Distillation without inhibition under reduced pressure led to the formation of a small amount of polymer. The monomers used were redistilled under reduced pressure in the presence of copper resinate. In two instances the monomer was recrystallized prior to use.

Homopolymerization

VDA has been homopolymerized in bulk, solution and emulsion systems. The experimental data are given in Table I. The polymers from the three systems were obtained as white powders. The lower conversion and lower inherent viscosities showed poorer polymerizability as compared to vinyl tetrahydroabietate. The infrared spectra of the polymers indicated absorption bands characteristic for a substituted aromatic ring at 1495, 820, and 625 cm.^{-1} . These bands could also be seen in the monomer.

TABLE I
Homopolymers of VDA^a

Run no.	System	Catalyst		Con- version, %	η_{inh}^c
		Type ^b	Content, %		
1	Bulk	AIBN	5	54	0.066
2	Bulk	DEABIB	5	37	0.068
3	Solution ^d	AIBN	5	23	0.045
4	Solution ^d	DEABIB	5	30	0.046
5	Emulsion ^e	AIBN	5	51	0.056 ^f
6	Emulsion ^e	DEABIB	5	44	0.065
7	Emulsion ^e	K ₂ S ₂ O ₈	5	33	0.055
8 ^g	Emulsion ^e	K ₂ S ₂ O ₈	5	46	0.057
9	Emulsion ^e	K ₂ S ₂ O ₈	2.5	4	0.052
10 ^g	Emulsion ^e	K ₂ S ₂ O ₈	2.5	6	0.060

^a All of the polymerizations were conducted at $60 \pm 2^\circ\text{C}$. by tumbling the tubes end-over-end for 48 hr. and with 4.0 g. of monomer.

^b AIBN = azobisisobutyronitrile; DEABIB = diethylazobisisobutyrate.

^c Determined on a solution of 0.400–0.410 g./100 ml. of tetrahydrofuran at 30°C .

^d Benzene (12 ml.) was used as a solvent.

^e Air-free distilled water (12 ml.), and 1% of Siponate DS-10 were used.

^f Calcd. for C₂₂H₃₀O₂: C, 80.93%; H, 9.26%. Found for monomer: C, 80.94%; H, 9.39%. Found for this polymer: C, 80.78%; N, 9.25%.

^g Recrystallized monomer was used.

Because of the tertiary hydrogens, curing of the bulk homopolymer was investigated as compared to the homopolymer of vinyl tetrahydroabietate. If the curing compositions contained 10% of dicumyl peroxide (Di-Cup, Hercules Powder Company, 96–99% pure) or more, completely insolubilized materials were produced within 30 min. at 160°C . This result was the same as shown in the homopolymer of vinyl tetrahydroabietate. The cured materials were brittle.

TABLE II
Emulsion Copolymers of VTA with VDA^a

Run no.	Charged composition		Conversion, %	η_{inh}^b	Analysis (found)		Composition ^c	
	VTA, wt.-%	VDA, wt.-%			C, %	H, %	VTA, %	VDA, %
12	75	25	70	0.103	79.76	10.37	67	33
13	65	35	64	0.091	80.07	10.32	59	41
14	50	50	60	0.085	80.42	10.08	42	58
15	38	62	57	0.073	80.35	9.83	37	63

^a All of the polymerizations were conducted at $60 \pm 2^\circ\text{C}$. by tumbling the tubes end-over-end for 48 hr. and with 4.0 g. of total monomers, 12 ml. of air-free distilled water, 0.04 g. of Saponate DS-10 as emulsifier, and 0.2 g. of AIBN as catalyst.

^b Determined on solutions of 0.400-0.404 g./100 ml. of tetrahydrofuran at 30°C .

^c Based on analysis for C, H in the copolymer.

TABLE III
 Emulsion Copolymers of Vinyl Chloride with VDA^a

Run no.	Charged composition			Conversion, %	η_{inh}^b	Analysis (found)			Composition ^c	
	VCl, wt.-%	VDA, wt.-%				C, %	H, %	Cl, %	VCl, %	VDA, %
17	96	4		92	0.90	5.06	55.79	97	3	
18	91	9		88	0.61	5.40	53.04	91	9	
19	78	22		79	0.53	6.13	42.55	73	27	
20	70	30		61	0.40	6.26	38.24	68	32	
21	59	41		53	0.29	6.52	36.11	63	37	
22	50	50		35	0.20	6.40	33.25	59	41	
23	38	62		44	0.10	7.36	23.60	41	59	

^a All of the polymerizations were conducted at $60 \pm 2^\circ\text{C}$. by tumbling the tubes end-over-end for 48 hr. and with the use of 5.0 g. of total monomers, 0.1 g. of Siphonate DS-10 as emulsifier, 0.1 g. of potassium persulfate as catalyst, and 15 ml. of air-free distilled water.

^b Determined on solutions of 0.296-0.382 g./100 ml. of tetrahydrofuran at 30°C .

^c Based on analysis for C, H, and Cl in the copolymer.

Copolymerization

Vinyl Tetrahydroabietate-VDA Copolymers. A set of vinyl tetrahydroabietate and VDA copolymers was prepared to see whether some special properties may be obtained in the copolymer. The experimental data are given in Table II. All of the copolymers were white powders and formed transparent, very brittle films as did both of the homopolymers. Conversions and inherent viscosities were linearly reduced with increase of VDA in the charged composition.

Vinyl Chloride-VDA Copolymers. Emulsion copolymers of vinyl chloride and VDA were prepared. The experimental data are given in Table III. The per cent ester incorporated was calculated from the percentage of C and Cl in the copolymer. Copolymers were obtained as white or light tan powders soluble in tetrahydrofuran and could be molded into

TABLE IV
Fractionation Data of VCl-VDA Copolymer^a

Sample	Weight		Cl, %	VDA, wt.-% ^b	η_{inh}^c
	g.	%			
Entire sample	2.00		42.55	27	0.53
Fraction 1	0.61	30.6	44.74	21	1.39
Fraction 2	0.13	6.5	39.48	29	0.32
Fraction 3	0.70	34.9	43.71	23	0.29
Fraction 4	0.19	9.4	42.61	25	0.28
Fraction 5	0.28	14.1	40.31	28	0.13
Total recovered	1.91	95.5			

^a The fractionation was conducted at room temperature with the use of tetrahydrofuran as solvent and methanol as nonsolvent.

^b Based on analysis for C, H, and Cl in the copolymer.

^c Determined on solutions of 0.391-0.417 g./100 ml. of tetrahydrofuran at 30°C.

transparent films at about 160°C. A tough copolymer could be obtained when the VDA in the charged composition was 4% or less. All other compositions gave colored brittle films.

In order to get information on the homogeneity of vinyl chloride-VDA copolymer, fractionation of the 73/27 copolymer (run 19, Table III) was conducted. The fractionation data are given in Table IV. It is noted that the homogeneous copolymer was produced in spite of the considerable difference in the r_1r_2 value of the vinyl ester and vinyl chloride. The homogeneity of vinyl chloride-VDA copolymer is significantly different from vinyl chloride-vinyl tetrahydroabietate copolymer.¹ The molecular weight distribution of the VDA copolymer was broad and one-third of the copolymer had as high an inherent viscosity as the vinyl chloride homopolymer. The recovery in the fractionation was 95.5%, and the greatest unrecovered portion seemed to be a copolymer having a very low inherent viscosity which was washed out with the methanol.

Vinyl Acetate-VDA Copolymers. Two sets of vinyl acetate and VDA copolymers were prepared by using AIBN and potassium persulfate as initiators.

Emulsion copolymerizations of vinyl acetate and VDA with AIBN have been conducted in five compositions. The experimental data are given in Table V. All of the copolymers were obtained as snow-white powders, soluble in tetrahydrofuran and toluene. They formed transparent, very brittle films. Inherent viscosities of copolymers were higher than that of the VDA homopolymer, but were not so high as to show a good mechanical property.

TABLE V
Emulsion Copolymers of Vinyl Acetate with VDA with AIBN Catalyst^a

Run no.	Charged composition		Conversion, %	η_{inh}^b	Analysis (found)		Composition ^c	
	VAc, wt.-%	VDA, wt.-%			C, %	H, %	VAc, %	VDA, %
24	80	20	72	0.32	61.79	7.49	76	24
25	68	32	67	0.22	65.35	7.97	62	38
26	57	43	60	0.18	68.16	8.09	51	49
27	50	50	43	0.16	70.13	8.38	43	57
28	40	60	37	0.14	72.31	8.61	34	66

^a All of the copolymerizations were conducted at $60 \pm 2^\circ\text{C}$. by tumbling the tubes end-over-end for 48 hr. and with the use of 2% of Siponate DS-10 as emulsifier and 4% of AIBN as catalyst.

^b Determined on solutions of 0.402-0.416 g./100 ml. of tetrahydrofuran at 30°C .

^c Based on analysis for C,H in the copolymer.

The intensity of infrared absorption bands characteristic for VDA was consistent with the content of VDA in copolymer based on C,H analysis.

Some emulsion copolymers of vinyl acetate and VDA were prepared with the use of potassium persulfate as a catalyst. The experimental data are given in Table VI.

All of the copolymers were obtained as white powders or light tan materials soluble in tetrahydrofuran and chloroform. However, insoluble polymers were obtained when prolonged polymerizations were conducted with 10% or less VDA in the charged composition.

Butadiene-VDA Copolymers. Several different emulsion copolymers of butadiene-VDA have been made. The experimental data are given in Table VII. As the chain-transfer activity of VDA was assumed to be sufficient, no chain-transfer agent was used in the copolymerization. The copolymers were obtained as white or light tan rubbery crumbs with one exception, in which the copolymer was obtained as tacky material by unbuffered copolymerization of a butadiene-VDA 20/80 charged composition. Most of the copolymers were not completely soluble in hot tetrahydrofuran, benzene, or mixtures of both solvents. All of the soluble

TABLE VI
Emulsion Copolymers of Vinyl Acetate with VDA with Potassium Persulfate Catalyst^a

Run no.	Charged composition		Polymerization Time, hr.	Conversion, %	η_{inh}^b	Analysis (found)		Composition ^c	
	VAc, wt.-%	VDA, wt.-%				C, %	H, %	VAc, %	VDA, %
30	96	4	5	87	1.13	57.21	7.18	94	6
32	90	10	5	74	0.70	58.94	7.29	88	12
34	84	16	48	74	0.60	60.72	7.61	80	20
35	71	29	48	77	0.25	64.71	7.94	65	35
36	59	41	48	69	0.19	68.51	8.30	49	51
37	50	50	48	58	0.16	71.24	8.51	38	62
38	39	61	48	48	0.12	73.74	8.73	28	72

^a All of the polymerizations were conducted at $60 \pm 2^\circ\text{C}$. by tumbling the tubes end-over-end, and with the use of 2% of Siponate DS-10 as emulsifier, and 5.0 g. of total monomers.

^b Determined on solutions of 0.052–0.416 g./100 ml. of tetrahydrofuran at 30°C .

^c Based on analysis for C,H in the copolymer.

TABLE VII
 Butadiene-VDA Copolymers^a

Run no.	Charged composition		Conversion ^b %	Soluble part, ^e wt.-%	η_{inh}^d	Analysis (found)		Composition ^e	
	BD, wt.-%	VDA, wt.-%				C, %	H, %	BD, %	VDA, %
40	90	10	83	12	0.32	88.53	10.74	96	4
41	80	20	86	32	0.64	87.87	10.93	88	12
42	60	40	60	26	0.58	87.16	10.89	79	21
43	60	40	48 ^f	58	0.54	87.65	11.03	85	15
44	51	49	55	21	0.50	87.28	10.84	80	20
45	41	59	42	17	0.36	86.83	10.81	75	25
46	31	69	23	25	0.38	86.01	10.82	6	35
47	20	80	13	23	0.38	82.65	11.03	23	77

^a All of the polymerizations were conducted at $60 \pm 2^\circ\text{C}$. by tumbling the tubes end-over-end for 48 hr. and with the use of 5.0 g. of total monomers, 2% of potassium persulfate as catalyst, and 2% of Siponate DS-10 as emulsifier.

^b In the buffered system of pH = 7.00.

^c Soluble in hot tetrahydrofuran.

^d Determined on solutions of 0.089-0.572 g./100 ml. of tetrahydrofuran at 30°C .

^e Based on analysis for C, H in the copolymer.

^f Unbuffered.

part of the copolymers, however, indicated about the same or higher inherent viscosities as compared to a sample of polybutadiene.

In view of the reactivities of both monomers, the amount of butadiene in the copolymer was larger than that of charged butadiene. It was shown that VDA was more difficult to incorporate in the copolymer with butadiene as compared to vinyl tetrahydroabietate.¹ Though the fractionation could not be done for these copolymers, the infrared spectrum of both soluble and insoluble parts showed that compositions containing both components were obtained.

As consistent with all of the existing butadiene copolymer literature, the infrared spectra of copolymers appeared to contain a high 1,4-*trans* structure (characteristic absorption bands for out-of-plane vibration of hydrogen attached to the double bond at 967, 1355 cm^{-1}).^{11,12} The determination of internal unsaturation for the soluble fraction of the copolymers were conducted according to the titration with perbenzoic acid.^{3,13} The titration data are given in Table VIII. These data indicated a high 1,4-adduct being in accord with the infrared data.

TABLE VIII
Amount of Internal Unsaturation in BD-VDA Copolymers

Run no.	Composition		Copolymer containing 1 eq. of unsaturation, g.	Internal unsaturation, %	Ratio 1,4/1,2
	BD, wt.-%	VDA, wt.-%			
41	88	12	89	69	69/31
43	85	15	67	93	93/7
42	79	21	83	82	82/18
44	80	20	81	84	84/16
45	75	25	109	66	66/34
46	65	35	92	90	90/10

Styrene-Acrylonitrile-VDA Terpolymers. Five emulsion terpolymers of varying compositions were prepared in order to study the copolymerization of styrene-acrylonitrile-VDA composition. The experimental data are given in Table IX.

All of the terpolymers were obtained as white powders, soluble in *N,N*-dimethylformamide but only slightly soluble in tetrahydrofuran. The terpolymers could be molded into transparent but brittle films at about 180°C.

EXPERIMENTAL

Standard polymer-forming reactions were used for the homopolymerization and copolymerizations. The methods in general were those used in the work on vinyl tetrahydroabietate.¹

TABLE IX
 Styrene-Acrylonitrile-VDA Terpolymers^a

Run no.	Charged composition			Con- version, %	η_{inh}^b	Analysis (found)			Composition ^c		
	VDA, wt.-%	Styrene, wt.-%	Acrylo- nitrile, wt.-%			C, %	H, %	N, %	VDA, %	AN, %	St, %
48	10	60	30	90	4.32	83.38	7.06	8.32	12	31	57
49	20	50	30	81	3.12	82.48	7.15	9.07	13	34	53
50	30	40	30	73	1.96	80.62	6.96	9.93	20	38	42
51	40	30	30	56	2.37	79.87	7.40	10.87	21	41	38
52	50	20	30	67	1.47	77.66	7.31	10.44	43	40	17

^a All of the polymerizations were conducted at $60 \pm 2^\circ\text{C}$. by tumbling the tubes end-over-end for 24 hr. and with the use of 5.0 g. of total monomers, 2% of potassium persulfate as catalyst, and 2% of Siponate DS-10 as emulsifier.

^b Determined on solutions containing 0.330-0.404 g./100 ml. of *N,N*-dimethylformamide.

^c Based on analysis for C, H, and N in the polymer.

This is a partial report of work done under contract with the Western and Southern Utilization Research and Development Division, Agricultural Research Service, U.S. Department of Agriculture and authorized by the Research and Marketing Act. The contract is supervised by Dr. Glenn Fuller of the Western Division.

We are indebted to Dr. Glen W. Hedrick for furnishing the vinyl dehydroabietate, Mr. Noah Halbrook for preparation of pure dehydroabietic acid, and Mr. John Lewis for synthesis of vinyl dehydroabietate, all of the Naval Stores Research Laboratory of the Southern Utilization Research and Development Division of the Agricultural Research Service, U.S.D.A., Olustee, Florida.

References

1. R. Liepins and C. S. Marvel, *J. Polymer Sci. A-1*, **4**, 2003 (1966).
2. J. R. Sowa and C. S. Marvel, *J. Polymer Sci. B*, **4**, 431 (1966).
3. R. W. Magin, C. S. Marvel, and E. F. Johnson, *J. Polymer Sci. A*, **3**, 3815 (1965).
4. C. S. Marvel, R. A. Malzahn, and J. L. Comp, *J. Polymer Sci. A*, **3**, 961 (1965).
5. M. Modena, R. B. Bates, and C. S. Marvel, *J. Polymer Sci. A*, **3**, 949 (1965).
6. R. A. Malzahn, J. H. Griffith, C. S. Marvel, G. W. Hedrick, J. B. Lewis, C. R. Mobley, and F. C. Magne, *J. Polymer Sci. A*, **2**, 5047 (1964).
7. T. Shono and C. S. Marvel, *J. Polymer Sci. A*, **1**, 1543 (1963).
8. C. S. Marvel, J. R. Hanley, Jr., and D. T. Longone, *J. Polymer Sci.*, **40**, 551 (1959).
9. N. J. Halbrook and R. V. Lawrence, *J. Org. Chem.*, **31**, 4246 (1966).
10. J. B. Lewis and G. W. Hedrick, *J. Polymer Sci. A-1*, **4**, 2026 (1966).
11. J. L. Binder, *J. Polymer Sci. A*, **1**, 47 (1963).
12. D. O. Hummel, *Infrared Spectra of Polymers*, Interscience, New York, 1966, p. 15.
13. I. M. Kolthoff, T. S. Lee, and M. A. Mairs, *J. Polymer Sci.*, **2**, 206, 220 (1947).

Received September 11, 1967

Monomer Reactivity Ratios for the Copolymerization of Styrene with 1,2,4-Trivinyl and *p*-Divinylbenzenes

RICHARD H. WILEY and TAE-OAN AHN, *Graduate Division, Hunter College, The City University of New York, New York, New York 10021*

Synopsis

The copolymerization kinetics of 1,2,4-trivinylbenzene (TVB) with styrene do not clearly resemble those of *o*-, *m*-, or *p*-divinylbenzene (DVB), structural elements of which are present in TVB. A control determination of the reactivity ratios for the styrene-*p*-DVB pair under different conditions (70°C., pre-gel point conversion), run for comparison with the TVB data, show values ($r_1 = 0.77$; $r_2 = 1.46$) similar to those previously recorded ($r_1 = 0.77$; $r_2 = 2.08$).

In the preceding reports¹⁻³ we have described the copolymerization characteristics of *p*-, *m*-, and *o*-divinylbenzenes and commented on the significance of their differences. Briefly, the styrene (St)-*p*-DVB system gives values of $r_1 = 0.77$ and $r_2 = 2.08$; the St-*m*-DVB system gives values of $r_1 = 0.605$ and $r_2 = 0.88$; and the St-*o*-DVB system gives values of $r_1 = 0.94$ and $r_2 = 0.99$. For the system with *o*-DVB, noncross-linked copolymers are obtained, based on their solubility. They appear to have approximately one double-bond per DVB unit, based on the infrared absorption characteristics.⁴ This peculiar behavior of *o*-DVB indicates that the two vinyl groups therein are nonplanar, as is consistent with the NMR data for the isomers,⁵ and that one of the vinyl groups does not copolymerize. On this basis, 1,2,4-TVB might presumably copolymerize 1,3-(*meta*) or 1,4-(*para*) leaving the *ortho* vinyl group unreacted; the reactivity ratio values should distinguish which of the two behavior types predominates.

We have now studied the copolymerization kinetics of the St-1,2,4-TVB system and report its apparent uniqueness as compared to DVB systems. The kinetics were followed by using ¹⁴C-labeled styrene and analysis techniques described previously^{1,4} at 70°C. Since this is a lower temperature than those (80, 100°C.) used before for our studies of such systems, we have repeated the St-DVB determinations at this temperature (70°C.). Also, we have stopped this set of copolymerizations (both DVB and TVB) at incipient gel formation instead of at an arbitrary low conversion. The conversion at this point is about 2-5% and varies with the amount of divinylbenzene present. Since conversion percentages are

difficult to measure accurately in these systems, we feel that gel point termination may offer improved reproducibility.

Under these conditions (70°C., incipient gel formation conversions) the copolymerization plots show values of $r_1 = 0.77$ and $r_2 = 1.46$ for the St-*p*-DVB systems (Fig. 1). These agree reasonably well with values (0.77, 2.08) observed previously under slightly different conditions. The data for the St-1,2,4-TVB system do not provide a definitive solution for the copolymerization equation (Fig. 2). If the sets of data for high concentration of TVB are set aside, the values obtained from the remaining sets of data are $r_1 = 1.80$ and $r_2 = 1.12$. These values do not closely resemble those of any of the three DVB isomers.

It can be concluded, therefore, that TVB does not copolymerize as either a *m*- or as a *p*-DVB with an inert *o*-DVB vinyl unit. It can also be concluded that the primary gel network units, to the extent that they are determined by kinetically controlled distributions of the crosslinking units, are different and distinguishable in the three systems.

EXPERIMENTAL

Monomers

Styrene- β - ^{14}C , supplied by Tracerlab Inc., having a specific activity of 0.17 mc./mmole, was diluted as previously² described with 150 volumes of freshly diluted styrene (n_D^{20} 1.5465) and was stored at -20°C. with 2,6-di-*tert*-butyl-*p*-cresol as stabilizer. *p*-Divinylbenzene was separated by preparative gas chromatography from a sample about 90% pure *para* supplied by Cosden Chemical Co. by the procedure described previously.⁶ Gas-chromatographic analysis showed that the sample was 99+ % pure. Trivinylbenzene prepared as previously described,^{7,8} and the isomeric

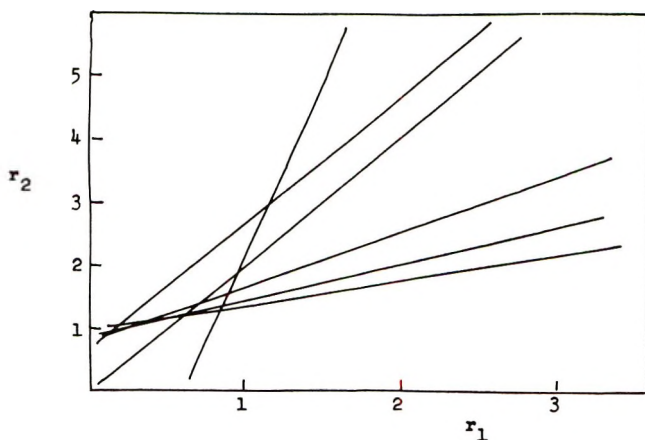


Fig. 1. Intersect plot for the copolymerization of styrene ($r_1 = 0.77$) and *p*-divinylbenzene ($r_2 = 1.46$) at 70°C. with benzoyl peroxide initiator and conversion to incipient gel formation.

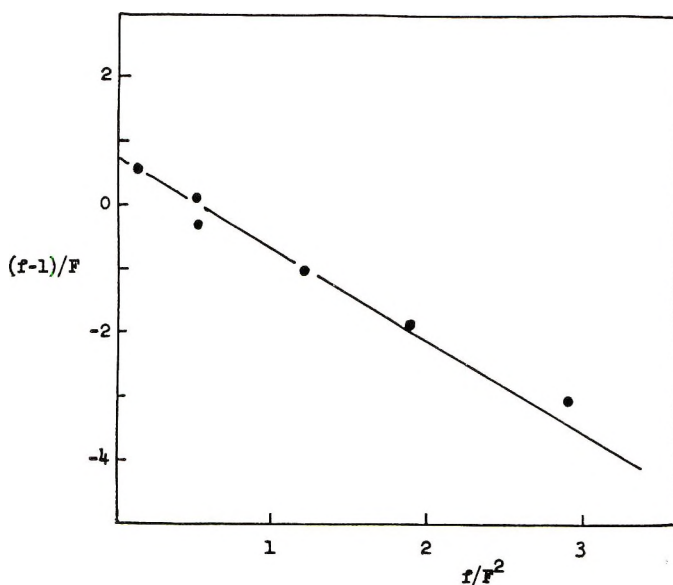


Fig. 2. Fineman-Ross plot for the copolymerization of styrene ($r_1 = 0.77$) and *p*-divinylbenzene ($r_2 = 1.46$) at 70°C. with benzoyl peroxide initiator and conversion to incipient gel conversion.

mixture of 1,2,4- and 1,3,5-trivinylbenzene was separated by preparative gas chromatography.⁸ Gas-chromatographic analysis showed that the sample was 99.8+ % 1,2,4-trivinylbenzene with 0.2% or less of 1,3,5-trivinylbenzene.

Copolymerization

The monomer mixture was prepared by vacuum line techniques previously used.²⁻⁴ The copolymerizations were carried out at $70 \pm 0.1^\circ\text{C}$. in a water bath with 0.1 wt.-% of dibenzoyl peroxide as initiator and were stopped at incipient gelation to give yields of 2.0–5.2%. The precipitated copolymer was swollen with benzene and methanol-washed three to five

TABLE I
Monomer Feed Composition in Copolymerization of Styrene (M_1) and *p*-Divinylbenzene (M_2) at 70°C.

Expt. no.	Monomer feed, g.		M_1/M_2	Styrene, wt.-%	<i>p</i> -DVB, wt.-%	Styrene, mole-%
	Styrene	<i>p</i> -DVB				
1	0.2519	0.5957	0.53	28.4	71.6	34.5
2	0.3692	0.5735	0.81	39.2	60.8	44.5
3	0.4601	0.4969	1.16	48.1	51.9	53.4
4	0.5510	0.3229	2.14	63.1	36.9	68.2
5	0.6031	0.2613	2.89	69.8	30.2	74.4
6	0.7377	0.1017	9.09	87.9	12.1	77.2

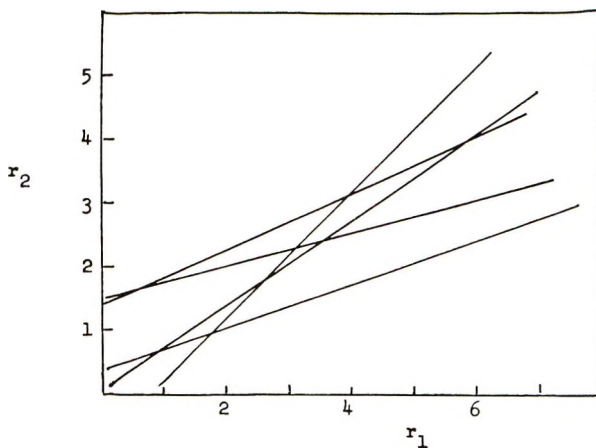


Fig. 3. Intersect plots for the copolymerization of styrene ($r_1 = 1.80$) with 1,2,4-trivinylbenzene ($r_2 = 1.12$) at 70°C . with 0.1% benzoyl peroxide initiator and conversion to incipient gel formation. The top two lines are for 91.2 and 94.2% trivinylbenzene compositions and are not included in assigning r_1 and r_2 values.

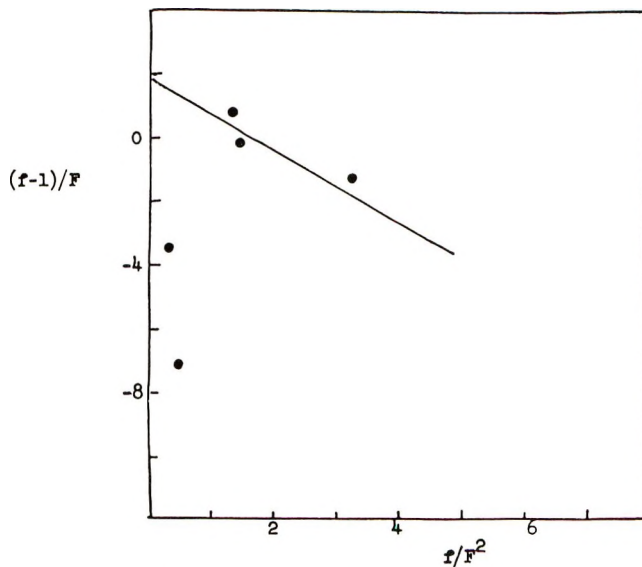


Fig. 4. Fineman-Ross plots for the copolymerization of styrene ($r_1 = 1.80$) with 1,2,4-trivinylbenzene ($r_2 = 1.12$) at 70°C . with 0.1% benzoyl peroxide initiator and conversion to incipient gelation. The two points not included in the extrapolations are those for 91.2 and 94.2% trivinylbenzene compositions.

times to remove monomers prior to final drying. In the copolymerization of styrene with *p*-DVB and also with 1,2,4-trivinylbenzene, increasing amounts of *p*-divinylbenzene or 1,2,4-trivinylbenzene in monomer mixture results in decreased time of gelation and of conversion at the gel point.

TABLE II
Copolymer Composition in Copolymerization of Styrene (M_1) and
p-Divinylbenzene (M_2) at 70°C.: Ionization-Chamber Assay

Expt. no.	Specific charge, mv./mg./sec. \times 10^{-2}	Molar ratio		
		M_1 , wt.-%	M_2 , wt.-%	M_2/M_1
1	1.300	13.9	86.1	4.98
2	1.815	19.6	80.4	3.27
3	2.286	24.6	75.4	2.45
4	2.950	31.7	68.3	1.72
5	3.931	45.6	54.4	0.96
6	6.923	69.2	30.8	0.27

TABLE III
Monomer Feed Composition in Copolymerization of Styrene (M_1) and
1,2,4-Trivinylbenzene (M_2) at 70°C.

Expt. no.	Monomer feed, g.		M_1/M_2	Styrene, wt.-%	1,2,4-TVB, wt.-%	Styrene, mole-%
	Styrene	1,2,4-TVB				
1	0.2732	0.8625	0.44	24.1	75.9	32.2
2	0.3662	0.7536	0.73	32.7	67.3	42.2
3	0.4656	0.5935	1.17	44.0	56.0	54.0
4	0.7036	0.4225	2.37	62.5	37.5	70.3
5	0.8326	0.3038	4.11	73.3	26.7	80.3

TABLE IV
Copolymer Composition in Copolymerization of Styrene (M_1) and
1,2,4-Trivinylbenzene (M_2) at 70°C.: Ionization-Chamber Assay

Expt. no.	Specific charge, mv./mg./sec. \times 10^{-2}	Molar ratio		
		M_1 , wt.-%	M_2 , wt.-%	M_2/M_1
1	0.532	5.8	94.2	10.84
2	0.807	8.8	91.2	6.90
3	2.273	24.8	75.2	2.05
4	3.432	37.5	62.5	1.11
5	5.251	57.3	42.7	0.50

Radioactivity Assay

Copolymer composition was determined by means of radioactivity assay of its styrene- β - ^{14}C content with the ionization chamber (Cary model 31 vibrating-reed electrometer) technique previously employed by us.³ Copolymer compositions and assay data are given in Table I-IV and plotted in Figures 1-4.

This research was supported in part under Contract AT (30-1)-3644 between the U.S. Atomic Energy Commission and Hunter College and by a Faculty Research Grant from the Graduate Division of the City University of New York.

References

1. R. H. Wiley, W. K. Mathews, and K. F. O'Driscoll, *J. Macromol. Sci.*, **A1**, 503 (1967).
2. R. H. Wiley and E. E. Sale, *J. Polymer Sci.*, **42**, 491 (1960).
3. R. H. Wiley and B. Davis, *J. Polymer Sci. B*, **1**, 463 (1963).
4. R. H. Wiley and B. Davis, *J. Polymer Sci.*, **62**, S132 (1962).
5. R. H. Wiley, T. H. Crawford, and N. F. Bray, *J. Polymer Sci. B*, **3**, 99 (1965).
6. R. H. Wiley and R. M. Dyer, *J. Polymer Sci. A*, **2**, 3153 (1964).
7. R. H. Wiley, G. DeVenuto, and A. DeVenuto, *J. Polymer Sci.*, in press.
8. F. W. Hoover, O. W. Webster, and C. T. Handy, *J. Org. Chem.*, **26**, 2234 (1961).

Received August 4, 1967

Effect of Urethane Groups on the Reaction of Alcohols with Isocyanates

H. A. SMITH, *The Dow Chemical Company, Midland, Michigan 48640*

Synopsis

Recently Reegen and Frisch reported the urethane catalysis of the alcohol-isocyanate reaction. We have made similar observations on a broader variety of reactants and catalysts including mono- and polyfunctional reactants, and tertiary amine, cobalt salt, and tin salt catalysts. We have found that the point in the reaction when urethane catalysis occurs is a function of the catalyst, the number of hydroxyl groups in the alcohol, and the effect of the interaction of the catalyst, alcohol, and isocyanate on the geometry of the reactive complex.

Introduction

Recently Reegen and Frisch¹ reported results on the alcohol-isocyanate reaction, which indicated catalysis of the reaction by the urethane formed. Their work was carried out with the use of phenyl isocyanate and 1-methoxy-2-propanol as reactants and dibutyltin dilaurate as catalyst. The following is a report on similar studies with monofunctional and polyfunctional alcohols and isocyanates and with tertiary amine, cobalt salt, and tin salt catalysts.

Experimental

For the purposes of this study the reactions were carried out as follows.² A solution of 5 meq. of the alcohol, 5 meq. of isocyanate, and 0.125 mmole of catalyst was added to toluene to give a total volume of 100 ml. Aliquots of 6-7 ml. of this solution were sealed into test tubes which were simultaneously immersed in the constant temperature bath maintained at 35.56°C. The sealed tubes were withdrawn at appropriate intervals, starting with a "zero" sample after 3 min. of immersion. The samples were immediately quenched by adding 1.00 ml. of 0.3*N* di-*n*-butylamine in 10 ml. of toluene to 4.95 ml. of reaction mixture, heating to boiling, and then diluting with 20 ml. of methanol. The isocyanate remaining in each sample at the end of its reaction period was then analyzed by titrating the di-*n*-butylamine remaining after reaction with the residual isocyanate with 0.0100*N* HCl to a bromphenol blue endpoint.

The alcohols used for this study were 1-butanol, 2-hydroxybutyl butyl ether (M-I), 1-ethyl-1-(2-hydroxybutoxy)-2-butoxyethane (M-II), a polyether polyol containing only secondary hydroxy groups (P-I), a polyether

polyol with 50% primary and 50% secondary hydroxyl groups (P-II), and an amine-based polyol with 50% primary and 50% secondary hydroxy groups (P-III). The isocyanates were phenyl isocyanate and tolylene diisocyanate (80/20 mixture of 2,4- and 2,6-isomers). The catalysts were triethylenediamine, cobaltous stearate, and stannous 2-ethylhexoate.

Results

The data for the reaction of a monohydroxylic alcohol, M-II, and phenyl isocyanate, shown in Figure 1, verify the catalytic effect observed by earlier workers.^{1,3-5} However, the point in the reaction where this catalysis becomes noticeable, by deviation of the kinetic plot from linearity, appears to vary with the catalysts used. Thus, with stannous 2-ethylhexoate, deviation occurs after 37-40% reaction; with cobaltous stearate,

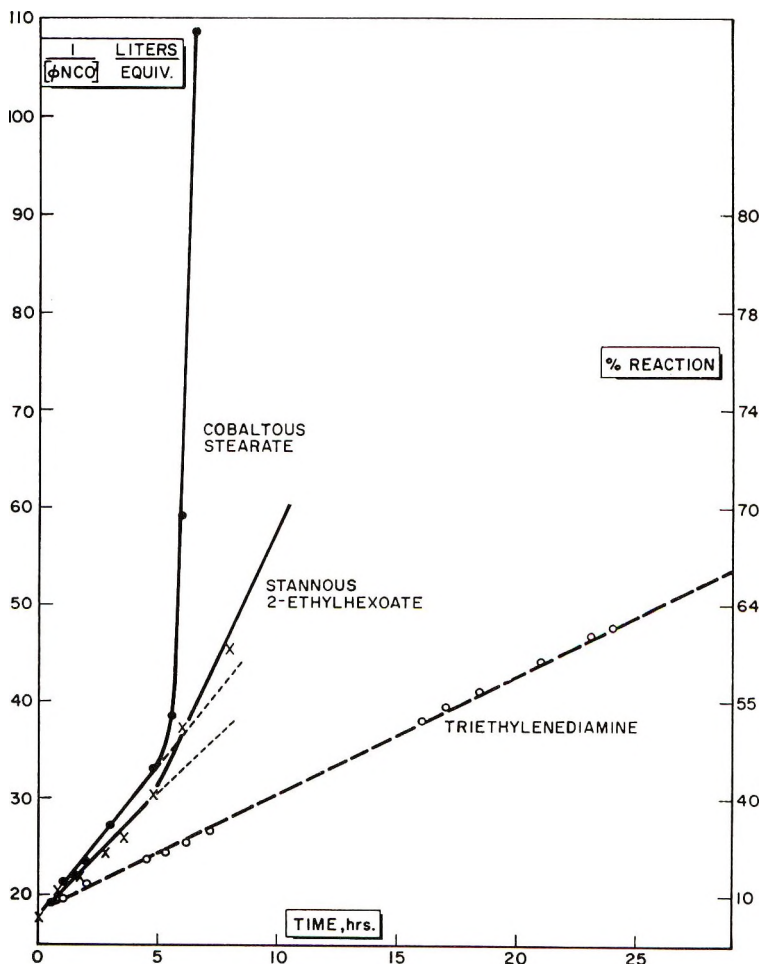


Fig. 1. Reaction of alcohol M-II with phenyl isocyanate with various catalysts.

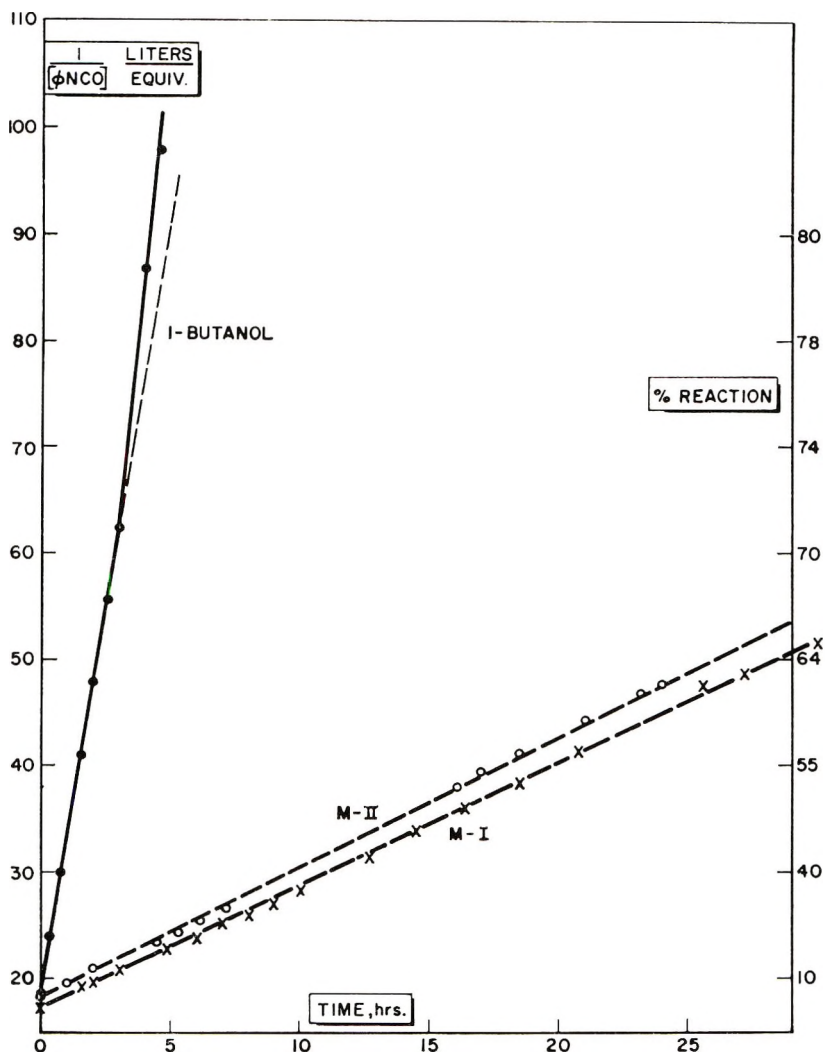


Fig. 2. Reaction of monofunctional alcohols with phenyl isocyanate with triethylenediamine catalysis.

it is at 45–50% reaction, while with triethylenediamine no deviation occurs until > 65% reaction.

The data in Figure 2 appear to indicate that the type of hydroxyl group, primary or secondary, or the presence of other functional groups in the molecule, such as ethers, do not appear to influence the point where the deviation begins. The sole effect of these groups appears to be on the rate only. Thus, 1-butanol deviates from linearity at 72–74% reaction, while the secondary alcohols M-I and M-II exhibit no deviation prior to this stage of the reaction under tertiary amine catalysis. Reegen and Frisch¹ found deviation with 1-methoxy-2-propanol at 40–50% reaction

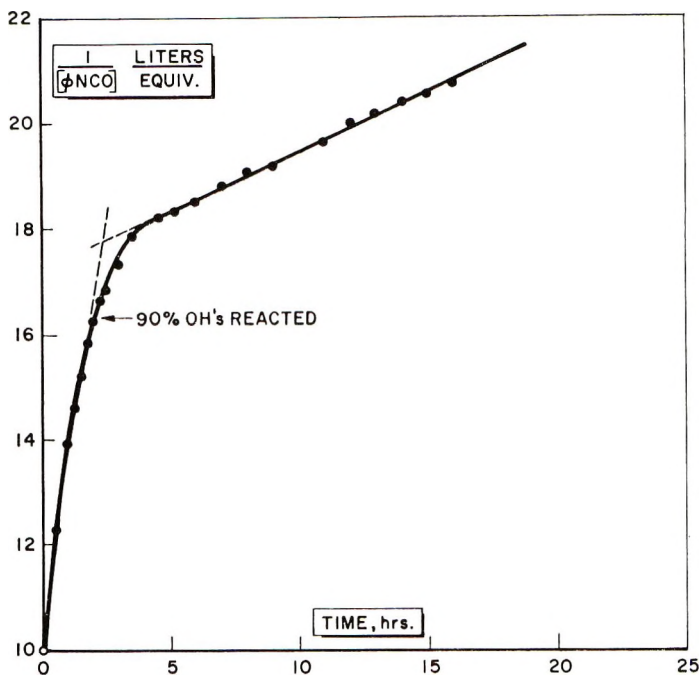


Fig. 3. Reaction of 1-butanol with excess phenyl isocyanate.

under dibutyltin dilaurate catalysis. This approaches the results obtained in this study with stannous 2-ethylhexoate and alcohol M-II. In these cases, also, the type of functional groups appears to influence the rate of reaction only.

One other effect was noted with the monofunctional alcohols due to the use of excess isocyanate. Reegen and Frisch used a 10% excess of isocyanate and obtained essentially the same results as presented here for equivalent amounts of reactants. However, if a 100% excess of phenyl isocyanate is used with 1-butanol under triethylenediamine catalysis, a linear plot is obtained up to 90% reaction of the hydroxyls, as shown in Figure 3. Subsequently, the rate decreases to that characteristic for the reaction of phenyl isocyanate with a urethane linkage to form the allophanate. No rate acceleration due to catalysis by the urethane of the alcohol-isocyanate reaction was observed in this case, in contrast with the results in Figure 2 where equivalent amounts of reactants were used.

In the case of the alcohols containing several hydroxyl groups, the results differed in some cases from those obtained with the monohydroxyl compounds (Fig. 4). The triethylenediamine-catalyzed reaction is the only one that gives a result similar to that obtained with the monohydroxyl alcohols, deviating from linearity at 66–70% reaction. With cobaltous stearate, deviation occurs at 34–40% reaction with the polyhydroxyl alcohols versus 45–50% reaction with the monohydroxyl. Stannous 2-ethylhexoate deviates at 80–85% reaction (Fig. 4) versus 34–40% (Fig. 1).

As in the case of the monohydroxyl alcohols, the type of hydroxyl, primary and secondary and the presence of ether or amine functions in the alcohol molecule do not appear to affect the point at which deviation occurs but affect only the reaction rate (Fig. 4).

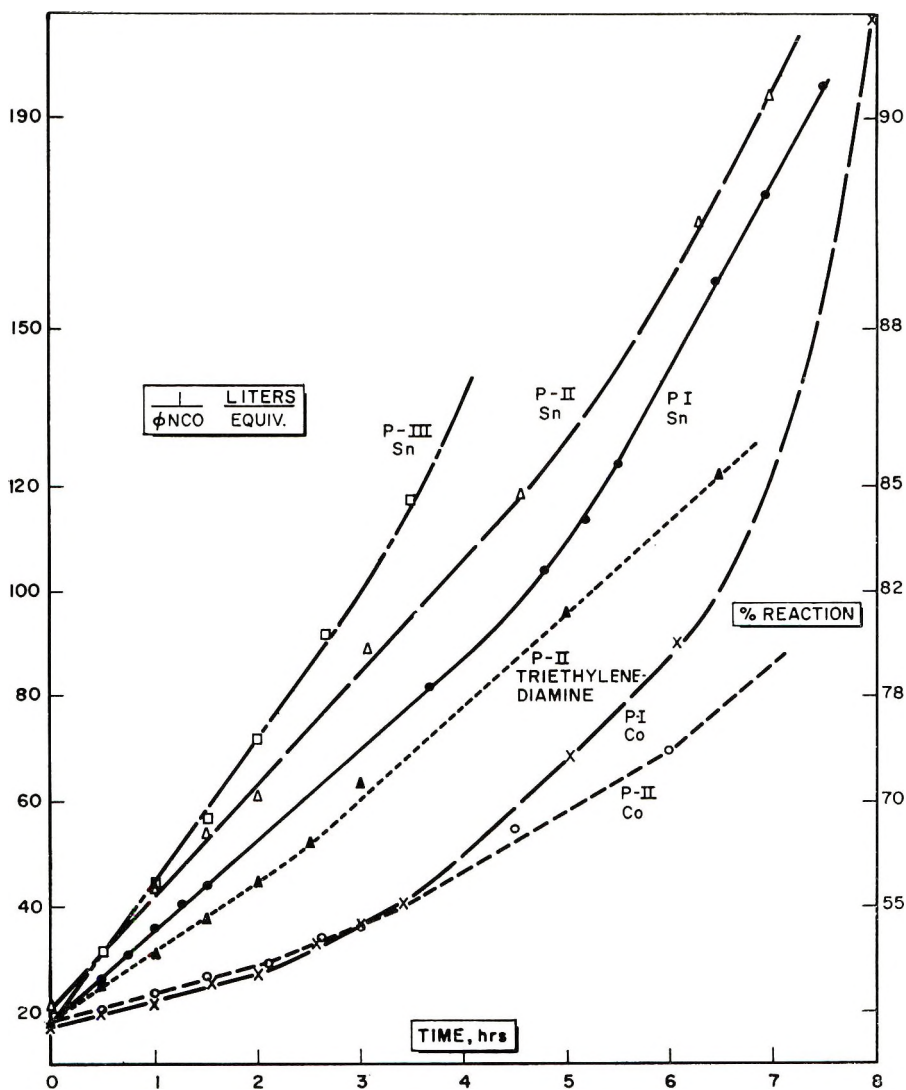


Fig. 4. Reaction of polyhydroxy alcohols with phenyl isocyanate.

When a diisocyanate, tolylene diisocyanate, is substituted for the phenyl isocyanate used to obtain the results in Figure 4, the data in Figure 5 are obtained. The tertiary amine catalyst shows the same behavior as before, deviating from linearity at 72-75% reaction. However, the tin catalyst curve shows no deviation from linearity up to > 93% reaction.

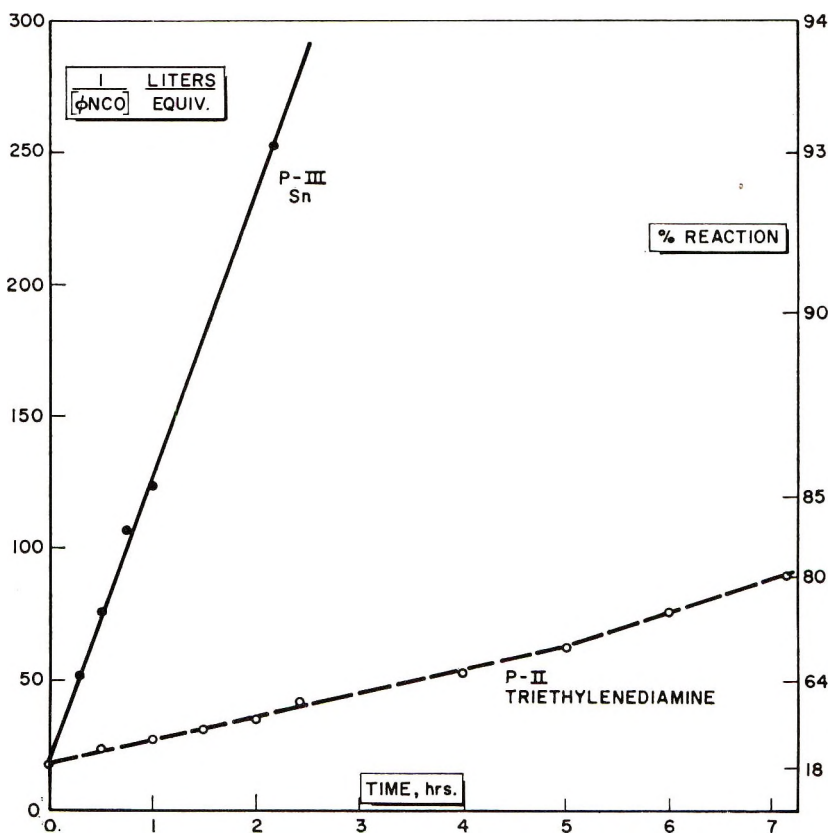


Fig. 5. Reaction of polyhydroxy alcohols with tolylene diisocyanate.

Discussion

The differences in behavior exhibited in alcohol-isocyanate reactions appear to be a function of catalyst and number of hydroxyl or isocyanate groups per molecule. Consequently, an analysis of the proposed mechanisms for the catalysis of these reactions might lead to an explanation for these results.

In the case of the tertiary amine, triethylenediamine, it has been well substantiated that such compounds catalyze these reactions by activating the isocyanate group.^{3,6,8} Therefore, polyfunctionality would not be expected to affect the results with this catalyst, as observed, since one activated isocyanate group would be reacting with one hydroxyl in all cases.

In the case of the cobalt salt, a different situation exists. This material can bind one or more hydroxyl, ether, urethane, or isocyanate groups into a tetrahedral complex (Fig. 6).²

In the case of polyhydroxyl alcohols, such as shown in Figure 6, the urethane produced by the reaction of a hydroxyl group with an isocyanate would be prevented by the remaining part of the alcohol molecule which is

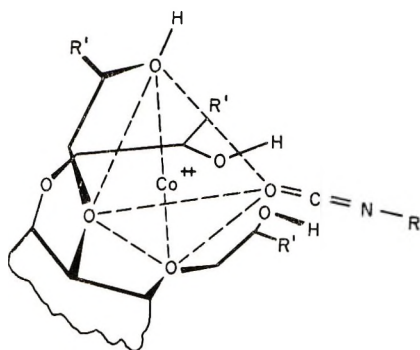


Fig. 6. Cobaltous complex.

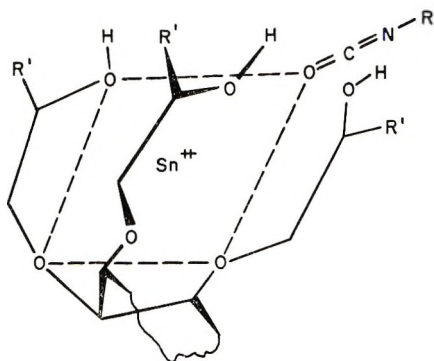


Fig. 7. Stannous complex.

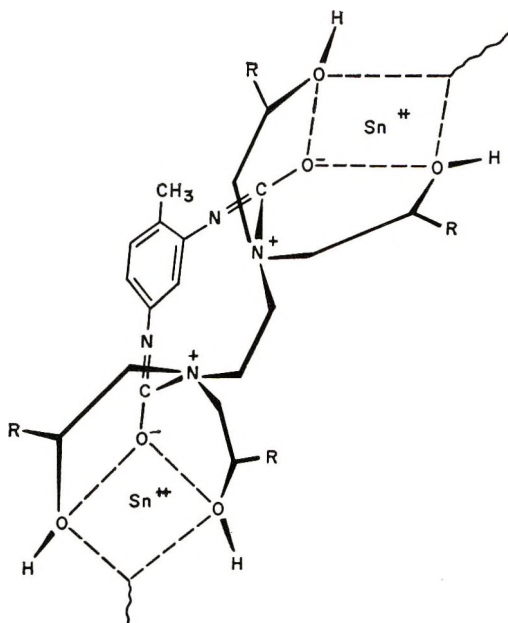


Fig. 8. Polyol P-III and tolylene diisocyanate under tin catalysis.

complexed from leaving the site of the complex. Consequently, it would be more available to act as a secondary catalyst than in the monohydroxyl case where such a trapping effect is not present. Thus, deviation from linearity due to urethane catalysis would be expected to occur at an earlier point in the cobalt catalyzed reaction with polyhydroxyl than with monohydroxyl alcohols as was observed.

The case of the tin catalyst is also different. It forms a square planar complex with both reactants, as shown in Figure 7.² Because of this, hydroxyls which are not directly complexed, but are held near the complex by ether groups, can very readily attain a configuration where the —O—H bond is parallel to the —N=C— bond of the isocyanate. This would allow reaction to occur more readily than it would with the directly complexed hydroxyls where this cannot take place. Consequently, it is difficult for the urethane linkages formed during reaction to improve upon the quite reactive situation already present. Therefore, their catalytic effects should not become apparent until later in the reaction than the monohydroxyl reagents where only less reactive complexed hydroxyls would be reacting. This, again, is the observed result.

The reaction of alcohol P-III with tolylene diisocyanate with the use of the tin catalyst is a special case of the system just discussed. Alcohol P-III is amine-based polyol which has the proper dimensions to activate both isocyanate groups of tolylene diisocyanate simultaneously via its tertiary amine groups in addition to the activation due to the tin catalyst (Fig. 8).² Since the amine groups are more basic than the urethane formed by the reaction and are always present in larger concentration, the urethane groups would be expected to have little or no effect on the alcohol-isocyanate reactions. It was observed that urethane groups did not catalyze in this reaction (Fig. 5) as predicted from the proposed mechanism for catalysis.

In summation, it appears that the factors governing the amount of urethane catalysis of the alcohol-isocyanate reaction are the catalyst, the alcohol, and the effect of the interaction of these two materials and the isocyanate on the geometry of the reactive complex.

References

1. S. L. Reegen and K. C. Frisch, *J. Polymer Sci. A-1*, **4**, 2321 (1966).
2. H. A. Smith, *J. Appl. Polymer Sci.*, **7**, 85 (1963).
3. J. W. Baker and J. B. Holdsworth, *J. Chem. Soc.*, **1947**, 713.
4. H. Okada and Y. Iwakura, *Makromol. Chem.*, **64**, 91 (1963).
5. M. Sato, *J. Org. Chem.*, **27**, 819 (1962).
6. J. W. Baker, J. Gaunt, and M. M. Davies, *J. Chem. Soc.*, **1949**, 9.
7. J. J. Tazema and H. K. Latourette, paper No. 35, presented at the 130th meeting of the American Chemical Society, Division of Paint, Plastics, and Printing Ink Chemistry, Atlantic City, New Jersey, Sept. 1956.
8. A. Farkas and K. G. Flynn, *J. Am. Chem. Soc.*, **82**, 642 (1950).

Received June 2, 1967

Revised August 24, 1967

Electron Spin Resonance Study of the Radiation-Induced Polymerization of *N*-Vinylcarbazole

P. B. AYSCOUGH and A. K. ROY,* *School of Chemistry, University of Leeds, Leeds, 2, England*, and R. G. CROCE and S. MUNARI, *Istituto di Chimica Industriale, Università di Genova, Genova, Italy*

Synopsis

When crystals of *N*-vinylcarbazole are γ -irradiated at 77°K., the ESR spectrum observed before warming consists of three peaks attributed to a radical-cation with the unpaired spin associated mainly with the nitrogen atom. Above 90°K. polymerization occurs, initiated by the cation, and the spectrum changes to that of an alkyl type of radical, $=\text{N}-\dot{\text{C}}\text{H}-\text{CH}_2$, trapped in the polymer. Single crystals were used for a detailed analysis of the nuclear hyperfine parameters of the observed radicals.

N-vinylcarbazole may be polymerized with great facility in the presence of free-radical¹ or cation²⁻⁴ initiators, (either inorganic or organic), or when subjected to ionizing radiation.^{5,6} The polymerization has also been studied in the presence of a wide range of organic electron acceptors such as chloranil, trinitrobenzene, and tetranitromethane⁷ and inorganic acceptors such as chlorine, bromine, and iodine.⁸

The mechanism of the reaction in the presence of electron acceptors has been discussed by Ellinger⁷ and by Scott et al.,⁹ who advanced the theory that initiation involves the reaction of a monomer-acceptor complex with a second similar complex when the reaction is carried out in solution, or with a monomer molecule during bulk polymerization. ESR spectra observed in solid *N*-vinylcarbazole during polymerization in the presence of halogens consist of single lines, varying in width from 7 to 12 Gauss depending on the nature of the complex.⁸ It was suggested that the species responsible for these spectra are molecular cations with the unpaired electron delocalized into the aromatic system.

Chapiro and Hardy⁶ studied the γ -irradiation of *N*-vinylcarbazole below its melting point and proposed a radical mechanism for the reaction. The evidence supporting this view is largely kinetic in nature and depends primarily on the observation of post-polymerization caused by the presence of trapped radicals in the irradiated solid. However, an ionic mechanism is not incompatible with these observations.

* Present address: Department of Physics, University of Dacca, Dacca 2, East Pakistan.

Evidence is accumulating to support the view that radiation-induced polymerization of olefinic compounds in the solid state proceeds mainly by cationic processes¹⁰⁻¹² and it seemed desirable to examine an *N*-vinyl compound with this evidence in mind. Accordingly we have investigated the electron spin resonance spectra of γ -irradiated *N*-vinylcarbazole between 77 and 300°K. and identified the paramagnetic species observed, using single crystals as an aid to identification. At 77°K. the main paramagnetic species appears to be a radical-cation which is replaced on warming by a dimeric or polymeric radical. The proposed reaction mechanism has some features in common with those discussed earlier for *N*-vinylcarbazole and for terminal olefins.

EXPERIMENTAL

N-Vinylcarbazole (Koch-Light Laboratories Ltd.) was recrystallized from methanol (observed m.p. 64°C., literature value 64.7°C.). Single crystals were grown by slow evaporation of a solution in methanol. A 1700 cu. ⁶⁰Co source was used for γ -irradiation: the total dose was about 4×10^6 rad for the single crystals, about 10^6 rad for powder samples. Details of the procedure for mounting the crystals and examining them in the ESR spectrometer (Decca type X2) have been given earlier.¹³

Polyvinylcarbazole was prepared by post-polymerization at 35°C. of monomer γ -irradiated at room temperature.^{2,5} Monomer was removed by extraction with hot methanol, and the polymeric sample was dried at 80°C.

RESULTS

Powder samples of *N*-vinylcarbazole irradiated and examined at 77°K. show ESR spectra consisting of three lines, with peak to peak separation of 20.5 Gauss. The central peak has almost twice the height of the outer peaks but is also appreciably narrower (about 8 Gauss peak-to-peak).

Single crystals have the form of an elongated flat hexagon. We have been unable to find any details of the crystal structure, though reference has been made to changes in crystallinity during irradiation.¹⁴ For study of the ESR spectra the reference axes were chosen so that *x* is parallel to one of the long edges and *z* perpendicular to the flat face. (See Fig. 1.)

The ESR spectra observed during rotations about the *x*, *y*, and *z* axes show no measurable anisotropy (the variation of the hyperfine splittings was less than 0.5 Gauss). The average isotropic component is 20.3 ± 0.3

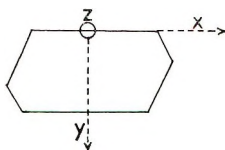


Fig. 1. Orientation of reference axes with respect to the principal faces of single crystal *N*-vinylcarbazole.

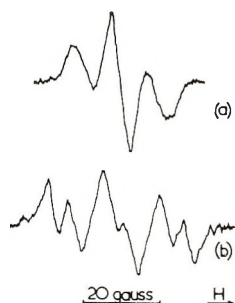


Fig. 2. Electron spin resonance spectrum of single crystal *N*-vinylcarbazole after γ -irradiation at 77°K.: (a) spectrum observed at 77°K. immediately after irradiation; (b) spectrum observed at room temperature, magnetic field parallel to z axis.

Gauss. These observations appear to rule out the possibility that the interacting nuclei are in a $-\text{CH}_2$ group and it is more likely that a single nitrogen atom is involved.

On warming the irradiated powder to about 90°K., the three relatively narrow lines are replaced by four much broader lines, average separation about 25 Gauss. This spectrum is unchanged up to room temperature and is stable for several days. The change is irreversible.

Single crystals, either irradiated at 77°K. and warmed to room temperature or irradiated at room temperature, show four-line spectra (1:3:3:1) at some orientations and six lines (1:1:2:2:1:1) at others (see Fig. 2). This behavior is characteristic of radicals containing one α proton and two β protons, and a detailed analysis was carried out to confirm this interpretation.

The procedure has been described earlier. Fortunately the axes chosen for rotation are close to the principal axes of the hyperfine tensor, so that formulae based on the first-order Hamiltonian for the interaction of electron

TABLE I
Hyperfine Coupling Constants for the Radical Trapped in *N*-Vinylcarbazole at 300°K.

Proton	Coupling constants, Gauss			Direction cosines		
	Principal values	Isotropic component ^a	Anisotropic components ^a			
α	25.7	-19.2	-6.5	1	0	0
	20.4		-1.2	0	0.99	0.13
	11.4		+7.8	0	-0.13	0.99
β_1	24.5	28.1	-3.6			
	29.8		+1.7			
	30.1		+2.0			
β_2	32.6	30.8	+1.8			
	29.8		-1.0			
	30.1		-0.7			

^a Signs assumed; estimated precision ± 0.3 Gauss.

and nuclei in the magnetic field¹³ provide a good estimate of the off-diagonal elements in the first stage of the analysis. Theoretical curves for rotations about the x , y , and z axes were then constructed by using the second-order Hamiltonian and the first estimates of the tensor elements in order to obtain a second approximation. The values so obtained are shown in Table I. Direction cosines were not estimated for the β protons since the anisotropic components are too small for useful calculations. The isotropic components are in good agreement with the conventional relationship:

$$a^H = Q^H_{\text{CCH}} \cos^2 \theta$$

between a^H , Q^H_{CCH} , and the dihedral angle θ between the β C—H bond and the axis of the carbon $2p$ orbital of the unpaired spin, with $Q^H_{\text{CCH}} = 41$ Gauss, $\theta_1 = 28^\circ$, $\theta_2 = 148^\circ$. These values correspond to an almost symmetrical configuration for the β protons in the $\text{>}\dot{\text{C}}\text{H—CH}_2\text{—}$ group.

It is of interest that the maximum and minimum values of the anisotropic components of the α -proton tensor are about 25% lower than those normally observed for these species, but are in very good agreement with the values observed for the radical $\text{NH}_3^+\text{CH}_2\text{CONH}\dot{\text{C}}\text{HCOO}^-$ in γ -irradiated glycyl glycine hydrochloride,¹⁵ or N -carbamyl glycine.¹⁶ Evidently the presence of a nitrogen atom in the β position causes some reduction in the unpaired spin density in the carbon $2p$ orbital, presumably as a result of polarization through the C—C—N linkage. There seems little doubt therefore that the radical observed at room temperature has the structure $\text{>}\dot{\text{N}}\text{—}\dot{\text{C}}\text{H—CH}_2\text{—}$.

Polyvinyl carbazole (powder) was γ -irradiated at 77°K. to a total dose of about 4×10^6 rads. The ESR spectrum observed at 77°K. consists of a single symmetric line of width 10–15 Gauss which decreases in intensity on warming but is otherwise unchanged between 77 and 300°K. The signal is significantly weaker than that in the monomer treated in the same manner.

DISCUSSION

Paramagnetic Species Trapped at 77°K.

In view of the large doses of radiation required to obtain an adequate concentration of radicals for the single-crystal studies it was necessary to establish that the species observed were not those produced by radiation damage to the polymer. The singlet spectrum obtained on irradiating the polymer is obviously different from that observed in the irradiated monomer, and is much more like that observed when the monomer reacts with electron acceptors such as halogens.⁸ Such spectra are often associated with radicals in which the unpaired electron is extensively delocalized in an aromatic or polyenyl system. It has also been shown that the yield of polymer at 77°K. in irradiated N -vinylcarbazole is very small.¹⁷

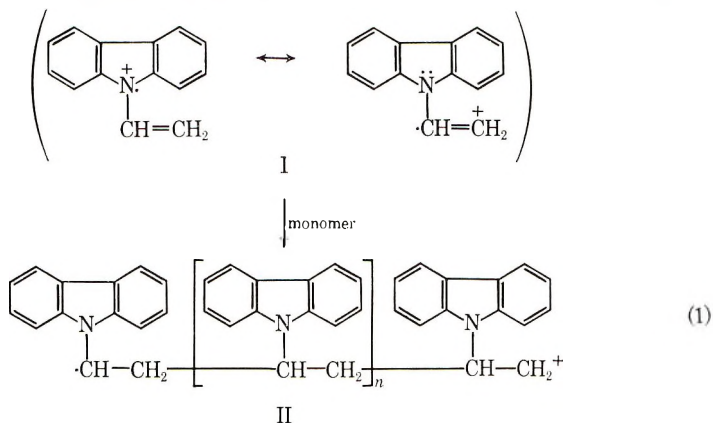
The isotropic three-line spectrum observed in the monomer between 77 and 90°K. is therefore to be associated with a transient species which is formed from the monomer and is converted almost quantitatively to the stable $\text{>N}-\dot{\text{C}}\text{H}-\text{CH}_2-$ radical. We have proposed that the triplet splitting is to be associated with N in the radical-cation formed by loss of one of the N lone-pair electrons in the monomer, rather than with $-\text{CH}_2$. However ESR evidence is not compelling. The difficulties are (1) the unequal intensities of the three lines, (2) the absence of anisotropic components. (The absence of observable interaction with the β proton in the species $\text{>}\dot{\text{N}}-\text{CH}=\text{CH}_2$ is not a serious problem, since this proton is likely to be in the nodal plane of the p orbital of the unpaired electron. The same comment would apply to any alternative species with the unpaired spin in the $-\text{CH}_2$ group.)

Regarding the first difficulty, unequal line widths and intensities have been observed for numerous nitrogen-containing radical-ions in solution⁸ and for radicals such as NO_2 in glassy matrices.¹⁹ This effect is usually attributed to relaxation processes involving motional modulation of the g and A tensors²⁰ which can produce differential broadening. This mechanism is unlikely to be effective in a crystalline solid at 77°K. Nuclear quadrupole interactions would probably have a similar effect but the likely magnitude is not known. However, there is independent evidence that the nitrogen triplet peaks can show marked differences in intensity when observed in solid matrices at 77°K. This is provided in two papers^{21,22} on γ -irradiated pyridine and pyridine- d^5 in which the species observed is thought to be $\text{C}_5\text{H}_5\text{N}^+$. We have observed similar spectra in nitrogen heterocyclic compounds such as substituted pyridines, indoles, and pyrroles,²³ though no detailed interpretations of these phenomena have been put forward.

The absence of hyperfine anisotropy is perhaps more unexpected, since the isotropic coupling is large and similar to that observed in several other nitrogen-containing radical-cations, e.g., $\cdot\text{NR}_3^+$, which show considerable anisotropy in the solid-phase spectra.²⁴⁻²⁶ Of this group, examined in single crystals, only $\cdot\text{NH}_3^+$ shows a predominantly isotropic spectrum, and this is thought to be caused by essentially free rotation of the radical.²⁷ The suggestion that there is free rotation in the radical-cation of *N*-vinylcarbazole is quite unreasonable. We believe that the explanation may be based on some delocalization of spin from the N $2p$ orbital into the aromatic system. This has been suggested in the studies of pyridine^{21,22} and is confirmed by studies of methyl-substituted pyridines.²³ In constructing a suitable molecular orbital for the unpaired electron in such systems it is necessary to propose a significantly greater contribution from nitrogen $2s$ (or σ) orbitals. In view of the great sensitivity of the s/p ratio for the unpaired spin in nitrogen-containing radicals to the nature of the groups attached to the nitrogen this is not unreasonable. Further details will be published elsewhere.

Mechanism of Polymerization

We believe that the change observed in the ESR spectrum between 77 and 90°K. can be represented by reaction (1), where n is very small (prob-



ably 0 or 1 at 90°K.). The polymerization is initiated by the carbonium ion form of I but probably does not proceed beyond the dimeric or trimeric stage until a temperature is reached which permits some relaxation of the crystalline lattice. We have found no evidence relating to the direction of the subsequent additions though this must be controlled by molecular orientation in the crystalline lattice. Propagation is likely to occur perpendicular to the planes of the vinyl groups. Unfortunately the ESR spectra give no information since the unpaired spin is left on the non-active end of the chain (II). It is presumably trapped there after termination has occurred at the growing end by charge neutralization or transfer. These neutral trapped radicals are the likely cause of the post-polymerization observed by Chapiro and Hardy.⁶ This mechanism is essentially similar to that proposed for the radiation-induced polymerization of hexadecene and other unsaturated hydrocarbons.^{10,11}

Our conclusions regarding the mechanism of the polymerization are therefore in general agreement with those advanced by Tsuji et al.⁸ but differ in the identity of the species trapped at room temperature. Clearly the presence of several mole per cent of free halogen in the sample examined by these authors makes it unlikely that the free cation exists in such systems at any stage. Our conclusions also give strong support to the views expressed in a recent paper by Pàc and Plesch.²⁸ The only difference is in the reversed locations of the unpaired spin and the positive charge in the cation. We believe that the ESR evidence is conclusive on this point, though this does not seriously affect the proposed mechanism.

References

1. H. Davidge, *J. Appl. Chem.*, **9**, 553 (1959).
2. O. F. Solomon, M. Dimonie, and M. Tomescu, *Makromol. Chem.*, **56**, 1 (1962).
3. O. F. Solomon, M. Dimonie, K. Ambrozh, and M. Tomescu, *J. Polymer Sci.*, **52**, 205 (1961).

4. J. Heller, D. O. Tieszen, and D. B. Parkinson, *J. Polymer Sci. A*, **1**, 125 (1963).
5. A. J. Restiano, R. B. Mesrobian, H. Morawetz, D. S. Ballantine, C. D. Dienes, and D. J. Metz, *J. Am. Chem. Soc.*, **78**, 2939 (1956).
6. A. Chapiro and G. Hardy, *J. Chim. Phys.*, **59**, 993 (1962).
7. L. P. Ellinger, *Polymer*, **5**, 559 (1964).
8. K. Tsuji, K. Takakura, M. Nishii, K. Hayashi, and S. Okamura, *J. Polymer Sci. A-1*, **4**, 2028 (1966).
9. H. Scott, G. A. Miller, and M. M. Labes, *Tetrahedron Letters*, **1963**, 1073.
10. P. B. Ayscough, A. P. McCann, C. Thomson, and D. C. Walker, *Trans. Faraday Soc.*, **57**, 1487 (1961).
11. E. Collinson, F. S. Dainton, and D. C. Walker, *Trans. Faraday Soc.*, **57**, 1732 (1961).
12. C. D. Wagner, *J. Phys. Chem.*, **66**, 1158 (1962).
13. P. B. Ayscough and A. K. Roy, *Trans. Faraday Soc.*, **63**, 1106 (1967).
14. J. Kroh and W. Pekala, *Bull. Acad. Polon. Sci.*, **12**, 419 (1964).
15. D. V. G. L. N. Rao and M. Katayama, *J. Chem. Phys.*, **37**, 383 (1964).
16. H. C. Box, H. G. Freund, and K. T. Liliga, *J. Chem. Phys.*, **38**, 2100 (1963).
17. S. Munari, G. Tealdo, F. Vigo, and G. Bonta, *Proceedings of the 2nd Tihany Symposium on Radiation Chemistry*, J. Dobò and P. Hedrig, Eds., Akademiai Kiado, 1967, p. 573.
18. P. B. Ayscough, F. P. Sargent, and R. Wilson, *J. Chem. Soc.*, **1963**, 5418.
19. P. W. Atkins, N. Keen, and M. C. R. Symons, *J. Chem. Soc.*, **1962**, 2873.
20. A. Carrington, A. Hudson, and G. R. Luckhurst, *Proc. Roy. Soc. (London)*, **A284**, 584 (1965).
21. C. David, G. Geuskens, and A. Verhasselt, *Mol. Phys.*, **11**, 257 (1967).
22. K. Tsuji, H. Yoshida, and K. Hayashi, *J. Chem. Phys.*, **45**, 2894 (1966).
23. P. B. Ayscough and R. G. Croce, unpublished observations.
24. J. R. Rowlands and D. H. Whiffen, *Nature*, **193**, 61 (1962).
25. J. R. Morton, *J. Phys. Chem. Solids*, **24**, 209 (1963).
26. A. J. Tench, *J. Chem. Phys.*, **38**, 593 (1963).
27. T. Cole, *J. Chem. Phys.*, **35**, 1169 (1961).
28. J. Pàc and P. H. Plesch, *Polymer*, **8**, 237 (1967).

Received June 1, 1967

Revised September 11, 1967

Peroxide Crosslinking of Poly(*n*-alkyl Methacrylates)

J. BARTOŇ, *Laboratory of Polymers, Slovak Academy of Sciences,
Bratislava, Czechoslovakia*

Synopsis

The action of dicumyl peroxide on poly(*n*-butyl methacrylate) and poly(*n*-nonyl methacrylate) produces degradation and crosslinking reactions in both polymers. Crosslinking and degradation of poly(*n*-alkyl methacrylates) are influenced also by the initial molecular weight of the polymer as well as by the type of alkyl group. The ratio of degradation to crosslinking p/q determined on the basis of the equation of Charlesby and Pinner, $S + S^{0.5} = (p/q) + (1/qP_n)$ is for poly(*n*-butyl methacrylate) of viscosity molecular weight 0.923×10^6 and 2.16×10^6 of 0.78 and 0.60, respectively; for poly(*n*-nonyl methacrylate) of weight average molecular weight 3.83×10^5 , p/q is 0.16. Crosslinking efficiencies (moles of crosslinks per mole of decomposed dicumyl peroxide) of the above polymers are relatively very low: 0.014, 0.005, and 0.039, respectively. The critical concentration of dicumyl peroxide necessary for the formation of gel, provided it undergoes complete decomposition, is for the above polymers 1.82, 1.65, and 0.98 wt.-%, respectively. Under the critical concentration of dicumyl peroxide the limiting viscosity number of poly(*n*-butyl methacrylate) increases with increasing concentration of dicumyl peroxide. An initial decrease of the value of the limiting viscosity number, which is characteristic for polymers undergoing simultaneous degradation and crosslinking, was not observed.

Free radicals acting on polymers bring about either their degradation or formation of branched and crosslinked structures. The final effect is influenced by the structure of the basic unit of the polymer. A typical example is provided by polyolefins. While polyethylene crosslinks by the effect of free radicals, the crosslinking of polypropylene is considerably more difficult, and polyisobutylene undergoes degradation exclusively.

Interesting results are provided by the introduction of alkyl groups in the side chain of the macromolecules. Schultz and Bovey¹ and Burlant et al.² investigated the effects of ionizing radiation on poly(alkyl acrylates); Graham studied poly(alkyl methacrylates),³ poly(aryl methacrylates) and poly(aryl acrylates).⁴ It can be concluded from their results that the proportion of crosslinking reactions increases with increasing length of the alkyl of the ester group in the side chain of the macromolecule. The highest effects, particularly with poly(alkyl methacrylates), are achieved with *n*-alkyl esters; secondary and tertiary alkyl esters have a lower proportion of crosslinking reactions and require higher doses of radiation for the formation of gel. Crosslinking of poly(alkyl acrylates) proceeds more easily in comparison with poly(alkyl methacrylates); this can be

attributed to the presence of the hydrogen on the tertiary carbon atom adjacent to the ester group.³

Lal and McGrath⁵ investigated the conditions of crosslinking of poly(alkyl vinyl ethers) by free radicals. In this case too, the lengthening of the alkyl in the poly(vinyl alkyl ether) favorably influenced crosslinking reactions. This was attributed to the higher ratio of the number of hydrogen atoms on secondary carbon atoms to hydrogen on tertiary carbon in the main chain. The branching of the alkyl in poly(vinyl butyl ether) did not influence the values of the ratio of degradation and crosslinking p/q , but crosslinking efficiency by branching was remarkably affected.

Recently Mantell et al.⁶ published results of a study of crosslinking of poly(dioxanyl methacrylates) and poly(dioxanyl acrylates) by dicumyl peroxide. Crosslinking of the acrylates took place more easily than crosslinking of the methacrylates. Crosslinking of methacrylates was conditioned by the presence of hydrogen atoms on the carbon atom between two oxygen atoms of the *m*-dioxane ring.

In this work we have tried to make clear the influence of the initial molecular weight of the polymer and of the length of the alkyl of the ester group in the side chain on crosslinking of poly(alkyl methacrylates) by the effect of free radicals from thermal decomposition of dicumyl peroxide.

EXPERIMENTAL

Dicumyl peroxide was recrystallized from ethanol, m.p. 39.0°C.; α, α' azobisisobutyronitrile from diethyl ether, m.p. 103.5°C. Analytical grade benzene was shaken thoroughly with sulfuric acid and rectified. Methyl ethyl ketone for viscometric work was of analytical grade.

Monomers

n-Nonyl methacrylate was synthesized by ester interchange of methyl methacrylate and *n*-nonyl alcohol.⁷

ANAL. Calcd. for $C_{13}H_{24}O_2$: C, 73.54%; H, 11.39%. Found: C, 73.50%; H, 11.20%.

n-Butyl methacrylate was the commercially available product.

Polymers

Monomers for polymerization were washed with a 10% solution of sodium hydroxide, sulfuric acid, distilled water, dried with calcium chloride, and redistilled at reduced pressure of nitrogen. The polymers were prepared by radical polymerization of monomers in benzene solution to a 10% conversion for *n*-butyl methacrylate and 30% conversion for *n*-nonyl methacrylate. α, α' -Azobisisobutyronitrile was used as initiator. The polymerization temperature was 60°C.

Mixtures of the polymers with dicumyl peroxide were prepared from benzene solution by evaporation of the solvent at 40°C. and 10 torr.

Procedures

Tempering of the mixture of polymers with dicumyl peroxide was carried out in sealed glass ampules in nitrogen atmosphere in a temperature-controlled bath at $145 \pm 0.2^\circ\text{C}$. for 4 hr. Under these conditions decomposition of more than 99% of dicumyl peroxide is attained.⁸

The insoluble part of the tempered samples was determined by extraction in an excess of benzene at $19\text{--}23^\circ\text{C}$. for 72 hr. in the dark. The solvent was changed every 24 hr. The percentage of gel was calculated from the weight of the insoluble part of the sample and from its initial weight before extraction.

Before the extraction, the tempered samples were vacuum-dried to constant weight in order to remove decomposition products of dicumyl peroxide.

The limiting viscosity number of poly(*n*-butyl methacrylates) as well as of the samples of poly(*n*-butyl methacrylates) after tempering was determined in methyl ethyl ketone at 23°C . Measurements were made with a dilution-type (Ubbelohde) viscometer. The molecular weight of poly(*n*-butyl methacrylate) was calculated from the equation:⁷ $[\eta] = 1.56 \times 10^{-5} \bar{M}_v^{0.81}$.

The given values of the limiting viscosity number are the arithmetical average of two determinations.

Light-scattering measurements were made at 24°C . with a Brice-Phoenix photometer with the 5461 A. green line as light source. Scattered intensities of methyl ethyl ketone solutions filtered through sintered glass G-5 were measured at angles of 45° , 90° , and 135° to the primary beam for series of four concentrations ranging from 0.003 g./ml. to 0.006 g./ml. The refractive index increment was determined on a Zeiss laboratory interferometer.

Errors in Measurement

When calculating per cent of gel the arithmetical average of at least three measurements was taken as result. The standard deviation of the arithmetical average was $\pm 0.25\%$.

RESULTS

First of all it was necessary to explain the relation between the amount of the insoluble part and of the initial molecular weight of the polymer. We used for this purpose poly(*n*-butyl methacrylates) of different molecular weight and two different concentrations of dicumyl peroxide. Results are shown in Figure 1. It is obvious from the dependence on Figure 1 that the initial molecular weight of the polymer has a considerable influence on the crosslinked portion of the polymer.

In order to express the influence of dicumyl peroxide concentration on the amount of the crosslinked portion of the polymer we used the modified equation of Charlesby and Pinner.¹⁰ For polymers with the most probable

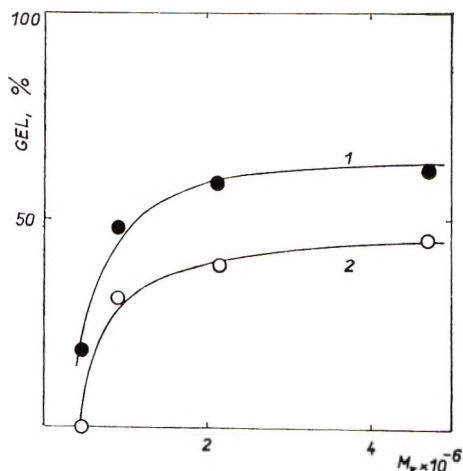


Fig. 1. Dependence of per cent gel of poly(*n*-butyl methacrylate) on the initial viscosity-average molecular weight of poly(*n*-butyl methacrylate) at various concentrations of dicumyl peroxide: (1) 5 wt.-%; (2) 3 wt.-%. Reaction time, 4 hr.; reaction temperature, 145°C.

distribution of molecular weight and assuming that the ratio of degradation to crosslinking p/q is constant, we have

$$S + S^{0.5} = (p/q) + (1/qP_n) \quad (1)$$

In eq. (1) S is the weight fraction of the soluble portion, p and q are fractions of the basic units of the polymer undergoing degradation and crosslinking, respectively, related to the total number of basic units, and P_n is the number-average degree of polymerization of the polymer before crosslinking. Further it holds that

$$q = 2m[C] \quad (2)$$

where m is the molecular weight of the basic unit of the polymer and $[C]$ is the concentration of crosslinks of the crosslinked polymer in moles/gram. From the definition of crosslinking efficiency E of the polymer it follows:

$$[C] = E[i] \quad (3)$$

where $[i]$ is the concentration of decomposed dicumyl peroxide in mole/g. and the crosslinking efficiency E is given by the number of moles of crosslinks per mole of decomposed peroxide.

Supposing that the crosslinking efficiency E is independent of concentration of dicumyl peroxide, which is fulfilled for dicumyl peroxide, as shown in the previous paper,^{11,12} we obtain from eqs. (2) and (3) by substituting in eq. (1) the relation

$$S + S^{0.5} = \frac{p}{q} + \frac{1}{2mEP_n[i]} \quad (4)$$

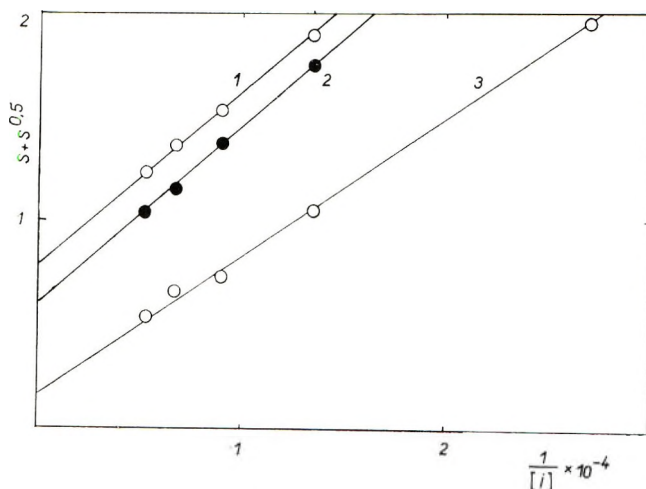


Fig. 2. Dependence of $S + S^{0.5}$ on reciprocal value of decomposed dicumyl peroxide (mole/g.) for: (1) poly(*n*-butyl methacrylate), $M_v = 9.23 \times 10^5$; (2) poly(*n*-butyl methacrylate), $M_v = 21.6 \times 10^5$; (3) poly(*n*-nonyl methacrylate), $M_w = 0.383 \times 10^6$. Reaction time, 4 hr.; reaction temperature, 145°C.

The graphical dependence given by eq. (4) is presented in Figure 2 for poly(*n*-butyl methacrylate) of different molecular weights and for poly(*n*-nonyl methacrylate).

From Figure 2 we obtained the values of the ratio p/q as an intercept on the ordinate axis and from the coordinate of the intersection point of the straight lines for the ordinate value $S + S^{0.5} = 2$ the critical concentration of dicumyl peroxide, necessary for gel formation. Crosslinking efficiency was calculated from the slopes of lines on Figure 2 and from eq. (4). The results are tabulated in Table I.

The values of P_n of poly(*n*-butyl methacrylate) were calculated for the most probable distribution of molecular weights from relation $\bar{M}_v/\bar{M}_n = 1.92$ determined for the exponent of the Mark-Houwink equation $\alpha = 0.81$.¹³ We further assumed, when calculating crosslinking efficiency, that poly(*n*-nonyl methacrylate) has also the most probable distribution of molecular weights.

TABLE I
Values of Ratio of Degradation and Crosslinking p/q , of Critical Concentrations of Dicumyl Peroxide Necessary for Gel Formation, and of Crosslinking Efficiencies of Poly(*n*-butyl Methacrylate) and Poly(*n*-nonyl Methacrylate)

Polymer	$\bar{M}_w \times 10^6$	p/q	E	Dicumyl peroxide critical concentration, wt.-%
Poly(<i>n</i> -butyl methacrylate)	0.923	0.78	0.014	1.82
	2.16	0.60	0.005	1.65
Poly(<i>n</i> -nonyl methacrylate)	0.383 ^a	0.16	0.039	0.98

^a Weight-average molecular weight.

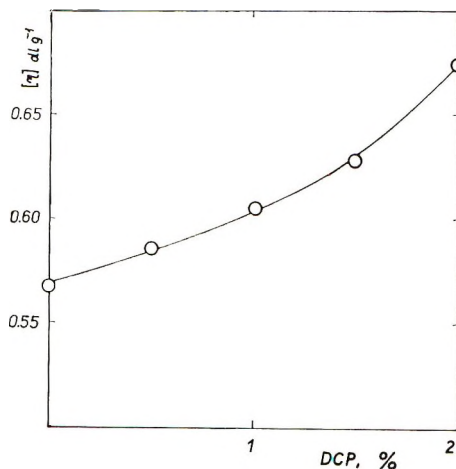


Fig. 3. Dependence of limiting viscosity number of poly(*n*-butyl methacrylate) in methyl ethyl ketone at 23°C. on concentration of decomposed dicumyl peroxide per cent by weight. Reaction time, 4 hr.; reaction temperature, 145°C.

The effects of free radicals on poly(*n*-butyl methacrylate) in the pregel region were investigated viscometrically in the range of dicumyl peroxide concentrations under the critical concentration necessary for formation of a gel for the given molecular weight of the polymer. The limiting viscosity number increases continuously with increasing concentrations of dicumyl peroxide. This dependence is shown for poly(*n*-butyl methacrylate) in Figure 3.

DISCUSSION

The influence of the initial molecular weight with irradiation of a polymer was mentioned by Schultz and Bovey.¹ Their work shows that the increase of the initial molecular weight of a polymer influences the value of the minimal dose of radiation necessary for gel formation and to a certain extent also the ratio of degradation and crosslinking. In further works of Burlant et al.,² Graham,^{3,4} and Lal and McGrath⁵ attention was given first of all to the influence of the length and type of alkyl in the side chain on crosslinking of the polymer. Because the initial molecular weights of the polymers were considerably different, comparison of the results is difficult.

The distribution of molecular weights of the polymer plays here an important role. The Charlesby-Pinner relation⁸ holds for polymers with the most probable distribution of molecular weights. Such distribution emerges upon polymerization within a narrow range of monomer conversion provided that macroradicals are terminating by disproportionation. In our case of polymerization of *n*-butyl methacrylate in benzene solution to a conversion of 10% it can be supposed that the ratio \bar{M}_w/\bar{M}_n is in the range 1.5–2. This is confirmed by the established linear course of depend-

ence of $S + S^{0.5}$ on the reciprocal of concentration of decomposed dicumyl peroxide. The determined dependence of the soluble portion of poly(*n*-alkyl methacrylates) points to the importance of the value of their initial molecular weights. Differences of the amounts of the soluble portion upon crosslinking of poly(*n*-alkyl methacrylates) of different alkyl lengths might be obscured as a result of different values of initial molecular weights.

Radical processes on crosslinking of poly(*n*-alkyl methacrylates) could go on according to the following scheme. Transfer reactions of cumyloxy radicals (or methyl radicals) with hydrogens of the polymer produce macroradicals. The formation of an unpaired electron on the alkyl in the side chain creates the prerequisite for further reactions, to some extent similar to reactions occurring upon decomposition of peroxides in polyolefins, whereby the probability of such reactions increases with increasing length of the alkyl. Recombination of two macroradicals leads to formation of C-C crosslinks, which in case of intermolecular recombination leads to formation of a crosslinked or branched structure. Disproportionation of macroradicals as well as intramolecular recombination are ineffective from the point of view of formation of a crosslinked product, as in both cases they reduce crosslinking efficiency.

Degradation of bonds in side chains of the macromolecule leads to formation of low molecular products as established by Fox et al.¹⁴ upon ultraviolet irradiation of poly(methyl acrylate). Analogically Burnett et al.¹⁵ established formation of gaseous products upon thermal block polymerization of *n*-propyl methacrylate and *n*-butyl methacrylate. They took these gaseous products for propylene and butylene and considered their formation to be a consequence of transfer reactions to the alkyl of the ester group and of subsequent degradation of the resulting macroradical. These reactions might also influence the crosslinking efficiency and the ratio of degradation and crosslinking, p/q .

Degradation of the main chain, which leads to reduction of the molecular weight of the polymer, can be imagined as being in accordance with the scheme given by Tobolsky and Norling¹⁶ for poly(methyl methacrylate).

The number of primary transfers of cumyloxy radicals to the hydrogens of the alkyl of the ester group of poly(*n*-alkyl methacrylate) will be higher in comparison with the number of transfers to the hydrogens of the $-\text{CH}_2-$ groups in the main chain, which are, in addition, hindered by the methyl and the ester group. The number of transfers to hydrogen atoms in the side chain will increase with increasing length of the alkyl of the ester group. This is indicated by the observed dependence of the decrease of the ratio p/q from poly(*n*-butyl methacrylate) to poly(*n*-nonyl methacrylate). If the value of p is constant, the ratio p/q will increase with decreasing q ; that is to say, if intramolecular recombination, disproportionation, and degradation of macroradicals having an unpaired electron in the side chain occur to a considerable extent, which is also indicated by low values of crosslinking efficiency, then the ratio p/q is higher than would correspond to the number of cleaved bonds in the main chain of the

macromolecule. Thus the ratio p/q does not reflect the real proportion of degradation and crosslinking reactions of poly(n -alkyl methacrylates). The relatively low values of crosslinking efficiencies of poly(n -butyl methacrylate) and poly(n -nonyl methacrylate) with regard to the values of the ratio p/q reflect exactly the high proportion of reactions of macroradicals not involving degrading (from the viewpoint of main chain cleavage) and crosslinking. Of course it should be taken into consideration whether all conditions necessary for the calculation of crosslinking efficiency were fulfilled. Owing to experimental difficulties the equilibrium volume fraction of the polymer v_2 in gel after its swelling was not determined. However, it can be concluded that the values v_2 are considerably low, which would indicate low values of crosslink concentration.

The values of the limiting viscosity number of poly(n -butyl methacrylate) are influenced also by branching of the macromolecule as well as degradation. The course of the dependence of the limiting viscosity number on concentration of decomposed dicumyl peroxide is different from the course of this dependence for atactic polypropylene and atactic poly-1-butene. In these two polymers, values of the limiting viscosity number decrease at the beginning and only later increase,¹⁷ which is the consequence of simultaneously proceeding crosslinking and degradation reactions. It can be concluded from the continuous increase of the limiting viscosity number of poly(n -butyl methacrylate) with increasing concentration of decomposed dicumyl peroxide that the influence of branching and degradation of macromolecules is overshadowed by crosslinking reactions of poly(n -butyl methacrylate) macroradicals.

The determination of the molecular weight of poly(n -nonyl methacrylate) by the light-scattering method was carried out by Mr. D. Lath.

References

1. A. R. Schultz and F. A. Bovey, *J. Polymer Sci.*, **22**, 485 (1956).
2. W. J. Burlant, J. Hinsch, and C. Taylor, *J. Polymer Sci. A*, **2**, 57 (1964).
3. R. K. Graham, *J. Polymer Sci.*, **38**, 209 (1959).
4. R. K. Graham, *J. Polymer Sci.*, **37**, 441 (1959).
5. J. Lal and J. E. McGrath, in *International Symposium on Macromolecular Chemistry, Prague, 1965* (*J. Polymer Sci. C*, **16**), O. Wichterle and B. Sedláček, Eds., Interscience, New York, 1966, p. 33.
6. G. Mantell, D. Rankin, and F. Galiano, *J. Appl. Polymer Sci.*, **9**, 3625 (1965).
7. T. A. Sokolova, L. A. Ovsyannikova, and I. I. Tikhodeeva, *Zh. Obshch. Khim.*, **33**, 1502 (1963).
8. D. F. Doehnert and O. L. Mageli, *Mod. Plastics*, **36**, 142 (1959).
9. M. Kurata and W. H. Stockmayer, *Fortschr. Hochpolymer.-Forsch.*, **3**, 196 (1963).
10. A. Charlesby and S. H. Pinner, *Proc. Roy. Soc. (London)*, **A249**, 367 (1959).
11. J. Bartoň and M. Lazár, in *International Symposium on Macromolecular Chemistry, Prague, 1965* (*J. Polymer Sci. C*, **16**), O. Wichterle and B. Sedláček, Eds., Interscience, New York, 1966, p. 361.
12. J. Bartoň, *Chem. Zvesti*, **20**, 169 (1966).
13. A. Charlesby, *Atomic Radiation and Polymers*, Pergamon Press, London, 1960, p. 132.

14. R. B. Fox, L. G. Isaacs, S. Stokes, and R. E. Kagarise, *J. Polymer Sci. A*, **2**, 2085 (1964).
15. G. M. Burnett, P. Evans, and H. W. Melville, *Trans. Faraday Soc.*, **49**, 1096, 1105 (1953).
16. A. V. Tobolsky and P. M. Norling, *J. Polymer Sci. A*, **3**, 1435 (1965).
17. J. Bartoň and E. Stehliková, *Vysokomolekul. Soedin.*, **9B**, 734 (1967).

Received November 4, 1967

Determination of Propagation and Termination Rate Constants for Some Methacrylates in Their Radical Polymerizations

KENJI YOKOTA,* MASARU KANI, and YOSHIO ISHII,
*Department of Synthetic Chemistry, Faculty of Engineering,
 Nagoya University, Nagoya, Japan*

Synopsis

Rotating sector determinations of k_p and $2k_t$ for ten methacrylates undergoing radical polymerization were carried out at 30°C. Ester groups in the monomers were: isopropyl, ethyl, β -cyclohexylethyl, methyl, γ -phenylpropyl, β -phenylethyl, β -methoxyethyl, benzyl, β -chloroethyl, and phenyl. Values of k_p obtained were 121, 126, 1190, 141, 149, 228, 249, 1250, 254, and 411 l./mole-sec., respectively; values of $2k_t \times 10^{-6}$ were 4.52, 7.35, 32.8, 11.6, 0.813, 1.88, 9.30, 41.9, 6.71, and 11.9 l./mole-sec., respectively.

Omitting the data for the β -cyclohexylethyl and benzyl esters, a Taft correlation, $\log k_p = (0.70 \pm 0.18)\sigma^* + 2.2$, was established, where σ^* denotes Taft's polar substituent constants for the above-mentioned ester groups. The steric substituent constants E_s were found to have no influence on k_p . Combination of k_p with τ_2 data from copolymerization studies with styrene or methyl methacrylate as M_1 comonomer revealed that the more reactive monomer gave rise to the more reactive polymer radical. Monomer viscosities and molar volumes of the ester groups were found to correlate with $2k_t$.

INTRODUCTION

A satisfactory, precise quantitative correlation of reactivities of vinyl monomers and of derived radicals with their structures has not yet been achieved. In the homopolymerization process, the rate of propagation of a given monomer involves two separate reactivities, i.e., that of monomer and that of the derived radical; the latter is considered to be more important. Hence as a whole, a monomer with larger resonance contribution is more reactive, gives rise to a less reactive radical, and consequently shows a smaller k_p value.

A detailed correlation requires a study of monomers in which systematic structural variations have been made. Recent studies by Imoto et al.^{1,2} on *p*-substituted styrenes established the Hammett correlations of propagation rate constants, of reactivities of monomers, and of derived radicals. In this paper, a rotating sector determination of a series of methacrylate monomers is described, and Taft correlations of k_p and of derived radical reactivities are discussed. Termination rate constants $2k_t$ were also correlated with monomer structures.

* Present address: Nagoya Institute of Technology, Nagoya, Japan.

EXPERIMENTAL

Preparation and Purification of Monomers

Methyl methacrylate was kindly supplied by the Mitsubishi Rayon Co. Ltd. Ethyl methacrylate was the commercially available product. β -Cyclohexylethyl, γ -phenylpropyl, β -phenylethyl, β -methoxyethyl, benzyl, and β -chloroethyl methacrylates were prepared in nearly quantitative yields by ester exchange between appropriate alcohols and a 4*M* excess of methyl methacrylate free from inhibitor in the presence of a small amount of *p*-toluenesulfonic acid as a catalyst. Isopropyl methacrylate was prepared similarly but with an excess of isopropyl alcohol. Phenyl methacrylate was prepared by the reaction of methacryl chloride and sodium phenoxide in water. The crude monomers were repeatedly fractionated through a Widmer column under nitrogen at reduced pressure until impurities (mostly alcohols) were not detected by gas chromatography. Non-volatile cuprous chloride was used as inhibitor. Monomers were identified by their boiling points, refractive indices, infrared, ultraviolet, and nuclear magnetic resonance spectra, as well as elementary analyses for some polymers. These results are given in part in Table I.

The monomers thus prepared were washed with saturated sodium bisulfite, 5% sodium hydroxide, 20% sodium chloride, and distilled water successively, dried over anhydrous sodium sulfate, distilled, and stored in a refrigerator. They were again distilled after prepolymerization immediately before use.

Other Reagents

α,α' -Azobisisobutyronitrile (AIBN), commercially available, was recrystallized twice from ethyl alcohol, m.p. 102–103°C. α,α' -Azobiscyclohexanecarbonitrile was prepared according to Overberger's description⁴ and recrystallized twice from ethyl alcohol, m.p. 113–114°C. β,β -Diphenyl- α -picrylhydrazyl (DPPH), commercially available, was recrystallized twice from benzene–petroleum ether and obtained as the benzene complex, m.p. 132–133°C. Benzene was successively washed with concentrated sulfuric acid, dilute sodium hydroxide, and distilled water, dried over calcium chloride, and fractionated under nitrogen.

Density Measurements

Densities of monomers and monomer–polymer mixtures were measured in a pycnometer at 30.0°C., and the results were used to calibrate the dilatometry.

Viscosity Measurements

Viscosities of monomers were measured at 30.0°C. with an Ostwald viscometer. Solution viscosities of polymers (η_{sp}/c) were measured also with an Ostwald viscometer at the same temperature in benzene, $c = 0.3$ g./100 ml.

TABLE I
 Properties of Monomers^a

Ester group	Boiling point, °C./mm. Hg	n_D^{20}	d_{40}^{30} g./cc.	d_{40}^{30} (polymer)	η_{inh}^{30} cP.	Found ^b C, %	Found ^b H, %	Calcd. C, %	Calcd. H, %
Isopropyl	65-67/95 (120/760)	1.4107 ²⁰ (1.4122 ²⁰)	0.8765	1.0505	0.610	65.35	9.16	65.59	9.44
Ethyl	116-117/760 (116-117/760)	1.4120 ²¹ (1.4147 ²⁰)	0.9045 (0.9135 ²⁰)	1.0795	0.565				
β -Cyclohexylethyl	99-102/3	1.4641 ¹⁸	0.9423	1.0613	2.79	73.81	10.30	73.43	10.27
Methyl	33-34/55 (100/760)	1.4163 ²¹ (1.4162 ²⁰)	0.9296 (0.9313)	1.2036 (1.1834)	0.516				
γ -Phenylpropyl	108-114/3	1.5084 ²¹	0.9967	1.1097	3.42				
β -Phenylethyl	100-105/3 (110-117/5)	1.5058	1.0123 (1.0018)	1.1427	2.98				
β -Methoxyethyl	75-76/22 (65-67/10)	1.4280 ²¹ (1.4283 ²¹)	0.9818 (0.990 ²⁰)	1.1378 1.18	1.03	57.65	8.33	57.31	8.39
Benzyl	88-90/3 (104-106/6)	1.5112 ²¹ (1.514 ²⁰)	1.0299	1.1819	2.09				
β -Chloroethyl	81-85/42 (61-64/11)	1.4498 ¹⁸ (1.4515 ²⁰)	1.0942 (1.106 ²⁰)	1.3002	0.933	49.02	6.21	48.50	6.11
Phenyl	81-82/5 (83-84/4)	1.5149 ²¹ (1.5156 ²⁰)	1.0485 (1.053 ²⁰)	1.1665	3.14	73.77	6.45	74.05	6.21

^a Values in parentheses are literature values.³^b Analysis of polymer samples.

Rate of Polymerization

Rates of polymerization were followed by dilatometry. Gravimetric experiments in sealed ampules gave satisfactory agreement with dilatometric results.

Rate Dependences on Monomer Concentration and on Initiator Concentration

Those experiments were carried out at $30.0 \pm 0.005^\circ\text{C}$. in the dark in a 10-ml. glass ampule connected with a capillary tube. Freshly distilled monomer, AIBN, and benzene were taken in a calibrated ampule. The contents were subjected to repeated freezing, pumping, and thawing under nitrogen (purified on hot copper net) and finally *in vacuo*. Then the contents were transferred to a polymerization ampule *in vacuo*, sealed off, and subjected to polymerization in a bath at a constant temperature. The concentration of initiator was $2\text{--}20 \times 10^{-2}$ mole/l. in neat monomer. The concentration of monomer examined ranged from bulk to 1 mole/l. in benzene.

Rate of Initiation

Rates of initiation were determined under the same conditions as above but with a small amount of DPPH in 80 vol.-% of monomer in benzene and calculated from the inhibition periods and the amounts of added inhibitor.

Radical Lifetime

Radical lifetimes were determined by the rotating sector method. Polymerizations were carried out in thin drum-shaped Pyrex ampules by use of azobiscyclohexanecarbonitrile as sensitizer under illumination with a 300 w. mercury lamp through a slit and a Toshiba UVD1C filter (passes 340–380 $m\mu$). The sector was made of a 60-cm. diameter black aluminum disk cut off at two positions so that the dark to light period ratio was three. The sector was driven by a 10-w. reaction synchronous motor 4SQ10 (Oriental Motor Co. Ltd.) and its speeds were accurately varied by using several combinations of gear heads (supplied by the same maker). Corrections for the dark rates were made according to the equations derived by Matheson et al.⁵ [eqs. (6), (7), and (8) in their paper]. Computed figures for the corrections are collected in Table II.

Copolymerization

Copolymerizations with styrene or methyl methacrylate were carried out for isopropyl and β -methoxyethyl methacrylates at 60°C . with AIBN to less than 10% conversions. Copolymer compositions were calculated from carbon contents for styrene copolymers and from appropriate NMR peak area ratios for methyl methacrylate copolymers.

TABLE II
Theoretical Values of $(p + 1)^{1/2}R_{pt}/R_p$, $p = 3$ as a Function of Flash Time t and Dark Rate/Steady Light Rate $\eta^{1/2}$ a

Flash time t , sec.	$(p + 1)^{1/2}R_{pt}/R_p$															
	$\eta^{1/2} = 0$	$\eta^{1/2} = 0.01$	$\eta^{1/2} = 0.02$	$\eta^{1/2} = 0.03$	$\eta^{1/2} = 0.04$	$\eta^{1/2} = 0.05$	$\eta^{1/2} = 0.06$	$\eta^{1/2} = 0.07$	$\eta^{1/2} = 0.08$	$\eta^{1/2} = 0.09$	$\eta^{1/2} = 0.10$	$\eta^{1/2} = 0.11$	$\eta^{1/2} = 0.12$	$\eta^{1/2} = 0.13$	$\eta^{1/2} = 0.14$	$\eta^{1/2} = 0.15$
0.1	0.9991	0.9992	0.9997	1.0004	1.0015	1.0028	1.0045	1.0064	1.0086	1.0112	1.0140	1.0171	1.0205	1.0242	1.0281	1.0323
0.2	0.9963	0.9965	0.9969	0.9977	0.9987	1.0001	1.0017	1.0036	1.0059	1.0085	1.0113	1.0145	1.0178	1.0216	1.0255	1.0298
0.3	0.9919	0.9920	0.9925	0.9932	0.9943	0.9957	0.9974	0.9993	1.0016	1.0042	1.0070	1.0102	1.0136	1.0174	1.0214	1.0257
0.5	0.9787	0.9789	0.9794	0.9802	0.9813	0.9827	0.9844	0.9865	0.9888	0.9915	0.9944	0.9977	1.0012	1.0051	1.0092	1.0137
0.7	0.9616	0.9618	0.9623	0.9631	0.9643	0.9658	0.9676	0.9697	0.9722	0.9749	0.9780	0.9814	0.9852	0.9892	0.9935	0.9981
1	0.9326	0.9328	0.9333	0.9342	0.9355	0.9371	0.9390	0.9414	0.9440	0.9470	0.9504	0.9541	0.9581	0.9625	0.9671	0.9721
2	0.8440	0.8442	0.8450	0.8462	0.8479	0.8501	0.8528	0.8559	0.8595	0.8636	0.8681	0.8730	0.8784	0.8841	0.8903	0.8968
3	0.7838	0.7842	0.7851	0.7867	0.7889	0.7918	0.7952	0.7993	0.8039	0.8090	0.8147	0.8209	0.8276	0.8347	0.8423	0.8503
5	0.7140	0.7145	0.7159	0.7182	0.7214	0.7255	0.7304	0.7361	0.7425	0.7496	0.7573	0.7656	0.7744	0.7836	0.7933	0.8034
7	0.6745	0.6751	0.6769	0.6800	0.6841	0.6894	0.6956	0.7027	0.7106	0.7191	0.7283	0.7381	0.7483	0.7590	0.7700	0.7814
10	0.6386	0.6395	0.6420	0.6460	0.6515	0.6583	0.6661	0.6748	0.6844	0.6945	0.7053	0.7164	0.7280	0.7399	0.7521	0.7645
20	0.5858	0.5874	0.5919	0.5989	0.6076	0.6176	0.6286	0.6402	0.6523	0.6648	0.6777	0.6907	0.7040	0.7175	0.7310	0.7448
30	0.5638	0.5661	0.5723	0.5813	0.5918	0.6034	0.6157	0.6285	0.6416	0.6549	0.6684	0.6822	0.6960	0.7100	0.7240	0.7382
50	0.5433	0.5469	0.5556	0.5668	0.5791	0.5921	0.6054	0.6191	0.6329	0.6469	0.6611	0.6753	0.6896	0.7040	0.7184	0.7329
70	0.5333	0.5380	0.5483	0.5606	0.5737	0.5872	0.6010	0.6151	0.6292	0.6435	0.6579	0.6724	0.6869	0.7014	0.7160	0.7306
100	0.5251	0.5312	0.5428	0.5559	0.5696	0.5835	0.5977	0.6120	0.6265	0.6410	0.6555	0.6701	0.6848	0.6995	0.7142	0.7290
200	0.5143	0.5231	0.5364	0.5504	0.5648	0.5793	0.5939	0.6085	0.6232	0.6380	0.6528	0.6676	0.6824	0.6972	0.7121	0.7270
300	0.5102	0.5204	0.5343	0.5486	0.5632	0.5778	0.5926	0.6073	0.6222	0.6370	0.6518	0.6667	0.6816	0.6965	0.7114	0.7263

a According to eqs. (6), (7), and (8) of Matheson et al.⁵ R_p = rate of polymerization in steady light, R_{pt} = rate of polymerization in flash time t , p = dark to light period ratio.

RESULTS

From the rate dependences on initiator and monomer concentrations collected in Table III, it is clear that the present polymerizations can be treated by the four simple reactions given in eqs. (1)–(4).



with $R_i = 2k_d f [I]$



with $R_p = k_p [M_j \cdot] [M] = k_p (k_d f / k_t)^{1/2} [M] [I]^{1/2}$



with $R_t = 2k_t [M \cdot]^2$

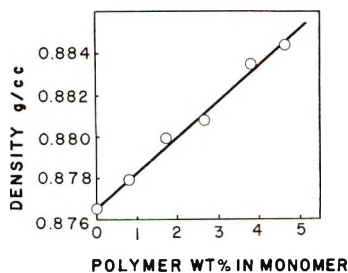


Fig. 1. Densities of monomer and monomer-polymer mixtures for isopropyl methacrylate.

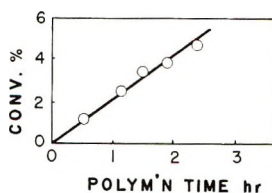


Fig. 2. Comparison of (—) dilatometric and (O) gravimetric determinations of rate of polymerization for isopropyl methacrylate.

Because of the kinetic results and of the fairly high specific viscosities of isolated polymers (Table III), degradative chain transfer or other unimolecular terminations are not important. Rate dependences on monomer concentration were over unity for some monomers, and in such cases, however, it had been consistently attributed to the complication in the initiation stage⁶ and also need not be considered here. Since rates of polymerization after the consumption of DPPH were only slightly smaller than that without inhibitor, the rate of initiation R_i and the radical lifetime τ determined separately were combined to calculate the propagation rate

TABLE III
Rate Constants and Related Quantities for the Radical Polymerizations of Methacrylates at 30°C.

Ester group	m^a	n^a	$R_i \times 10^9$, mole/l.-sec. ^b	f^c	$k_p^2/2k_t \times 10^3$, l./mole-sec.	τ , sec. ^d	$k_p/2k_t \times 10^5$	k_{tr} , l./mole-sec.	$2k_t \times 10^{-6}$, l./mole-sec.	η_{sp}/c , dl./g. ^e
Isopropyl	1.00	0.50	9.30	0.69	3.22	2.30	2.67	121	4.52	4.3
Ethyl	1.00	0.50	10.1	0.74	2.17	1.84	1.72	126	7.35	3.6
β -Cyclohexylethyl	1.12	0.50 _s	2.85	0.22	43.0	1.29	3.63	1190	32.8	6.1
Methyl	1.00	0.50	8.25	0.63	1.71	1.56	1.21 _s	141	11.6	3.9
γ -Phenylpropyl	1.00	0.51	5.00	0.38	27.0	5.90	18.1	149	0.813	6.4
β -Phenylethyl	1.11	0.50	6.78	0.52	27.6	4.81	12.3	228	1.88	3.2
β -Methoxyethyl	0.98	0.52	8.33	0.63	6.67	1.40	2.68	249	9.30	1.2
Benzyl	1.15	0.51	3.62	0.27	37.5	1.26	2.99	1250	41.9	5.4
β -Chloroethyl	1.00	0.50	7.63	0.58	9.95	2.70	3.85	254	6.71	1.2
Phenyl	1.10	0.50	7.93	0.60	15.3	1.70	3.46	411	11.9	3.2

^a In $R_p = k_p(k_{tr}/k_t)^{1/2}[M]^m[I]^n$.

^b $[I] = 5 \times 10^{-7}$ /sec. $[M] = 80$ vol.-% in benzene.

^c $k = 1.31 \times 10^{-7}$ /sec. assumed, $f = R_i/2k_d[I]$.

^d $[I] = 4.10 \times 10^{-3}$ mole/l., monomer bulk.

^e Measured in benzene at 30°C., $c = 0.3$ g./100 ml. for the polymer obtained at $[I] = 5 \times 10^{-2}$ mole/l., $[M] = 80$ vol.-% in benzene.

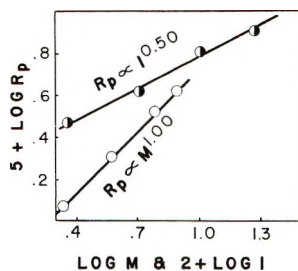


Fig. 3. Rate dependences on (●) initiator concentration and (○) on monomer concentration for isopropyl methacrylate.

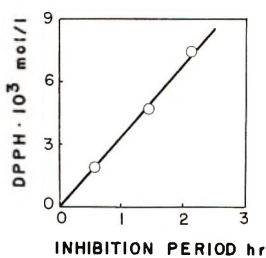


Fig. 4. Determination of rate of initiation for isopropyl methacrylate.

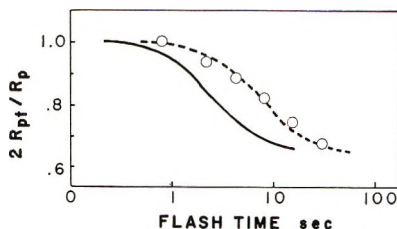


Fig. 5. Determination of radical lifetime for isopropyl methacrylate: (—) $\tau = 1$ sec, dark rate/steady light rate = 0.07; (- - -) $\tau = 2.30$ sec. (R_p = rate of polymerization in steady light, R_{pt} = rate of polymerization in flash time t .)

constant k_p and the termination rate constant $2k_t$ according to eqs. (5) and (6):

$$k_p^2/2k_t = R_p^2/R_i[M]^2 \quad (5)$$

$$k_p/2k_t = R_p\tau/[M] \quad (6)$$

Typical results of a series of experiments are shown in Figures 1–5 for isopropyl methacrylate, and satisfactory plots are observed. All results are summarized in Table III.

For methyl methacrylate, $k_p = 141$ l./mole-sec. and $2k_t = 11.6 \times 10^6$ l./mole-sec. are obtained. These values are in good accordance with the values, $k_p = 143$ l./mole-sec. and $2k_t = 12.2 \times 10^6$ l./mole-sec. at 30°C . reported by Matheson et al.,⁵ whose description of the apparatus and

calculation we followed. We estimate, however, that the accumulated experimental errors may amount to about $\pm 40\%$ at the final k_p and $2k_t$ values.

The more important problem is the discrepancies among reported k_p values far beyond the experimental errors for a given monomer by several investigators. For example, Table IV shows the compiled k_p values⁷ for

TABLE IV
 k_p for Methyl Methacrylate^a

k_p , l./mole-sec.	Temperature, °C.	Method
143	30	Rotating sector
310 \pm 20	23.6	"
410 \pm 50	35.9	"
248	30	"
512.6	25	"
128	22	Single period, highly sensitive dilatometer
106	32	Single period, thermocouple
384	22.5	" "

^a Literature values for k_p .⁷

methyl methacrylate at about 30°C. There is a fivefold difference between the largest and the smallest values. Matheson⁸ thoroughly discussed this problem, without fully revealing the cause. We consider that a series of experiments by one investigator's apparatus would greatly minimize systematic errors at least, and the results of such experiments should be useful for the discussion of the relative reactivities.

Copolymerization experiments afforded the following four sets of monomer reactivity ratios obtained by the Fineman-Ross plots. Errors were calculated at the level of 95% confidence: For styrene (M_1) and isopropyl methacrylate, $r_1 = 0.47 \pm 0.06$ and $r_2 = 0.74 \pm 0.05$; for styrene (M_1) and β -methoxyethyl methacrylate, $r_1 = 0.50 \pm 0.01$ and $r_2 = 0.58 \pm 0.04$; for methyl methacrylate (M_1) and isopropyl methacrylate, $r_1 = 0.89 \pm 0.21$ and $r_2 = 1.20 \pm 0.20$; for methyl methacrylate (M_1) and β -methoxyethyl methacrylate, $r_1 = 0.86 \pm 0.11$ and $r_2 = 1.06 \pm 0.11$.

DISCUSSION

From the individual rate constants of ten methacrylates as summarized in Table III, the correlations between rate constants and monomer structures can be discussed. It seems that the Taft polar and steric substituent constants, σ^* and E_s , are most adequate to characterize the electronic and spatial natures of ester groups.^{9,10} Substituent constants for the ten ester groups studied are collected in Table V, a part of which is estimated as indicated.

TABLE V
Taft Substituent Constants for the Ester Groups

Ester group	σ^{*a}	E_s^b
Isopropyl	-0.190	-0.47
Ethyl	-0.100	-0.07
β -Cyclohexylethyl	-0.02 ^c	
Methyl	0.00	0.00
γ -Phenylpropyl	0.020	-0.45
β -Phenylethyl	0.080	-0.43
β -Methoxyethyl	0.19 ^c	-0.77
Benzyl	0.215	-0.38
β -Chloroethyl	0.385	-0.90
Phenyl	0.600	-0.90

^a Data of Taft.⁹

^b Data of Taft.¹⁰

^c Estimated as $\sigma^*/2.8$ for the NCH_2 group.¹¹

Rate of Propagation

Propagation rate constants k_p are plotted against σ^* values in Figure 6. In spite of inevitable experimental errors in obtaining individual k_p as estimated in the Results section, we find an essential increase of k_p as σ^* becomes larger with a correlation coefficient of 0.99. In other words, the monomer with the stronger electron-attracting ester group tends to propagate with greater ease. β -Cyclohexylethyl and benzyl monomers show extraordinarily large k_p . These monomers will be discussed later and are omitted as exceptions in the following analysis. Application of the method of regression analysis gives slope = $+0.70 \pm 0.18$ at the level of 95% confidence. The scatterings of individual determinations as in Figures 1-5 reflect an inaccuracy of the slope of ± 0.18 . The estimation of experimental errors up to $\pm 40\%$ in the Results section is apparently too large. The absence of any steric effect of ester groups on k_p is clear from Figure 7, where the benzyl monomer is again an exception. (The E_s value for the β -cyclohexylethyl group is not known.) Hence the Taft-Ingold or the Taft equation

$$\log(k/k_0) = \rho^*\sigma^* + \delta E_s \quad (7)$$

for the present reaction reduces to

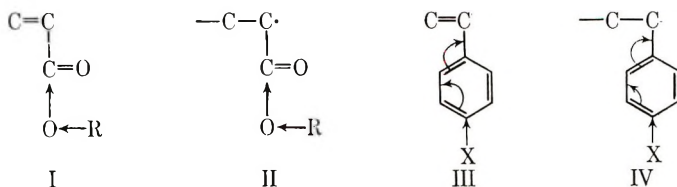
$$\log k_p = 0.70\sigma^* + 2.2 \quad (8)$$

Burnett et al.¹² and Grant and Grassie¹³ concluded that k_p values remained virtually constant and independent of the ester groups from their experiments on methyl, *n*-propyl, *n*-butyl, and *tert*-butyl methacrylates. The apparent disagreement with our conclusion unquestionably comes from the difference in the range of polar character of ester groups examined.

Imoto et al.¹ obtained a similar relationship for a series of *p*-substituted styrenes, where

$$\log k_{pX}/\log k_{pH} = +0.6\sigma \quad (9)$$

and X = *p*-methoxy, *p*-methyl, *p*-fluoro, *p*-chloro, *p*-bromo, *p*-cyano, and hydrogen. It is interesting to note that in the present methacrylate system, there is no direct conjugation between a vinyl group or unpaired electron and ester group R, (I and II), whereas there is in the styrene



system, (III and IV), and that the reaction constant ρ^* for the present nonconjugative system is not smaller than that for a conjugative styrene system.

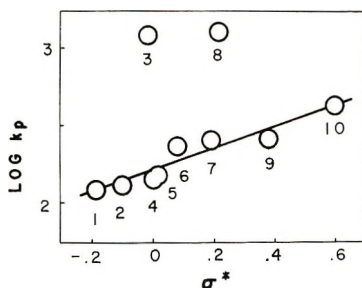


Fig. 6. Taft correlation between $\log k_p$ and σ^* of ester groups: (1) isopropyl; (2) ethyl; (3) β -cyclohexylethyl; (4) methyl; (5) γ -phenylpropyl; (6) β -phenylethyl; (7) β -methoxyethyl; (8) benzyl; (9) β -chloroethyl; (10) phenyl.

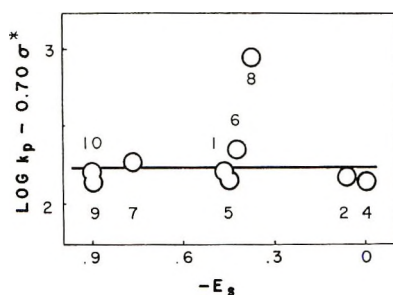


Fig. 7. Taft correlation between $\log k_p - 0.70\sigma^*$ and E_s of ester groups. (1)–(10) as in Fig. 6.

Ötsu et al.¹⁴ studied the relative reactivities ($1/r_1$) of methacrylate monomers towards the polystyrene radical and established the Taft equation,

$$\log 1/r_1 = +0.33\sigma^* + \text{constant} \quad (10)$$

Similar correlation of the relative reactivities of methacrylates towards the poly(methyl methacrylate) radical from the data reported by Bevington and Malpass,¹⁵ by Ōtsu et al.,¹⁶ and by Yokota and Ishii¹⁷ gives

$$\log 1/r_1 \simeq +0.2\sigma^* + \text{constant} \quad (11)$$

again with a positive slope. These results indicate that a monomer with a stronger electron-attracting ester group is more reactive towards two reference polymer radicals. This was attributed¹⁶ to the larger resonance contribution of such monomers.

Combination of r_2 from such copolymerization studies with k_p from the present study enables us to discuss the relative reactivities (k_{21}) of various polymethacrylate radicals as shown in Table VI.

$$k_{21} = k_p/r_2 \quad (12)$$

TABLE VI

Ester group	Reactivity vs. styrene		Reactivity vs. methyl methacrylate	
	r_2	k_{21} , l./mole-sec.	r_2	k_{21} , l./mole-sec.
Isopropyl	0.74	164	1.20	101
Ethyl	0.41 ^a	308	1.08 ^b	117
Methyl	0.46 ^a	307	1.0	141
β -Phenylethyl	0.51 ^c	443	1.33 ^c	171
β -Methoxyethyl	0.60	415	1.06	235
Benzyl	0.51 ^a	2540	1.05 ^b	1190
β -Chloroethyl	0.46 ^d	552	1.13 ^d	225
Phenyl	0.60 ^a	685	1.72 ^b	239

^a Data of Ōtsu et al.¹⁴

^b Data of Bevington and Malpass.¹⁵

^c Data of Yokota and Ishii.¹⁷

^d Data of Ōtsu et al.¹⁶

The difference of reaction temperature (60°C. for copolymerization and 30°C. for homopolymerization) is not considered. Figure 8 shows the correlations of such reactivities with σ^* values of ester groups towards styrene and methyl methacrylate. The slopes, i.e., the reaction constant ρ^* , were calculated as 0.68 ± 0.25 for styrene and 0.48 ± 0.30 for methyl

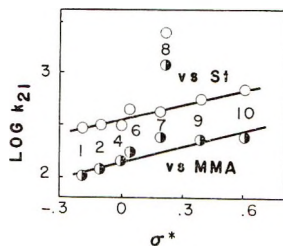


Fig. 8. Taft correlations of polymer radical reactivities and σ^* of ester groups: (○) reactivity vs. styrene; (●) reactivity vs. methyl methacrylate; (1)–(10) as in Fig. 6.

methacrylate. We can safely conclude that a polymethacrylate radical with a stronger electron-attracting ester group is more reactive towards the both reference monomers of opposite polar characters and that the more reactive monomer gives rise to the more reactive polymer radical, contrary to the general picture in vinyl polymerization. The explanation of reactivities based on the resonance contribution is invalidated and the polar contribution should be important, although the precise scheme is not clear. It should be noted that the sum of σ^* in eq. (11) and that from Figure 8 (0.48 ± 0.30) is roughly equal to σ^* in eq. (8).

Rate of Termination

Unlike the k_p values above discussed, termination rate constants $2k_t$ can not be arranged according to the polar character of ester groups. As to the theory of the rate of termination reaction of vinyl radical polymerization, the most plausible may be the diffusion-controlled mechanism developed by North.¹⁸ According to this theory, the termination process consists of three stages; the first stage is a translational diffusion of two polymer radicals to a proximity, the second, concluded by North to be rate-determining, is a segmental diffusion of both chains, and the third is a chemical interaction between two radicals to produce one or two inactive polymer chains. Ōtsu et al.¹⁹ reported a linear correlation between $k_p/k_t^{1/2}$

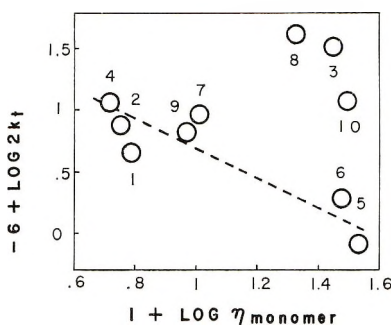


Fig. 9. Correlation between termination rate constant $2k_t$ and monomer viscosity.

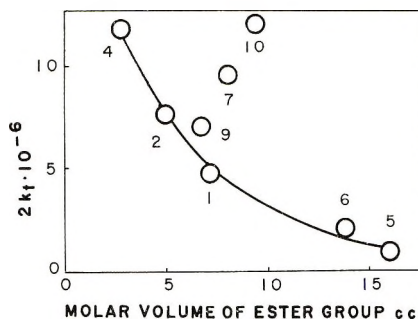


Fig. 10. Correlation of termination rate constant $2k_t$ and molar volume of ester group.

and reciprocals of viscosities of eleven alkyl methacrylates. Now it is possible to discuss $2k_t$ directly instead of the complex $k_p/k_t^{1/2}$. In Figure 9, $2k_t$ and η_{monomer} are plotted in logarithmic scale. It is necessary to omit as before the points for the β -cyclohexylethyl and benzyl esters as well as the point (10) for the phenyl ester, which is only one phenolic ester, to find a rough correlation. In addition, when $2k_t$ and molar volumes of ester groups are plotted in Figure 10, an inversely proportional relationship is observed.* North²⁰ showed that the rate of termination should be inversely proportional to the macroscopic viscosity of the system and to the square root of some characteristic segmental chain length. Here the involvements of monomer viscosity and steric factor of the side chain are meaningful, although the correlation is yet unsatisfactory.

Rate of Initiation

Because of the difficulties in obtaining the rate of initiation R_i , it is difficult to correlate it with structure. In Table III, R_i is transformed into the more straightforward quantity f , initiation efficiency by using the relation

$$R_i = 2k_d f [I] \quad (13)$$

with $k_d = 1.31 \times 10^{-7}/\text{sec.}$ at 30°C. , as calculated by the equation of Van Hook and Tobolsky.²¹ With few exceptions, f values fall in the range of 0.5–0.8. Points (3) and (8), which showed extraordinarily large k_p , are again exceptions and show small f . It is conceivable for these anomalies that some transfer reactions might be involved; (3) β -cyclohexylethyl has tertiary hydrogen and benzyl has a benzylic hydrogen. But, this is puzzling, as some of other monomers also have such active and easily abstractable hydrogens. Moreover, the monomers which show anomalous behavior exhibit regular kinetics as described before. Monomer reactivities in copolymerizations and tacticities of polymers²² are also regular. Further investigations are necessary to clarify this.

References

1. M. Imoto, M. Kinoshita, and M. Nishigaki, *Makromol. Chem.*, **86**, 217 (1965).
2. M. Imoto, M. Kinoshita, and M. Nishigaki, *Makromol. Chem.*, **94**, 238 (1966).
3. J. Kumanotani, R. Ishino, M. Kurokawa, and C. Matsuyama, *Kōbunshi Kagaku*, **11**, 929 (1962).
4. C. G. Overberger, M. T. O'Shaughnessy, and H. Shalit, *J. Am. Chem. Soc.*, **71**, 2661 (1949).
5. M. S. Matheson, E. E. Auer, E. B. Bevilacqua, and E. J. Hart, *J. Am. Chem. Soc.*, **71**, 497 (1949).
6. A. D. Jenkins, *J. Polymer Sci.*, **29**, 215 (1958).
7. J. Brandrup and E. H. Immergut, *Polymer Handbook*, Interscience, New York, 1966, p. II-59.
8. M. S. Matheson, E. E. Auer, E. B. Bevilacqua, and E. J. Hart, *J. Am. Chem. Soc.*, **73**, 1700 (1951).

* For the deviation of point (7), a transfer reaction to the ether methylene group may be involved. Rate dependence on initiator concentration is slightly smaller than unity.

9. R. W. Taft, Jr., *J. Am. Chem. Soc.*, **75**, 4231 (1953).
10. R. W. Taft, Jr., *J. Am. Chem. Soc.*, **74**, 3120 (1952).
11. R. W. Taft, Jr., in M. S. Newman, *Steric Effects in Organic Chemistry*, Wiley, New York, 1956, Chap. 13.
12. G. M. Burnett, P. Evans, and H. W. Melville, *Trans. Faraday Soc.*, **49**, 1096, 1105 (1953).
13. D. H. Grant and N. Grassie, *Trans. Faraday Soc.*, **55**, 1042 (1959).
14. T. Ōtsu, T. Itō, and M. Imoto, *J. Polymer Sci. B*, **3**, 113 (1965).
15. J. C. Bevington and B. W. Malpass, *European Polymer J.*, **1**, 19 (1965).
16. T. Ōtsu, T. Itō, and M. Imoto, *Kōgyō Kagaku Zasshi*, **69**, 986 (1966).
17. K. Yokota and Y. Ishii, *Kōgyō Kagaku Zasshi*, **69**, 1057 (1966).
18. A. M. North, *Quart. Rev. (London)*, **20**, 421 (1966).
19. T. Ōtsu, T. Itō, and M. Imoto, *J. Polymer Sci. A*, **2**, 2901 (1964).
20. S. W. Benson and A. M. North, *J. Am. Chem. Soc.*, **84**, 935 (1962).
21. J. P. Van Hook and A. V. Tobolsky, *J. Am. Chem. Soc.*, **80**, 779 (1958).
22. K. Yokota, unpublished data.

Received September 20, 1967

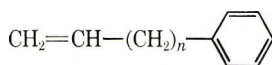
Synthesis and Crystal Structure of Isotactic Poly-4-phenyl-1-butene

F. J. GOLEMBA, J. E. GUILLET, and S. C. NYBURG,
Department of Chemistry, University of Toronto, Toronto, Ontario, Canada

Synopsis

Poly-(4-phenyl-1-butene) was prepared by using a titanium tetrachloride-triethylaluminum catalyst. The crystalline polymer melts at 158°C. Double orientation could not be obtained but all the reflections on the x-ray fiber diagram can be indexed on the basis of a hexagonal cell ($a = 20.8$ Å., c (fiber repeat) = 6.61 Å.). However the crystal structure proposed does not belong to a hexagonal space group but to the monoclinic (pseudo-orthorhombic) space group Pa ($a = 10.4$ Å., $b = 18.0$ Å., $c = 6.61$ Å.). The 3_1 helix, common to systems of this type, is consistent with an isotactic (not syndiotactic) configuration for the polymer chain.

Polyolefins from monomers of the general type:



are of interest because the presence of the bulky phenyl ring places steric constraint on the possible modes of packing. The first member of this series, crystalline polystyrene, was shown by Natta¹ to crystallize as 3_1 helices with six helices to the hexagonal unit cell, space group $R\bar{3}c$ or $R3c$, and with a calculated crystalline density of 1.124 g./cc.

In the present work a higher homolog ($n = 2$) of styrene was studied and the crystal structure compared to that of polystyrene.

Polymerization

4-Phenyl-1-butene was distilled from lithium hydride through a packed column under reduced pressure. Polymerizations were carried out under nitrogen in sealed bottles as follows.

Freshly distilled 4-phenyl-1-butene (10.0 ml., 0.076 mole) was added to 8.0 ml. (0.0056 mole) of triethylaluminum solution, (0.7*mM* in heptane) and 7.5 ml. (0.0053 mole) of titanium tetrachloride solution (0.7*mM* in heptane) under an atmosphere of dry nitrogen.

The bottles were sealed and shaken at 55°C. for one week. The catalyst was deactivated with ethanol, and the polymer was precipitated in ethanol in a Waring Blendor. It was then filtered, washed with ethanol, and dried in air. The yield of solid polymer ranged from 10–40%.

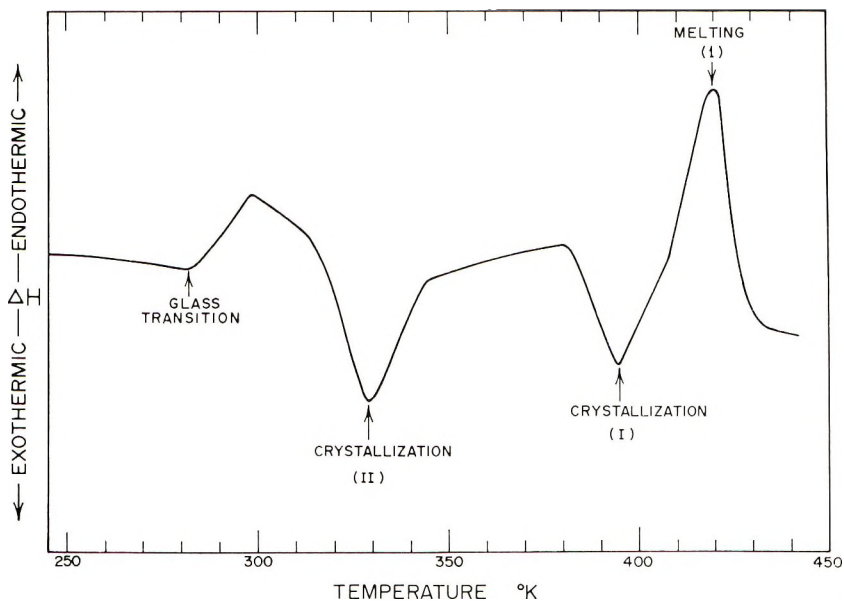


Fig. 1. DSC curve of poly-4-phenyl-1-butene.

The polymer was a white, powdery solid with a crystalline melting point of 158°C., measured by disappearance of birefringence on a hot-stage microscope. The intrinsic viscosity $[\eta]$ of the polymer determined at 80°C. in tetralin was 0.63 dl./g.

Differential Thermal Analysis

A Perkin-Elmer differential scanning calorimeter was used to study the thermal properties of the polymer. A typical scan in which the slope of the machine has been adjusted to give a zero slope for the amorphous polymer is shown in Figure 1. A positive increase in slope characteristic of the glass transition of the amorphous, non-oriented polymer² occurred at about 10°C. The region of the scan between 40 and 160°C. contained two exotherms and an endotherm. By holding the sample at the crystallization temperature (I) for extended periods, the melting peak increased in area, indicating the polymer must be annealed at elevated temperatures to reach maximum crystallinity.

If the sample was kept at the crystallization temperature (II) for several minutes an endotherm appeared on the scan over a temperature range of 59–69°C. An increase in the area of the endotherm resulted when the sample was annealed at 54°C. for extended periods. The exotherm, designated crystallization (II), is attributed to a second crystalline form of poly-4-phenyl-1-butene.

The samples for x-ray examination were annealed for 1 week under vacuum at 120°C. A scan of these samples from 20–170°C. showed only one melting peak and no crystallization peak indicating the sample

contained only one crystalline form. From five DSC curves for these samples a value of the molar heat of fusion ΔH_m (850 cal./monomer unit with a standard deviation of 30 cal./monomer unit) was obtained.

X-Ray Examination

For x-ray studies the polymer was extracted with boiling methyl ethyl ketone and the insoluble fraction dried in air. It was then molded in a Carver press into rectangular pellets at 160°C. and 15,000 psi.³ Samples were stretched 2-3 times their original length in boiling water or pressed through calendaring rolls. The samples, about 1 mm. thick, were then annealed at 120°C. under vacuum for 1 week.

X-ray fiber diagrams (Fig. 2) were taken with Ni-filtered $\text{CuK}\alpha$ radiation with the use of a cylindrical camera of 57.3 mm. diameter. Both stationary and Weissenberg photographs were taken with the fiber axis coaxial with the film holder and normal to the beam. Photographs taken at liquid nitrogen temperatures did not show an increase in the number of observable reflections. No double orientation could be obtained, as evidenced on Weissenberg photographs. The fiber repeat, averaged from a number of photographs, was 6.61 ± 0.05 Å. With related polymers, such repeat distances are characteristic of hexagonal or tetragonal cells.⁴

Indexing of the reflections was carried out with the aid of a Bernal chart. It was found that the ξ values for the reflections on every layer line was consistent with a hexagonal unit cell $a = 20.8$, $c = 6.61$ Å. To show the agreement between observed and calculated positions of the reflections, we list in Table I their distances s from the meridian.

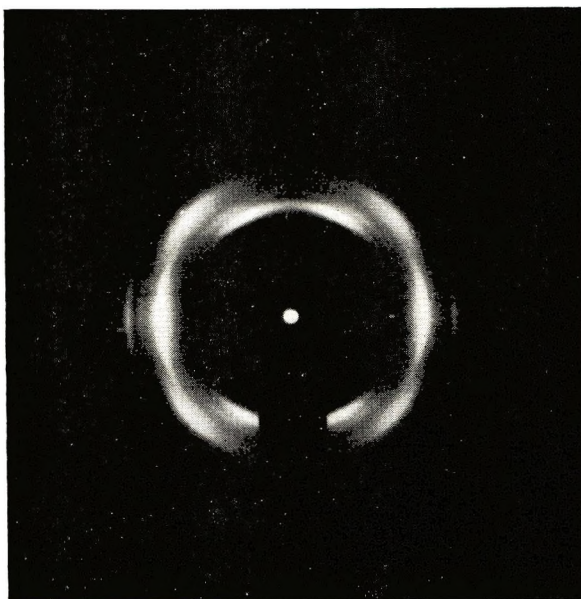


Fig. 2. X-ray fiber diagram of poly-4-phenyl-1-butene.

TABLE I
Comparison of Measured and Calculated Distances s , from the Meridian

Reflections	s , mm.		I (obs.)
	Obs.	Calc.	
<i>hk0</i>			
110	4.27	4.26	MS
200, $2\bar{2}0^a$	4.86	4.86	M
310	8.95	8.92	WM
400, $4\bar{4}0$	9.69	9.72	VS
$5\bar{1}0$	11.7	11.73	S
330	12.8	12.81	WM
510	14.0	13.94	WM
$7\bar{7}0$	16.9	17.01	WM
440, $8\bar{4}0^b$ }		17.08	
620, $8\bar{6}0$	17.9	17.84	M
800, $8\bar{8}0$	19.45	19.44	WM
550	21.4	21.30	W
11, $\bar{1}1$, 0	26.7	26.73	W
<i>hk1</i>			
$1\bar{1}1$	2.4	2.43	WM
111	4.3	4.26	VS
201, $2\bar{2}1$	4.8	4.86	S
$3\bar{1}1$	6.55	6.60	M
221, $4\bar{2}1$ }	8.6	8.52	VS
311		8.92	
401, $4\bar{4}1$	9.7	9.72	MS
$5\bar{5}1$	12.25	12.15	W
421, $6\bar{4}1$	13.0	13.2	W
<i>hk2</i>			
112	4.25	4.26	WM
$3\bar{1}2$	6.55	6.60	WM
312	9.0	8.92	W
402, $4\bar{4}2$	9.8	9.72	W

^a $s_{h00} = s_{h\bar{h}0}$

^b $s_{h10} = s_{2h, \bar{h}0}$

With 12 monomer units to the unit cell, the calculated density of the polymer is 1.070 g./cc. The density of the annealed sample measured by flotation in sulfuric acid-water solution was 1.045 g./cc. An amorphous sample was prepared by heating the annealed sample above the melting point and quenching in a Dry Ice-acetone slurry; the density of this amorphous polymer measured by flotation in a water-acetone solution was 0.962 g./cc.

From these data it is possible to estimate the degree of crystallinity from the relation:

$$\% \text{ crystallinity} = 100[1 - (\rho_c - \rho_e)/(\rho_c - \rho_a)]$$

where ρ_c is the fully crystalline density calculated from x-ray data, ρ_e is the density of the sample used for x-ray work, and ρ_a is the measured amorphous

density. By using this expression a value of 77% is obtained for the fully annealed polymer.

Crystal Structure

With the above hexagonal cell, reflections hkl are systematically absent for $(h + k)$ odd. This implies a C -centered cell (Fig. 3).

The disposition of the 3_1 helices along the fiber axis and their sense of screw were decided by the following considerations. The initial disposition was based on that proposed for polypropylene by Keith.⁹ The packing of the helices in the hexagonal cell was then determined by steric considerations, making sure that all intermolecular distances fell within accepted values. A number of postulates were examined by comparing structure factors and observed intensities for all the possible hkl values. Since the conformational energies of both right- and left-handed versions of the same absolute polymer configuration are the same an equal number of each type of helix is expected. The sense of screw was arbitrarily assigned for one chain and the agreement between $F_c^2(hkl)$ and observed intensities allowed

TABLE II
Comparison of Calculated Structure Factors and
Observed Intensities for the Hexagonal Cell

hkl	$F_c^2 \times 10^{-3}$	I (obs.)
110	31.3	MS
200, $\bar{2}\bar{0}$	10.2	M
310	4.7	WM
400, $\bar{4}\bar{0}$	24.8	VS
$5\bar{1}0$	4.5	S
330	0.8	WM
510	2.3	WM
770	0.3	WM
440, $\bar{8}\bar{4}0$	1.3	
620, $\bar{8}\bar{6}0$	5.7	M
800, $\bar{8}\bar{8}0$	3.4	WM
550	0.1	W
11, $\bar{1}\bar{1}$, 0	0.7	W
$\bar{1}\bar{1}1$	23.0	WM
111	28.8	VS
201, $\bar{2}\bar{2}1$	31.3	S
$3\bar{1}1$	2.9	M
221, $\bar{4}\bar{2}1$	16.3	VS
311	3.8	
401, $\bar{4}\bar{4}1$	12.4	MS
$5\bar{5}1$	1.4	W
421, $\bar{6}\bar{4}1$	5.5	W
112	4.1	WM
$3\bar{1}2$	4.5	WM
312	1.3	W
402, $\bar{4}\bar{4}2$	1.7	W

the assignment of a sense of screw to each of the remaining helices in the cell. The structure factors, $F(hkl)$, were calculated, the necessary multiplicity m being taken into account.

The intensity of a reflection is

$$I(hkl) = mL_p F^2(hkl)\phi$$

assuming negligible absorption. Here L_p is the Lorentz polarization factor which was ignored; ϕ is the crystallite disorientation factor, also ignored: $F(hkl)$ is the structure factor:

$$F^2(hkl) = A^2(hkl) + B^2(hkl)$$

where $A(hkl)$ is $\sum_r f_r \cos 2\pi(hX_r + kY_r + lZ_r)$ and $B(hkl)$ is $\sum_r f_r \sin 2\pi(hX_r + kY_r + lZ_r)$.

Here X_r, Y_r, Z_r is the fractional atomic coordinate of the r th atom, f_r is its scattering factor, where

$$f_r = f_0 \exp \{-B \sin^2 \theta / \lambda^2\}$$

f_0 (taken from the literature⁶) being for the atom at rest and B , the temperature factor, taken as $5 \times 10^{-16} \text{ cm}^2$. Hydrogen atoms were omitted.

Apart possibly from 510, there is seen (Table II) to be good general agreement between the calculated F^2 and observed intensities.

The Space Group

The proposed structure is based on hexagonal packing, but gives rise to systematic absences hkl absent for $(h+k)$ odd. These systematic ab-

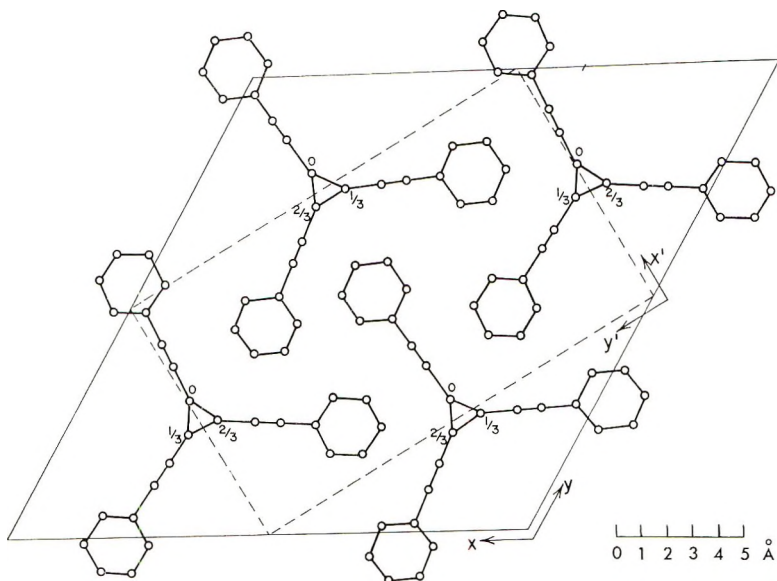


Fig. 3. Crystal structure of poly-4-phenyl-1-butene.

sences destroy the Laue symmetry $6/mmm$. The question then arises whether the structure is not more rationally described in the orthorhombic system by choosing new axes x' and y' but preserving z (Fig. 3). The fact that the Laue symmetry with respect to these axes is mmm cannot of course be used by itself as evidence for the orthorhombic system since all fiber diagrams of uniaxial polymers of all crystal systems have this symmetry. However, the proposed structure lacks some of the necessary symmetry axes or planes required by the orthorhombic system and in fact it belongs to the monoclinic Pa space group. If the origin is chosen to lie on the a glide, then the atomic general positions are related as $x', y', z; x' + 1/2, 1/2 - y', z$.

The transformation from hexagonal (unprimed) to monoclinic (pseudo-orthorhombic) (primed) axes yields

$$\begin{aligned}h' &= 1/2(h + k) \\k' &= 1/2(k - h)\end{aligned}$$

In Pa , $h'0l$ are systematically absent for h' odd which would give, for hexagonal indexing, hhl absent for h odd. However, for a hexagonal cell the reflections hhl and $2h, h, l$ (in general present) coincide on a fiber diagram, so that the systematic absences cannot be checked unless double orientation is present.

Discussion

From the per cent crystallinity of the polymer sample and the measured ΔH_m , the true ΔH_m^* may be calculated from the following relation

$$\Delta H_m^* = 100\Delta H_m / (\% \text{ crystallinity})$$

ΔH_m^* is 1.1 kcal./monomer unit. The only other member of this series for which the heat of fusion has been measured is polystyrene. The values reported are 2.15 and 2.00 kcal.^{7,8}

The length of each monomer unit in the helix is 2.20 Å, the carbon-carbon chain being arranged in such a way that alternate carbon-carbon bonds are parallel to the fiber axis while the others form an angle of $64^\circ 37'$ with this axis. This gives rise to a C—C—C bond angle of $115^\circ 23'$, which is close to that proposed for polystyrene (116°), indicating that the radial and axial adjustments which are necessary to provide space for the side groups are similar. This angle is generally formed with polymers that have small or flat side groups (polypropylene, polystyrene) with three monomer units per helix turn.

Both polystyrene and poly-4-phenyl-1-butene may be assigned to pseudo-hexagonal cells,⁵ and in both cases the true space group is monoclinic.

Hexagonal cells containing four 3_1 helices have been proposed for polypropylene⁹ and poly(*N,N*-di-*n*-butyl acrylamide),¹⁰ although crystal structures have not been examined in detail.

Natta¹¹ has reported a fiber repeat of 6.55 Å. for poly-4-phenyl-1-butene. He also found that the crystalline polymer consisted of 3_1 helices.

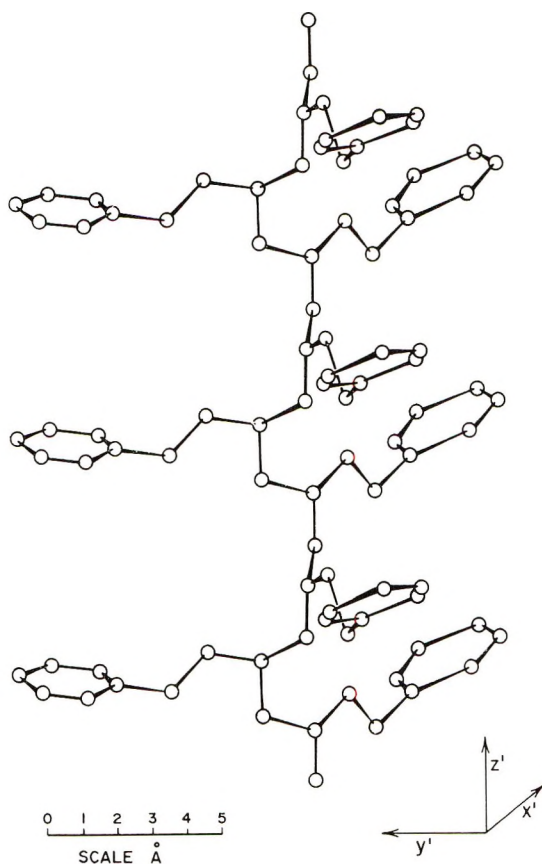


Fig. 4. Proposed conformation of poly-4-phenyl-1-butene.

Figure 4 depicts the proposed conformation of poly-4-phenyl-1-butene. The fractional positions of the independent carbon atoms (nonsymmetry related) based on the hexagonal cell are given in Table III.

TABLE III

X	Y	Z
0.296	0.288	0.000
0.296	0.288	0.233
0.365	0.351	0.310
0.417	0.397	0.113
0.486	0.462	0.191
0.548	0.459	0.268
0.492	0.529	0.268
0.615	0.517	0.345
0.558	0.591	0.345
0.621	0.586	0.422

Conclusions

Poly-4-phenyl-1-butene may be assigned an hexagonal cell with dimensions close to that of the hexagonal cell of polystyrene ($a = 21.9$ A., $c = 6.65$ A.). The densities of poly-4-phenyl-1-butene and of polystyrene are quite similar and show the expected trend, thus their packing densities are not very different. The packing of poly-4-phenyl-1-butene is therefore more favorable for a group of four units than six (as in polystyrene).

Poly-4-phenyl-1-butene is more rationally assigned to a monoclinic (pseudo-orthorhombic) unit cell of dimensions ($a = 10.4$ A., $b = 18.0$ A., $c = 6.61$ A.), space group Pa .

The poly-4-phenyl-1-butene samples studied in this work must be isotactic, as a syndiotactic polymer would be incompatible with a 3_1 helix. The first and fourth side groups must have the same configuration, which is satisfied only if the polymer is isotactic.

The financial support of the National Research Council of Canada and an N.R.C. Fellowship (F.J.G.) are gratefully acknowledged.

References

1. G. Natta, *J. Polymer Sci.*, **16**, 143 (1955).
2. J. A. Price, *J. Polymer Sci.*, **51**, 541 (1961).
3. T. W. Campbell and A. C. Haven, Jr., *J. Appl. Polymer Sci.*, **1**, 73 (1959).
4. H. D. Noether, in *International Symposium on Macromolecular Chemistry, Prague, 1965* (*J. Polymer Sci. C*, **16**), O. Wichterle and B. Sedláček, Eds., Interscience, New York, 1967, p. 725.
5. G. Natta and P. Corradini, *Makromol. Chem.*, **16**, 77 (1955).
6. *International Tables for Crystallography*, Vol. 3. C. H. MacGillavry and G. D. Rieke, Kynoch Press, Birmingham, England, 1962, pp. 202-203.
7. A. B. Thompson and D. W. Woods, *Nature*, **176**, 78 (1955).
8. R. Dedeurwaerder and J. F. M. Oth, *J. Chim. Phys.*, **56**, 940 (1959).
9. H. D. Keith, F. J. Padden, Jr., N. M. Waller, and H. W. Wyckoff, *J. Appl. Phys.*, **30**, 1485 (1959).
10. D. V. Badami, *Polymer*, **1**, 273 (1960).
11. G. Natta, *Makromol. Chem.*, **35**, 93 (1960).

Received April 14, 1967

Revised October 4, 1967

Thermostability of Some Isomeric Polyoxadiazoles

V. V. RODÈ, E. M. BONDARENKO, V. V. KORSHAK,
A. L. RUSANOV, E. S. KRONGAUZ, D. A. BOCHVAR, and
I. V. STANKEVICH, *Institute of Elemento-Organic Compounds, Academy
of Sciences of the U.S.S.R., Moscow, U.S.S.R.*

Synopsis

The thermal stability of the isomeric poly-1,2,4-oxadiazole (PO-2) and poly-1,3,4-oxadiazole (PO-3) was investigated. The isomerism of the ring substantially influenced polymer thermostability. The weight losses in PO-2 occur above 220–230°C. *in vacuo*, but PO-3 degrades only at 280–300°C. The weight changes in isomeric polyoxadiazole at lower temperatures are connected with the completion of the cyclization process. At higher temperatures degradation of the oxadiazole ring takes place, and as a result carbon and nitrogen oxides, 4,4'-dicarboxy (diphenyl ether) dinitrile and other products are evolved. The mechanism of polymer thermal degradation is examined; it is shown that the weakest bonds are C—O and N—O. These data are in a good agreement with the results of calculation of the π -electron systems of unsubstituted oxadiazole cycles in the framework of the molecular orbital treatment in the Hückel approximation. It is shown that the oxygen in the oxadiazole ring oxidizes the products of thermal degradation of polymers and a cell effect takes place. The thermal oxidation of isomeric polyoxadiazoles does not differ essentially from the degradation *in vacuo*. It was found that the formation of intermediate products such as peroxides and hydroperoxides does not take place, and oxygen does not act as an initiator of polymer degradation.

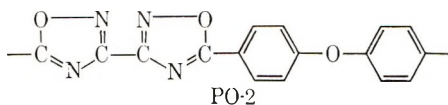
Intramolecular polyheterocyclization is one of the best ways of obtaining attractive thermostable polymers containing aromatic carbo- and heterocycles. It may be carried out as a two-stage process. The linear polymers formed in the first stage of the reaction are usually soluble in organic solvents and thus may be worked up into films and fibers. Polyheterocyclization is carried out on prepared articles, and the insoluble and infusible polyheteroarylenes formed do not need any additional workup. In this connection investigation of the thermostability of polyheteroarylenes is of great interest; in addition, their exploitation temperature range is limited by their degradation temperature.

Among the polymers containing in their main chains recurring aromatic heterocycles, polyoxadiazoles of high thermostability attract a rather great attention.

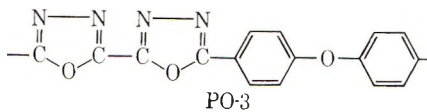
In literature there are some data concerning syntheses of such polymers and their behavior at elevated temperatures. However it should be mentioned that in most cases only TGA and DTA data are shown. Frazer et al.¹⁻³ have found that aromatic 1,3,4-polyoxadiazoles decompose in the

temperature range of 450–500°C.; aliphatic derivatives are less stable and decompose at 400–450°C. According to the DTA data, Frazer and Sarasohn³ have found three stages in polyhydrazide–polyoxadiazole conversion: the liberation of absorbed water, cyclodehydration, and decomposition of poly-1,3,4-oxadiazole. Other authors^{4–7} have also used only TGA and DTA analyses data to describe the high thermostability of poly-1,3,4-oxadiazoles. Therefore, detailed investigation of the dependence of the isomeric polyoxadiazoles with heteroatoms in the 1,2,4- and 1,3,4- positions on their thermostability is of great interest.

The polymers studied in the present investigation were poly-1,2,4-oxadiazole (PO-2) obtained from oxamidoxime and 4,4'-dicarboxy(diphenyl ether) dichloride



and poly-1,3,4-oxadiazole (PO-3) from oxalic acid dihydrazide and 4,4'-dicarboxy(diphenyl ether) dichloride



Experimental

The synthesis of PO-2 and PO-3 was carried out as a two-stage process.^{8,9} In the first stage of the PO-2 synthesis, poly-*O*-acyloylamidoxime was obtained; the reaction was carried out in hexamethylphosphoramide (HMPA) solution with cooling, with the use of equimolecular amounts of oxamidoxime and 4,4'-dicarboxy(diphenyl ether) dichloride. The polymer was cyclized *in vacuo* (2 torr) at 200°C. for 2 hr. PO-2 was obtained as a white powder soluble in concentrated H₂SO₄; $[\eta]$ (in 0.5% solution of concentrated H₂SO₄) was 0.22.

In the first stage of PO-3 synthesis a polyhydrazide was obtained. The reaction was carried out in HMPA solution with cooling by interaction of equimolecular amounts of oxalic acid dihydrazide and 4,4'-dicarboxy(diphenyl ether) dichloride. The polyhydrazide obtained was cyclodehydrated *in vacuo* (2 torr) at 270–280°C. for 20 hr. PO-3 was obtained as a black powder soluble without decomposition in concentrated H₂SO₄ and having $[\eta]$ (in 0.5% solution of concentrated H₂SO₄) of 0.41.

The thermostability of polymers was investigated in the temperature range of 225–500°C. Thermal degradation was carried out in the previously described device^{10,11} *in vacuo* (10⁻² to 10⁻³ torr) while thermooxidation was carried out in the same device in statical conditions under oxygen pressure of 120 torr. The solid and gaseous degradation products analyzed by gas, thin-layer and column chromatography.

Results and Discussion

It was shown that the polyoxadiazole thermostability depends on oxadiazole cycle isomerism. As is shown in Figure 1, the weight losses of PO-2 occur at 220–230°C. in 1 hr. while some changes in PO-3 weight occur at 280–300°C. No noticeable changes in polymer PO-2 take place up to temperatures of 250–275°C., and total weight losses reach 4% (at 275°C.). Infrared spectroscopy data indicate that the main weight losses

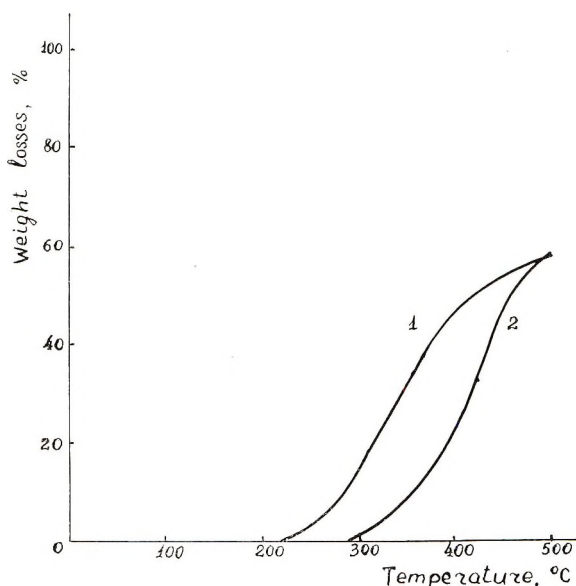


Fig. 1. Degradation of isomeric polyoxadiazoles *in vacuo* for 1 hr.: (1) PO-2; (2) PO-3.

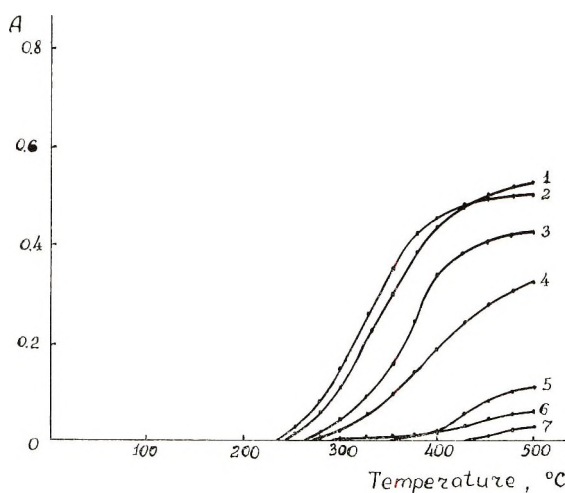


Fig. 2. Composition of PO-2 degradation products vs. temperature (heating *in vacuo* for 1 hr.): (1) DN; (2) O₂; (3) CO₂; (4) N₂; (5) CO; (6) NO; (7) (CN)₂.

TABLE I
Composition of Products of Degradation of PO-2 *in vacuo* for 1 hr.

Tem- per- ature, °C	Low molecular weight solids			Gaseous products															
	4,4'-Dicarboxy- (diphenyl ether) dinitrile			N ₂	CO	CO ₂	NO	NO ₂	(CN) ₂	Total, %	Weight, %	A × 10 ^{3a}	Weight, %	A × 10 ^{3a}	Weight, %	A × 10 ^{3a}	Weight, %	A × 10 ^{3a}	
	Total, %	Weight, %	A × 10 ^{3a}																Weight, %
225	0.53	0.53	—	—	—	—	—	—	—	—	—	—	—	—	—	—	—	—	—
250	2.42	1.53	0.54	0.8	—	—	—	—	—	—	—	—	—	—	—	—	—	—	—
275	6.11	2.12	2.62	3.9	—	—	—	—	—	—	—	—	—	—	—	—	—	—	—
300	12.78	2.41	6.97	10.4	0.08	0.9	—	—	—	—	—	—	—	—	—	—	—	—	—
325	20.17	2.43	12.15	18.1	0.25	2.6	0.05	0.5	0.61	4.2	0.15	1.5	2.34	15.5	—	—	—	—	—
350	31.12	2.44	20.37	30.1	0.46	5.0	0.06	0.7	1.26	8.7	0.18	1.8	3.63	24.0	—	—	—	—	—
375	39.91	2.46	25.92	38.6	0.78	8.5	0.08	0.9	2.19	15.2	0.19	1.9	5.17	34.3	—	—	—	—	—
400	46.63	2.47	30.12	44.8	1.28	14.1	0.10	1.1	3.77	26.0	0.20	2.0	6.18	41.0	—	—	—	—	—
425	50.60	2.49	32.32	32.11	1.75	19.0	0.18	1.9	4.96	34.2	0.23	2.3	6.92	46.0	—	—	—	—	—
450	53.40	2.50	33.79	33.48	2.22	24.2	0.44	4.8	5.63	38.8	0.27	2.7	7.14	47.3	0.08	0.5	—	—	—
475	55.98	2.51	35.33	34.90	2.58	28.1	0.73	8.0	5.79	40.2	0.44	4.4	7.37	48.8	0.20	1.2	—	—	—
500	57.67	2.51	36.24	35.72	2.80	30.1	0.90	9.8	6.00	41.4	5.01	5.2	7.57	50.1	0.36	2.1	—	—	—
					2.97	32.3	0.97	10.5	6.31	43.6	0.57	5.8	7.66	50.6	0.41	2.6	—	—	—

^a Moles of compound per mole of structural unit.

TABLE II
Composition of Products of Degradation of PO-3 *in vacuo* for 1 hr.

Tem- per- ature, °C.	Total Amount of weight, loss, water,		Low molecular weight solids		Gaseous products									
	%	%	Total, Weight, %	A Weight, × 10 ^{3a} %	Oligo- mers, %	O ₂	N ₂	CO ₂	CO	H ₂	(CN) ₂			
						Weight, %	Weight, %	Weight, %	Weight, %	Weight, %	Weight, %			
300	0.81	0.63	—	—	—	—	0.18	—	—	—	—			
325	3.95	1.67	1.61	1.61	—	—	0.53	0.13	0.01	—	—			
350	8.06	2.45	4.09	4.09	6.1	—	1.05	0.42	2.9	0.05	—			
375	12.45	2.56	7.05	7.05	10.5	—	1.78	0.96	6.7	0.10	—			
400	21.09	2.59	13.22	13.22	19.7	—	3.24	1.78	12.3	0.21	—			
425	34.81	2.61	23.48	23.48	35.0	Traces	4.46	3.68	25.4	0.46	—			
450	46.90	2.62	31.53	31.68	47.2	0.25	5.18	5.68	39.2	1.04	—			
475	55.017	2.63	37.49	37.10	55.0	0.39	5.69	6.67	46.0	1.51	0.17			
500	58.194	2.63	39.69	39.17	58.4	0.52	5.90	6.94	47.9	1.57	0.39			
												4.0		

^a Moles of compound per mole of structural unit.

at that temperature are due to completion of cyclization. As shown by infrared spectroscopy the frequency 1740 cm.^{-1} , which corresponds to the acylated amidoxime carbonyl group, disappears in this temperature range. The cyclization process is connected with liberation of water from the polymer. Table I shows that the amount of water in PO-2 degradation products approaches some limit (about 2.4%) with temperature rise up to $300\text{--}325^\circ\text{C}$. Absolute water amounts do not change at further PO-2 heating, but the relative amount of water in the degradation products decreases rapidly. Thus, at low temperatures ($250\text{--}300^\circ\text{C}$), the weight losses are connected with completion of the cyclization process.

The PO-3 weight losses at temperatures up to 400°C . are also connected with completion of the polycyclization process and liberation of water (Table II). The uncyclized parts in macromolecular chains in both

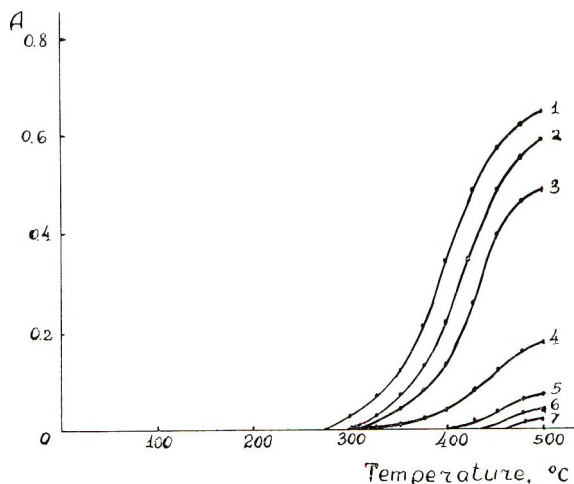


Fig. 3. Composition of PO-3 degradation products vs. temperature (heating *in vacuo* for 1 hr.): (1) N_2 ; (2) ND; (3) CO_2 ; (4) CO; (5) O_2 ; (6) $(\text{CN})_2$; (7) H_2 .

PO-2 and PO-3 are probably almost equal, because the water amount liberated from PO-3 with increasing temperature rise, reaches 2.4%.

The chain degradation of poly-1,2,4-oxadiazole PO-2 accompanied by the formation of considerable amounts of gaseous and low molecular weight solid products takes place above $250\text{--}275^\circ\text{C}$. (Fig. 2, and Table I). The degradation process is completed in 1 hr.

Nitrogen, nitrogen oxides, carbon monoxide, and carbon dioxide were found among degradation products of polymer PO-2. At temperatures above 425°C . small amounts of oxalic acid dinitrile were found. In Figure 2 and subsequent figures, the mole fraction of the various products is plotted as the function A , defined as the moles of compound per mole of structural unit.

The low molecular weight products of PO-2 degradation consist almost completely of 4,4'-dicarboxy(diphenyl ether)dinitrile (DN). At high

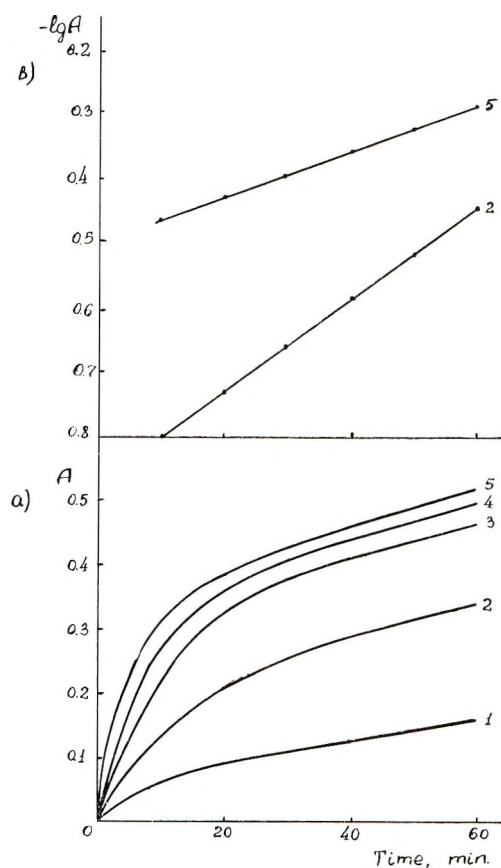


Fig. 4. Kinetic curves (a) of the liberation of nitrogen dioxide from PO-2 and (b) semi-logarithmic plots derived from some curves: (1) 300°C.; (2) 350°C.; (3) 400°C.; (4) 450°C.; (5) 500°C.

temperatures small amounts of diphenyl ether, diphenyl, benzonitrile, benzene, and HCN are found.

The infusible, insoluble solid residue after degradation seems to be a carbonized three-dimensional skeleton consisting mainly of phenylene rings. This conclusion is in a good agreement with results of elementary analysis and infrared spectroscopy.

The formation of solid and gaseous products in poly-1,3,4-oxadiazole degradation takes place at higher temperatures than in the case of PO-2 (Fig. 3 and Table II). Among the gaseous degradation products of PO-3 obtained above 325–350°C., carbon oxides and nitrogen prevail. It must be noted that at above 400°C. a small amount of free oxygen is formed, and hydrogen and oxalic acid dinitrile are found in gaseous products of PO-3 degradation at higher temperatures.

Of the low molecular weight solids formed on degradation of PO-3, DN prevails. Small amounts of diphenyl ether, diphenyl, benzonitrile,

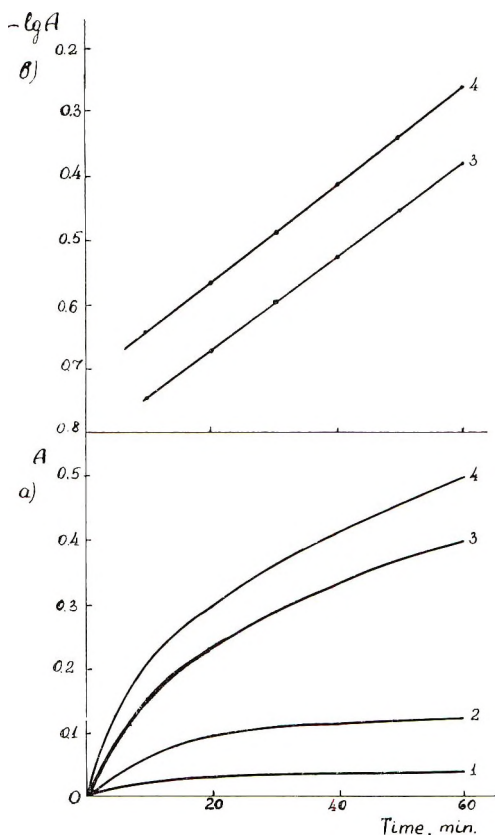


Fig. 5. Kinetic curves (a) of the liberation of carbon dioxide from PO-3 and (b) semi-logarithmic plots derived from some curves: (1) 350°C.; (2) 400°C.; (3) 450°C.; (4) 500°C.

benzene, and HCN were also formed. The infusible solid residue seems to be a carbonized three-dimensional skeleton consisting mainly of phenylene rings. This conclusion is in a good agreement with results of elementary analysis and infrared spectroscopy.

The composition of the products formed in thermal degradation of isomeric polyoxadiazoles leads one to consider the polymer degradation as beginning from the oxadiazole.

In PO-2 containing 1,2,4-oxadiazole rings, cleavage of O—N and O—C bonds with simultaneous conjugated cleavage of one of the C=N bonds probably takes place first. Obviously O—N cleavage leads to the formation of carbon oxides and carbonized residue, but nitrogen and oxalic acid dinitrile may be also formed. The O—C bond cleavage leads to the formation of nitrogen oxides and DN. In this case the formation of the carbonized residue or nitrogen volatilization may also take place. As shown in Table I, there is a good correlation between the molar fraction of DN formed and the total nitrogen oxides.

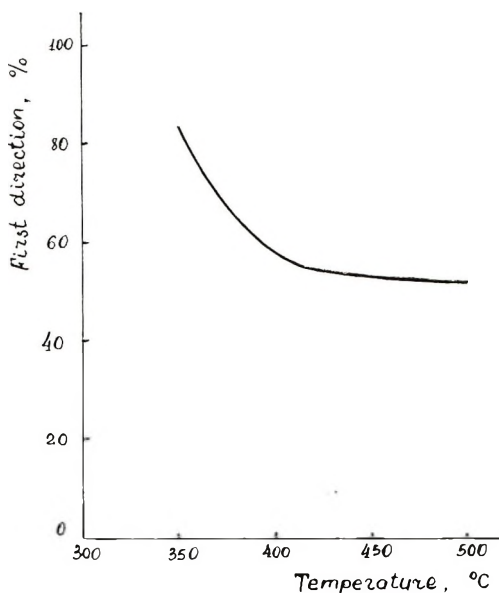


Fig. 6. Dependence of the first direction for PO-3 degradation on temperature.

The presence of not only NO and CO but also NO₂ and CO₂ in the gaseous products from degradation of PO-2 indicates that during the ring cleavage free oxygen is liberated and immediate oxidation of NO and CO takes place. Investigations of volatilization kinetics in PO-2 degradation showed that the formation of any gas (including NO₂ and CO₂) and thermodegradation processes are described by a first-order equation and follow the Arrhenius law. Figure 4 represents the kinetic curves of nitrogen dioxide formation and also semilogarithmic plots derived from some of the curves. Such kinetic regularity allows one to assume that a cell effect takes place during oxidation of NO and CO to NO₂ and CO₂.

The composition of the PO-3 thermodegradation products suggests that the polymer degradation may also begin with cleavage of the oxadiazole ring. The degradation probably occurs simultaneously in two directions. In the first case cleavage of the C—O—C bond takes place and oxygen, carbon monoxide, and carbon dioxide are liberated. This cleavage, as a rule, is accompanied by conjugated cleavage of the N—N bond. As a result, considerable amounts of DN are formed. The amount of DN evolved changes parallel with liberation of carbon oxides (Table II).

The second direction of the degradation is connected with C=N bond cleavage. As a result considerable amounts of nitrogen are formed, and simultaneously the formation of the carbonized residue takes place.

The process of CO₂ formation in degradation of PO-3 is connected with oxidation of CO by oxygen liberated in degradation of the oxadiazole. Probably in this case the cell effect takes place too. This assumption is supported by CO₂ formation kinetics which is described by the first-order equation and follows the Arrhenius law. Figure 5 shows the kinetic

curves for CO₂ formation from PO-3 and also some semilogarithmic plots derived from them. The comparison of the PO-3 degradation rates in first and second directions indicates that the first one connected with C—O—C and N—N bond cleavage, predominates. At relatively low temperatures (275–400°C.) the first direction part significantly predominates over the second (Fig. 6 and Table II). However, with increasing temperature, the probability of reaction in the first direction decreases and at 500°C. reaches 53%.

These data are in a good agreement with the results of calculation of the π -electron systems of the oxadiazole cycles in the framework of the MO treatment in Hückel approximation.

The calculation was carried out for 1,2,4-oxadiazole (O-2) and 1,3,4-oxadiazole (O-3).

The Coulomb and resonance integrals of the atomic orbitals centered on atoms X and Y are denoted by α_x and β_{xy} . The following assumptions were made:

$$\alpha_N = \alpha_C + 0.4\beta$$

$$\alpha_O = \alpha_C + 2.0\beta$$

$$\beta_{CN} = 1.0\beta$$

$$\beta_{CO} = 0.9\beta$$

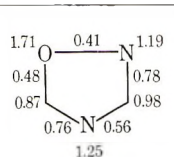
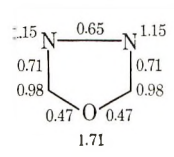
$$\beta_{NN} = 1.5\beta$$

$$\beta_{NO} = 1.0\beta$$

The parameter β_{NN} corresponds to the value given by Polansky et al.;¹² the β_{NO} value is taken from Bochvar and Bagaturianz,¹³ and the values of the remaining parameters are from Pullman and Pullman.¹⁴

The molecular diagrams and energy levels of the isomeric oxadiazoles are given in Table III. It is seen that the total energy E of the π -electrons in the ground state (i.e., the sum of energies of the π -electrons occupying the lower energy levels) for the O-2 system is $E_1 = 10.2882\beta$; respectively for the O-3 system it is $E_2 = 10.8066\beta$.

TABLE III
Molecular Diagrams of Energy Levels of the Isomeric Oxadiazoles

Compound	Molecular diagram	Energy level ^a
O-2 	×+×+×+×	-1.4304
	×+×+×+×	-0.9138
	×-×-×-×	0.8160
	×+×+×+×	1.4476
	±-±-±-±	2.8805
	×-×-×-×	
	×-×-×-×	
O-3 	×-×-×-×	-1.6913
	±-±-±-±	-0.9120
	×-×-×-×	0.5913
	±=±=±=±	1.9365
	×-×-×-×	2.8755
	±=±=±=±	
	±=±=±=±	

^a The energy zero is α ; the β unit is β_{CC} .

This shows somewhat greater stability for the O-3 in comparison with the O-2 ring, since β is negative.

The comparison of molecular diagrams of the systems under consideration demonstrates that bond orders in O-3 are more smoothed out than in O-2. The lowest bond order in the O-2 cycle is 0.41 (for the N—O

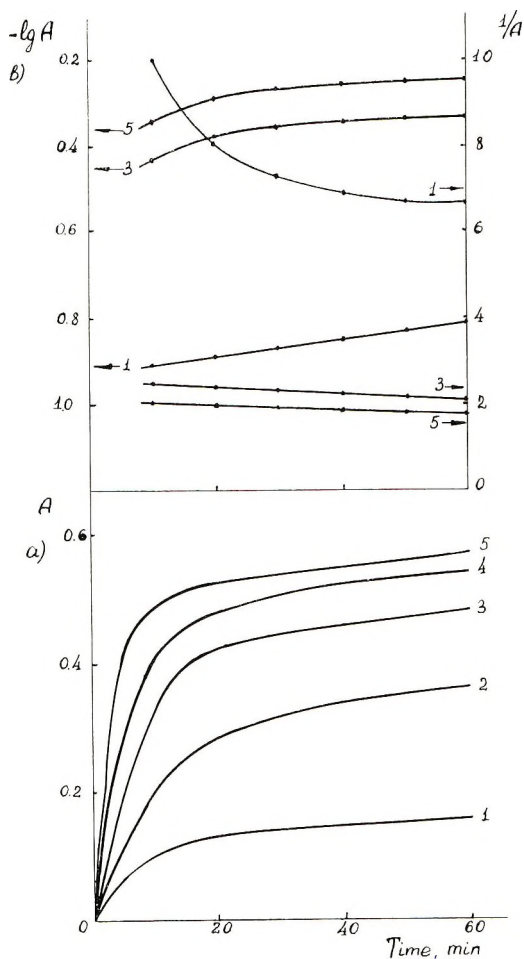


Fig. 7. Kinetic curves (a) of the liberation of nitrogen dioxide from thermally oxidized PO-2 and (b) semilogarithmic plots derived from the curves: (1) 300°C.; (2) 350°C.; (3) 400°C.; (4) 450°C.; (5) 500°C.

bond) and the highest one is 0.78 for the N—C bond. In the O-3 system, accordingly, the lowest bond order corresponds to the C—O bond (0.47) and the highest, to the N—C bond (0.71).

The data on thermal stability of isomeric polyoxadiazoles show that poly-1,3,4-oxadiazoles are actually more stable. Probably the greater stability of PO-3 is conditioned not only by greater stability of the π -

TABLE IV
Composition of Products of Thermooxidative Degradation of PO-2 for 1 hr.

Tem- per- ature, °C.	Total weight loss, %	Amount of water, %	Low molecular weight solids										Gaseous products						
			4,4'-Dicarboxy- (diphenyl ether) dinitrile			Oligo- mers, %			N ₂		CO		CO		NO ₂		(CN) ₂		
			Total, %	Weight, %	A × 10 ^{3a}	Total, %	Weight, %	A × 10 ^{3a}	Weight, %	A × 10 ^{3a}	Weight, %	A × 10 ^{3a}	Weight, %	A × 10 ^{3a}	Weight, %	A × 10 ^{3a}	Weight, %	A × 10 ^{3a}	
225	0.54	—	—	—	—	—	—	—	—	—	—	—	—	—	—	—	—	—	—
250	2.44	1.57	0.60	0.60	0.9	—	—	—	—	—	—	—	—	—	—	—	—	—	—
275	6.56	2.15	3.16	3.16	4.7	—	—	—	—	—	—	—	—	—	—	—	—	—	—
300	13.09	2.40	7.52	7.52	11.2	—	—	—	—	—	—	—	—	—	—	—	—	—	—
325	21.67	2.44	13.51	13.51	20.1	—	—	—	—	—	—	—	—	—	—	—	—	—	—
350	31.78	2.45	20.50	20.50	30.5	—	—	—	—	—	—	—	—	—	—	—	—	—	—
375	39.70	2.47	25.61	25.61	38.1	—	—	—	—	—	—	—	—	—	—	—	—	—	—
400	46.11	2.49	29.34	29.34	43.7	Traces	—	—	—	—	—	—	—	—	—	—	—	—	—
425	51.13	2.50	32.34	32.12	47.8	0.22	—	—	—	—	—	—	—	—	—	—	—	—	—
450	54.39	2.51	34.09	33.78	50.3	0.31	—	—	—	—	—	—	—	—	—	—	—	—	—
475	56.62	2.52	35.25	34.81	51.8	0.44	—	—	—	—	—	—	—	—	—	—	—	—	—
500	57.75	2.52	35.91	35.38	52.7	0.53	—	—	—	—	—	—	—	—	—	—	—	—	—

^a Moles of compound per mole of structural unit.

TABLE V
Composition of Products of Thermooxidative Degradation of PO-2 for 1 hr.

Tem- per- ature, °C.	Total weight loss, %	Amount of water, %	Low molecular weight solids			Gaseous products						
			4,4'- Dicarboxy- (diphenyl ether) dinitrile			Total, %	N ₂ Weight, % × 10 ^{3a}	CO ₂ Weight, % × 10 ^{3a}	CO Weight, % × 10 ^{3a}	H ₂ Weight, % × 10 ^{3a}	(CN) ₂ Weight, % × 10 ^{3a}	
			Total, %	Weight, % × 10 ^{3a}	Oligo- mers, %							
300	0.95	0.65	—	—	0.30	0.23	2.5	0.07	0.5	—	—	—
325	4.04	1.66	1.61	2.4	0.77	0.54	5.9	0.19	1.3	0.04	0.4	—
350	8.17	2.46	4.03	6.0	1.68	1.01	11.0	0.59	4.1	0.08	0.9	—
375	12.96	2.58	7.17	10.7	3.21	1.89	20.5	1.16	8.0	0.16	1.8	—
400	22.65	2.60	14.51	21.6	5.54	3.23	35.1	2.07	14.3	0.24	2.6	—
425	35.47	2.62	23.68	35.3	9.17	4.62	50.2	4.12	28.5	0.43	4.7	—
450	47.611	2.63	32.44	47.9	12.541	5.33	57.8	6.42	44.4	0.64	6.9	0.15
475	54.547	2.64	37.40	55.1	14.507	5.77	62.7	7.59	52.5	0.81	8.8	0.33
500	57.843	2.64	39.85	58.6	15.383	5.82	64.2	8.05	55.7	0.89	9.7	0.57

^a Moles of compound per mole of structural unit.

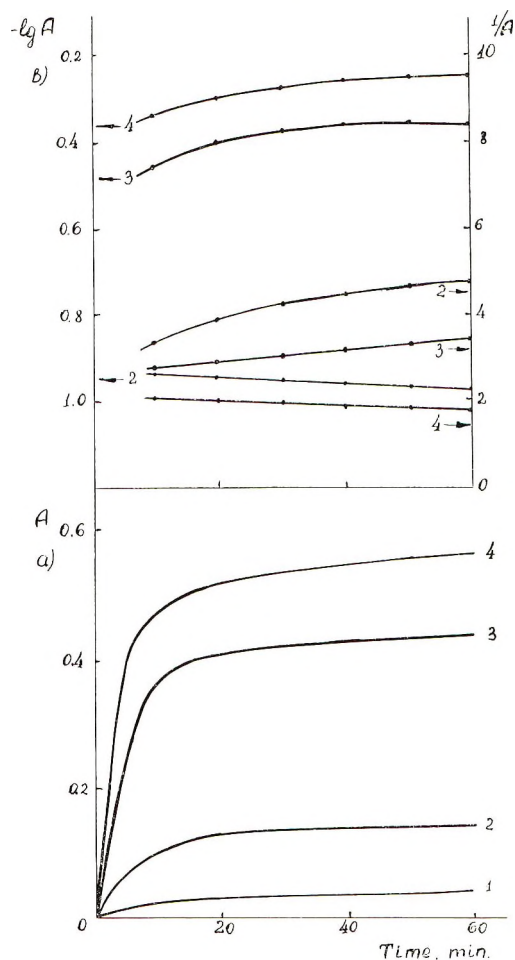


Fig. 8. Kinetic curves (a) of the liberation of carbon dioxide from thermally oxidized PO-3 and (b) semilogarithmic plots derived from the curves: (1) 350°C.; (2) 400°C.; (3) 450°C.; (4) 500°C.

electron system of the 1,3,4-oxadiazole but also the larger conjugation energy for PO-3 than for PO-2.

Thus, the stability of the isomeric polyoxadiazoles is different. However in both cases, for PO-2 as well as for PO-3, the weakest bonds in the rings are bonds between oxygen and neighboring atoms. The cleavage of these bonds leads to the formation of polymer oxidation products.

It was therefore interesting to elucidate the changes in composition and ratio of degradation products of isomeric polyoxadiazoles in the oxidation process.

The experiments carried out under steady-state conditions at an oxygen pressure of 120 torr showed that the pattern of thermal degradation of the isomeric polyoxadiazoles remains almost the same. As shown in

Tables IV and V the thermooxidation products of the polyoxadiazoles are identical to their thermal degradation products.

The general differences lie in the kinetics of CO₂ and NO₂ formation for PO-2 and in that of CO₂ formation for PO-3. As shown in Figures 7 and 8, the kinetics of gas formation is described by a first-order equation only up to 325–350°C. for PO-2 and up to 400°C. for PO-3. Above these temperature ranges the kinetics of nitrogen and carbon oxides formation is described by a fractional order; at high temperatures it approaches second-order. This phenomenon means that on thermooxidation of polyoxadiazoles not only a cell effect, but also ordinary oxidation takes place.

The kinetics characteristics found show that isomeric polyoxadiazole oxidation does not proceed through intermediate formation of peroxides and hydroperoxides. The regularities found confirm the opinion expressed previously¹⁵ that in fully aromatic polymer systems oxygen does not act as an initiator of polymer degradation.

References

1. A. H. Frazer and F. T. Wallenberger, *J. Polymer Sci. A*, **2**, 1171 (1964).
2. A. H. Frazer, W. Sweeny, and F. T. Wallenberger, *J. Polymer Sci. A*, **2**, 1157 (1964).
3. A. H. Frazer and I. M. Sarasohn, *J. Polymer Sci. A-1*, **4**, 1649 (1966).
4. C. I. Abshire and C. S. Marvel, *Makromol. Chem.*, **44–46**, 388 (1961).
5. I. Iwakura, K. Uno, and S. Hara, *J. Polymer Sci. A*, **3**, 45 (1965).
6. T. Umishi and M. Hasegawa, *J. Polymer Sci. A*, **3**, 3191 (1965).
7. J. Preston and W. B. Black, *J. Polymer Sci. B*, **4**, 267 (1966).
8. V. V. Korshak, E. S. Krongauz, and A. L. Rusanov, *Dokl. Akad. Nauk SSSR*, **166**, 356 (1966).
9. A. L. Rusanov, V. V. Korshak, E. S. Krongauz, and I. B. Nemirovskaya, *Vysokomolekul. Soedin.*, **8**, 804 (1966).
10. V. V. Rodè, I. V. Zhuravleva, S. R. Rafikov, V. V. Korshak, S. V. Vinogradova, and S. N. Salazkin, *Vysokomolekul. Soedin.*, **6**, 994 (1964).
11. I. V. Zhuravleva, V. V. Rodè, and S. R. Rafikov, *Izvest. Akad. Nauk SSSR, Ser. Khim.*, **1965**, 216.
12. O. E. Polansky and G. Derfingler, *Monatsh. Chem.*, **92**, 1114 (1961).
13. D. A. Bochvar and A. A. Bagaturianz, *Zh. Fiz. Khim.*, **39**, 1631 (1965).
14. B. Pullman and A. Pullman, *Quantum Biochemistry*, Interscience, New York, 1962.
15. V. V. Rodè and I. V. Zhuravleva, *Vestnik Tekhn. Ekonom. Inform.*, **1964**, No. 12, 13.

Received May 23, 1967

Revised October 27, 1967

The Radiation-Induced Copolymerization of Tetrafluoroethylene and 3,3,3-Trifluoropropene under Pressure*

DANIEL W. BROWN and LEO A. WALL, *National Bureau of Standards, Washington, D.C. 20234*

Synopsis

A study was made of the gamma-ray-induced copolymerization of tetrafluoroethylene and 3,3,3-trifluoropropene. Copolymerizations were carried out at 100°C. and 5000 atm. pressure and at 21°C. and various pressures up to 8000 atm. The reactivity ratios calculated from the composition data indicate that the propagation rate constants favor addition of trifluoropropylene by a factor of 3-7; individual values depended little on the polymerization pressure and temperature. Polymerization rates changed little with monomer composition between 0 and 75% tetrafluoroethylene; between 75 and 95% tetrafluoroethylene they increased by a factor of 10. As many as 850,000 molecules were polymerized per 100 e.v. absorbed. The copolymers are soluble in hexafluorobenzene at 29.6°C. if they contain less than 70% tetrafluoroethylene. Intrinsic viscosities range from 0.1 to about 10 dl./g. From various considerations it appears likely that the degree of polymerization is about equal to the kinetic chain length in high-pressure polymerizations at 21°C.; at autogenous pressure or at 5000 atm and 100°C., monomer transfer reduces the value considerably.

INTRODUCTION

Poly(3,3,3-trifluoropropene) of high molecular weight has been prepared by irradiating the monomer at high pressure.¹ It is amorphous, and its glass transition temperature has been reported to be 35°C.² Tetrafluoroethylene was copolymerized with 3,3,3-trifluoropropene in the hope of obtaining elastomers of interest. This paper describes the polymerization behavior and makes a preliminary evaluation of the copolymers.

Apparently no previous paper describes this copolymerization, even made at low pressure.

EXPERIMENTAL

The polymerization techniques at high pressure have been described previously.^{3,4} In essence, a known amount of degassed monomer mixture of known composition was exposed at known temperature and pressure to radiation of known intensity from cobalt-60. After irradiation, the pressure

* Presented at the 152nd American Chemical Society Meeting, New York, N.Y., September, 1966.

vessels were cooled to -80°C . and opened and unconverted monomer was removed. The polymer was removed as quantitatively as possible, heated *in vacuo* for several hours at 180°C ., to remove dissolved monomer, and weighed.

Polymerizations at autogenous pressure were performed in sealed glass tubes about 90% full of liquid.

The tetrafluoroethylene was obtained from Peninsular ChemResearch, Gainesville, Florida. It was freed from inhibitor (turpentine) by flash distillations, first at room temperature and then at -80°C .; a residue amounting to about 10% of the first distillate was discarded after the second distillation. The mass spectrometric analysis of the second distillate gave C_2F_4 99.83%, C_2F_6 0.07%, and cyclic C_4F_8 0.10%. The 3,3,3-trifluoropropene was prepared by reaction between acrylic acid and sulfur tetrafluoride.⁵ Mass spectrometric and vapor-phase chromatographic analysis of the washed, distilled product gave no evidence of any impurity.

The initial composition of the monomer charge was calculated by use of the perfect-gas laws, from the measured pressure and volume of each component put in the bomb. The final monomer composition was calculated from the initial composition, the polymer composition, and the conversion.

Elemental analyses of the polymers were performed on a Sargent Carbon and Hydrogen Combustion apparatus. Copolymer compositions were calculated from the carbon contents.

Solution viscosities were determined in hexafluorobenzene at 29.6°C . Intrinsic viscosities were obtained from three to five relative viscosities in the range 1.08–2.0 by plotting reduced viscosity against concentration and extrapolating a straight line through the plotted values linearly to zero concentration.

RESULTS

Polymerizations

Results of successful polymerizations are listed in Table I. Quantities included are the polymerization pressure, temperature, and radiation intensity, the fraction of tetrafluoroethylene in the polymer and in the monomer before and after the polymerization, the fraction of monomer polymerized, 10^3R_p (the polymerization rate, expressed as 10^3 times the fraction of monomer converted per hour), and the intrinsic viscosity $[\eta]$ of the polymer. Mole fractions are used exclusively; however, the maximum difference between mole and weight fraction is 0.01, because the molecular weights of the monomers differ by only 4%.

The rates were calculated from the conversion and radiation time. One experiment was performed for the purpose of detecting any variation of rate with conversion. A sample was irradiated in several increments; after each dose measurements were made of the piston displacement required to restore the pressure to its original value. Since the piston diame-

TABLE I
Copolymerization of 3,3,3-Trifluoropropene and Tetrafluoroethylene
(21°C., 1400 rad/hr. except as specified)

Press., atm.	Mole fraction C ₂ F ₄			Fract. convn.	10 ³ R _p , 10 ³ /hr.	[η], dl./g.
	Init.	Final	Polymer			
auto	0.85	0.85	0.53	0.018	0.27	0.18
auto	0.75	0.76	0.39	0.026	0.19	0.13
auto	0.45	0.46	0.22	0.024	0.18	0.13
auto	0	0	0	0.015	0.12	0.10
auto	0.66	0.70	0.37	0.11	5.1	0.062 ^a
auto	0.51	0.53	0.27	0.093	4.3	0.065 ^a
auto	0.20	0.21	0.14	0.069	3.2	0.065 ^a
auto	0	0	0	0.17	2.0	— ^a
1000	0.88	0.92	0.70	0.24	3.9	2.2 ^b
1800	0.88	0.90	0.61	0.064	4.0	2.1
1800	0	0	0	0.098	1.0	1.0
3500	0.88	0.91	0.64	0.11	19	5.0
5000	0.95	0.97	0.85	0.11	120	—
5000	0.90	0.95	0.64	0.15	32	9.7
5000	0.88	0.90	0.56	0.069	21	5.3
5000	0.72	0.86	0.42	0.32	17	5.0
5000	0.80	0.82	0.39	0.053	10	3.4
5000	0.67	0.68	0.29	0.027	5.8	3.5
5000	0.49	0.57	0.19	0.22	11	3.4
5000	0	0	0	0.14	10	3.4
5000	0.84	0.85	0.53	0.024	~30	7.7 ^c
5000	0.70	0.72	0.30	0.056	76	3.2 ^d
5000	0.44	0.46	0.16	0.068	51	2.3 ^d
5000	0	0	0	0.10	68	1.0 ^d
8000	0.82	0.87	0.42	0.115	82	8.3
8000	0.70	0.72	0.29	0.075	77	8.2
8000	0.32	0.36	0.10	~0.15	~100	8
8000	0	0	0	0.13	78	8.5

^a 250,000 rad/hr.

^b A portion of this sample formed in a small recess in the bomb. F_A for it was found to equal 0.90. Since this value differs insignificantly from f_A , the material in the recess was regarded as completely converted. The values listed apply to material not in the recess.

^c 100°C., not irradiated.

^d 100°C.

ter was known, the volume contractions associated with these displacements could be calculated. The cumulative results are plotted in Figure 1. Since volume change on polymerization is usually proportional to conversion, the linearity of the plot implies that the polymerization proceeded at a constant rate during the radiation periods. Attempts were made to detect polymerization in the absence of radiation in the same experiment by making a second determination of each piston position after a period of about 20 min. In each case duplicate positions were found, indicating that the polymerization rate due to the combination of thermal rate and

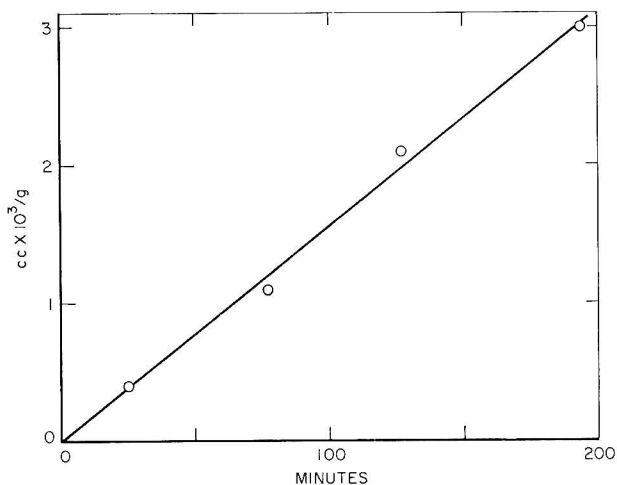


Fig. 1. Isobaric volume change vs. irradiation time, 1400 rad/hr., 21°C., 5000 atm., 89% C₂F₄. After 194 min. conversion was 6.9%.

any long-term after-effect was much smaller than the radiation-induced rate.

The experiment described above was performed because formation of a second liquid phase occurred during irradiation of the samples run at auto-genous pressure. Phase separation sometimes is associated with rate acceleration or postpolymerization so it seemed worth while to look for these effects in a run at high pressure.

Significant thermal polymerization did occur only in one experiment (that indicated by note c in Table I). On bringing the sample to the desired pressure a second time before irradiation (our standard procedure) a larger value was found for the piston penetration than was originally required. A third approach to the desired pressure required still more penetration, indicating that a reaction definitely was occurring. Therefore, the sample was not irradiated; the pressure was reduced after about 45 min. Isolation of the polymer permitted calculation of the listed conversion and rate; the latter is uncertain, because it is not known exactly when the reaction started.

Trace amounts of nonpolymeric reaction products were detected (but not identified) only in the monomer recovered from all samples polymerized at 100°C.

Three unlisted experiments gave only traces of polymer but very large amounts of carbon and carbon tetrafluoride. The reaction conditions will be given because of the possible hazard implied for others who may work with this system. The formation of carbon and carbon tetrafluoride occurred first when pressure was applied at 100°C. to a sample that contained 90% tetrafluoroethylene. At about 5000 atm. the pressure rose abruptly to about 7000 atm. and then dropped sharply. The products were as indicated above. Carbon was formed at 22°C. and both 5000 and

3500 atm during the irradiation of samples having 88% tetrafluoroethylene. In the latter two experiments a bomb of twice the normal bore was involved (sample dimensions in these two runs were 2.5 cm. diameter and 7.5 cm. length). In the run at 3500 atm. pressure, in which carbon and carbon tetrafluoride were formed, pressure measurements had indicated that the sample condition was still satisfactory when one-third the final dose had accumulated. A repeat run in the same bomb, but for a shorter time, gave polymer. In our regular bombs there was a successful polymerization with a charge containing 95% tetrafluoroethylene.

Properties of the Copolymers

Solubility. The homopolymer of 3,3,3-trifluoropropene is soluble in acetone and hexafluorobenzene at 29.6°C. The copolymer containing 10% tetrafluoroethylene is swollen by, but is insoluble in, acetone. It was assumed that samples containing more tetrafluoroethylene also would be insoluble in acetone, so no further test was made with it. Polymers containing up to 70% tetrafluoroethylene are soluble in hexafluorobenzene at 29.6°C. The sample containing 85% tetrafluoroethylene was enormously swollen at 29.6°C. by hexafluorobenzene. The gellike precipitate occupied one-third of the total volume when the polymer represented but 0.3% of the total weight. This sample was soluble at 190°C. (in a sealed tube) but reprecipitated as a loose gel at about 150°C. The sample containing

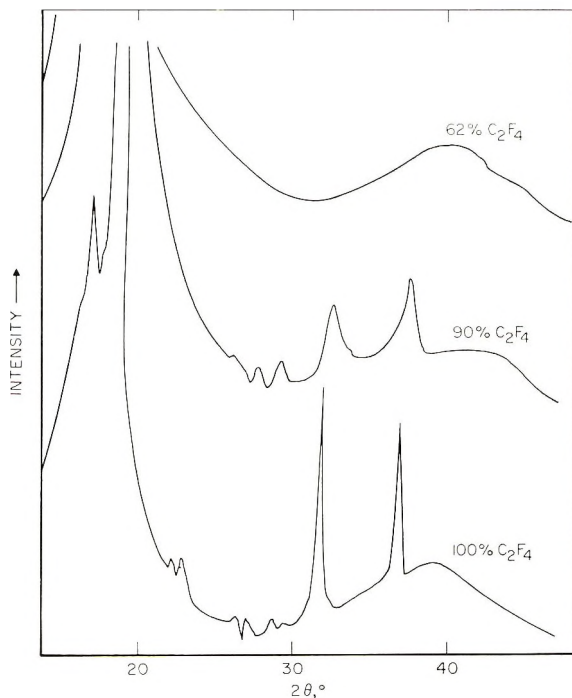


Fig. 2. X-ray intensity vs. Bragg angle $\times 2$; films 0.1 mm. thick, on glass plate.

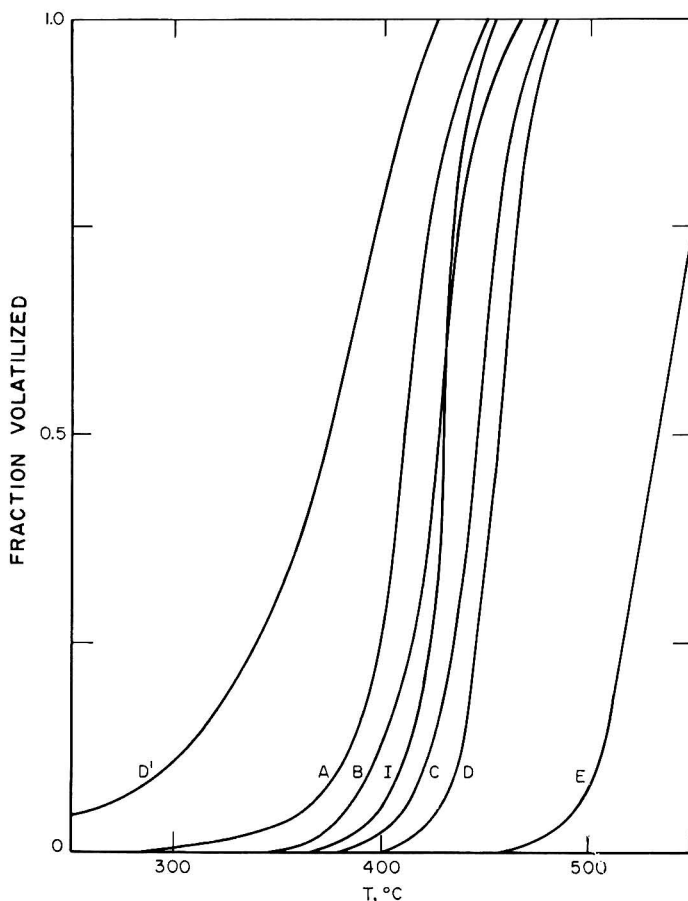


Fig. 3. Thermogravimetry of C_2F_4 - $C_3F_3H_3$ copolymers, heating rate $1.8^\circ C./min.$: (I) polyethylene; (A) 0% C_2F_4 ; (B) 42% C_2F_4 ; (C) 64% C_2F_4 ; (D) 85% C_2F_4 ; (D') 85% C_2F_4 after 280 Mrad.; (E) Teflon.

90% tetrafluoroethylene was not much swollen by hexafluorobenzene at any temperature up to $225^\circ C$. This is near the critical temperature for this solvent, so perfluorobiphenyl was used at still higher temperatures. It dissolved this sample at $300^\circ C$. but not at $190^\circ C$.

Bulk Behavior. At room temperature the polymers become much softer as the content of tetrafluoroethylene increases from zero to 70%; hardness increases progressively at contents of 70 to 85 to 90% tetrafluoroethylene. The glass transitions of these copolymers are being measured by the dilatometric method, using mercury as the confining fluid. There is a progressive decrease in the glass transition as the content of tetrafluoroethylene is increased.⁶

Crystallinity. It is natural to suspect crystallinity as the cause of the insolubility and the increased stiffness that occurs at tetrafluoroethylene contents of 70–85%. In Figure 2 x-ray diffraction curves obtained from

two thin copolymer films are compared with the curve from a commercial Teflon film of about the same thickness. The individual curves are placed arbitrarily on the ordinate axis; the values of 2θ are matched. The underlying glass plate is the cause of the broad maximum. Peaks indicative of crystallinity are the sharper ones, such as occur at 2θ equal to 32° and 38° , for the Teflon sample and the copolymer containing 90% tetrafluoroethylene. Such peaks are absent from the pattern of the sample containing 62% tetrafluoroethylene.

A repeat run on the sample containing 62% tetrafluoroethylene after it had been exposed to 200 Mrad still showed no sharp peaks.

Thermal Stability. Thermogravimetric analyses are given in Figure 3; curves for polyethylene and polytetrafluoroethylene are included for comparison. There is a measurable increase in thermal stability as the content of tetrafluoroethylene is increased. Prior exposure of one sample to gamma radiation decreased its thermal stability. A similar effect has been observed with other polymers.⁷

Effect of Gamma Radiation. Samples of copolymers containing 42, 62, 85, and 90% tetrafluoroethylene were placed in well-evacuated tubes and exposed to radiation from cobalt-60. The gel content was determined after shaking of the irradiated samples in solvents known to dissolve the unirradiated polymer: i.e., hexafluorobenzene at 29.6°C . for the polymers containing 42 and 60% tetrafluoroethylene, hexafluorobenzene at 190°C . for the sample with 85% tetrafluoroethylene, and perfluorodiphenyl at 300°C . for the sample with 90% tetrafluoroethylene. The results are given in Table II; they imply that all polymers but the one with 90% tetrafluoroethylene form gel when irradiated.

TABLE II
Apparent Effect of Gamma Radiation

C ₂ F ₄ , %	Mrad	Gel, %
42	140	82
62	12	77
62	280	92
85	12	63
85	280	91
90	12	0

However, the gels were re-extracted with hot, degassed perfluorobiphenyl. As the temperature was slowly increased, the samples containing 42 and 64% tetrafluoroethylene dissolved very suddenly at 300°C . The sample containing 85% tetrafluoroethylene dissolved less rapidly at 340°C .

DISCUSSION

The polymerization data have been considered in terms of homogenous kinetics by using the conventional reactivity ratio concept and copolymer

rate equation. The results of this analysis are given below because they are consistent with many of the data. One anticipates some difficulties with this approach, in view of the observed phase separation at autogenous pressure.

The copolymerizations probably proceed by a free-radical chain mechanism. The G value (yield per 100 e.v. absorbed) for monomer units converted to polymer is between 120 and 850,000, indicating that a long kinetic chain exists. The polymerization rate of samples of about the same composition increases with temperature. At autogenous pressure the polymerization rates increase by a factor of 24–27 when the radiation intensity increases by a factor of 180; that is, about as the 0.6 power of the intensity. The rates of free-radical chain reactions increase with temperature and, ideally, as the 0.5 power of the intensity; the rates of ionic polymerizations usually decrease when temperature is increased and are proportional to intensity. Thus, our results are more like those expected from a radical than an ionic mechanism.

Composition Diagram

When the chain length is long, the copolymer composition depends on the monomer composition and four propagation constants. These constants are denoted k_{AA} , k_{AB} , k_{BB} , and k_{BA} , where A and B refer to tetrafluoroethylene and 3,3,3-trifluoropropene, respectively. In each constant the first subscript indicates the kind of radical end and the second indicates

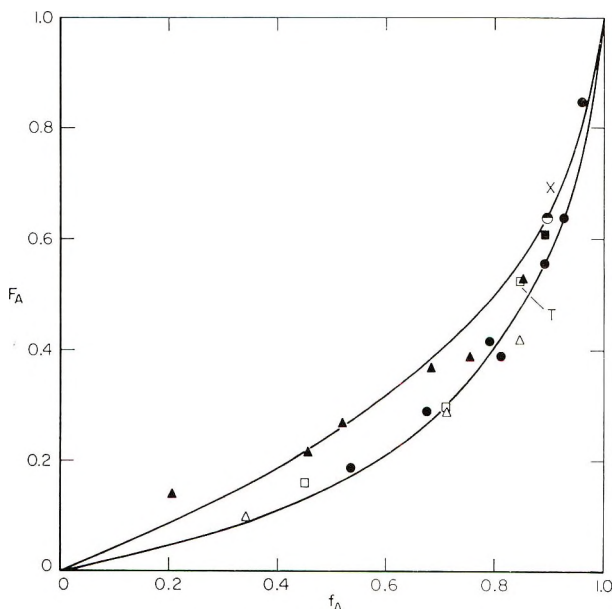


Fig. 4. Fraction C_2F_4 in polymer vs. fraction in monomer. Curves according to eq. (1): (upper) $r_1 = 0.15$, $r_2 = 2.5$; (lower) $r_1 = 0.12$, $r_2 = 5.0$. At 21°C., except (□). Pressure: (▲) autogenous; (×) 1000 atm.; (■) 1800 atm.; (⊙) 3500 atm.; (●) 5000 atm.; (Δ) 8000 atm.; (□) 5000 atm. 100°C.

the monomer that is added. Equations relating the instantaneous polymer and monomer compositions have been derived in various forms.^{8a} One is

$$F_A = (r_1 f_A^2 + f_A f_B) / (r_1 f_A^2 + 2f_A f_B + r_2 f_B^2) \quad (1)$$

where F_A and f_A are the mole fractions of tetrafluoroethylene in polymer and monomer, respectively, f_B is the mole fraction of 3,3,3-trifluoropropene, and r_1 and r_2 are the rate constant ratios k_{AA}/k_{AB} and k_{BB}/k_{BA} , respectively.

Figure 4 is a plot of F_A versus f_A . Symbols represent experimental values taken from Table I. The arithmetic mean of the initial and final value of f_A is used to minimize the effect of the small-to-moderate composition change that occurred during each polymerization. The uncertainty in F_A is regarded as 0.03 unit. The lines were calculated by using eq. (1) and the indicated values of r_1 and r_2 . Values of r_1 and r_2 equal to 0.12 and 5.0, respectively, fit most results reasonably well (lower curve). The upper curve is a better fit for most results from polymerizations at auto-genous pressure, but the changes in r_1 and r_2 are not great. Thus, under all conditions tried both radicals add 3,3,3-trifluoropropene in preference to tetrafluoroethylene, since r_1 is less than 1 and r_2 is greater than 1. Furthermore, there is only a small effect of pressure and temperature changes in this preference.

The result for the thermal polymerization (the point marked T, Figure 4) falls in with the other data. If the thermal and radiation-induced polymerizations proceeded by different mechanisms, different reactivity ratios would be expected to apply, and the point marked T would very likely be remote from the other points. A thermal polymerization at 100°C. more rapid than any at 21°C. certainly is thought to be free-radical in nature. Therefore, the observed position of point T supports a free-radical mechanism of the radiation-induced polymerizations.

The Alfrey-Price Q and e parameters were calculated for 3,3,3-trifluoropropene for each of the two sets of reactivity ratios by making use of a published value for tetrafluoroethylene.⁹ It was assumed that pressure had no effect on Q_A and e_A . The average values of Q_B and e_B believed applicable are 0.13 and 0.42, respectively. Values such as these imply a low general activity (Q) combined with a moderate polar term (e). The Q and e values for 3,3,3-trifluoropropene are similar to those of vinyl chloride, 0.044 and 0.20 respectively; both contain radicals of approximately the same electronegativity attached to vinyl radicals.

Copolymerization Rates

In the conventional theory of copolymerization rates the termination rate constants are assumed independent of the monomer composition.^{8b,10} If the G value for initiation also is independent of monomer composition, besides pressure and temperature, the rate equation can be put in a form of rather general utility. It is

$$R_p/R_B = (R_A/R_B)[r_1 f_A^2 + 2f_A f_B + r_2 f_B^2] / \{r_1^2 f_A^2 + 2\Phi f_A f_B r_1 r_2 (R_A/R_B) + [r_2 f_B (R_A/R_B)]^2\}^{1/2} \quad (2)$$

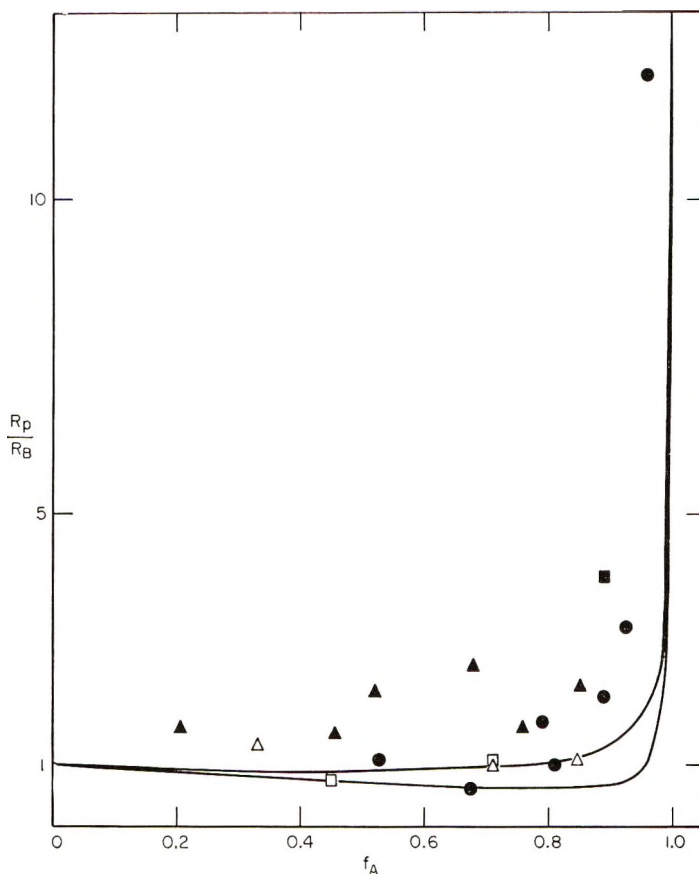


Fig. 5. Relative polymerization rate vs. fraction C_2F_4 in monomer. Curves according to eq. (2): (upper) $r_1 = 0.15$, $r_2 = 2.5$; (lower) $r_1 = 0.12$, $r_2 = 5.0$; (both) $R_A/R_B = 10$, $\Phi = 1$, and $R_A/R_B = 10^3$, $\Phi = 1$ and 100. At 21°C., except (\square). Pressure: (\blacktriangle), autogenous; (\blacksquare) 1800 atm.; (\bullet) 5000 atm.; (\triangle) 8000 atm.; (\square) 100°C., 5000 atm.

In this equation the polymerization rates of mixed A and B, pure B, and pure A are R_p , R_B , and R_A , respectively. The quantity Φ is equal to $k_{t_{AB}}/2k_{t_{AA}}^{1/2}k_{t_{BB}}^{1/2}$, where the k 's are rate constants for cross termination and the two types of like termination, respectively. Values of Φ substantially greater than 1 are commonly observed.

Calculations were made by using assumed values of R_A/R_B and Φ in eq. (2). The results are plotted in Figure 5 with the observed rate ratios. Most of the latter are above the theoretical curves, which are insensitive to chosen values of R_A/R_B and Φ over the experimental range of compositions. Obtaining good agreement between curves and experimental data requires the use of negative Φ 's, which have no physical meaning.

Departure from the rate theory usually is attributed to a composition dependence of the initiation or termination rate constants, or both. In

this case it also may be connected with phase separation, since it appears that higher values of R_p/R_B are associated with the high conversion results. A plausible picture is that rates are higher in the dense phase, but the combined rate is not much affected if conversion is so low that little dense phase is present. This would explain the proportionality between conversion and time implied by the data in Figure 1, all of which are at low conversion.

Equation (2) contains additive combinations of several temperature- and pressure-dependent terms. It follows that activation terms are not simple sums of values for two or more elementary reactions and would not be expected to be independent of temperature or pressure even at constant composition. For this reason no attempt is made to consider the dependence of such terms on monomer composition. For empirical use values may be taken as $-15 \text{ cm.}^3/\text{mole}$ and 5 kcal./mole for the activation volume and enthalpy, respectively.

Molecular Weight

An examination of the intrinsic viscosities listed in Table I reveals two types of variation with composition. In polymerization at room temperature and high pressure or at autogenous pressure, when the radiation intensity is high, the intrinsic viscosity varies little with composition until it increases with the rate in the region of 80–90% tetrafluoroethylene. In polymerizations at 100°C. and 5000 atm. or at room temperature and autogenous pressure at low radiation intensity the intrinsic viscosity increases gradually with the content of tetrafluoroethylene. It appears that variations in the importance of monomer transfer account for this behavior; we illustrate this with Figure 6. This is a plot of the intrinsic viscosity of poly(3,3,3-trifluoropropene) versus its viscosity-average molecular weight (10^{-5}) (symbol \ominus and the straight line); superimposed on this is a plot of intrinsic viscosity versus a function of the kinetic chain length for all samples except those with intrinsic viscosities lower than 0.1, different symbols being used for different reaction conditions. The viscosity-average molecular weights were obtained by means of a relation determined previously.¹ The function of the kinetic chain length is so chosen that it is numerically equal to the viscosity-average molecular weight (10^{-5}) if transfer is negligible, termination is by disproportionation, and the G value for initiation is equal to 4. The numbers under each symbol are the percentages of combined tetrafluoroethylene.

None of the viscosity data have been so treated as to eliminate the decrease due to the shear rate in the viscometers (maximum values were about 500–1000 sec.^{-1}). Where the apparent intrinsic viscosities are in the range 8 to 10 dl./g. the correction is expected to be appreciable.¹¹ Correction is not possible without extensive work but, if made, might result in a closer approach of the high-viscosity data to the line.

Consider now the agreement between the function of the kinetic chain length and the viscosity-average molecular weight of poly(3,3,3-trifluoro-

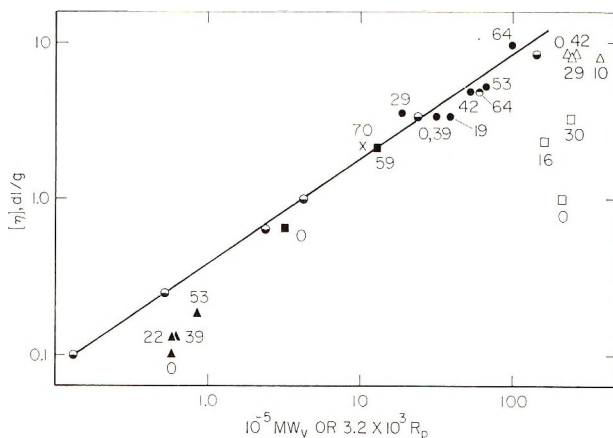


Fig. 6. Intrinsic viscosity of poly-3,3,3-trifluoropropene in hexafluorobenzene vs. (\bullet) $M_v (\times 10^{-5})$ and also intrinsic viscosity of homo- and copolymers vs. kinetic chain-length function at 1400 rad/hr. At 21°C., except (\square). Pressure: (\blacktriangle) autogenous; (\times) 1000 atm.; (\blacksquare) 1800 atm.; (\odot) 3500 atm.; (\bullet) 5000 atm.; (\triangle) 8000 atm.; (\square) 100°C., 5000 atm. The number associated with each point is the percentage of tetrafluoroethylene in the polymer.

propene). In polymerizations at 21°C. and pressures of 1800, 5000, and 8000 atm. the values are very similar (compare the abscissa values of the line and of points with a zero), indicating that transfer is negligible. Under such conditions the presence of tetrafluoroethylene changed the intrinsic viscosity only when the kinetic chain length changed. At 21°C. and autogenous pressure or at 100°C. and 5000 atm. the kinetic chain-length function is much larger than the viscosity-average molecular weight, indicating that transfer is important. Under these conditions the intrinsic viscosities increased with the content of tetrafluoroethylene, even when the kinetic chain length was constant. Our interpretation is that increasing the amount of tetrafluoroethylene decreases the importance of transfer, but this can affect the molecular weight appreciably only if the polymerization pressure and temperature are such that transfer is important in the homopolymerization of 3,3,3-trifluoropropene.

In consequence, the values of the kinetic chain-length function chosen should be about equal to the copolymer molecular weight (10^{-5}) when the polymerization pressure is high at 21°C. A correlation of such values with intrinsic viscosity for various polymer compositions, as in Figure 6, suggests that there is little influence of polymer composition on the relation between intrinsic viscosity and molecular weight. Thus, for rough purposes the line drawn for the homopolymer can be applied to the copolymers as well.

Radiation Effects

Ordinarily one believes a polymer crosslinks when irradiated if exposure to radiation renders it incompletely soluble in materials in which it pre-

viously had dissolved. The finding that the insoluble materials listed in Table II dissolved at about 300°C. can be interpreted in at least two ways. Irradiation might induce crystallization, as found in the case of polytetrafluoroethylene.¹² If so, the materials would be insoluble only at temperatures well below the melting temperature of polytetrafluoroethylene (327°C.), as observed. However, the x-ray pattern of an irradiated sample shows no evidence of crystallinity. An alternative explanation is that the large doses of radiation used decrease the thermal stability so much that the solution process results from thermal degradation of the gel. The marked effect of prior irradiation on thermal stability (compare lines D' and D in Fig. 3) and the negative x-ray result mentioned above make us favor the second explanation.

Acknowledgment

The authors thank the following persons at the National Bureau of Standards for their assistance: Rolf Paulson for the elemental analysis, Sidney Straus for the thermogravimetric analysis, William Dorko for the mass spectrographic analysis, and Howard Swanson for the x-ray diffraction.

This work was based on research supported by the U.S. Army Research Office, Durham, North Carolina.

References

1. D. W. Brown, *Am. Chem. Soc. Polymer Preprints*, **6**, 965 (1965).
2. E. M. Sullivan, E. W. Wise, and F. P. Reding, U.S. Pat. 3,110,705 (1963).
3. L. A. Wall, D. W. Brown, and R. E. Florin, *Am. Chem. Soc. Polymer Preprints*, **2**, 366 (1961).
4. D. W. Brown and L. A. Wall, *J. Phys. Chem.*, **67**, 1016 (1963).
5. W. R. Hasek, W. C. Smith, and V. A. Engelhardt, *J. Am. Chem. Soc.*, **82**, 543 (1960).
6. H. Yu, private communication, National Bureau of Standards.
7. S. Straus and L. A. Wall, *SPE Trans.*, **4**, 61 (1964).
8. P. J. Flory, *Principles of Polymer Chemistry*, Cornell Univ. Press, Ithaca, N.Y., 1953: (a) p. 178; (b) p. 200.
9. L. J. Young, *J. Polymer Sci.*, **54**, 411 (1961).
10. G. N. Burnett, *Mechanism of Polymer Reactions*, Interscience, New York, 1954, p. 290.
11. T. G. Fox, J. C. Fox, and P. J. Flory, *J. Am. Chem. Soc.*, **73**, 1901 (1951).
12. A. Nishioka, M. Tajuna, and M. Owaka, *J. Polymer Sci.*, **28**, 617 (1958).

Received July 31, 1967

Revised September 27, 1967

Alternating Copolymerization through the Complexes of Conjugated Vinyl Monomers-Alkylaluminum Halides

MASAAKI HIROOKA, HIROSHI YABUUCHI, JIRO ISEKI, and
YASUTO NAKAI, *Central Research Laboratory, Sumitomo Chemical Co.
Ltd., Takatsuki, Osaka, Japan*

Synopsis

A vinyl monomer that has the nitrile or carbonyl group conjugated to the C=C double bond, such as acrylonitrile, methyl acrylate, and methyl methacrylate, forms a complex with an alkylaluminum halide, and the complex reacts spontaneously with a hydrocarbon monomer such as styrene, propylene, or ethylene, giving a high molecular weight copolymer. The copolymers always contain the two monomer units in 1:1 ratio. Thus styrene, copolymerized with methyl acrylate or methyl methacrylate in the presence of ethylaluminum sesquichloride in homogeneous toluene solution, gives such an equimolar copolymer regardless of the initial monomer compositions. The NMR spectra of these copolymers are distinctly different from those of the equimolar copolymers obtained with azobisisobutyronitrile as initiator and have simpler and well separated patterns. The copolymers and the corresponding radical copolymers appear to be amorphous, judged by their x-ray diffraction patterns and their differential thermal analyses. Their infrared spectra resemble each other very closely. Hence, the difference in the NMR spectra may be ascribed to the matter of the sequence distribution. The infrared spectrum of ethylene-methyl acrylate copolymer shows no absorption near 720 cm.^{-1} due to the methylene sequence arising from ethylene-ethylene linkage. These experimental data lead to the inference that the equimolar copolymers obtained in this work may have an alternating sequence.

INTRODUCTION

The authors¹ previously found that the acrylonitrile-ethylaluminum dichloride complex or a mixture of them *in situ* copolymerized spontaneously with olefinic hydrocarbon monomers, such as propylene, styrene, isobutylene and hexene-1, in high yield even at such low temperatures as -78°C . It was particularly noteworthy that an equimolar copolymer was obtained over a wide range of experimental conditions. Furthermore, some experimental results suggested that these equimolar copolymers have alternating monomer sequences. The crucial fact in this type of copolymerization appears to be that acrylonitrile is coordinated to an alkylaluminum halide. It was also interesting that copolymers of such novel monomer combinations as propylene and polar vinyl monomer were obtained, such copolymerization reactions having been scarcely known to take place.

The authors have extended the studies of this type of reaction and of the properties of the copolymer. The present work relates to a similar copolymerization with methyl acrylate or methyl methacrylate in place of acrylonitrile. Emphasis has been placed on the clarification of the sequence distribution in the copolymers through the inferences obtained from the copolymerization process itself, the NMR and IR spectra, and other properties of the copolymers.

EXPERIMENTAL

Materials

Monomers. Methyl acrylate, methyl methacrylate, acrylonitrile, and styrene were purified, distilled, and dried in the usual way. Propylene and ethylene were polymerization grade, from the Sumitomo Chemical Co.

Solvents. *n*-Heptane was ASTM pure grade obtained from the Enjay Chemical Co. and further refined by being treated with concentrated sulfuric acid, washed with water, dried and distilled. Toluene, a commercial G.R. grade, was used after drying over silica gel.

Organoaluminums. Ethylaluminum sesquichloride and ethylaluminum dichloride, obtained from the Ethyl Corporation Ltd. were distilled under nitrogen atmosphere, diluted into purified *n*-heptane or toluene, and stored in glass ampules.

Polymerization

The polymerization procedure may be illustrated by an example of the copolymerization of methyl acrylate and styrene with ethylaluminum sesquichloride.

In a 200-ml. four-necked flask equipped with a stirrer, a thermometer, and a gas inlet tube, toluene and methyl acrylate were mixed under nitrogen atmosphere and cooled to -78°C . by a mixture of solid carbon dioxide and methanol. When a toluene solution of ethylaluminum sesquichloride was added to this, the mixture became a homogeneous pale-yellow solution. Then the solution was brought to 25°C . No polymer was produced. Upon the addition of styrene a polymerization commenced. According to the progress of the copolymerization, the yellow, clear solution became viscous and yet remained homogeneous. At the end of the polymerization, the reaction mixture was poured into a large amount of methanol and white solid copolymer was coagulated. The copolymer was washed with methanol, dried *in vacuo*, and weighed. The purification of the copolymer was carried out by reprecipitation from acetone solution into methanol.

The copolymerizations with other monomer combinations were carried out by similar procedures. The copolymerization with propylene was conducted in a 300 ml. glass pressure vessel with a stirrer and that with ethylene in a 300 ml. stainless steel autoclave.

Measurements

Intrinsic Viscosity. Viscosity measurements were carried out, in benzene solution in the case of methyl acrylate or methyl methacrylate copolymers and in dimethylformamide solution in the case of acrylonitrile copolymers, at 30°C. with an Ubbelohde viscometer.

NMR Measurements. A 100 Mc./sec. high-resolution NMR spectrometer Model JNM4H-100, made by Japan Electron Optics Laboratory Inc., was used. The NMR spectra of the copolymers were obtained at 70–80°C. in deuterated chloroform as about 10% solution. Tetramethyl silane or hexamethyl disiloxane was used as the internal standard.

Infrared Measurements. Infrared measurements of the copolymers were carried out with a Perkin-Elmer Model 125 infrared spectrophotometer.

RESULTS

Copolymerization

Various Monomer Combinations

Conjugated polar monomers that have the carbonyl or nitrile group, such as methyl acrylate, methyl methacrylate, and acrylonitrile, form complexes with alkylaluminum halides. In the presence of the conjugated monomer and an alkylaluminum halide a hydrocarbon monomer such as propylene, styrene, or ethylene rapidly reacts and produces copolymer with high molecular weight. Typical results of the copolymerization with *n*-heptane or toluene as solvent are given in Table I. The copolymers were purified against the alkylaluminum component by reprecipitation from acetone, benzene, or dimethylformamide into methanol. The compositions of the copolymers according to elementary analyses agreed well with the calculated value for the 1:1 copolymer. The results are similar to those of the copolymerization of acrylonitrile and olefins with alkylaluminum halides, reported in a previous paper.¹ Although the copolymerization of acrylonitrile proceeded heterogeneously in all cases, methyl acrylate or methyl methacrylate copolymerized in the homogeneous system if toluene was used as solvent. Thus, in the copolymerization system of styrene and methyl acrylate (MA) or methyl methacrylate (MMA) with toluene as solvent both the complex of ethylaluminum sesquichloride and MA or MMA and the resulting copolymer were soluble in the solvent, and the copolymerization proceeded homogeneously at a moderate rate at about room temperature. The authors have therefore chosen these homogeneous copolymerization systems for further detailed study.

Methyl Acrylate and Styrene

The results of copolymerizations effected over a wide range of monomer composition and given in Table II. Ethylaluminum sesquichloride was used in one-half the molar amount of methyl acrylate, in order to prevent the

TABLE I
Copolymerization with Various Monomer Combinations

Expt. no.	Monomer, ^a g.		Organoaluminum, mmoles	Solvent, ml.	Time, min.	Temp., °C.	Phase	Yield, g.	[η], dl./g.	Elem. anal., ^b %		
	A	B								C	H	N
1	Pr, 100	AN, 2	AlEtCl ₂ , 50	<i>n</i> -heptane, 150	5	-78	heter.	2.48	0.63	—	—	14.46 (14.72)
2	"	"	"	toluene, 30	10	-78	"	2.87	1.84	—	—	14.39
3	"	MA, 4	"	—	10	-78	"	1.64	4.95	65.50 (65.60)	9.46 (9.44)	—
4	St, 10	AN, 2	AlEt _{1.5} Cl _{1.5} , 25	<i>n</i> -heptane, 20	10	-10	"	2.93	1.88	83.71 (84.04)	7.84 (7.05)	9.02 (8.91)
5	"	MA, 3	"	"	62	25	"	3.85	0.91	75.84 (75.76)	6.92 (7.42)	—
6	"	"	"	toluene, 62	240	25	homo.	3.46	3.18	75.76	7.85	—
7	"	MMA, 3	"	"	62	25	"	1.54	2.02	76.12 (76.40)	7.80 (7.90)	—
8	E, 100	MA, 4	"	<i>n</i> -heptane, 20	180	-78	heter.	0.82	1.53	63.22 (63.13)	9.11 (8.83)	—

^a Pr, propylene; St, styrene; E, ethylene; AN, acrylonitrile; MA, methyl acrylate; MMA, methyl methacrylate.

^b Figures in parentheses indicate value calculated for 1:1 copolymer.

TABLE II
 Copolymerization of Methyl Acrylate and Styrene^a

Expt. no.	Monomer concn., moles/l.		Polymn. time, min.	Yield, g.	Elem. anal., %		MA mole-% in polymer	Convsn., % of MA	[η], dl./g.
	MA	St			C	H			
1	0.40	1.20	60	1.72	75.61	7.72	50.4	28.3	4.69
2	"	"	240	3.34	75.44	7.58	50.9	54.9	4.64
3	"	0.60	60	1.65	76.21	8.41	48.8	27.2	2.84
4	"	"	240	3.46	75.76	7.85	50.0	56.9	3.18
5	"	"	360	4.17	76.02	8.32	49.3	68.5	2.85
6	"	0.30	60	1.03	75.95	7.67	49.5	16.9	3.02
7	"	"	240	2.75	—	—	—	45.2	2.64
8	"	"	360	3.74	75.41	7.18	51.0	61.4	2.16
9	"	0.11	20	0.52	75.96	7.80	49.5	8.5	1.66
10	"	"	240	1.43	75.90	7.39	49.7	23.6	1.27

^a Polymerization condition: 25°C.; AIEt_{1.5}Cl_{1.5}, 0.2 mole/l.; solvent, toluene; total liquid volume, 80 ml.

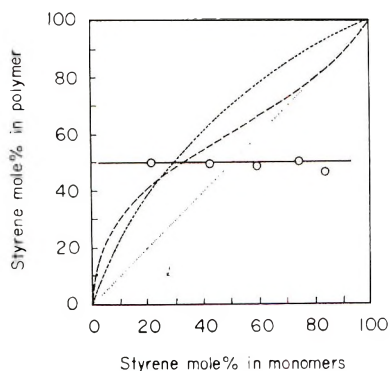


Fig. 1. Copolymerization of methyl acrylate and styrene: (O) with $\text{AlEt}_{1.5}\text{Cl}_{1.5}$: (---) radical,^{2,3} $r_1(\text{St}) = 0.75$, $r_2(\text{MA}) = 0.18$; (- - -) cationic,⁴ $r_1(\text{St}) = 2.2$, $r_2(\text{MA}) = 0.4$.

homopolymerization of styrene by free ethylaluminum sesquichloride. In this condition no homopolymer of methyl acrylate was produced. The copolymerization proceeded homogeneously, and the viscosity of the clear, yellow solution gradually increased. Although the composition of the unreacted monomer varied according to the progress of the copolymerization, the resulting copolymer always contained each monomer component in equimolar proportions; this relationship held independently of initial monomer composition. All the compositions of the copolymers in elementary analyses represented extremely good agreement with the calculated value for the 1:1 copolymer. The molecular weights of the copolymers in general were high and increased in proportion to the increase of styrene concentration.

Figure 1 indicates the relationship between monomer feed and polymer composition in the present copolymerization compared with those of conventional cationic and radical copolymerizations. The polymer composition in either the cationic or the radical process varies according to the monomer composition, but the present copolymerization apparently differs from these conventional ones in monomer reactivity.

Methyl Methacrylate and Styrene

Table III gives the results of copolymerizing methyl methacrylate and styrene under conditions similar to those of methyl acrylate and styrene. In this case the effect of monomer composition was investigated under the condition of constant total monomer concentration and varying ratios of monomer components. Ethylaluminum sesquichloride was used in one-half the molar amount of methyl methacrylate. As the concentration of ethylaluminum sesquichloride increased, the polymer yield increased. The copolymerization was stopped at a relatively low conversion, 3–10%. The copolymer compositions may be seen to be equimolar over the wide range of monomer composition.

TABLE III
Copolymerization of Methyl Methacrylate and Styrene^a

Expt. no.	Monomer concn., ^b moles/l.		AIEt _{1.5} Cl _{1.5} concn., moles/l.	Polymn. time, min.	Yield, g.	Elem. anal., %		MMA in polymer, %	Convsn., % of MMA	[η], dl./g.
	St	MMA				Tot.	C			
11	2.0	0.5	2.5	90	1.08	75.82	7.85	51.9	10.6	2.72
12	1.5	1.0	"	60	1.23	75.60	8.07	52.6	6.1	3.81
13	1.0	1.5	"	15	1.61	74.82	7.95	55.0	5.3	3.58
14	0.5	2.0	"	7	1.14	74.79	7.96	55.1	2.8	3.30

^a Polymerization conditions: 25°C.; MMA/AIEt_{1.5}Cl_{1.5} molar ratio, 2.0; solvent, toluene; total liquid volume, 100 ml. Theoretical value of elementary analysis for alternating copolymer: C, 76.44%; H, 7.90%.

^b St, Styrene; MMA, methyl methacrylate.

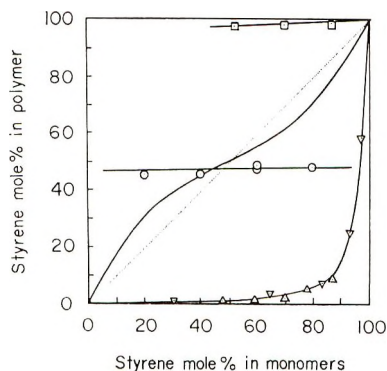


Fig. 2. Copolymerization of methyl methacrylate and styrene. (—) radical;⁵ (□) cationic;⁶ (Δ) anionic, Na catalyst;⁷ (▽) anionic, BuLi catalyst;⁷ (○) with $\text{AlEt}_{1.5}\text{Cl}_{1.5}$.

Figure 2 shows the relationship between monomer feed and copolymer composition compared with those in the conventional radical, cationic, and anionic copolymerizations. It is apparent that the results of the present copolymerization do not agree with any conventional relation.

Preparations and Properties for NMR and IR Analyses

The properties of the copolymers of the present copolymerization and of radical copolymerization, obtained for NMR and IR analyses, are summarized in Table IV. Random copolymers were prepared in bulk with azobisisobutyronitrile (AIBN) as initiator. To produce 1:1 copolymer, the initial monomer compositions were deduced from the monomer reactivity ratio. The reactions were stopped at a low conversion. The copolymers were purified by the reprecipitation procedure.

NMR Spectra of Copolymers

Styrene-Methyl Methacrylate Copolymers

The NMR spectra of the copolymers were obtained from the 10% deuterated chloroform solution at the resonance frequency of 100 Mc./sec. Figure 3 shows typical spectra of copolymers of 1:1 composition, prepared with $\text{AlEt}_{1.5}\text{Cl}_{1.5}$ and AIBN. Spectrum *B* is identical with that reported by Harwood and Ritchey,^{8,9} but the spectrum *A* differs from them and also from the spectrum of block copolymer.¹⁰ Spectrum *A* is comparatively simplified, and the resonance splits are sharp.

The authors¹¹ have analyzed the spectra of these copolymers and discussed the assignments of the resonances and sequence of the monomer units. By comparing spectra *A* and *B* the following facts may be summarized:

(1) The diamagnetic shift of the *ortho* proton in the phenyl group is seen in spectrum *B* but not *A*.

TABLE IV
Properties of Copolymers for NMR and IR Analyses^a

Expt. no.	Monomer		Catalyst	Elem. Anal., ^b %			Polym. compn., mol.-%	[η], dl./g.
	A	B		C	H	N		
1	St	MA	AlEt _{1.5} Cl _{1.5}	75.62 (75.76)	7.39 (7.42)	—	MA 50.4	5.37
2	"	"	AIBN	75.58	7.66	—	MA 50.5	1.11
3	St	MMA	AlEt _{1.5} Cl _{1.5}	75.93 (76.40)	7.50 (7.90)	—	MMA 51.6	3.83
4	"	"	AIBN	76.38	7.89	—	MMA 50.2	1.00
5	St	AN	AlEt _{1.5} Cl _{1.5}	83.88 (84.04)	7.59 (7.05)	8.71 (8.91)	AN 48.9	2.13
6	"	"	AIBN	82.48	7.83	9.71	AN 53.3	2.54
7	E	MA	AlEt _{1.5} Cl _{1.5}	63.22 (63.13)	9.11 (8.83)	—	MA 49.6	1.53
8	"	"	radical initiator	64.21	8.61	—	MA 45.4	2.05

^a St, styrene; E, ethylene; MMA, methyl methacrylate; MA, methyl acrylate; AN, acrylonitrile; AIBN, azobisisobutyronitrile.

^b Figures in parentheses indicate value calculated for 1:1 copolymer.

(2) The resonance of the methoxy proton in the range of 6.4–7.7 τ is broad in spectrum *B* but splits sharply into three peaks at 6.6 (I), 7.0 (II), and 7.6 (III) τ in the case of spectrum *A*.

(3) The methylene and methine resonances are also simplified in spectrum *A*.

(4) A broad peak between 9 and 9.5 τ in spectrum *B* has been assigned to the α -methyl proton. The corresponding resonance in spectrum *A* splits into three distinct peaks at 9.0 (IV), 9.3 (V), and 9.4 (VI) τ .

(5) The resonance intensity ratio of phenyl proton to either methoxy or α -methyl proton is exactly 5:3 in both spectra *A* and *B*, as is to be expected from the 1:1 copolymer composition. Furthermore, the corresponding peak intensity ratios of methoxy to α -methyl protons, i.e., (I) to (VI), (II) to (V), and (III) to (IV), are all equal and unity.

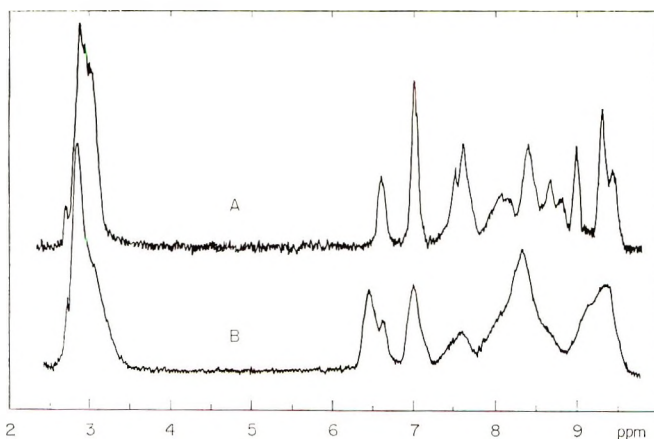


Fig. 3. NMR spectra of styrene-methyl methacrylate copolymers: (A) with $\text{AlEt}_{1.5}\text{Cl}_{1.5}$; (B) with AIBN.

In spectrum *A* the configurational influence or the difference in the sequence of monomer units may be alternatively considered as the reason for the shift of the methoxy and α -methyl proton with the three well-separated peaks. The relationship of the resonance intensities between the methoxy and α -methyl groups, however, can be explained only by the shifts' being due to the configurational effect. This leads to the conclusion that the possible sequence is an alternating one. This is also supported by the lack of the *ortho* proton shift in the phenyl group and the absence of an MMM methoxy triad at 6.4 τ , which appears in the spectrum of poly-(methyl methacrylate).

Three methoxy peaks are assigned to cosyndiotactic, coheterotactic, and coisotactic triads, respectively, from low to high field. The existence of these three configurations means that the copolymer obtained with $\text{AlEt}_{1.5}\text{Cl}_{1.5}$ is atactic.

Styrene-Methyl Acrylate Copolymers

Figure 4 shows the NMR spectra of styrene and methyl acrylate copolymers obtained with $\text{AlEt}_{1.5}\text{Cl}_{1.5}$ and AIBN. A distinct difference between them is observed. The split of the methoxy proton resonances into three peaks may be explained as analogous to that of styrene-methyl methacrylate copolymer. In this case, however, the diamagnetic shift of the *ortho* proton in the phenyl group is observed also in spectrum *A*.

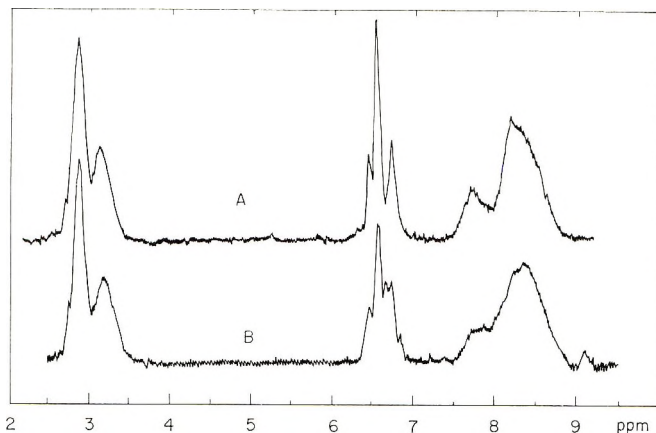


Fig. 4. NMR spectra of styrene-methyl acrylate copolymers: (A) with $\text{AlEt}_{1.5}\text{Cl}_{1.5}$; (B) with AIBN.

As to the split in the phenyl resonance, it is generally understood that it is due, not only to the successive styrene unit, but also to all environmental groups.¹² Therefore the possibility of an alternating sequence of the monomer unit is not excluded. In both spectra *A* and *B* the ratio of the resonance areas for the phenyl and methoxy protons is observed to be 5:3. Consequently, it is confirmed that each copolymer has a 1:1 composition.

IR Spectra of Copolymers*Copolymers Containing Styrene*

The infrared spectra of the copolymers formed with $\text{AlEt}_{1.5}\text{Cl}_{1.5}$ and the 1:1 radical copolymers were compared over the range of 400–4000 cm^{-1} . The spectra of styrene-methyl acrylate and styrene-acrylonitrile copolymers are shown in Figures 5 and 6. Both the spectra of the present copolymer and of the radical one are not clearly distinguished from each other except by a slight difference in the absorbance in a few bands. This is in contrast to the fact that there is a great difference between the NMR spectra of both copolymers.

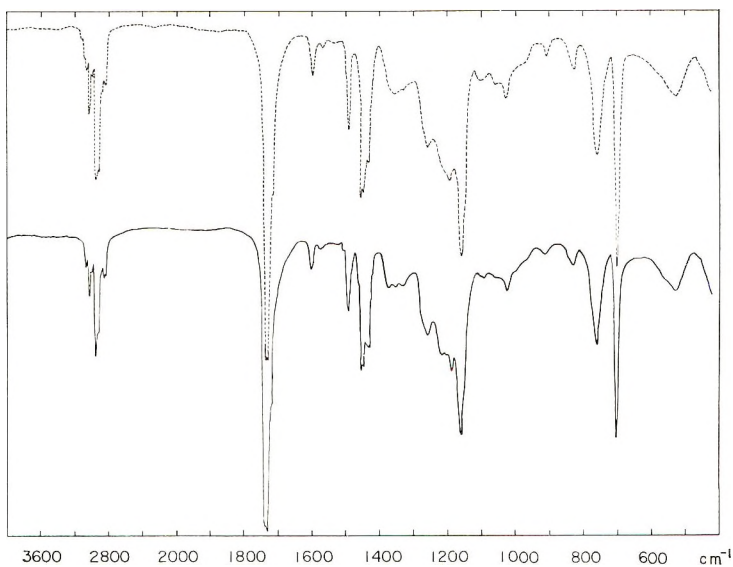


Fig. 5. IR spectra of styrene-methyl acrylate copolymers: (---) with AIBN; (—) with $\text{AlEt}_{1.5}\text{Cl}_{1.5}$.

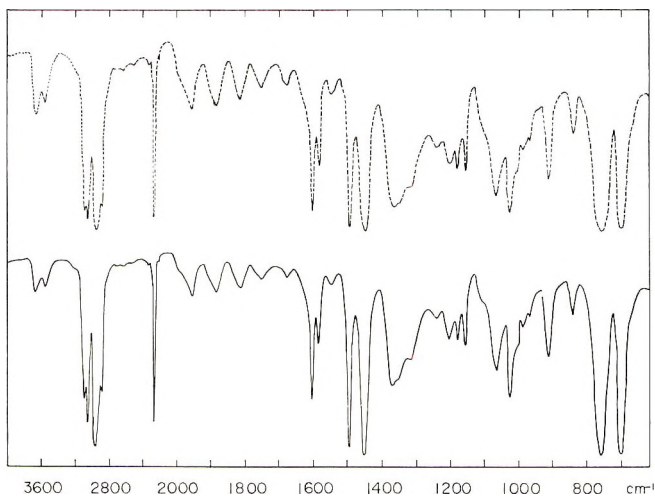


Fig. 6. IR spectra of styrene-acrylonitrile copolymers: (---) with AIBN; (—) with $\text{AlEt}_{1.5}\text{Cl}_{1.5}$.

IR Spectra of Ethylene-Methyl Acrylate Copolymers

Figure 7 shows the IR spectra of ethylene-methyl acrylate copolymers over the range of $700\text{--}900\text{ cm}^{-1}$ with a scale expander. Between the spectrum of the copolymer prepared from a monomer complex and that of the radical copolymer prepared by a high-pressure polymerization technique there is a clear difference. The absorption band at 750 cm^{-1}

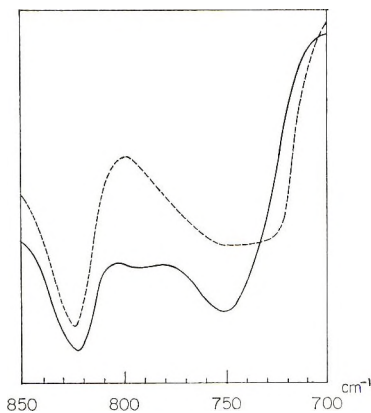


Fig. 7. IR spectra of ethylene-methyl acrylate copolymers: (- - -) with peroxide. (—) with $\text{AlEt}_{1.5}\text{Cl}_{1.5}$.

in the present copolymer was sharp and may be due to the skeletal vibration that can be seen also in the spectrum of poly(methyl acrylate). The corresponding absorption for the radical copolymer was broad and spread almost to 720 cm.^{-1} . This may be ascribed to the existence of a long chain of the methylene group; it is known that the rocking mode of at least four adjacent straight-chain methylene linkages appears near 720 cm.^{-1} . The lack of this kind of band in the spectrum of the present copolymer indicates that there is no substantial linkage of ethylene to ethylene. This may be considered in relation to the alternating sequence of the copolymer.

DISCUSSION

In a previous paper¹ attention was drawn to the fact that the copolymerization of acrylonitrile and an olefin in the presence of an alkylaluminum halide gave a copolymer of equimolar composition. Subsequent work, as shown in the present paper, has revealed that similar equimolar copolymers were obtained also when methyl acrylate or methyl methacrylate was used in place of acrylonitrile. When an alkylaluminum chloride alone was complexed with methyl acrylate or methyl methacrylate, polymerization did not occur and no homopolymer was produced. Unsaturated olefinic hydrocarbons, however, reacted instantaneously with the conjugated vinyl monomers in the presence of alkylaluminum halides, producing copolymers. The reaction gave 1:1 copolymer over a wide range of initial monomer composition and also independently of polymerization time. Consequently, each fact mentioned above supports the assumption that the present copolymer prepared through the monomer complex may have an alternating sequence.

Equimolar copolymers can be prepared also by conventional radical copolymerization. These copolymers, such as styrene-methyl acrylate and styrene-acrylonitrile copolymers, have not only 1:1 polymer composition

but also patterns in their x-ray diagrams, differential thermal analyses, and infrared spectra that are indistinguishable from the corresponding copolymers formed with $AlEt_{1.5}Cl_{1.5}$. The data also indicate that both the radical and the present copolymers are amorphous. Nevertheless, the NMR spectra of styrene-methyl acrylate and styrene-methyl methacrylate copolymers formed in the present copolymerization were shown to be very different from those of conventional radical copolymers and to be simpler. We have analyzed these spectra and obtained confirmation that the styrene-methyl methacrylate copolymer prepared with $AlEt_{1.5}Cl_{1.5}$ has an alternating sequence. Besides, the lack of the absorption band near 720 cm.^{-1} in the IR spectrum of ethylene-methyl acrylate copolymer from the present copolymerization means that a block sequence of ethylene-ethylene is not substantially included. On the basis of the results and considerations presented above it can be inferred that the 1:1 copolymer from the present copolymerization has an alternating sequence.

Although alternating copolymers from conventional radical polymerizations have been known to be obtained only from specific monomers such as maleic anhydride, vinylidene cyanide, and fumaric esters, which have little or no ability to homopolymerize, the authors have failed to find any report that an alternating copolymer was prepared from a monomer combination from which a random copolymer can be easily obtained. For this reason, the fact that alternating copolymers were obtained in the present copolymerization is noteworthy. If the conclusion concerning the alternating sequence of the copolymer is valid, it may be said that the present copolymerization is a peculiar process that enables us to compare an alternating copolymer with a random copolymer from the same monomer combination.

For an alternating copolymer a specific relationship between the monomer reactivity ratios, $r_1 = r_2 = 0$, is necessary. This means that the homopolymers do not appear and only copolymerization takes place. Such a phenomenon was observed in the copolymerization of acrylonitrile and propylene in the presence of ethylaluminum dichloride, as described in the previous paper. In the present work, too, it was confirmed that the complex of methyl acrylate or methyl methacrylate and ethylaluminum sesquichloride did not polymerize of itself. As shown in the present paper, the monomer reactivity in the present copolymerization cannot be explained by a conventional radical or ionic polymerization mechanism. The peculiarity of this copolymerization seems to consist in that the reaction proceeds through the complex of an alkylaluminum halide with a conjugated vinyl monomer. These complexes could be clearly recognized by means of IR spectroscopy in the cases of methyl acrylate, methyl methacrylate, and acrylonitrile. The complex is formed between aluminum and the carbonyl or nitrile group. It is considered that through the formation of the complex the electron density on the carbon-carbon double bond in the position conjugated to the polar group decreases and that the reactivity of the polymerization may be modified, as if it possessed the same character-

istics as a monomer that is likely to give an alternating copolymer, such as maleic anhydride, fumaric ester, or vinylidene cyanide. It seems to be important that the C=C double bonding in this kind of monomer is located in the position conjugated to the polar group. Since this kind of complex does not polymerize of itself, it is believed that the activation of the complex may arise through the attack of a donor monomer possessing a polarity opposite of that of the complexed monomer. It is judged that in the present copolymerization the complex formation and the donor-accepter interaction play important roles in the activation of the copolymerization and at the same time induce a tendency to alternation.

The effect of metallic compounds on the polymerization of vinyl compounds has been studied in recent years. Imoto et al.¹³⁻¹⁵ found that zinc chloride promotes the radical polymerization of acrylonitrile and methyl methacrylate and considered that the monomer reactivity varies because of the coordination of zinc chloride with the nitrile or carbonyl group. They further disclosed that when the copolymerization of acrylonitrile and vinylidene chloride was carried out in the presence of zinc chloride, the monomer reactivity ratios changed according to the increase of zinc chloride concentration.

A British patent applied for by Esso Research and Engineering Co.¹⁶ outlines a method of producing copolymers that consists of copolymerizing a monomer having an electronegative group, such as acrylonitrile or methyl acrylate, and a second monomer that promotes a Friedel-Crafts polymerization but has no ability for radical polymerization, such as 2-methylpentene-1, isobutylene, or hexene-1, with a Friedel-Crafts halide, in the presence of a radical initiator. In this reaction system a complex formation between the first monomer and a metal halide is suggested. It is interesting that a copolymer can be obtained from the combination that includes a monomer known to be difficult to polymerize with a radical initiator. The compositions of the copolymers obtained, however, are random and differ from the present copolymers.

Although both the studies made by Imoto et al. and the Esso patent are characterized by the modification of a vinyl monomer through complex formation between the polar group of the vinyl monomer and a metal halide such as zinc chloride, other alternating copolymers have not been prepared. Consequently, it is evident that the tendency to an alternating sequence cannot be ascribed only to the coordination effect of the polar group in a conjugated vinyl monomer to a metal halide.

It is well known that the combination of trialkyl boron or trialkyl aluminum and oxygen or a peroxide acts as an initiator in radical polymerization. Hoechst's patent¹⁷ indicates that the trialkyl aluminum-organic peroxide system initiates the copolymerization of a conjugated vinyl compound and an olefin, such as propylene, ethylene or isobutylene, which is known to polymerize with difficulty with a radical initiator. This means that these catalysts have different abilities to copolymerize with a conventional radical initiator. Further, Wexler and Manson¹⁸

studied the polymerization reaction with trialkylaluminum and found that the copolymerization of methyl methacrylate and styrene could not be explained by a conventional radical mechanism. They concluded that the polymerization is neither clearly free-radical nor ionic, and some form of coordination may take place. From these reports it is deduced that the initiating action of trialkylaluminum cannot be identified with that of a conventional radical initiator but that an alkylaluminum compound itself does not cause alternating copolymerization.

It may be summarized that in the present copolymerization the coexistence of at least one alkyl group and one halogen atom attached to the aluminum metal is important, and an alternating copolymer can be obtained when the aluminum component is coordinated with a polar group of a conjugated monomer and the resulting complex is attacked by a donor monomer. Furthermore, it can be pointed out as a characteristic feature of the present copolymerization that it is not necessary to use deliberately a radical source and that the polymerization proceeds spontaneously.

The authors wish to express their gratitude to S. Kodama, K. Nakaguchi, and S. Kawasumi for their kind guidance and encouragement, Y. Kubota for his continued interest and helpful discussions, H. Oi, K. Shirayama, and T. Okada for determining and interpreting the infrared spectra and K. Sudo, T. Ishiyama, and T. Kawai for their assistance in the experimental work.

References

1. M. Hirooka, H. Yabuuchi, S. Morita, S. Kawasumi, and K. Nakaguchi, *J. Polymer Sci. B*, **5**, 47 (1967).
2. K. W. Doak, *J. Am. Chem. Soc.*, **72**, 4681 (1950).
3. F. M. Lewis, C. Walling, W. Cummings, E. R. Briggs, and F. R. Mayo, *J. Am. Chem. Soc.*, **70**, 1519 (1948).
4. Y. Lander, *J. Polymer Sci.*, **8**, 63 (1952).
5. G. E. Ham, *Copolymerization*, Interscience, New York, 1964, p. 791.
6. T. Higashimura and S. Okamura, *J. High Polymer (Japan)*, **17**, 635 (1960).
7. K. F. O'Driscoll and A. V. Tobolsky, *J. Polymer Sci.*, **37**, 363 (1959).
8. H. J. Harwood, *Chem. Eng. News*, **41**, 36 (1963).
9. H. J. Harwood and W. M. Ritchey, *J. Polymer Sci. B*, **3**, 419 (1965).
10. K. Ito and Y. Yamashita, *J. Polymer Sci. B*, **3**, 631 (1965).
11. J. Iseki, to be published.
12. F. A. Bovey and G. V. D. Tiers, *Fortschr. Hochpolymer-Forsch.*, **3**, S139 (1963).
13. M. Imoto, T. Otsu, and S. Shimizu, *Makromol. Chem.*, **65**, 174 (1963).
14. M. Imoto, T. Otsu, and Y. Harada, *Makromol. Chem.*, **65**, 180 (1963).
15. M. Imoto, T. Otsu, and M. Nakabayashi, *Makromol. Chem.*, **65**, 194 (1963).
16. Esso Research and Engineering Co., Brit. Pat. 946,052 (Jan. 8, 1964).
17. Farbwerke Hoechst A.-G., U.S. Pat. 3,156,675 (Nov. 10, 1964).
18. H. Wexler and J. A. Manson, *J. Polymer Sci. A*, **3**, 2903 (1965).

Received June 26, 1967

Revised October 2, 1967

**Inorganic Coordination Polymers. X.* Observations
on the Formation and Nature of
Poly(di- μ -diphenylphosphinato-
hydroxyaquochromium(III)), $\{Cr(H_2O)(OH)-$
 $[OP(C_6H_5)_2O]_2\}_z$**

K. D. MAGUIRE and B. P. BLOCK, *Technological Center, Pennsalt
Chemicals Corporation, King of Prussia, Pennsylvania 19406*

Synopsis

Under different conditions two products, one green and one brown, were obtained by the air oxidation of chromium(II) diphenylphosphinate. Air oxidation of an aqueous suspension of the phosphinate apparently yields a mixture in which the green form predominates. As initially isolated, the green form is a low molecular weight polymer corresponding to $\{Cr(H_2O)(OH)[OP(C_6H_5)_2O]_2\}_n$, with n approximately 11. It spontaneously polymerizes further in organic solvents to high molecular weight polymers of the same composition, with n in the range 150-200. This polymerization reaction involves the elimination of water and is probably a reaction between endgroups resulting in a basically linear polymer. The brown product, corresponding to low molecular weight $\{Cr_2(H_2O)(OH)_2[OP(C_6H_5)_2O]_4\}_p$, also polymerizes spontaneously but at a faster rate and to a gel. The polymer so produced is less soluble than that produced from the low molecular weight green product and is probably crosslinked.

INTRODUCTION

In an earlier publication from this laboratory² it was reported that the quality of the polymer $\{Cr(H_2O)(OH)[OP(C_6H_5)_2O]_2\}_z$ depended on the details of its preparation. Differences in the product, noted particularly during solution polymerization of the oxidized chromium(II) diphenylphosphinate, were attributed to the presence of varying amounts of acetate. We now wish to report results that shed further light on the cause of this deviation and have led to a more satisfactory procedure for the preparation of $\{Cr(H_2O)(OH)[OP(C_6H_5)_2O]_2\}_z$.

EXPERIMENTAL

General

Viscosity data were collected as before.² The apparent intrinsic viscosities were calculated by plotting either η_{sp}/C or $\ln \eta_{rel}/C$ or both against

* Part IX of this series in Dahl and Block.¹

concentration and extrapolating to infinite dilution. Gel permeation chromatograms were obtained with a Waters Associates apparatus and dimethylformamide (DMF) as solvent. Infrared spectra were obtained with a Perkin-Elmer Model 337 grating spectrophotometer for mulls in hexachlorobutadiene or Nujol. Visible-light spectra were measured with a Beckman DB spectrophotometer in conjunction with a Photovolt Varicord Model 43 recorder. Molecular weight data were obtained for $\bar{M}_n < 10,000$ with a Mechrolab Model 301A Vapor Pressure Osmometer and purified chloroform solutions and for $\bar{M}_n > 10,000$ with a Hewlett-Packard Model 502 high-speed membrane osmometer equipped with a 0-8 Schleicher and Schuell membrane and DMF solutions at 30°C. The molecular weight values reported were obtained by extrapolation to infinite dilution.

All reagents were ACS reagent-grade or better and were used without further purification unless specifically indicated otherwise. Diphenylphosphinic acid was prepared by the procedure described by Ocone et al.³ Its sodium and potassium salts were prepared by neutralizing a methanol solution of the appropriate hydroxide with solid diphenylphosphinic acid to pH of about 6.5. Filtration and concentration of the solution (almost all the methanol has to be removed), followed by addition of acetone to the cooled concentrated solution, precipitated the salt. The salts were washed with acetone and dried in a vacuum oven at 80°C.

Chromium(II) Diphenylphosphinate

All operations involving chromium(II) compounds were carried out under an atmosphere of nitrogen. Because both acetate and zinc ions are difficult to remove from chromium(II) diphenylphosphinate, its synthesis via chromium(II) acetate² was abandoned.

Warm 2*M* HCl reacts readily with excess highly purified chromium metal (99.999%, from Schmelztechnik G.m.b.H., München, Germany, through United Mineral and Chemical Corporation, 129 Hudson Street, New York, New York, 10013, as shot 3–5 mm. in diameter), yielding a bright blue chromium(II) chloride solution, which contains very little free acid.^{4,5} Thus 110 ml. of 2*M* HCl was added to 10 g. of Cr shot, and the mixture was allowed to evolve hydrogen for 30–60 min. Then it was gently heated to, and kept at, reflux until reaction ceased (approximately 30 min.). This solution was transferred under nitrogen to the reaction flask. A solution of 51.2 g. of KOP(C₆H₅)₂O (200 mmoles) in 1500 ml. of methanol (deoxygenated by boiling 15 min. and cooling in a stream of nitrogen) was added slowly (about 1 hr.) to the CrCl₂ solution, while the mixture was stirred continuously with a magnetic stirrer. The blue-gray solid that precipitated initially soon assumed the bright pink color of chromium(II) diphenylphosphinate. Toward the end of the reaction the addition of the phosphinate was interrupted briefly, and the supernatant liquid was examined visually for the presence of excess chromium(II). (There should be some chromium(II) in the solution when the addition is completed. Excess phosphinate, if present, coprecipitates with the chromium(II) phosphinate

and is detrimental to the final polymer.) After the mixture was stirred for 30 min., the solid pink product was filtered out of the mixture and washed with a deoxygenated 1:1 v/v mixture of methanol and water, until the acidified washings gave no precipitate with aqueous silver nitrate solution (four to six washings with 50 ml. portions, accompanied by sufficient shaking to break up the filter cake each time, were required).

The product is insoluble in all common solvents with which it does not react and is very readily oxidized by air.

ANAL. Calcd. for $C_{24}H_{22}CrO_5P_2$: C, 57.15%; H, 4.40%; P, 12.28%. Found: C, 56.34%; H, 4.42%; P, 12.21%.

A sample of the pink chromium(II) diphenylphosphinate hydrate was dried by evacuation to 10^{-1} torr for 6 hr. at room temperature (about 25°C.). A sample of the dry hydrate (2.0045 g.) was sealed to a high vacuum system and dehydrated by heating to 150–180°C. for 3 hr. at 10^{-3} torr; the evolved water was collected and weighed (0.0667 g.).

Calcd. for monohydrate: H_2O , 3.57%; for dihydrate: 6.90%. Found: H_2O , 3.33%.

Oxidation in Aqueous Suspension

Pink chromium(II) diphenylphosphinate prepared on the scale just described was transferred to a large open beaker containing 2 liters of distilled water, and the suspension was stirred overnight at room temperature (about 25°C.) in contact with the air. The resulting solid was filtered, washed with water, and dried in a vacuum oven at 65°C.; yield 43–44 g., approximately 85%, based on the $KOP(C_6H_5)_2O$.

The product is a pale-green powder readily soluble in chloroform, benzene, tetrahydrofuran (THF), and dioxane but insoluble in diethyl ether, ethanol, and water. A freshly prepared solution in chloroform has an intrinsic viscosity in the range 0.03–0.04 dl./g. The viscosity–time

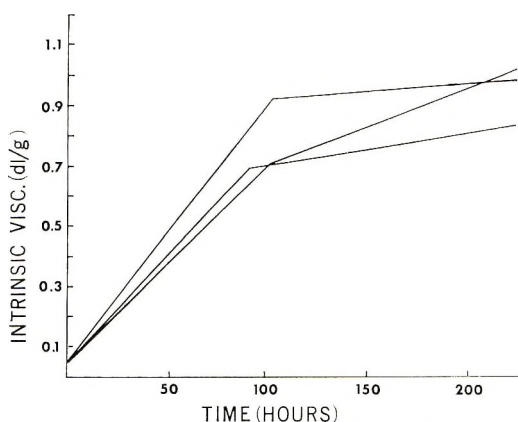


Fig. 1. Change in intrinsic viscosity with time at 55°C. for chloroform solutions of different portions of a sample of pink $Cr[OP(C_6H_5)_2O]_2 \cdot H_2O$ oxidized in aqueous suspension.

data obtained with this material are not reproducible. A typical example is shown in Figure 1.

The elemental analysis and the infrared spectrum are indistinguishable from those of the low molecular weight green polymer (described later). However, the visible-light spectrum of a chloroform solution (1 g. per 100 ml.) shows evidence of the absorption characteristic of the low molecular weight brown polymer (described later) at 400–350 $m\mu$; see Figure 2.

Green Low Molecular Weight $\{\text{Cr}(\text{H}_2\text{O})(\text{OH})[\text{OP}(\text{C}_6\text{H}_5)_2\text{O}]_2\}_n$

Pink chromium(II) diphenylphosphinate, prepared on the scale described herein, was transferred to an open beaker containing 1 liter of a 70:30 v/v mixture of THF and water with the aid of a small volume of the solvent mixture in such a way that it did not come in contact with the air until the transfer was complete; that is, the suspension was introduced below the surface of the solvent mixture. The mixture was stirred while exposed to the air, until the pink solid was completely oxidized and a clear bright-green solution had formed (3–4 hr.). The green solution was then poured into an ice-cold 1% NaCl solution (4 liters), whereupon the polymer precipitated as a green solid. After the solid had settled (usually overnight), it was filtered off, washed free from chloride with water, and dried in a vacuum oven at 65°C. for 8 hr.; yield 43–44 g., or about 85%, based on $\text{KOP}(\text{C}_6\text{H}_5)_2\text{O}$.

The product is a pale-green powder readily soluble in chloroform, benzene, THF, and dioxane but insoluble in diethyl ether and ethanol. A freshly prepared solution in chloroform has an intrinsic viscosity ranging from 0.03 to 0.04 dl./g. The intrinsic viscosity increases slowly when a chloroform solution (1–5 g. per 100 ml.) is allowed to stand at temperatures up to 55°C. and may reach as high as 1.0 dl./g. after several days. A sample with $[\eta] = 0.04$ dl./g. (chloroform, 30°C.) has a molecular weight of 6160 (VPO, chloroform, 30°C.).

ANAL. Calcd. for $\text{C}_{24}\text{H}_{22}\text{CrO}_6\text{P}_2$: C, 55.29%; H, 4.45%; Cr, 9.97%; P, 11.88%. Found: C, 55.9%; H, 4.57%; Cr, 10.02%; P, 12.16%.

In the visible-light spectrum of a chloroform solution there are two peaks of approximately equal intensity (molar absorbance ≈ 35) at 420 and 615 $m\mu$. If the product is free from the brown, low molecular weight polymer, there is no major absorption band in the region 400–300 $m\mu$ (Fig. 2).

The infrared spectrum is identical with that reported previously.²

Brown Low Molecular Weight Polymer

Pink chromium(II) diphenylphosphinate monohydrate prepared on one-half the scale described herein was dried by passing a stream of warm (40°C.) dry nitrogen through the solid for 6 hr. The dried solid was then oxidized by passing a mixture of dry air and nitrogen, containing approximately 1% oxygen, through the solid. The composition of the gas mixture was maintained by keeping the flow rate of nitrogen 20 times greater than

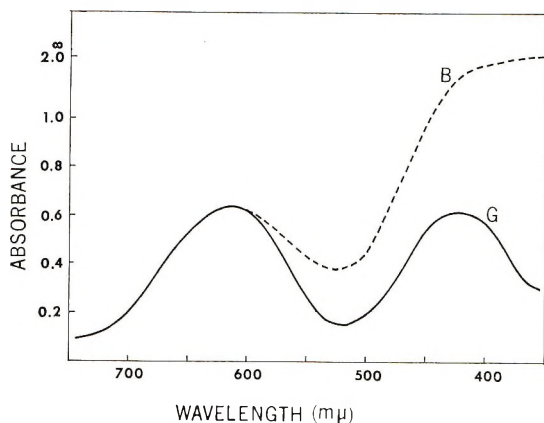


Fig. 2. Visible-light spectra of the brown oxidation product (*B*) and the green oxidation product (*G*) in chloroform solution (1 g. per 100 ml., 1 cm. cell).

that of the air; yield 15.4 g. The oxidation is highly exothermic, and if the dried chromium(II) compound is simply exposed to air, the oxidation is so vigorous that some charring usually occurs. Even when there is no charring, if the solid heats up unduly an insoluble product results.

Solutions of the brown oxidation product in chloroform increase in intrinsic viscosity rapidly at first and after a few days yield gels. The solutions change from brown to green.

ANAL. Calcd. for $C_{48}H_{44}Cr_2O_{11}P_4$: C, 56.3%. Found: C, 55.6, 56.4, 56.8, and 57.1% for different samples. The values for H, Cr, and P were within experimental error for either $\{Cr_2(H_2O)(OH)_2[OP(C_6H_5)_2O]_4\}_p$ or $\{Cr(H_2O)(OH)[OP(C_6H_5)_2O]_2\}_n$.

A weighed, dried sample of $Cr[OP(C_6H_5)_2O]_2 \cdot H_2O$ (0.4165 g.) was allowed to react with dry air, and the increase in weight was found to be 0.0125 g. This increase corresponds to a gain of 1 g.-atom of oxygen per Cr atom during the oxidation.

In the visible-light spectrum of a chloroform solution there are peaks at 615 $m\mu$ (molar absorbance ≈ 35) and 350–400 $m\mu$ (molar absorbance $\approx 10^3$); see Figure 2.

The infrared spectrum is virtually indistinguishable from that reported earlier for $\{Cr(H_2O)(OH)[OP(C_6H_5)_2O]_2\}_x$.²

Solution Polymerization

A freshly prepared solution of the green polymer in chloroform was placed in a bath thermostatically controlled to 30°C. ($\pm 0.02^\circ$). Samples were removed periodically, and the polymerization was followed by measuring the intrinsic viscosity of the samples. A sample of the brown polymer dissolved in chloroform was placed in a Ubbelohde viscometer in the 30°C. bath, and the efflux times were measured periodically. The results are collected in Table I.

TABLE I
 Polymerization of Low Molecular Weight Products at 30°C. in Chloroform^a

Green product			Brown Product	
Δt , hr.	$[\eta]^b$	η_{sp}^c	Δt , hr.	η_{sp}^c
0	0.034	0.0348	0	0.08
5	0.042	0.043	0.75	0.09
10	0.046	0.047	1.0	0.096
15	0.053	0.054	1.25	0.112
20	0.058	0.058	3.0	0.15
30	0.068	0.069	4.0	0.17
39	0.076	0.077	6.0	0.196
48	0.084	0.085	22.0	0.29

^a Concentration 1 g. per 100 ml. for both materials.

^b At 30°C., in chloroform, η_{sp}/C , where $C \rightarrow 0$.

^c For solution containing 1 g. per 100 ml. of chloroform.

Increasing the temperature of the polymerization increases the rate of polymerization, whereas changes in the concentration (range, 1–5 g. per 100 ml.) have only a small effect on the rate of increase of intrinsic viscosity. Samples of high molecular weight polymer were usually obtained by dissolving a requisite quantity of the green low molecular weight polymer ($[\eta] = 0.04$) in a suitable solvent, such as THF or chloroform, and placing the solution in a hot room at 55°C. for a number of days. Typical results are as follows, in which are given solvent, concentration (in grams per 100 ml.), time incubated (in hr.), $[\eta]$ of product at 30°C. in the same solvent: THF, 2.7, 168, 0.74; THF, 2.7, 312, 0.95; chloroform,

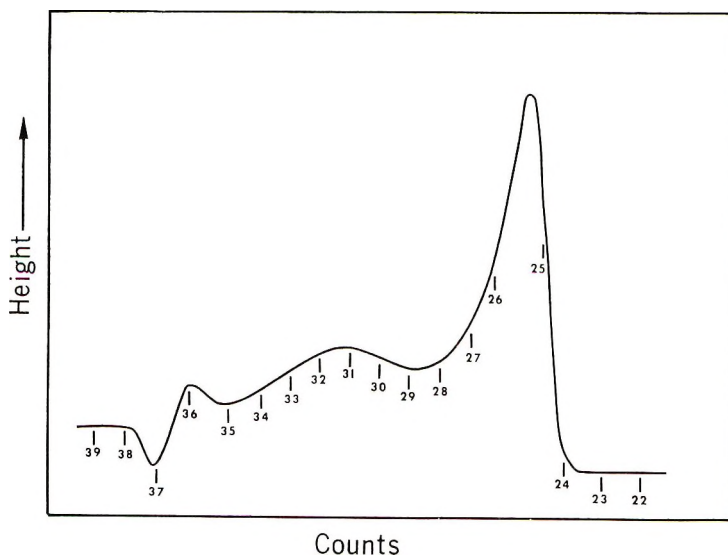


Fig. 3. Gel permeation chromatograph in DMF of a sample of whole polymer ($[\eta]_{\text{THF}} = 0.95$ dl./g.) made by incubation of the green oxidation product in THF.

2.7, 168, 0.86; benzene, 1.0, 18, 0.39; benzene, 2.5, 18, 0.39. Solid, green polymers were isolated by evaporation of the solvent followed by drying to constant weight in a vacuum oven at 65°C. One sample of polymer (THF, 2.7, 312, 0.95) had a molecular weight of 88,000 in DMF solution, according to membrane osmometry. The gel permeation chromatograph of a DMF solution of the same sample is reproduced in Figure 3. Samples of the brown polymer treated in a similar manner invariably gave gels.

Solution Polymerization By-product

A 1 g. sample of the green, low molecular weight polymer ($[\eta] = 0.04$) in a high-vacuum apparatus was completely freed from extraneous moisture by evacuating to a pressure of approximately 10^{-3} torr for 8 hr. at room temperature. Anhydrous THF (25 ml. dried over CaH_2) was then distilled onto the sample, and the reaction vessel was sealed under vacuum. The polymer solution was kept at 30°C. for 4 days; then the solvent was distilled into the vacuum system and collected over CaH_2 . The liberated hydrogen was collected in a Toepler pump and found to be 0.66 moles (14.95 ml. at STP). The intrinsic viscosity of the polymer increased from 0.04–0.14 dl./g. during the polymerization.

Polymerization Inhibition

Samples of green, low molecular weight polymer ($[\eta] = 0.04$) in chloroform (1 g. per 100 ml.) were treated with various reagents, and the viscosities of the solutions were compared with those of untreated samples after standing at 55°C. for a number of days. Samples polymerized in the dark or in ultraviolet light, in the presence of oxygen, or in the presence of 0.1% nitrobenzene gave viscosity increases similar to those of untreated samples. A sample treated with 0.1% benzoyl peroxide actually increased less than the control (the benzoic acid produced by decomposition of the peroxide presumably acting in a manner similar to that of acetate described in the introduction). Samples of the polymer solution, treated with 2,4-pentanedione, ethylenediamine, picolinic acid, or *o*-phenylenediamine and allowed to stand at 55°C. for seven days, showed no increase in viscosity.

TABLE II
Properties of Fractions of $\{\text{Cr}(\text{H}_2\text{O})(\text{OH})[\text{OP}(\text{C}_6\text{H}_5)_2\text{O}]_2\}_x$

Fraction	Wt., g.	$[\eta]$, ^a dl./g.	k'	Slope ^b	\bar{M}_n ^c	x
1	17.4	0.86	0.28	0.21	180,000	345
2	2.6	0.48	0.48	0.11	88,000	169
3	2.1	0.14	0.51	0.01	55,000	105
4	1.2	<0.05	—	—	—	—

^a THF at 30°C.

^b η_{sp}/C versus C .

^c Membrane osmometer in DMF at 30°C.

Fractional Precipitation

A partial separation was effected by the addition of ethanol to a dilute solution of high molecular weight polymer ($[\eta] = 0.95$ at 30°C . in THF) in THF. The polymer fractions were separated by centrifuging the suspension and were dried to constant weight at 50°C . under vacuum; see Table II.

DISCUSSION

The Oxidation Process

To eliminate the difficulties encountered in the earlier work, arising from the presence of acetate (presumably end-capping or competition with bridging phosphinates²), chromium(II) diphenylphosphinate was made from chromium(II) chloride. Chromium(II) diphenylphosphinate monohydrate prepared in this manner is a light-pink solid, whereas samples prepared from chromium(II) acetate are definitely gray. Oxidation of aqueous suspensions of the pink solid, however, still does not give polymer samples with reproducible properties. Visible-light spectra of solutions of the oxidation products and relationships of intrinsic viscosity versus time for their solutions vary from sample to sample and sometimes even for different portions of a single sample (Fig. 1). Frequently solution polymerization leads to gel formation. It appears that the oxidation process is yielding at least two different materials.

This difficulty can be avoided if the pink monohydrate of chromium(II) diphenylphosphinate is suspended in a mixture of 70:30 v/v THF and water and the suspension is then exposed to air for a few hours. The green solid isolated from the resultant deep-green solution is analyzed as $\{\text{Cr}(\text{H}_2\text{O})\text{-(OH)}[\text{OP}(\text{C}_6\text{H}_5)_2\text{O}]_2\}_n$. Its infrared spectrum shows the previously noted bands at 3600 cm.^{-1} (sharp) and $3300\text{--}3450\text{ cm.}^{-1}$ (broad, weak) assigned to coordinated OH^- and H_2O .² The visible-light spectrum of a chloroform solution (Fig. 2) shows two bands at 615 and $420\text{ m}\mu$ of approximately equal intensity (molar absorbance about 35 per mole of Cr), attributable to the $d\text{-}d$ transitions of octahedrally coordinated chromium(III). As initially isolated, this green product is a relatively low molecular weight polymer (intrinsic viscosity 0.04 dl./g. , \bar{M}_n about 6000), which is insoluble in water but readily soluble in organic solvents. When its solutions are allowed to stand at temperatures up to 60°C ., their intrinsic viscosities slowly increase to values as high as 1.0 dl./g. (Fig. 4) and their number-average molecular weights to values as high as 190,000. In contrast to the earlier samples² this spontaneous polymerization is quite reproducible from sample to sample of the green oxidation product.

When the dry, pink monohydrate of chromium(II) diphenylphosphinate is allowed to react *slowly* with air diluted with nitrogen (1.0% oxygen by volume), there is a highly exothermic reaction producing a brown solid, which is quite different from the earlier oxidation products.² Elemental

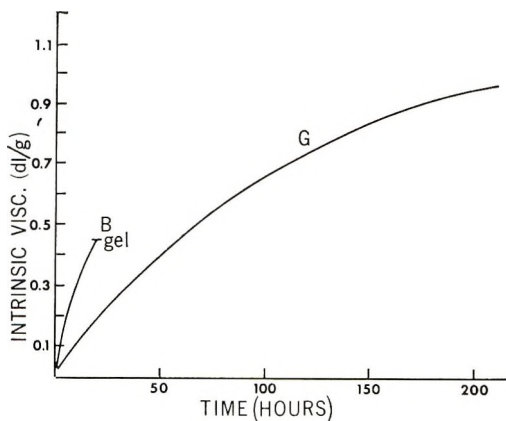
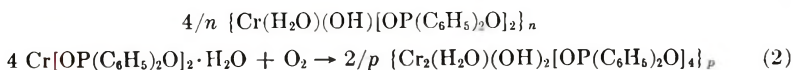
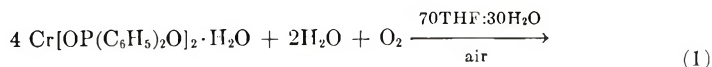


Fig. 4. Change in intrinsic viscosity with time at 55°C. for chloroform solutions of the brown oxidation product (*B*) and the green oxidation product (*G*) (1 g. per 100 ml.).

analyses of various preparations show some variation, but the composition approximates $\{\text{Cr}_2(\text{H}_2\text{O})(\text{OH})_2[\text{OP}(\text{C}_6\text{H}_5)_2\text{O}]_4\}_p$; that is, there is only 0.5 mole of water per chromium, not 1 mole, as in the green product. The stoichiometry of the oxidation agrees with this formulation. Although the two different oxidation products give essentially the same infrared spectra, their visible-light spectra differ. The peak at $615\text{ m}\mu$ is about the same in both, but the brown product gives a broader peak of much greater intensity (molar absorbance about 10^3 per mole of Cr) at $400\text{--}350\text{ m}\mu$ (Fig. 2).

The brown product is much less readily prepared in soluble form, and its characterization is less complete. The intrinsic viscosity of its solutions in organic solvents increases quite rapidly, compared to the rate of increase observed for the green product (Table I and Fig. 4), and after a few days at room temperature gels invariably form. It is quite obvious that the brown polymer is in some way trifunctional and that this leads to some crosslinking and gel formation. Since we were primarily interested in the soluble polymer, further characterization of the brown product was not undertaken. It should be noted, however, that the ultimate product of the solution polymerization of the brown oxidation product is a green polymer. It approximates $\{\text{Cr}(\text{H}_2\text{O})(\text{OH})[\text{OP}(\text{C}_6\text{H}_5)_2\text{O}]_2\}_x$ in composition and is quite similar to the polymer formed from the green oxidation production, except in solubility.

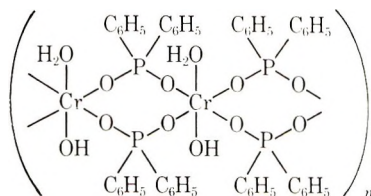
The isolation of two different products from the oxidation of chromium(II) diphenylphosphinate monohydrate explains the erratic behavior of the earlier products. The reactions involved may be summarized in the following equations:



Air oxidation of an aqueous suspension of chromium(II) diphenylphosphinate monohydrate must involve both reactions, leading to mixtures of the green and brown oxidation products. Spectral analysis indicates that the green product is predominant, but there is obviously sufficient brown product present to affect the intrinsic viscosity-time behavior. The lack of reproducibility of this behavior suggests that the relative amounts of the two products vary from sample to sample. Apparently in aqueous suspension the solid particles are not simultaneously exposed to sufficient oxygen and water to yield exclusively the completely hydrated green product, and the oxidized product always contains some minor amount of the brown product. In the THF-water medium, on the other hand, the oxidized product dissolves as rapidly as it is formed, and there is always sufficient water and oxygen to avoid formation of the coordinatively unsaturated brown product; see eq. (1). In the absence of water other than that contained in the chromium(II) diphenylphosphinate monohydrate, the water-deficient brown product which exhibits markedly different behavior from that of the green product is the major oxidation product.

Solution Polymerization of Green Oxidation Product

The most likely structure of the green polymer is a linear arrangement of doubly bridged chromium atoms with water and hydroxyl groups also coordinated to the chromium:

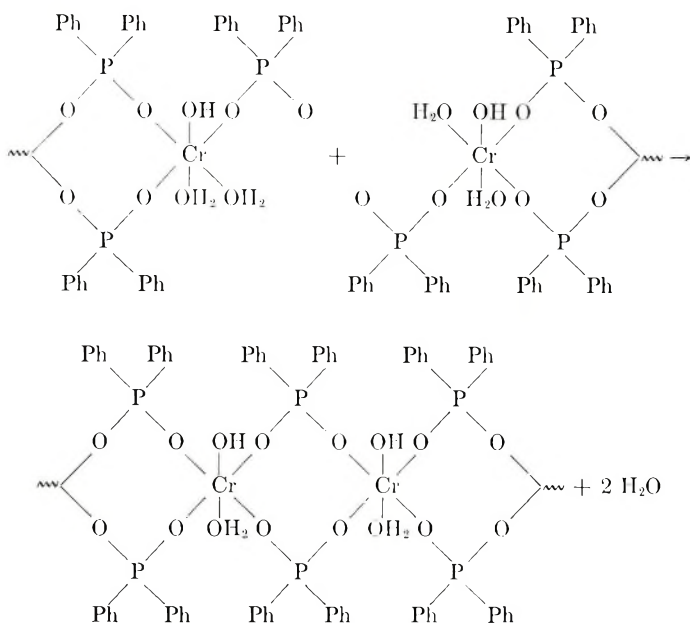


The recent x-ray structure studies of $(\text{CH}_3\text{COCHCOCH}_3)_2\text{Cr}[\text{OP}(\text{C}_6\text{H}_5)_2\text{O}]_2\text{Cr}(\text{CH}_3\text{COCHCOCH}_3)_2$ ⁶ and $\text{Mn}(\text{CH}_3\text{COOC}_2\text{H}_5)_2(\text{OPCl}_2\text{O})_2$ ⁷ lend plausibility to such a structure.

When low molecular weight, green $\{\text{Cr}(\text{H}_2\text{O})(\text{OH})[\text{OP}(\text{C}_6\text{H}_5)_2\text{O}]_2\}_n$ (intrinsic viscosity about 0.04 dl./g.) is allowed to polymerize in anhydrous THF, high molecular weight $\{\text{Cr}(\text{H}_2\text{O})(\text{OH})[\text{OP}(\text{C}_6\text{H}_5)_2\text{O}]_2\}_r$ and water are the only identifiable products. During the polymerization the visible spectrum of the solution remains virtually unchanged, as does the infrared spectrum of the solute. The polymerization does not show any noticeable acceleration in the presence of peroxides or ultraviolet radiation, nor is it prevented by the presence of radical scavengers that do not chelate with chromium(III). Thus, the solution polymerization appears to be more like a condensation than an addition polymerization.

The polymerization can be terminated by the addition of neutral or uninegative bidentate ligands, such as ethylenediamine or 2,4-pentanedione, which become attached to the chromium. This suggests that the polymerization takes place via sites on the chromium that are readily accessible

to these chelating agents. The bulk of the hydroxyl and water groups in the polymer are quite unreactive under the conditions of the solution polymerization. It therefore seems reasonable to conclude that the polymerization reaction involves endgroups. A plausible reaction follows:



In this reaction the nonbridging endgroup diphenylphosphinates substitute water in other endgroups and generate new double bridges. The retention of solubility throughout the solution polymerization suggests that the polymer remains linear, as required by the proposed reaction.

Attempts to study the kinetics of the solution polymerization by following the intrinsic viscosity of the solution were not successful. No simple rate laws fit the data. Further examination of the high molecular weight polymer explained the difficulties. A sample (intrinsic viscosity of 0.95 dl./g. in THF at 30°C., slope of η_{sp}/C versus C of 0.40, and \bar{M}_n of 88,000) was separated into four fractions, for which data are shown in Table II. Gel permeation chromatographs of the whole polymer indicate that there are three different types of component present (Fig. 3). The presence of three distinct components in varying amounts in the polymer makes any relation between intrinsic viscosity and molecular weight of dubious value and rules out measuring rates by following the intrinsic viscosity of the product as a function of time.

We are indebted to Messrs. F. D. Loomis, R. S. Grzymala, N. R. LeDonne, and J. Douglas for assistance with the experimental work and to our Analytical Department for the elemental analyses and molecular weight measurements.

This investigation was supported in part by the Office of Naval Research.

References

1. G. H. Dahl and B. P. Block, *Inorg. Chem.*, **6**, 1439 (1967).
2. A. J. Saraceno and B. P. Block, *Inorg. Chem.*, **3**, 1699 (1964).
3. L. R. Ocone, C. W. Schaumann, and B. P. Block, *Inorg. Syn.*, **8**, 71 (1966).
4. H. Lux and G. Illmann, *Ber.*, **91**, 2143 (1958).
5. J. P. Fackler, Jr. and D. G. Holah, *Inorg. Chem.*, **4**, 954 (1965).
6. C. E. Wilkes and R. A. Jacobson, *Inorg. Chem.*, **4**, 99 (1965).
7. J. Danielsen and S. E. Rasmussen, *Acta Chem. Scand.*, **17**, 1971 (1963).

Received August 21, 1967

Revised October 27, 1967

NOTES

Preparation and Analysis of Asymmetric Membranes

It has been shown, theoretically¹ and experimentally,² that a polymer membrane possessing an internal, fixed gradient of inhomogeneity (e.g., structure, composition, etc.), will exhibit anisotropic transport behavior, such as penetrant mass flow. The rate of flow of a soluble penetrant through such a membrane due to a chemical potential (concentration, vapor pressure) gradient across the membrane depends on the direction of that gradient relative to the direction of the membrane's fixed gradient of inhomogeneity. The same is true for other transport properties, e.g. heat transfer, etc.

This directional preference for mass flow of penetrant can be utilized in separation processes; the "valve effect,"³ superimposed on the natural separation capabilities of a homogeneous membrane⁴ will make the separation process more efficient. The analysis and elucidation of membrane structure is essential for the study and prediction of such behavior. Thus, a well-characterized membrane (as to structure, type, and amount of inhomogeneity) is a prime requisite.

This note describes some methods for preparation and characterization of polymer membranes possessing a fixed gradient of composition from one surface to the other. The primary technique uses a high-energy electron source to initiate polymerization of monomer sorbed in a prescribed manner in a polymer film. The resultant gradient of composition may be determined by spectroscopic analysis of slices obtained by microtoming the film sample perpendicular to the diffusion axis.

A typical diffusion-polymerization cell used for graded-membrane preparation is shown in Figure 1. The original polymer membrane (A) is placed above a monomer (B) reservoir and under a sintered stainless steel plate (void fraction >50%), to form a two-compartment chamber. The membrane acts as a barrier between the two compartments. Any transport of monomer from the lower compartment to the top one, which will take place when the top compartment is evacuated, will occur through the polymer membrane. The sintered stainless steel plate is rigid and prevents deformation of the polymer membrane due to the monomer vapor pressure differential across the membrane during the process. The porous plate does not hinder monomer transport.

After assembly, the top compartment is evacuated first, thus pulling the membrane against the porous plate—a position it keeps throughout the experiment. The bottom compartment, which contains the monomer, is then outgassed, insuring an atmosphere of pure monomer vapor in this compartment. The top compartment is continuously pumped out, so that a constant vapor pressure difference is maintained across the membrane.

The conditions described above lead to diffusion or permeation of penetrant B through barrier A under a concentration or vapor-pressure differential. This process has been treated mathematically⁵ and various factors effecting the transport process have been reviewed elsewhere.⁶

The concentration gradient of penetrant in the membrane at any time during the transport process can be determined by analytical or graphical methods.^{6,7} The concentration gradient is a function of time, temperature, and the concentration differential across the membrane for any polymer-penetrant system. When the penetrant flux reaches a steady state, i.e., when the penetrant moves across the membrane at a constant rate, the concentration gradient becomes time independent. By manipulating external conditions such as concentration, temperature, and time, any gradient shape from the very

shallow shape at the initial stages of permeation, to the final, time-independent, steady-state shape gradient can be achieved. Further modifications can be affected by introducing thermal gradients across the membrane.

Once the desired gradient of monomer concentration in the membrane has been obtained, the whole cup is irradiated with 6 M.e.v. electrons from a Van de Graaff generator at dose rates of 0.5–5.0 Mrad/min., to polymerize and graft monomer B in the membrane A. Trapped polymer B and graft copolymer AB will form; the relative amounts will depend on the system and conditions chosen.

The radiation must be of sufficiently high initial energy to penetrate the aluminum and porous steel barriers above the film sample and still retain the energy required for initiation of graft copolymerization in the film. The cell design, as shown, can be used with 6 M.e.v. electrons or ^{60}Co γ -radiation. If less penetrating radiation (e.g., 1 M.e.v. electrons) is used, the cell must be modified; for example, the porous steel barrier can be replaced with porous aluminum sheet or screening.

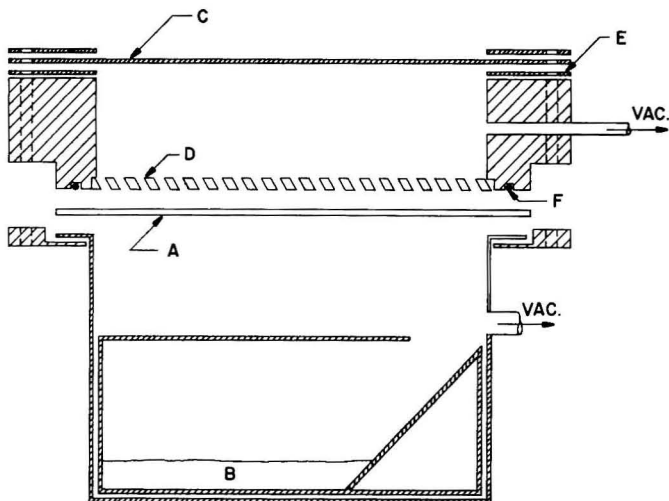


Fig. 1. Permeation-polymerization cell: (A) polymer membrane; (B) monomer liquid in radiation-shield container; (C) $\frac{1}{16}$ -in. aluminum plate; (D) $\frac{1}{8}$ -in. sintered stainless steel plate; (E) gasket; (F) O-ring.

The relative rates of diffusion and polymerization are crucial factors determining the shape of the final graft gradient. If the diffusion rate is negligible in comparison with the polymerization rate, the resulting gradient of B in A, assuming complete conversion to grafted polymer, is the theoretically predicted gradient of monomer concentration. If the rate of diffusion cannot be neglected, the resulting grafted gradient will be steeper than the calculated one, as more monomer diffuses in during the grafting process, and polymerizes after a short travel time, i.e., in the region of high monomer concentration.

There also is the possibility of surface layer formation of almost pure polymer B on the membrane surface, which is expected especially when polymerization can occur in the monomer vapor phase. This complication can be minimized by placing a porous barrier (e.g., filter paper) between the polymer membrane and the vapor phase.

The molecular weight of the grafted polymer is expected to be a function of, among other variables, the dose rate. If the membrane is sufficiently thin, no attenuation of radiation intensity through the membrane is expected and the dose distribution will be fairly uniform with thickness. Also, the small amount of sorbed monomer is not expected to affect the distribution of the active centers created by the radiation. High

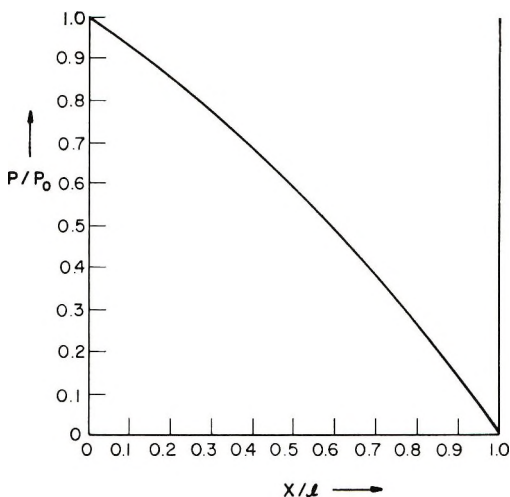


Fig. 2. Monomer distribution in membrane. Relative vapor pressure (P/P_0) of monomer in membrane vs. relative thickness (x/l).

dose rates will yield low molecular weight grafts, as a large number of active center per unit volume will be available at any time.

In some polymer-monomer systems, polymerization may continue after irradiation has stopped, resulting in a steeper gradient. Effectively, the polymerization reaction time has been extended, allowing more monomer to diffuse in. This effect can be minimized by rapidly exposing the membrane to oxygen or air after removal from the radiation source and/or by heating.

If a high overall graft concentration is required, the entire process can be repeated so that additional monomer will be grafted on the existing gradient. The shape of the final gradient will depend on the diffusion and solubility properties of monomer B in the copolymer AB.

To establish the shape of the grafted gradient experimentally, the membrane can be microtomed perpendicular to the diffusion axis and the microtomed slices analyzed by infrared or other techniques. A visual and photometric analysis is possible if the grafted and matrix polymers are of different color or optical properties. Microdensity measurements⁸ also have been utilized for this purpose. For thick films, sufficiently accurate data may be obtained by scanning slices cut parallel or diagonally to the diffusion axis. Other techniques, such as ATR-infrared, also may be useful.

The experimentally determined steady-state gradient of relative vapor pressure of vinyl acetate in a polyethylene ($\rho = 0.92$ g./ml.) film is shown in Figure 2. Since the solubility coefficient of vinyl acetate in polyethylene is essentially constant with vapor pressure, this also is the shape of the steady-state concentration of sorbed monomer. The steady-state, isothermal ($T = 24^\circ\text{C}.$) gradient of vinyl acetate was grafted by using 6 M.e.v. electrons at a dose rate of 1.0 Mrad/min. for 1.5 min. The membrane was washed in methanol, ethanol, and toluene to leach out any homopolymer. Weight loss was less than 2.0% of grafted polymer, which in turn was 1.5% of total weight. Bands at 1740 cm.^{-1} (carbonyl stretch), 1360 cm.^{-1} (CH_3 deformation), and 1235 cm.^{-1} (C—O stretch), were utilized to determine the shape of the gradient, the band at 725 cm.^{-1} (methylene rock) being used as internal thickness calibration. No surface layer of poly(vinyl acetate) was detected.

The gradient of grafted poly(vinyl acetate) in the polyethylene film, prepared by the method described above, is shown in Figure 3. The gradient of grafted copolymer corresponds with the steady-state gradient of sorbed, diffusing monomer at the time of

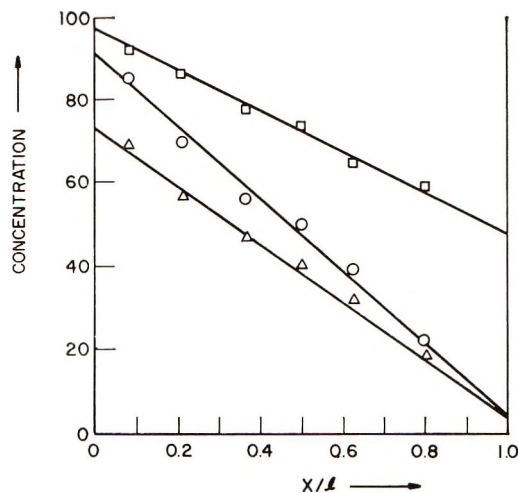


Fig. 3. Gradient of grafted poly(vinyl acetate) in polyethylene membrane. Concentration (in arbitrary units) of poly(vinyl acetate) vs. relative thickness (x/l).

radiation, shown in Figure 2, as calculated from knowledge of the solubility and diffusion coefficients for vinyl acetate in polyethylene as functions of vapor pressure and temperature.

Other methods for preparation of asymmetric membranes include the preparation of simple laminates,³ by many well known methods, to almost continuous gradients made by successive castings of different concentration films.⁹ The general technique described in this paper for the synthesis of continuous gradients, can be extended to include other methods of polymerization initiation, such as ultraviolet, x-ray, or γ -radiation, dispersed (uniformly or asymmetrically) radical initiators, such as azobisisobutyronitrile, or simple thermal activation such as for the reaction of oxygen or halogens during their unidirectional permeation through a viscous hydrocarbon substrate.

The monomer can enter the membrane either from the vapor phase or from the liquid phase, including solutions with a diluent liquid which may swell the polymer, thereby possibly promoting monomer sorption, or, which may otherwise effect the grafting reaction.¹⁰ Of course, the initially formed graded-graft copolymer can be modified further if the polymer is susceptible to some desired chemical or physical reaction. For example, polyethylene-graded graft-styrene membranes have been sulfonated to obtain graded ion-exchange membranes.¹¹ More complex membranes may be prepared by graded graft copolymerization of different monomers in the same or different directions through the same base membrane.

Structural gradients can be obtained by using nonmonomer penetrants which are radical chain-transfer reagents and/or which swell or otherwise affect the polymer film. The resultant crosslink density distribution and swelling induced changes in polymer structure and morphology will reflect the spatial distribution of penetrant at the time of radiation or other initiated reaction.

Many other modifications can be conceived; the method is both versatile and easily controllable, yielding, within a relatively short time, asymmetric membranes of unique structure and properties for a number of applications.¹¹ These asymmetric membranes also serve as model systems for studies of transport phenomena in multicomponent media, in terms of irreversible thermodynamics, with applications especially for biological systems.¹¹

Partial support of this investigation by grants from the E. I. du Pont de Nemours Co. and the National Science Foundation is gratefully acknowledged.

References

1. H. L. Frisch, *J. Polymer Sci. A*, **2**, 1115 (1964).
2. C. E. Rogers, in *Transport Phenomena in Polymeric Films (J. Polymer Sci. C, 10)*, C. A. Kumins, Ed., Interscience, New York, 1965, p. 93.
3. C. E. Rogers, V. Stannett, and M. Szwarc, *Ind. Eng. Chem.*, **49**, 1933 (1957).
4. S. A. Stern, in *Membrane Processes for Industry*, Southern Research Institute, Birmingham, Alabama, 1966, p. 196.
5. J. Crank, *The Mathematics of Diffusion*, Oxford Univ. Press, London, 1956.
6. C. E. Rogers, in *Physics and Chemistry of the Organic Solid State*, Vol. II, D. Fox, M. Labes, and A. Weissberger, Eds., Interscience, New York, 1965, Chap. 6.
7. P. E. Rouse, *J. Am. Chem. Soc.*, **69**, 1068 (1947).
8. S. Munari, F. Vigo, G. Tealdo, and C. Rossi, *J. Polymer Sci. B*, **4**, 547 (1966).
9. A. M. Liquori and C. Borte, *Ric. Sci.*, **6**, 71 (1964).
10. G. Odian, T. Acker, and M. Sobel, *J. Appl. Polymer Sci.*, **7**, 245 (1963).
11. C. E. Rogers and S. Sternberg, to be published.

C. E. ROGERS
S. STERNBERG

Division of Polymer Science
Case Western Reserve University
Cleveland, Ohio 44106

R. SALOVEY

Bell Telephone Laboratories
Murray Hill, New Jersey 07971

Received August 4, 1967

Rates of Sulfonation of Divinylbenzene-Crosslinked Polystyrene in Dimethyl Sulfoxide

The rate of sulfonation of bead copolymers of styrene crosslinked with 8 mole-% of isomeric divinylbenzenes has been found to be influenced by the nature of the swelling agent. We have observed an increase in the rate of sulfonation of beads swollen in dimethyl sulfoxide (DMS) as compared with those swollen in ethylene dichloride (EDC). In accordance with the previous observations,¹ enhanced rates have been found for beads crosslinked with approximately 2:1 mixture of *m*- and *p*-divinylbenzenes. Increase in the rate of sulfonation has been explained on the basis of the solubility of sulfuric acid in the swelling agent and on the higher dielectric constant of the solvent.

In the previous sulfonation rate studies,^{1,2} of bead copolymers of styrene and divinylbenzenes, ethylene dichloride (EDC) with which sulfuric acid is immiscible was used as a swelling agent. The swelling agent retained in the beads probably renders the reaction site more or less inaccessible to the sulfonating agent. Under these conditions the rate of diffusion of sulfuric acid into the swelling agent is probably a parameter controlling the rate of sulfonation. We have now investigated the sulfonation rates of bead copolymers using dimethyl sulfoxide (DMS), with which sulfuric acid is miscible and wish to report the results of these studies. Sulfonations in nitrobenzene have been reported recently by Freeman.⁶

Results and Discussion

The data obtained on the sulfonation of copolymer beads are summarized in Figures 1 and 2. An increase in the rate of sulfonation of beads swollen in DMS as compared with those swollen in EDC has been observed. For the *meta* crosslinked copolymer, sulfonation to the level of 4.69 meq./g. was reached in 9 hr. with DMS and in the same time to only 2.08 meq./g. with EDC. For the *para* crosslinked copolymer, the values are 4.53 meq./g. in DMS and 2.35 eq./g. in EDC in 3½ hr. For the 2:1/*m*:*p*-DVB crosslinked copolymer the values are 4.5 and 3.94 meq./g., respectively, in DMS and EDC in 60 min. The differences for the last would probably be greater at 60°C. A least-squares analysis of the initial linear portion shows slopes of 0.0670 (DMS)/0.0614 (EDC).

It does not appear that differences in swelling of the lattice by the two solvents can account for differences in the rates of sulfonation. DMS is known to have a higher solvent power than EDC and hence might swell the polymer lattice better. Qualitatively, however, we observed little or no difference in the amount of swelling in the two solvents. Furthermore, previous data on the swelling ratios of beads containing 8 mole-% of pure *meta*, pure *para*, and 2:1 *meta/para* divinylbenzene monomers prepared

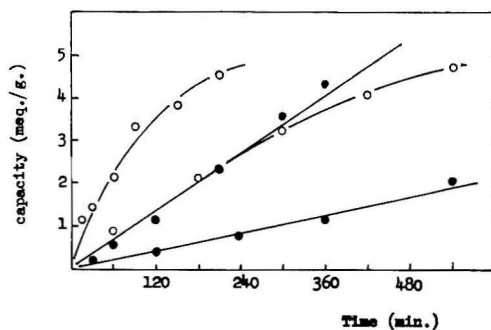


Fig. 1. Sulfonation of bead copolymers of styrene with 8% pure *m*- and pure *p*-divinylbenzene: (○) in dimethyl sulfoxide; (●) in ethylene dichloride. The upper pair of curves is for pure *para*, the lower pair for *meta*.

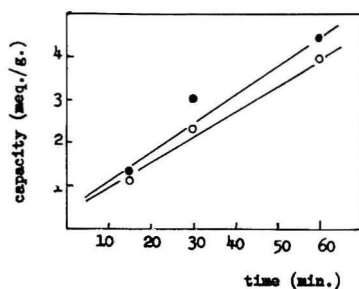


Fig. 2. Sulfonation of bead copolymers of styrene with 8% 2:1/*m*:*p*-divinylbenzene: (●) in dimethyl sulfoxide; (○) in ethylene dichloride.

with 0.5% benzoyl peroxide and their sulfonation rates indicate that there is not a direct correlation between swelling ratios (SR) and rate of sulfonation. Thus, the *para* cross-linked copolymer swells less than the *meta* (SR = 1.53/1.77) but sulfonates more rapidly (1.13/0.4 meq./g. at 2 hr.).^{1,3} Therefore, the rate enhancement can probably best be explained on the basis of the homogeneity of the solvent-sulfuric acid system and on the greater dielectric constant of the solvent. Under identical conditions the penetration of sulfuric acid into the beads is faster and its concentration inside the beads is likely to be higher for beads swollen in DMS than in EDC. Also, it may be noted from a practical point of view that EDC may not be a good choice for sulfonations at 80°C., which is very close to the boiling point of ethylene dichloride. This can lead to the cracking of beads, especially if sufficient swelling agent is retained in the beads.

Experimental

m-DVB (supplied by Centre de Recherches du Groupe Petrofina, Brussels) and *p*-DVB prepared by the decarboxylation of *p*-phenylenediacrylic acid (Aldrich Chemicals) were purified and characterized by methods reported earlier.⁴ Monomers thus obtained were 99.9+ % pure by gas chromatography (flame ionization detector, Perkin-Elmer R column). The mixture of *m*- and *p*-DVB was prepared from commercial DVB (Dow Chemical Co.) by the method reported earlier with the use of a Bentone column.⁵ The composition of the mixture was found by gas-chromatographic analysis (thermal conductivity detector) to be 73% *meta* and 27% *para*. Bead copolymerizations were carried out at 80°C. with 0.5% benzoyl peroxide as initiator and carboxymethylcellulose as dispersing agent. Sulfonations were run on 30 mesh beads swollen for 20 hr. in DMS (Eastman Organic Chemicals, n_D^{20} 1.4740) and EDC (Fisher Scientific, boiling range 82.5–83.5°C.) at 80°C., with 98% sulfuric acid prepared from C.P. 96% sulfuric acid and C.P. 30% oleum. The details of these methods have been published previously.^{1,3} The observed rates¹ are comparable to those reported previously for the *meta* beads but are somewhat (about one-half) less for the *para* beads. We have no explanation for the latter discrepancy at present. It is believed that the present data are self-consistent, having been checked by two observers, even though they are at variance in part with previous data obtained by another observer.

This work was supported in part by the U.S. Atomic Energy Commission under Contract AT-(30-1)-3644 with Hunter College of the City University of New York.

References

1. R. H. Wiley and T. K. Venkatachalam, *J. Polymer Sci. A*, **3**, 1063 (1965).
2. K. W. Pepper, *J. Appl. Chem. (London)*, **1**, 124 (1951).
3. R. H. Wiley, J. K. Allen, S. P. Chang, K. E. Musselman, and T. K. Venkatachalam, *J. Phys. Chem.*, **68**, 1776 (1964).
4. R. H. Wiley and R. M. Dyer, *J. Polymer Sci. A*, **2**, 3153 (1964).

5. R. H. Wiley, G. DeVenuto, and T. K. Venkatachalam, *J. Gas Chromatog.*, **5**, 590 (1967).
6. D. H. Freeman and A. S. Aiyar, *Anal. Chem.*, **39**, 1141 (1967).

RICHARD H. WILEY
T. O. AHN
Y. KAMATH

Graduate Division
Hunter College
The City University of New York
New York, New York 10021

Received September 14, 1967
Revised October 31, 1967